DEVELOPMENT OF LABORATORY METHODOLOGIES FOR EVALUATING THE EFFECTIVENESS OF REACTIVE TAILINGS COVERS

MEND Project 2.21.1

March 1992

DEVELOPMENT OF LABORATORY METHODOLOGIES FOR EVALUATING THE EFFECTIVENESS OF REACTIVE TAILINGS COVERS

Final Report

by

Ernest K. Yanful, Ph.D.

Project Manager : K.G. Wheeland
Centre de technologie Noranda
240 Hymus Boulevard
Pointe Claire, Quebec, H9R 1G5

DSS Contract Number KE 144-8-4464/01-SS
Environment Canada Scientific Authority : D. Vachon

December 1991

DISTRIBUTION

	Copies
Mr. D. Vachon (Environment Canada Scientific Authority)	5
Mr. G. Tremblay (Prevention and Control Coordinator, MEND Program)	20
Noranda Internal Distribution	15

ACKNOWLEDGEMENTS

The author wishes to thank Drs. R. Nicholson and R.W. Gillham of the University of Waterloo for undertaking the fundamental research work required to develop methodologies for cover evaluation. The results of this work were applied to the evaluation of candidate soils. Dr. Nicholson also developed the oxygen diffusion model used for estimating fluxes. The author also benefited from discussions with Dr. Kerry Rowe of the University of Western Ontario during modelling of several column experiments using the computer program, POLLUTE. Dr. L.S. Barbour of the University of Saskatchewan and L. St-Arnaud of NTC modelled the drainage of a two-layer cover system in a laboratory column. Technical review of this report by K.G. Wheeland of NTC is gratefully acknowledged. The bench work was conducted with the assistance of NTC's geotechnical technologist, K. Shikatani, and three University of Waterloo students: R. Sydor, B. Aubé and G. Cotta. J. D'Arcy typed, edited and assembled the entire report.

The project was jointly funded by Environment Canada, CANMET and DSS under the MEND program. Supplementary funding to complete additional tasks resulting from a change in scope was provided by Noranda Inc. The support of Mr. Hennie Veldhuizen in this regard is also acknowledged.

Mr. Jim Scott, formerly of Environment Canada, Hull, was the former Scientific Authority of the contract. The author acknowledges his cooperation and support of the work described in this report.

KEY WORDS

Acid Mine Drainage
Base Metal Tailings
Engineered Covers
Oxygen Flux
Diffusion Coefficient
Moisture Drainage
MEND Program

EXECUTIVE SUMMARY

This final report presents the results of an investigation conducted to develop laboratory and computer methodologies for evaluating the effectiveness of engineered soil covers for reactive sulphide tailings. The study was undertaken under a Supply and Services Canada (DSS) contract awarded to Noranda Technology Centre (NTC) in January 1989. Funding for the project was provided by Environment Canada, Canada Centre for Mineral Technology (CANMET), DSS and Noranda Inc. NTC subcontracted the initial fundamental aspects of the study to the University of Waterloo. NTC focused on the more-applied aspects of the work and later adopted some of the methods developed at Waterloo in the investigation of candidate natural soils from two active Canadian mine sites.

The transport of oxygen through tailings covers was shown to be mainly by molecular diffusion resulting from concentration gradients established between the atmosphere and soil void spaces. The rate of diffusion is controlled by the diffusion coefficient which is, in turn, dependent on the grain size, moisture content, porosity and other physical properties such as tortuosity or the flow path length. Oxygen diffusion coefficients, determined for one of the candidate soils, were observed to decrease with increasing water contents or degrees of water saturation. This trend was consistent with theoretical predictions and agreed with findings reported by previous workers. In the laboratory tests reported here, it was acknowledged that oxygen uptake by natural soils moulded at high moisture contents could be significant as a result of increased activity of soil micro-organisms under moist conditions. It was recommended that this factor be given serious consideration in any investigation.

Three laboratory columns were designed and constructed, and suitable instrumentations were adapted to provide reliable methodologies for soil cover evaluation. The developed apparatus were; a) a column for determining the diffusion coefficient of oxygen, b) a column for evaluating the hydraulic behaviour (moisture retention and drainage characteristics) of potential cover materials, and c) a demonstration column for estimating the low oxygen fluxes expected from saturated soil covers.

Experimental and theoretical pressure head profiles observed in a two-layered system (candidate till over sand layer) indicated drainage of the sand layer to residual saturation without a measurable drainage and therefore loss of moisture from the till layer. Experimental testing was extended to at least 100 days in the demonstration column. Similar trends in moisture contents were observed. The results suggested that, in the absence of other extraneous influences such as root penetration and cracking resulting from freezing, similar performance could be expected in the field. At most Canadian mine sites, 100 days will, most probably, be the maximum dry period when no recharge to the cover by infiltration would occur.

Estimates of oxygen concentration at the base of the demonstration column showed that only 600 ppm could be expected in a year. In terms of fluxes, this would amount to 6.5×10^{-3} moles/m^2/a of oxygen and an acid flux of 0.338 g/m^2/a of sulphuric acid (H_2SO_4). In comparison, maximum acid flux estimated in uncovered tailings in laboratory lysimeter tests at NTC (outside this project) was typically of the order of 1200 g/m^2/a of H_2SO_4.

Practical concepts were proposed for designing high performance soil covers. Critical material properties required for design and prediction of performance were identified to include the diffusion coefficient, moisture drainage characteristics and long-term critical moisture contents under dry conditions. It was concluded, from limited laboratory testing, that freezing and thawing cycles could play an important role in soil cover performance.

SOMMAIRE EXECUTIF

Ce rapport final présente les résultats d'une étude réalisée en vue de développer des méthodologies de laboratoire et informatiques qui permettront d'évaluer l'efficacité de recouvrements géologiques pour résidus sulfureux. Cette étude a été réalisée dans le cadre d'un contrat octroyé au Centre de technologie Noranda (CTN) par Approvisionnement et services Canada (MAS) en janvier 1989. Le projet a été financé par Environnement Canada, le Centre canadien de la technologie des minéraux et de l'énergie (CANMET), le MAS et Noranda Inc. Le CTN a donné les aspects fondamentaux de l'étude en sous-traitance à l'université de Waterloo. Le CTN s'est penché directement sur les aspects pratiques du projet et a par la suite adopté certaines des méthodes développées à Waterloo pour l'étude de sols naturels provenant de deux mines actives au Canada.

Il a été démontré que la pénétration d'oxygène dans les recouvrements se fait principalement par diffusion moléculaire résultant de gradients de concentration établis entre l'atmosphère et les vides dans le sol. Le taux de diffusion est contrôlé par le coefficient de diffusion qui dépend, à son tour, de la granulométrie, de l'humidité, de la porosité et d'autres propriétés physiques comme la tortuosité, ou longueur du trajet de l'écoulement. Dans l'un des deux sols à l'étude, les coefficients de diffusion d'oxygène diminuaient à mesure que la teneur en eau ou le niveau de saturation en eau augmentait. Cette tendance était compatible avec les prédictions théoriques et avec les observations d'études précédentes. Lors des essais de laboratoire rapportés dans ce document, on a constaté que l'absorption d'oxygène dans les sols naturels mis en place ayant une forte teneur en humidité pouvait être importante à cause de l'activité accrue des microorganismes contenus dans les sols humides. Il a été recommandé de tenir compte de ce facteur dans toute étude de recouvrements géologiques.

Le CTN a conçu et construit trois colonnes de laboratoire, et adapté des instruments appropriés pour assurer des méthodes fiables d'évaluation de recouvrements géologiques. L'équipement mis au point pour ce projet comprend: a) une colonne pour déterminer le coefficient de diffusion de l'oxygène; b) une colonne pour évaluer le comportement hydraulique (rétention de l'humidité et caractéristiques d'écoulement) des matériaux de recouvrement; c) une colonne d'essai pour évaluer les faibles taux de pénétration d'oxygène prévus dans les recouvrements géologiques saturés.

Des profils de potentiel hydraulique expérimentaux et théoriques observés dans un système à deux couches (till sur sable) ont indiqué que la couche de sable se drainait jusqu'à une saturation résiduelle, sans qu'il y de drainage mesurable - donc sans qu'il y ait de perte d'humidité - dans la couche de till. Les résultats observés dans la colonne d'essai, qui se sont prolongés sur 100 jours au moins, ont révélé des caractéristiques d'humidité semblables. Ces résultats suggèrent qu'en l'absence de facteurs externes tels que la pénétration de racines et la fissuration due au gel, on peut s'attendre à un rendement semblable sur le terrain. Sur la plupart des sites miniers canadiens, une période de 100 jours devrait fort probablement être la durée maximale sans recharge hydraulique du recouvrement par infiltration.

Selon une estimation de la concentration d'oxygène au bas de la colonne d'essai, l'accumulation annuelle d'oxygène ne devrait pas dépasser 600 ppm. En termes de flux, ceci représente 6,5 x 10^{-3} moles/m^2/an d'oxygène, et un flux maximum de 0,338 g/m^2/an d'acide sulfurique (H_2SO_4). En comparaison, selon des essais lysimétriques (non reliés à ce projet) effectués en laboratoire au CTN, le flux d'acide maximum estimé dans les résidus non recouverts serait typiquement de l'ordre de 1 200 g/m^2/an de H_2SO_4.

Des concepts pratiques ont été proposés pour la conception de recouvrements à haut rendement. Les propriétés critiques des matériaux requis pour la conception de ces recouvrements et la prédiction de leur rendement comprennent le coefficient de diffusion, les courbes caractéristiques de drainage, et les teneurs en eau critiques à long terme en conditions sèches. Par les résultats d'essais de laboratoire limités, il a été conclu que les cycles de gel et de dégel peuvent avoir une influence importante sur le rendement des recouvrements.

TABLE OF CONTENTS

Page

LIST OF TABLES

LIST OF FIGURES

1. INTRODUCTION

Acid mine drainage (AMD) is the single largest environmental problem facing the mining industry. Not only is effective management of AMD an important environmental question, but it can also strain the financial resources of a company. Today, many mining companies are spending large sums of money in order to meet environment compliance. Studies conducted between 1984 and 1987 to determine the extent of the AMD problem indicate that Canada has, in total, some 25,000 hectares of sulphidic tailings deposits. These deposits are acid-generating, and if not properly managed, threaten surrounding surface and groundwater resources. The projected cost of rehabilitation of these tailings deposits is more than $3 billion over the next 25 years (Filion and Ferguson, 1989). Thus, research is required to understand the problem more fully and to identify cost-effective solutions.

Existing major tailings management and decommissioning practices include: revegetation, disposal in natural water bodies, maintenance of water cover by means of engineered dams, disposal in flooded open pits, application of covers constructed from natural soils and/or synthetic membranes, blending of acid-generating and alkaline tailings, and long-term treatment of AMD. More than twenty years of research has shown that, while revegetation provides some stabilization and aesthetics to tailings surfaces and slopes, it does not improve drainage or seepage water quality. At many mine sites, AMD treatment by lime neutralization is still the most frequently used technique for control of AMD. In some cases, it is the only abatement technique. If this trend continues, the mining industry will be faced with perpetual maintenance of numerous sites, many years after cessation of operation.

With the recognition that perpetual treatment of AMD seepage may not be an acceptable long-term solution, industry and government in Canada initiated a joint program in 1983 to undertake and sponsor research on acidic drainage. This program subsequently evolved into the RATS (Reactive Acid Tailings Stabilization) program, now known as MEND (Mine Environment Neutral Drainage). The primary objective of MEND is to identify and/or develop reliable and cost-effective technologies for decommissioning of mine wastes. Recent interests in the design of saturated soil barriers for prevention and control of acid generation in sulphide tailings led to the initiation of a laboratory project on covers in 1989. The principal objective of the project was to

develop laboratory methodology and apparatus for evaluating the effectiveness of engineered soil covers for tailings. It was jointly funded by Environment Canada, Supply and Services Canada (DSS) and Canada Centre for Mineral Technology (CANMET), Energy Mines and Resources Canada, under the MEND program. Noranda Technology Centre (NTC) was the principal contractor of the project, and NTC subcontracted the fundamental and development aspects of the research to the University of Waterloo. The Waterloo team conducted research on the identification and evaluation of physical properties pertinent to cover performance, using standard soil materials such as clean silts and sands. The Waterloo work led to the design and fabrication of the demonstration column required for evaluating cover effectiveness. NTC evaluated the physical and geotechnical properties of natural soil materials from existing mine sites and later modified and tested the demonstration column using these natural soils.

2. OBJECTIVES AND SCOPE

In order to prevent or minimize contamination of the environment by acidic drainage from tailings impoundments, it would be necessary to limit the oxidation rates of constituent sulphide minerals and/or the rate of release of acid products from the tailings area. Consequently, ongoing MEND research on soil cover design is aimed at producing covers which would have two principal functions: (i) act as barriers against oxygen transport into the tailings, and (ii) reduce the amount of infiltration into the tailings mass and thereby the amount of contaminated water leaving the impoundment.

Differences between oxygen diffusivities in water and in air, discussed later in Section 2.2, imply that an effective soil barrier against oxygen diffusion would be one which is saturated with water and would maintain saturation for a considerable length of time. Therefore, the work conducted by NTC examined the diffusive properties of soil covers with respect to gaseous oxygen as well as their hydraulic properties or water-retention characteristics. The work undertaken by the University of Waterloo is presented as a separate report in Appendix A.

The original project contract required the development of a laboratory apparatus for evaluating the effectiveness of covers for reactive sulphide tailings. The evaluation was to include

measurement of oxygen fluxes and pertinent geotechnical properties of candidate natural materials. In this report, it is demonstrated that a proper evaluation of cover effectiveness would require assessment of oxygen diffusion as well as hydraulic behaviour. Consequently, the emphasis was placed on development of methodologies rather than on a single apparatus. Despite this shift in emphasis, it is noted that three different apparatus were developed in the course of the project: a) a column for determining oxygen diffusion coefficients, b) a column for investigating the hydraulic behaviour (moisture retention and drainage characteristics) and, c) another column (referred to as the demonstration column) for measuring the low oxygen fluxes expected in saturated soil covers. In addition, the diffusion coefficient of oxygen was determined at various degrees of water saturation for one of the candidate soils studied. The scope of geotechnical testing was also expanded to include the measurement of consolidation characteristics. These characteristics are required for estimates of any settlements that are likely to occur if any of the tested candidate soils are to be used for constructing covers on mine wastes. Thus the original project deliverables were exceeded in every respect.

This report presents a detailed description and analysis of the work conducted at NTC. The theory of sulphide oxidation and acid generation is briefly discussed as an introduction to the rationale for the specific testing techniques developed or adopted in the research. An overview of the utility of empirical and estimation methods relating diffusion coefficients to water contents is presented. The locations, geology and geotechnical properties of the candidate natural soils are described. A description of the laboratory methods and equipment used in determining the diffusion coefficients of the candidate natural soils is provided. The computer models used in modelling the various laboratory experiments and cover scenarios are discussed. In Section 5.2, the importance of the hydraulic characteristics of the cover is depicted, using soil index properties and drainage column experiments.

3. SULPHIDE OXIDATION AND ACID GENERATION IN TAILINGS.

3.1 Oxidation Process.

The milling of base metal sulphide ores results in the production of tailings which are generally

deposited in exposed impoundments. These sulphide tailings oxidize upon contact with air. In the presence of large quantities of infiltrating water, the oxidation leads to the formation of an acidic drainage with high concentrations of sulphate iron and heavy metals.

The principal sulphide minerals in most base metal tailings are pyrrhotite ($Fe_{1-x}S$) and pyrite (FeS_2). The reaction for pyrite oxidation has been more extensively studied and will be used here to illustrate the process of acid generation in sulphide tailings. The first important reaction in acid generation is the oxidation of pyrite into dissolved iron, sulphate and hydrogen ion :

$$FeS_2(s) + 7/2\ O_2(g) + H_2O(l) \rightarrow Fe^{2+}(aq) + 2SO_4^{2-}(aq) + 2H^+(aq) \qquad [1]$$

The dissolved Fe^{2+}, SO_4^{2-} and H^+ represent an increase in total dissolved solids and acidity of the drainage water and hence a decrease in pH, unless it is neutralized. In a low-pH environment (that is at pH 1.5 to 3.5), where oxygen is readily available, subsequent oxidation of ferrous iron, Fe^{2+}, will occur, producing ferric iron, Fe^{3+}, as follows :

$$Fe^{2+}(aq) + 1/4O_2(g) + H^+(aq) \rightarrow Fe^{3+}(aq) + 1/2\ H_2O(l) \qquad [2]$$

In the pH range 1.5 to 3.5, ferric oxidation to ferric iron, Equation [2], is sometimes catalyzed by the iron-oxidizing bacteria, Thiobacillus ferrooxidans.

The reactions in Equations [1] and [2] can be combined to yield :

$$FeS_2(s) + 15/4\ O_2(g) + 1/2\ H_2O(l) \rightarrow Fe^{3+}(aq) + 2SO_4^{2-}(aq) + H^+(aq) \qquad [3]$$

Equation [3] indicates that during pyrite oxidation both Fe^{2+} and S_2^{2-} of $FeS_2(s)$ can oxidize,

resulting in the formation of two moles of SO_4^{2-} and one mole of H^+ for each mole of FeS_2 oxidized. Ferric iron, Fe^{3+}, released as either in Equation [2] or Equation [3], will further oxidize pyrite, thereby generating additional acidity and dissolved ferrous iron, according to the following reaction :

$$14Fe^{3+}(aq) + FeS_2(s) + 8H_2O(l) \dashrightarrow 15Fe^{2+}(aq) + 2SO_4^{2-}(aq) + 16H^+(aq) \qquad [4]$$

A comparison of Equations [1] and [4] indicates that, at low pH, dissolved ferric iron will oxidize pyrite and generate more acidity than that produced from pyrite oxidation by gaseous oxygen. At slightly higher pH values (say 3.5 or greater), hydrolysis of Fe^{3+} will occur, resulting in the precipitation of ferric hydroxide and leaving little Fe^{3+} in solution while simultaneously lowering pH (through release of additional H^+) :

$$Fe^{3+}(aq) + 3H_2O(l) \dashleftarrow\dashrightarrow Fe(OH)_3(s) + 3H^+(aq) \qquad [5]$$

Thus, the oxidation and the subsequent acidification processes, once started, are self-perpetuating.

The foregoing discussions indicate that the principal ingredients for acid generation are: 1) sulphide minerals, 2) water or humid atmosphere, and 3) oxidants, principally oxygen from the atmosphere or from chemical sources and dissolved ferric iron. Thus the exclusion of oxygen and moisture will stop sulphide oxidation and acid generation. Although ferric iron is an important oxidant, examination of Equations [1] and [2] indicates that if oxygen is not available ferric iron will not form and the oxidation process will not occur. Thus, the role of the ferric iron is intermediate. Oxygen availability and transport therefore appears to be the most important consideration in any reactive tailings management strategy. Other factors found to influence pyrite oxidation are sulphide content, bacterial population density and ferric iron concentration.

3.2 Oxygen Transport by Diffusion

As already mentioned, oxygen is a key requirement for sulphide oxidation and acid generation. Most base metal tailings are usually fine-grained (mostly sandy silts or silty sands with occasional slimes). Consequently, gaseous oxygen will be transported through them principally by molecular diffusion. The role of advection or bulk gas flow, in comparison, will be minor. Diffusion occurs in response to concentration gradients usually established between the atmosphere and pore spaces within tailings deposit. The process may be assumed to be Fickian in behaviour so that the diffusive flux of oxygen into the soil or tailings mass can be described by Fick's first law as follows :

$$J = -\theta D \frac{\delta C}{\delta Z} \qquad [6]$$

where
- J = flux of oxygen $[ML^{-2}T^{-1}]$
- D = the diffusion coefficient $[L^2T^{-1}]$
- C = concentration $[ML^{-3}]$
- Z = depth in the tailings deposit [L]
- θ = gas-filled porosity $[L^3/L^3]$

The flux gives an indication of the mass of oxygen transported per unit area into the cover as well as into the uncovered tailings and is directly proportional to the potential acid flux. Thus it provides an indication of cover performance or effectiveness.

At any particular depth in the soil or tailings deposit, the rate of change in concentration can be determined from Fick's second law which can be expressed as follows :

$$\theta \frac{\delta C}{\delta t} = \theta D \frac{\delta^2 C}{\delta Z^2} - \theta KC \qquad [7]$$

Equation [7] has been written in the more general form to include a first order reaction rate constant, K, which is assumed to describe oxygen consumption by reactive sulphide tailings underneath a cover. It is obvious that, in an unreactive soil cover, K is equal to zero. The other terms in Equation [7] have the same meanings as those in Equation [6].

The diffusion process drives gaseous oxygen into the cover at a rate governed by the diffusion coefficient. For example, the diffusion coefficient of oxygen in air is 0.178 cm^2/s, compared to a value of 2×10^{-5} cm^2/s in water. Oxygen diffusion from the atmosphere into a tailings deposit can occur through air-filled cracks and pores in the tailings as well as through water-filled pores. The relative magnitude of the diffusion coefficients indicates that diffusion through the water-filled cracks and pores is less important. Generally, when oxygen transport into a tailings deposit is controlled by diffusion through air-filled pores, high (close to atmospheric values) gaseous oxygen concentrations are observed at or near the surface of the impoundment. These values decrease rapidly with depth to the zone where the oxygen is consumed by sulphide mineral oxidation.

The effective diffusion coefficient is highly dependent on the pore characteristics of the tailings. For oxygen, the effective diffusion coefficient, D_e, can be written as a function of the porosity, θ, and a tortuosity, τ, as follows :

$$D_e = D_o \theta \tau \qquad [8]$$

where D_o is the diffusion coefficient of oxygen in air. The tortuosity is introduced to account for obstruction caused by the presence of solids and liquids in the pathway. It is generally defined as the inverse of the normalized path length (Taylor, 1949; Nielsen et al., 1984; Nicholson et al.,1989).

To illustrate the calculation of flux, a 1 m thick tailings deposit with a porosity of 0.40 is assumed. If the tortuosity, τ, is taken to be 0.2, then the effective diffusion coefficient of gaseous oxygen is calculated from Equation [8] to be 1.42×10^{-2} cm^2/s. The flux of gaseous oxygen across the 1 m thick deposit then is 1.0 kilogram per square meter per month. On the other hand, if the tailings is fully saturated, the effective diffusion coefficient of oxygen in water is calculated to be 1.6×10^{-6} cm^2/s, using the parameters in Table 1 and Equation [8]. The resulting flux of oxygen through the water-saturated pores is 3.6×10^{-3} kilograms per square meter per month. Thus, the flux of oxygen as a result of aqueous diffusion is lower than by gaseous diffusion. These calculations ignore oxygen consumption by sulphide mineral oxidation. For this case, a reaction rate constant, K, can be incorporated in the expression for the flux, F, which, at steady state, is given by:

$$F = C_o(D_e\theta K)^{1/2} \qquad [9]$$

TABLE 1

PARAMETERS USED IN FLUX CALCULATIONS

Diffusion coefficient of oxygen in air	0.178 cm^2/s
Diffusion coefficient of oxygen in water	2×10^{-5} cm^2/s
Concentration of oxygen in air	2.8×10^{-4} g/cm^3
Concentration of oxygen in water	8.6×10^{-3} g/cm^3
Porosity of tailings, θ	0.4
Tortuosity, τ	0.2

Gaseous diffusion is particularly important in the reclamation of tailings impoundments because it is the mechanism by which oxygen enters such impoundments covered with engineered soils. As is shown later, the flux of oxygen into the tailings can be very small if the cover is designed

to have a high water content. Thus properly engineered soil covers may be an attractive option for reclamation of tailings areas. Even in cases where a water cover appears to be the best option because of economics, an engineered soil cover may still be required for exposed tailings beaches.

4. METHODS OF DETERMINATION OF DIFFUSION COEFFICIENTS.

4.1 Empirical and Estimation Methods.

An important aspect of accurate prediction of soil cover performance in reactive sulphide tailings is the estimation of oxygen diffusive fluxes. In order to determine fluxes, a precise knowledge of the diffusion coefficient is required. The diffusion coefficient can be measured in the laboratory. There are, however, several empirical equations which relate the effective diffusion coefficient to the gas-filled porosity and degree of saturation. Most empirical correlations express the effective diffusion coefficient as :

$$D_e = D_a^o.Q \qquad [10]$$

where D_a^o is the diffusion coefficient of oxygen in free air and Q is a relative diffusivity factor or diffusibility dependent on the structure of the gas-filled pore space and is a function of porosity, θ, moisture content θ_w, tortuosity, τ, and a constrictivity factor, δ. As already noted, the tortuosity, τ, accounts for the tortuous paths of real pores and the constrictivity for the variation of the cross-sectional area of the pore segment over its length (Collin and Rasmusson, 1988). Van Brakel and Heertjes (1974) expressed the diffusibility Q as a function of the tortuosity and constrictivity as follows :

$$Q = \frac{\theta\delta}{\tau^2} \qquad [11]$$

Values of τ and δ can generally be determined by means of mercury intrusion porosimetry. These authors concluded from laboratory experiments that δ/τ^2 lies between 0.5 and 1.0 for unidirectional binary gas diffusion in homogenous, isotropic macroporous media with a continuous pore space. Van Brakel and Heertjes (1974) also give an excellent review of the various relationships proposed for Q and the gas-filled porosity.

Other examples of empirical relations are those given by Troeh et al (1982) and Millington and Shearer (1971) for aggregated and nonaggregated soils.

The relation by Troeh et al is as follows:

$$D_e/D_o = [(S - u)] \ / \ (1 - u)]^v \qquad [12]$$

in which D_e is the effective gas diffusion coefficient, D_o the diffusion coefficient of gas in air, S the air-filled porosity (V_{gas} / V_{total}) and u and v are dimensionless parameters that are determined experimentally for a specific medium. Values of u and v calculated by Troeh et al., (1982) by comparison with data available in existing literature were in the order of 0.1 and 1.6, respectively, for soils with air-filled porosities of 0.2 to 0.7. The major difficulty with almost all empirical relations is that at high degrees of saturation they break down. The estimation method of Millington and Shearer (1971) models the porous medium as consisting of solid spheres which interpenetrate each other, and separated by spherical pores which also interpenetrate. The gas diffusivity for non-aggregated soils is given as:

$$D_e/D_o = (1 - S)^2 \ . \ [\epsilon(1 - S)]^{2x} \qquad [13]$$

where

D_e = effective diffusivity through air-filled pores in soil

D_o = diffusivity in free air

S = degree of saturation

ϵ = porosity

and x is given by

$$[\epsilon(1 - S)]^{2x} + [1 - \epsilon(1 - S)]^{x} = 1 \qquad [14]$$

Aggregated soils consists of porous particles separated by interped or inter-aggregate pores. It is conceivable that oxygen diffusion in aggregated soils will be higher than in non-aggregated soils at the same water content. In general, soil peds or aggregates have a fine pore- structure and will absorb in water, leaving the larger interped pores open for diffusion. For aggregated media, the expression for the diffusivity through gas-filled pores is more complex and incorporate both the inter-aggregate and intra-aggregate porosities and saturations. The expression is described in detail by Millington and Shearer (1971), and Collin (1987).

Millington and Shearer's equations were used in the present investigation to estimate effective diffusion coefficients from laboratory-measured moisture contents and porosities. These equations have generally been found to be fairly accurate for predicting diffusion coefficients (see examples in Collin, 1987).

4.2 Experimental Methods.

Several authors have conducted laboratory experiments to determine diffusion coefficients in soils. These experiments have generally involved measuring an experimental concentration profile at some defined time and matching it to a theoretical profile using appropriate measured material properties, such as water content and porosity. These methods have generally been used in the laboratory as well as in greenhouse experiments. Lemon and Erickson (1952) used a platinum electrode to measure oxygen diffusion rates in greenhouse soils. The method involved a correlation of the current flow produced by reduction of oxygen at the platinum surface to the corresponding flux of oxygen, by means of Fick's law. Reardon and Moddle (1985) used a conductimetric technique for the determination of diffusion coefficient for carbon dioxide in samples of uranium mill tailings. From the results of 22 separate determinations, they proposed an equation relating the diffusion coefficient to air-filled porosity. These authors have limited the applicability of the equation to porosities in the range of 0.06 to 0.46. A corresponding equation for oxygen was also derived. Papendick and Runkles (1965) used a solution of the classical transient-state diffusion equation to evaluate diffusion-porosity

relationships for several nonsoil materials (glass beads, beads, wool) and a moist soil. These authors recognized the important role of biochemical consumption of oxygen in moist soils and included an "activity" term (describing the mass of oxygen consumed per unit soil volume per unit time) in their equation. Their experimental apparatus for the soils consisted of a 7.6 cm diameter aluminum column and a 6.4 cm diameter Plexiglas column for the nonsoil materials. The columns were instrumented along their lengths with Beckman oxygen electrodes to measure gaseous oxygen concentrations in volume percent. Diffusion coefficients were then determined by matching experimental data and theoretical curves. Oxygen activity factor used in the matching exercise ranged from 1.25 to 1.60 μL/g/hr.

Lai et al., (1976) proposed a "nondisruptive" method for determining oxygen diffusion coefficient in soils using the theory of radial diffusion of a finite quantity of gas into a semi-infinite porous medium. The method involved monitoring the change in concentration of gaseous oxygen injected into a soil mass from a hypodermic needle. The method was verified in the laboratory with three Michigan soils and in the field as well. Discrepancy between field and laboratory diffusion coefficients was attributed by the authors to heterogeneity and presence of gravels and plant roots in the field soils which tended to impede gas diffusion.

5. LABORATORY DEVELOPMENT OF COVER TECHNOLOGY.

5.1 Candidate Soils.

5.1.1 Location, Geology and Mineralogy.

Soil Locations

Candidate natural soils used in the present investigation were glacial tills from the vicinities of Heath Steele and Faro mine sites located in New Brunswick and the Yukon Territory, respectively. The Heath Steele till was collected from a trench excavated in summer, 1989, at about 2 km south-east of the Heath Steele concentrator. An inter-till sand layer was also collected from the trench and included in the investigation of the capillary barrier concept, discussed later in Section 5.2.1. The Yukon till was received in a 45 gallon drum from Curragh

Resources Ltd., owners of the Faro mine. These candidate tills were selected because they were being considered by the respective mines for construction of covers on acid-generating waste rock.

Geology

The Heath Steele soils constitute part of a stratigraphic sequence in northern New Brunswick believed to consist of a unique depositional event of one till sheet. A 1987 Geological Survey of Canada drilling project confirmed this. Most of the area is covered by a till, generally less than 2 m thick, increasing to depths greater than 10 m in valleys. A detailed lithological study of the till indicates that it is mostly locally derived from the underlying bedrock. The till appears to have been moved only a few hundred metres to a couple of kilometres in the direction of ice movement. From erosional records such as till fabric and striae, and depositional features such as eskers, it has been noted that the oldest ice flow in the northern New Brunswick area was southeastward. The major, most intense, ice flow was from west to east. Rampton et al., (1984) have suggested these glacial events to be of late Wisconsian age (that is, about 10,000 to 20,000 years ago). The till at Heath Steele mines is a basal till of glaciolacustrine origin. The glaciolacustrine deposit consists of interstratified sand, silt and clay 2 to 10 m thick.

The Yukon till is part of the surficial deposits of the Anvil area. Studies on the quaternary geology of the area have been conducted by Keele (1910) and Hughes et al., (1969). The last glacial event in the Anvil area was the late Wisconsin-McConnell advance of the Selwyn lobe of the cordilleran ice sheet. The till comprised locally derived angular rock fragments and outwash transported by melt water streams formed from the deglaciation of the Selwyn lobe. The till is typically composed of well-sorted, sub-rounded grains of quartz, feldspar, and granite. The metal content of the till reflects the lithology of the underlying bedrock. The glacial overburden thickness generally exceeds 60 m and averages between 15 and 30 m in the Anvil area.

Mineralogy

Mineralogical characterization of a fine-grained soil provides useful information on its geotechnical behaviour. For example, the swelling and shrinkage potential of a soil can be

predicted from its mineralogy. This information is useful in considering soils for inclusion in cover systems.

The candidate soils were characterized for their mineralogy using X-ray diffraction and chemical techniques. X-ray methods involved random powder diffraction and oriented diffraction analysis of <2 μm fraction. The oriented diffraction work included air-dry, wet and potassium-saturated analyses of the <2 μm fraction of the tills. This work was conducted in order to define the clay mineral composition of the tills. Carbonate contents were obtained by gasometric analysis using the Chittick apparatus (Dreimanis, 1962). In addition, glycol retention and total potassium were measured to provide estimates of vermiculite and illite contents.

Mineralogical analyses of the Heath Steele tills indicated that they are composed of abundant quartz, feldspar(both orthoclase and plagioclase), illite, chlorite, and probably a trace of carbonate. A typical random X-ray powder diffractogram is presented in Fig. 1 for soil HS-C. Although a carbonate content of about 3 percent was obtained from gasometric analysis, this amount was too small to yield an X-ray peak on the diffractogram.

Figure 2 shows typical X-ray diffractograms for the natural and K^+-saturated oriented soil HS-C obtained on the < 2 μm fraction. The traces indicate the presence of abundant illite. The strong peaks at 0.72 and 1.45 nm on Fig. 2a suggest chlorite was present. However, heat treatment did not produce a strong 1.4 nm in confirmation. As shown, K^+-saturation seemed to greatly modify the traces without increasing the size of the 1.0 nm illite peak. This suggests the 1.42 and 0.72 nm peaks were produced by a smectite that actually expanded on contact with KCl solutions to produce the rather ragged traces on Fig. 2b.

The distribution of exchangeable cations in till I HS-C in milliequivalents per 100 gram of dry soil was found to be Na^+(0.28), K^+ (2.37), Ca^{++} (1.44), and Mg^{++} (2.21). This distribution gives a rather low cation exchange capacity of 6.30 meq/100 g, which probably suggests that the clay minerals are either present only in a very small amount or are inactive.

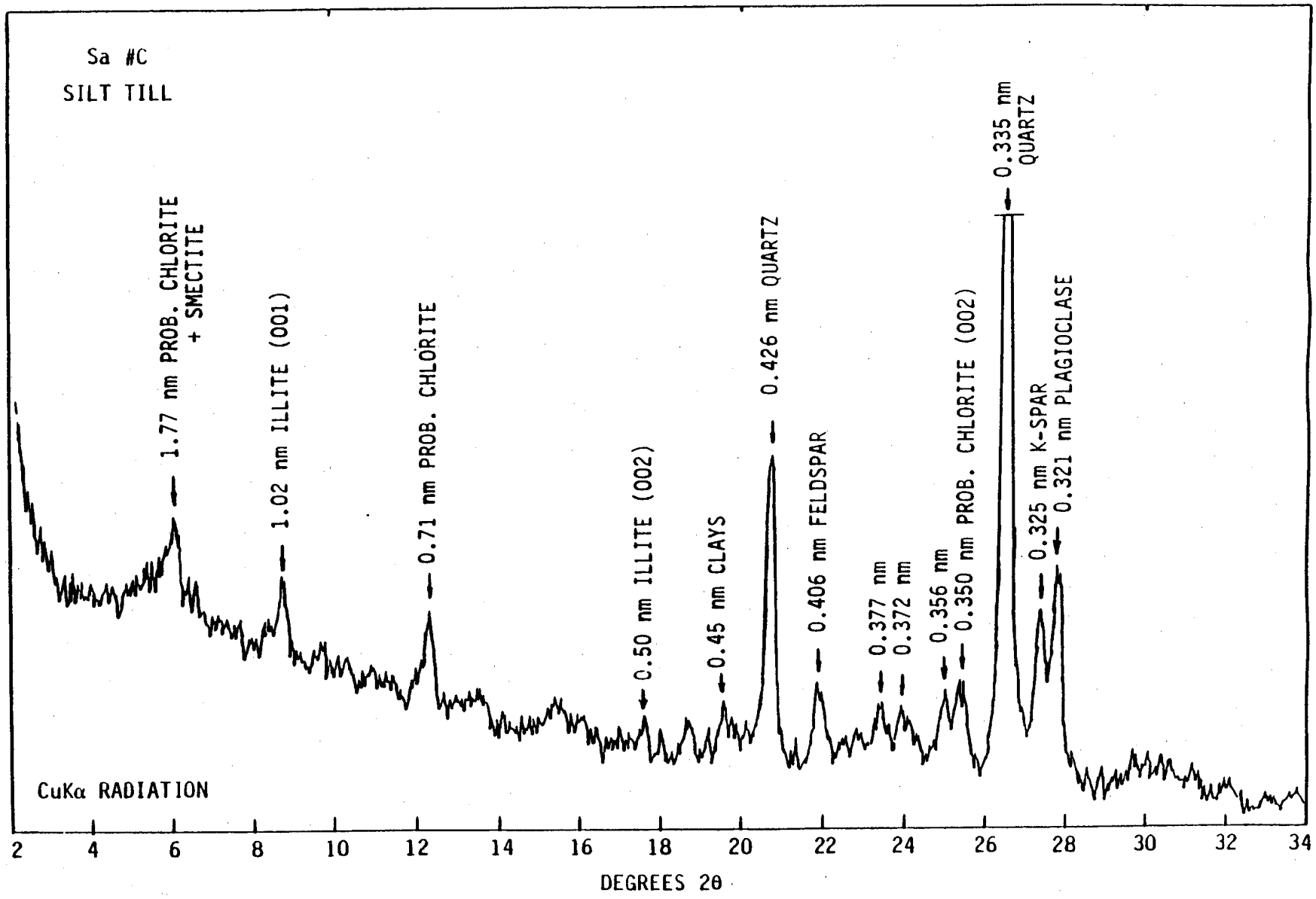

Figure 1 A random X-ray powder diffractogram of till HS-C.

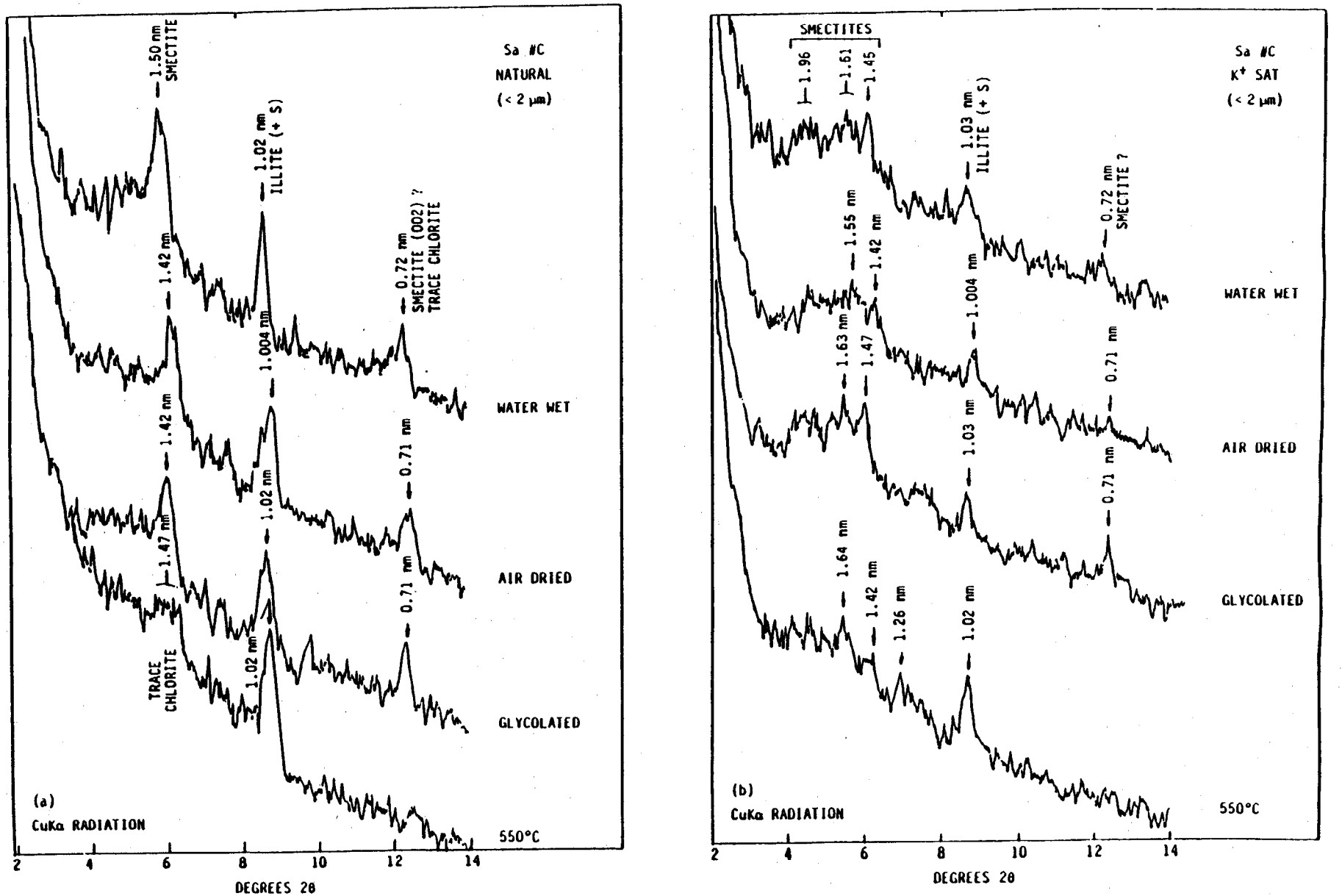

Figure 2 Oriented X-ray diffractograms of till HS-C.

The mineralogy of the Yukon till (bulk soil) is characterized by abundant quartz and plagioclase feldspar and minor amounts of clay minerals (illite and Fe-Mg trisoctahedral chlorite). Distribution of exchangeable cations on the less than 2 mm fraction (-No. 8 mesh) is as follows: Na^{+} (0.10), K^{+} (0.20), Ca^{++} (20.20) and Mg^{++} (3.60). This distribution gives a CEC value of 19.7 meq/100 g. Approximate mineralogical compositions of the <2 mm fraction are: quartz (55%), plagioclase (16%), amphibole (1%), Fe-Mg chlorite (16%) and illite (12%).

5.1.2 Geotechnical Properties.

Index Properties

The grain size distribution provides information for predicting the water retention and drainage characteristics of a soil. These characteristics control the performance of a saturated soil cover. The grain size also influences gas diffusion coefficients in soils. The Atterberg limits (liquid and plastic) describe the plasticity characteristics of a soil and reflect on mineralogy and water-holding capabilities.

The grain size curves of the Heath Steele soils, presented in Fig. 3, indicate the till is a sandy silt with about 8 percent clay fraction. The sand is medium to coarse with an appreciable fine gravel content.

The Yukon till is a silty sand with a 10.5 percent clay size fraction as shown in Fig. 3.

The moisture retention characteristics of the candidate soils are very important. Of particular significance is the capillary head. The capillary head is, by definition, the height above the water table at which air entry can occur by gravity drainage. It can be estimated from an empirical correlation between the head, h_e and D_{10}, the particle sizes at which 10 percent of the material is finer:

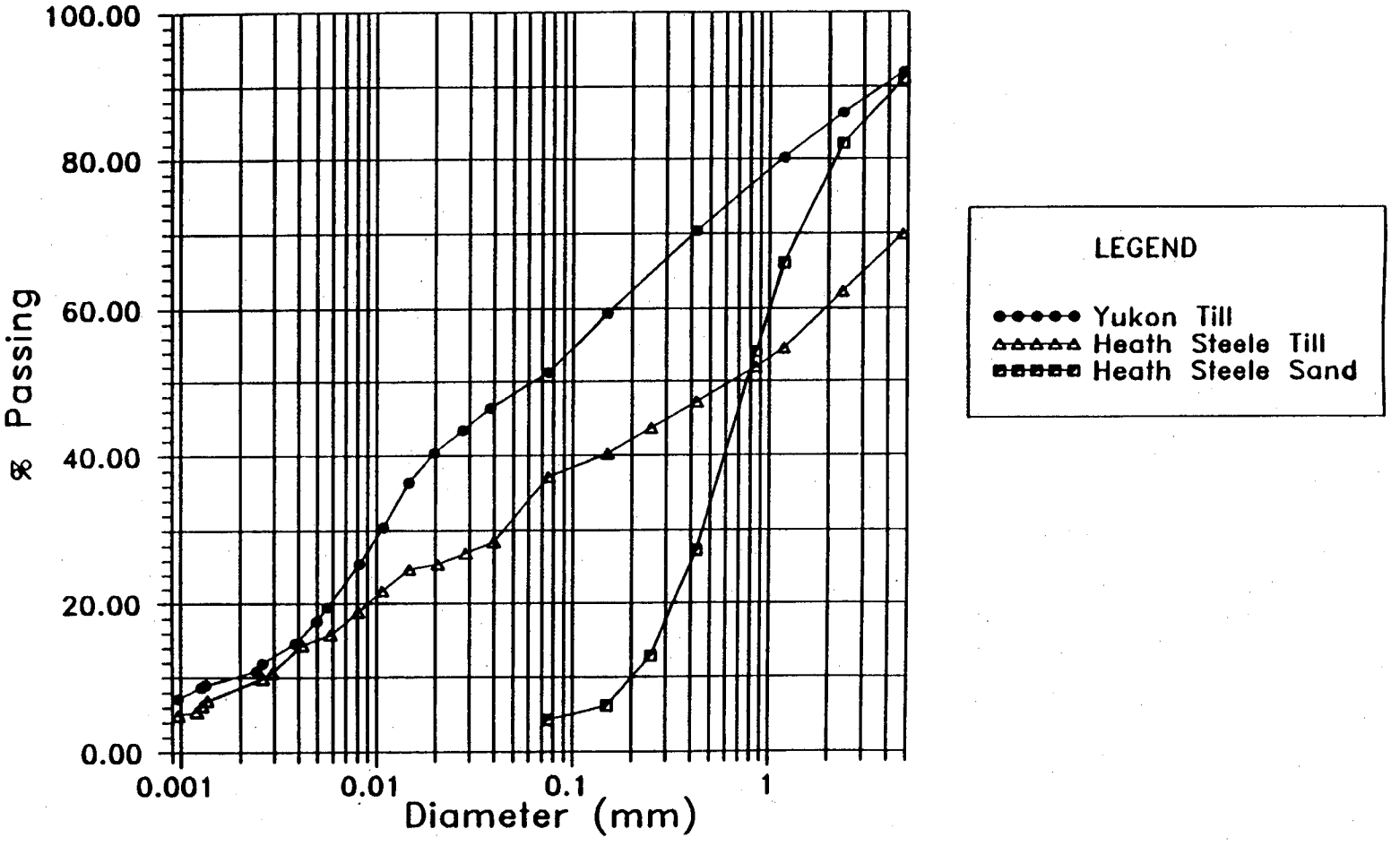

Figure 3 Grain size distribution of candidate tills.

$$= -0.01[-21.9 - 85.12(logD_{10})]$$

[15]

The above correlation is based on data from Lambe and Whitman (1969). In the above equation, h_e is in meters and D_{10} in millimeters. From the correlation, the capillary head for both the Heath Steele and Yukon tills is estimated to be about 2 m.

The index properties of the candidate soils are presented in Table 2.

TABLE 2
INDEX PROPERTIES OF CANDIDATE SOILS

SOIL	HEATH STEELE TILL	YUKON TILL
<2 μm (%)	8	10.5
<75 μm (%)	37	51
Specific Gravity	2.72	2.79
Plasticity Index	12.7	nonplastic

Compaction Parameters

In geotechnical engineering, compaction is performed in order to densify soils through removal of air from the pores. Laboratory compaction tests yield two important parameters: the optimum moisture content (OMC) and maximum dry density (MDD). These parameters are normally specified for placement of soils in field applications. Generally, the shear strength of the soil increases as water is added to the soil and compacted until the OMC is reached. The shear

strength begins to decrease beyond the OMC. The hydraulic conductivity (K) varies differently. As the soil is compacted, K decreases through a decrease in the void ratio and continues to decrease, although only slightly, beyond the OMC (Lambe, 1958; Mitchell, 1976; Daniel et al., 1985). Therefore, the hydraulic conductivity of a compacted soil attains its minimum value at a water content higher than the OMC.

Laboratory compaction tests were performed on the -No. 4 mesh fraction of the soils to provide information on the OMC and MDD. This information is needed for specifying field compaction densities if any of the soils are to be used as cover materials. The soils were all compacted using the modified Proctor energy of 42.5 kJ/m^3 with an automatic mechanical compactor. The procedure used is described in (ASTM D 1557-78).

Modified Proctor compaction curves for the two tills are presented in Fig. 4. Optimum moisture contents were 9 and 16 percent for the Heath Steele and Yukon tills, respectively. The corresponding maximum dry densities were 2.08 and 1.70 Mg/m^3. These compaction parameters are similar to those reported in the literature for inorganic clayey sandy silts and silty sands (Craig, 1974; Holtz and Kovacs, 1981). These curves can be used for the specification of field compaction and placement if these tills are to be used as covers. A high degree of moisture saturation (approximately 95 percent) can be attained by compacting at slightly wet of the optimum water content and relative compaction of about 96 percent (Yanful and St-Arnaud, 1991). In addition, a soil compacted at a moisture content above its optimum is less permeable and more resistant to cracking (less brittle) than a soil with the same density compacted at a moisture content below optimum.

Consolidation Characteristics

The compressibility of a soil can be determined from the results of a consolidation test. Consolidation is a process by which a soil is densified through removal of water from the pores. The densification occurs through a decrease in void ratio which, in most cases, results from the application of an external load. Consolidation can also occur through loss of water due to osmosis (Barbour, 1987).

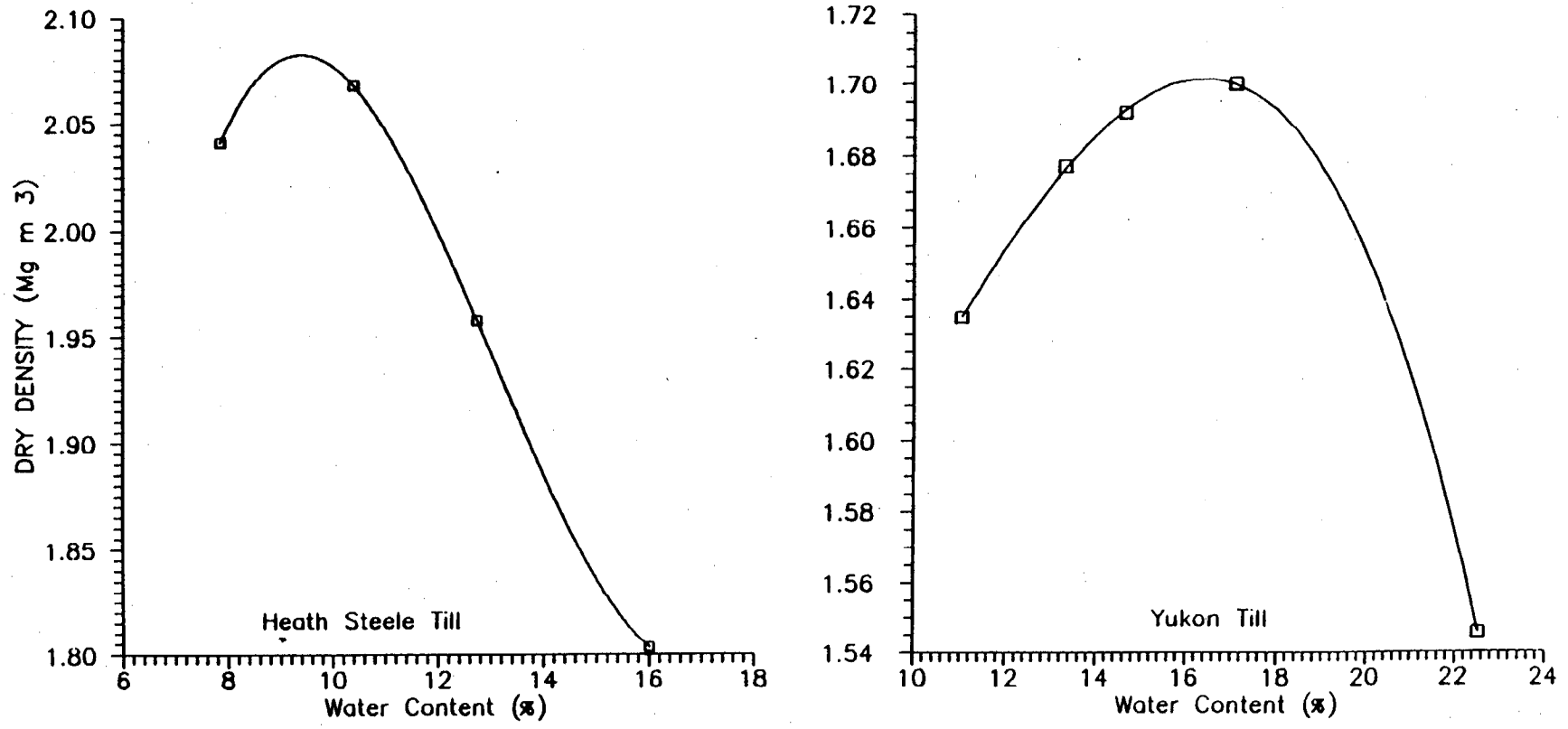

Figure 4 Modified Proctor compaction curves of candidate tills.

The most popular consolidation test used in geotechnical engineering is the oedometer test, the principles of which are based on Terzaghi's one-dimensional theory of consolidation. A consolidation test can also provide information on the rate at which water moves through a soil and therefore provides an estimate of the hydraulic conductivity. Since the compressibility of coarse-grained soils is low, oedometer tests are only carried out on fine-grained soils (clays and silts).

The oedometer tests were performed on till samples initially compacted at water contents of about 2 percent higher than the OMC. After compacting in 100 mm diameter split moulds, the soils were carefully removed and trimmed into 50 mm diameter and 20 mm thick oedometer rings. The rings containing the soils were immediately weighed to provide the mass of the test specimens and then loaded in a front-loading Control T302 consolidometer using a load increment ratio (LIR) of unity from 0 to 1600 kPa. The standard procedure used is described elsewhere (Taylor, 1948; Bowles, 1986).

The results of the oedometer tests are presented in Tables 3 and 4 for two sets of identical samples HS-C1, HS-C2, YK1 and YK2. For the Heath Steele tills, the coefficient of consolidation, c_v, at low average stresses (6 to 38 kPa) range from 3.5×10^{-3} cm^2/s to 7.9×10^{-3} cm^2/s, with the exception of the value for HS-C1 at 6 kPa. The tests were performed using a load increment ratio equal to one. Each applied load was maintained until most of the primary consolidation was deemed to have occurred.

Figure 5 shows plots of void ratio versus log pressure curves obtained from the tests. The curves indicate essentially linear virgin behaviour between 100 and 1600 kPa. An average compression index, C_c, of about 0.13 is estimated from the virgin compression. The preconsolidation pressure, σ_c', of compacted till HS-C, estimated from a Casagrande construction technique, is about 80 kPa. For the Yukon till, YK, the preconsolidation pressure of the compacted sample averages to be about 80 kPa as well.

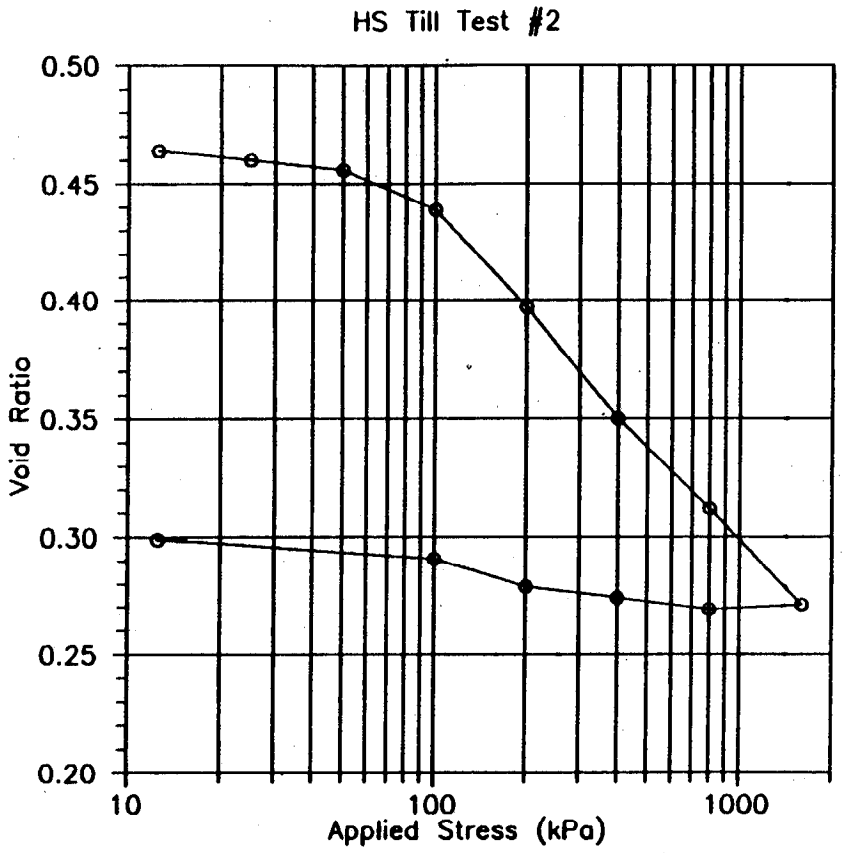

a)

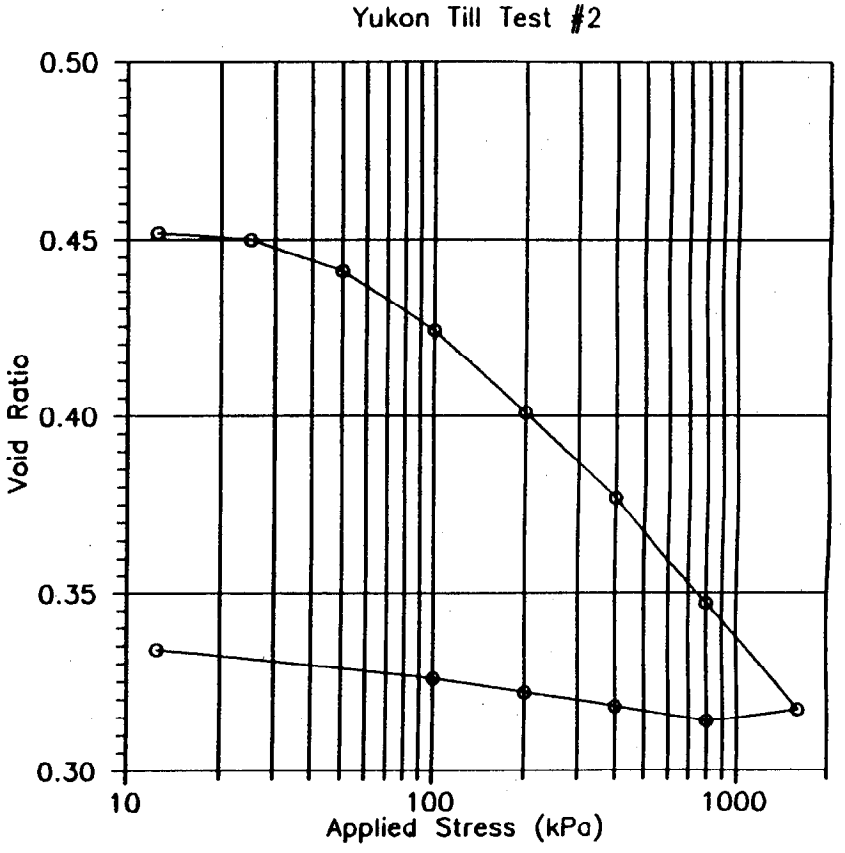

b)

Figure 5 Void ratio - log pressure curves for candidate tills.

TABLE 3

Heath Steele Consolidation Spreadsheet

CONSOLIDATION SPREADSHEET
HEATH STEELE TEST #1

APPLIED STRESS (kPa)	FINAL DIAL (mm)	DIAL CHANGE (mm)	SPEC. HEIGHT (mm)	MACH. CORR. (mm)	CORR. SPEC. HEIGHT (mm)	AVG. SPEC. HEIGHT (mm)	VOID HEIGHT (mm)	VOID RATIO	FITTING TIME (sec) t90	FITTING TIME (sec) t50	COEF. OF CONSOL. Cv (cm^2/s)	AVERAGE APPLIED STRESS (kPa)	da SQRT TIME (mm)	da LOG TIME (mm)	d90 (mm)	d100 (mm)	PRIMARY CONSOL RATIO	CHANGE VOID RATIO	COMPRES. INDEX Cc	COEF COMP Mv (kPa-1)	AVG VOID RATIO	K (cm/s)
0.00	12.000	0.000	20.000	0.000	20.000		6.3127	0.461														
12.50	11.836	0.164	19.836	0.010	19.846	19.923	6.1587	0.450	67.20		1.25E-02	6.25	11.890		11.870		0.1355	0.0113	0.0374	0.0026	0.455583	3.1926E-06
25.00	11.723	0.113	19.723	0.009	19.732	19.789	6.0447	0.442	105.10		7.90E-03	18.75	11.777		11.766		0.1278	0.0083	0.0277	0.0006	0.445793	4.9695E-07
50.00	11.545	0.178	19.545	0.022	19.567	19.650	5.8797	0.430	195.10		4.24E-03	37.50	11.620		11.587		0.2060	0.0121	0.0400	0.0005	0.435601	1.9299E-07
100.00	11.219	0.326	19.219	0.033	19.252	19.410	5.5647	0.407	90.49		8.83E-03	75.00	11.385		11.280		0.3579	0.0230	0.0765	0.0004	0.418066	3.8357E-07
200.00	10.707	0.512	18.707	0.041	18.748	19.000	5.0607	0.370	128.20		5.97E-03	150.00	10.900		10.775		0.2713	0.0368	0.1223	0.0004	0.388148	2.0755E-07
400.00	10.082	0.625	18.082	0.048	18.130	18.439	4.4427	0.325	126.02		5.72E-03	300.00	10.285		10.155		0.2311	0.0452	0.1500	0.0002	0.347161	1.2192E-07
800.00	9.537	0.545	17.537	0.046	17.583	17.857	3.8957	0.285	276.95		2.44E-03	600.00	9.750		9.590		0.3262	0.0400	0.1328	0.0001	0.304604	2.3025E-08
1600.00	8.993	0.544	16.993	0.066	17.059	17.321	3.3717	0.246	196.00		3.25E-03	1200.00	9.260		9.055		0.4187	0.0383	0.1272	0.0000	0.265480	1.4662E-08
800.00	9.035	-0.042	17.035	0.011	17.046	17.053	3.3587	0.245														
400.00	9.104	-0.069	17.104	0.025	17.129	17.088	3.4417	0.251														
200.00	9.176	-0.072	17.176	0.041	17.217	17.173	3.5297	0.258														
50.00	9.324	-0.148	17.324	0.088	17.412	17.315	3.7247	0.272														
12.50	9.461	-0.137	17.461	0.051	17.512	17.462	3.8247	0.279														

CONSOLIDATION SPREADSHEET
HEATH STEELE TEST #2

APPLIED STRESS (kPa)	FINAL DIAL (mm)	DIAL CHANGE (mm)	SPEC. HEIGHT (mm)	MACH. CORR. (mm)	CORR. SPEC. HEIGHT (mm)	AVG. SPEC. HEIGHT (mm)	VOID HEIGHT (mm)	VOID RATIO	FITTING TIME (sec) t90	FITTING TIME (sec) t50	COEF. OF CONSOL. Cv (cm^2/s)	AVERAGE APPLIED STRESS (kPa)	da SQRT TIME (mm)	da LOG TIME (mm)	d90 (mm)	d100 (mm)	PRIMARY CONSOL. RATIO	CHANGE VOID RATIO	COMPRES. INDEX Cc	COEF COMP Mv (kPa-1)	AVG VOID RATIO	K (cm/s)
0.00	11.000	0.000	20.000	0.000	20.000		6.370	0.467														
12.50	10.943	0.057	19.943	0.011	19.954	19.977	6.324	0.464	256.80		3.29E-03	6.25	10.971		10.956		0.2924	0.0034	0.0112	0.0008	0.4657	2.5196E-07
25.00	10.895	0.048	19.895	0.009	19.904	19.929	6.274	0.460	129.80		6.49E-03	18.75	10.927		10.920		0.1620	0.0037	0.0122	0.0003	0.4621	1.7974E-07
50.00	10.826	0.069	19.826	0.016	19.842	19.873	6.212	0.456	240.00		3.49E-03	37.50	10.868		10.854		0.2254	0.0045	0.0151	0.0002	0.4580	5.9933E-08
100.00	10.580	0.246	19.580	0.027	19.607	19.725	5.977	0.439	178.40		4.62E-03	75.00	10.785		10.638		0.6640	0.0172	0.0573	0.0003	0.4471	1.5053E-07
200.00	10.000	0.580	19.000	0.041	19.041	19.324	5.411	0.397	126.00		6.28E-03	150.00	10.200		10.084		0.2222	0.0415	0.1380	0.0004	0.4178	2.4634E-07
400.00	9.339	0.661	18.339	0.057	18.396	18.719	4.766	0.350	233.10		3.19E-03	300.00	9.556		9.417		0.2337	0.0473	0.1572	0.0002	0.3733	7.1191E-08
800.00	8.799	0.540	17.799	0.077	17.876	18.136	4.246	0.312	264.40		2.64E-03	600.00	9.100		8.870		0.4733	0.0382	0.1267	0.0001	0.3306	2.3750E-08
1600.00	8.240	0.559	17.240	0.086	17.326	17.601	3.696	0.271	290.10		2.26E-03	1200.00	8.865		8.335		1.0535	0.0404	0.1341	0.0000	0.2913	1.0782E-08
800.00	8.276	-0.036	17.276	0.020	17.296	17.311	3.666	0.269														
400.00	8.327	-0.051	17.327	0.031	17.358	17.327	3.728	0.274														
200.00	8.394	-0.067	17.394	0.037	17.431	17.395	3.801	0.279														
50.00	8.538	-0.144	17.538	0.058	17.596	17.514	3.966	0.291														
12.50	8.676	-0.138	17.676	0.028	17.704	17.650	4.074	0.299														

TABLE 4

Yukon Consolidation Spreadsheet

CONSOLIDATION SPREADSHEET
YUKON TEST #1

APPLIED STRESS (kPa)	FINAL DIAL (mm)	DIAL CHANGE (mm)	SPEC. HEIGHT (mm)	MACH. CORR. (mm)	CORR. SPEC. HEIGHT (mm)	AVG. SPEC. HEIGHT (mm)	VOID HEIGHT (mm)	VOID RATIO	FITTING TIME (sec) t90	t50	COEF. OF CONSOL. Cv (cm^2/s)	AVERAGE APPLIED STRESS (kPa)	ds SQRT TIME (mm)	LOG TIME	d90 (mm)	d100 (mm)	PRIMARY CONSOL. RATIO	CHANGE VOID RATIO	COMPRES. INDEX Cc	COEF COMP Mv (kPa-1)	AVG VOID RATIO	K (cm/s)
0.00	12.000	0.000	20.000	0.000	20.000		6.3127	0.461														
12.50	11.840	0.160	19.840	0.033	19.873	19.937	6.1857	0.452	135.00		6.24E-03	6.25	11.924		11.882	11.877	0.2917	0.0093	0.0308	0.0021	0.4566	1.3124E-06
25.00	11.800	0.040	19.800	0.027	19.827	19.850	6.1397	0.449	1058.40		7.89E-04	18.75	11.835		11.825	11.823	0.2778	0.0034	0.0112	0.0003	0.4502	2.0035E-08
50.00	11.616	0.184	19.616	0.037	19.653	19.740	5.9657	0.436	375.00		2.20E-03	37.50	11.780		11.699	11.690	0.4891	0.0127	0.0422	0.0005	0.4422	1.0577E-07
100.00	11.385	0.231	19.385	0.040	19.425	19.539	5.7377	0.419	95.75		8.63E-03	75.00	11.540		11.487	11.481	0.2549	0.0167	0.0553	0.0003	0.4275	2.7157E-07
200.00	11.087	0.298	19.087	0.046	19.133	19.279	5.4457	0.398	135.00		5.84E-03	150.00	11.315		11.239	11.231	0.2834	0.0213	0.0709	0.0002	0.4085	1.1757E-07
400.00	10.794	0.293	18.794	0.044	18.838	18.986	5.1507	0.376	60.00		1.27E-02	300.00	10.988		10.940	10.935	0.1820	0.0216	0.0716	0.0001	0.3871	1.2959E-07
800.00	10.439	0.355	18.439	0.044	18.483	18.660	4.7957	0.350	117.60		6.28E-03	600.00	10.665		10.605	10.598	0.1878	0.0259	0.0862	0.0001	0.3633	3.8431E-08
1600.00	10.048	0.391	18.048	0.050	18.098	18.291	4.4107	0.322	95.75		7.57E-03	1200.00	10.320		10.250	10.242	0.1989	0.0281	0.0934	0.0000	0.3363	2.5115E-08
800.00	10.079	-0.031	18.079	0.000	18.079	18.088	4.3917	0.321														
400.00	10.133	-0.054	18.133	-0.024	18.109	18.094	4.4217	0.323														
200.00	10.186	-0.053	18.186	-0.025	18.161	18.135	4.4737	0.327														
50.00	10.239	-0.053	18.239	-0.022	18.217	18.189	4.5297	0.331														
12.50	10.378	-0.139	18.378	-0.056	18.322	18.269	4.6347	0.339														

CONSOLIDATION SPREADSHEET
YUKON TEST #2

APPLIED STRESS (kPa)	FINAL DIAL (mm)	DIAL CHANGE (mm)	SPEC. HEIGHT (mm)	MACH. CORR. (mm)	CORR. SPEC. HEIGHT (mm)	AVG. SPEC. HEIGHT (mm)	VOID HEIGHT (mm)	VOID RATIO	FITTING TIME (sec) t90	t50	COEF. OF CONSOL. Cv (cm^2/s)	AVERAGE APPLIED STRESS (kPa)	ds SQRT TIME (mm)	LOG TIME	d90 (mm)	d100 (mm)	PRIMARY CONSOL RATIO	CHANGE VOID RATIO	COMP INDEX Cc	COEF COMP Mv (kPa-1)	AVG VOID RATIO	K (cm/s)
0.00	12.000	0.000	20.000	0.000	20.000		6.3127	0.461														
12.50	11.872	0.128	19.872	0.008	19.880	19.940	6.1927	0.452	54.15		1.56E-02	6.25	11.948		11.923	11.920	0.2170	0.0088	0.0291	0.0020	0.4568	3.0926E-06
25.00	11.817	0.055	19.817	0.024	19.841	19.861	6.1537	0.450	453.75		1.84E-03	18.75	11.859		11.846	11.844	0.2626	0.0028	0.0095	0.0002	0.4510	3.9664E-08
50.00	11.671	0.146	19.671	0.055	19.726	19.784	6.0387	0.441	240.00		3.46E-03	37.50	11.776		11.742	11.738	0.2588	0.0084	0.0279	0.0003	0.4454	1.0971E-07
100.00	11.412	0.259	19.412	0.083	19.495	19.611	5.8077	0.424	117.60		6.93E-03	75.00	11.581		11.530	11.524	0.2188	0.0169	0.0561	0.0003	0.4328	2.2095E-07
200.00	11.097	0.315	19.097	0.074	19.171	19.333	5.4837	0.401	93.75		8.45E-03	150.00	11.320		11.261	11.255	0.2081	0.0237	0.0786	0.0002	0.4125	1.8891E-07
400.00	10.783	0.314	18.783	0.068	18.851	19.011	5.1637	0.377	57.00		1.34E-02	300.00	10.996		10.945	10.939	0.1805	0.0234	0.0777	0.0001	0.3890	1.4836E-07
800.00	10.372	0.411	18.372	0.065	18.437	18.644	4.7497	0.347	114.15		6.46E-03	600.00	10.664		10.578	10.570	0.2325	0.0302	0.1005	0.0001	0.3621	4.6091E-08
1600.00	9.970	0.402	17.970	0.060	18.030	18.234	4.3427	0.317	199.83		3.53E-03	1200.00	10.228		10.173	10.166	0.1520	0.0297	0.0988	0.0000	0.3321	1.2378E-08
800.00	10.005	-0.035	18.005	-0.022	17.983	18.007	4.2957	0.314														
400.00	10.059	-0.054	18.059	-0.025	18.034	18.009	4.3467	0.318														
200.00	10.112	-0.053	18.112	-0.024	18.088	18.061	4.4007	0.322														
50.00	10.168	-0.056	18.168	-0.021	18.147	18.118	4.4597	0.326														
12.50	10.325	-0.157	18.325	-0.063	18.262	18.205	4.5747	0.334														

The variations of the compression index and the coefficient of consolidation with applied stress are shown in Fig. 6 for till HS-C. The compression index, C_c, increases with stress until the preconsolidation pressure is substantially exceeded and then begins to fall slightly. This suggests that the soil may have undergone some structural or fabric changes at these high stresses. The wavy shape of the c_v versus applied stress curve may be attributed to quasi-preconsolidation. Each applied load was maintained until there was no change in dial gauge readings or sample compression. The elapsed time for this phenomenon to occur was different for each applied load. Therefore, it was possible that some secondary compression occurred, resulting in a quasi-preconsolidation pressure that is larger than the maximum previous consolidation pressure (Leonards and Ramiah, 1959; Das, 1983).

Hydraulic Conductivity

The hydraulic conductivity, K, of a soil is a measure of the rate at which a liquid flows through it. Unlike the intrinsic permeability, k, it takes into account the density and viscosity of the flowing liquid. The two are related as follows:

$$K = \frac{\rho g}{\mu} k \qquad [16]$$

where ρ is the density, μ the viscosity of the liquid and g the acceleration due to gravity. Hydraulic conductivity, K, is usually reported in cm/s or m/s. From Equation [12], using appropriate dimensions for p, g, and μ, the corresponding units for the permeability will be cm^2 or m^2.

Hydraulic conductivity can vary by several orders of magnitude, depending on how it is measured. Several factors, such as gradient, confinement, type of permeating liquid, length of testing time, size of sample and type of equipment influence the magnitude of K. The different roles played by these factors are discussed in detail by several authors (Mitchell and Younger,1967; Olson and Daniel,1981; Fernandez and Quigley, 1985; Yanful et al., 1990b).

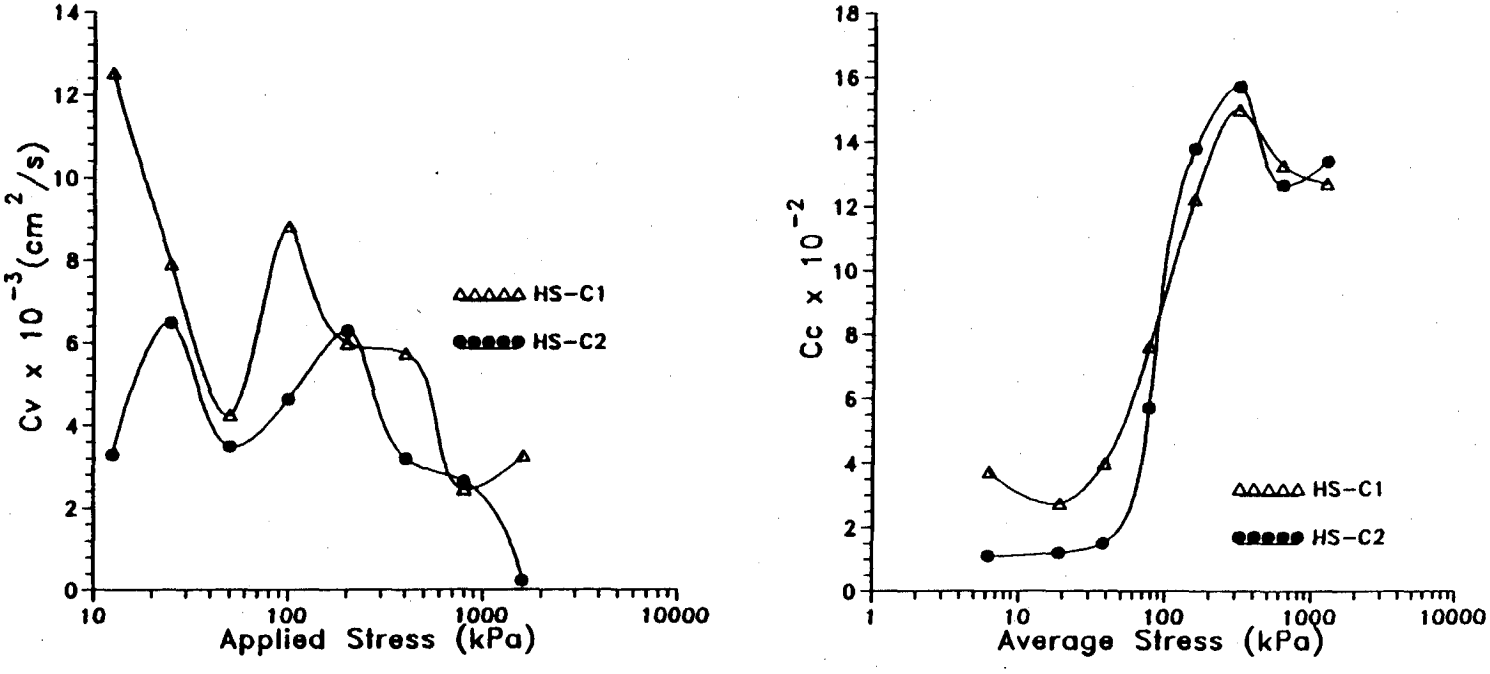

Figure 6 Variations of compression index, C_c, and coefficient of consolidation, c_v, with applied stress (Heath Steele till HS-C).

Laboratory measurements of hydraulic conductivity generally yield values which are 2 to 3 orders of magnitude lower than those measured in the field. This discrepancy has been attributed to the presence of micro and macro fissures or cracks in field soils. These cracks are normally absent in laboratory specimens. Consequently, researchers and practising engineers consider field measured values of K more reliable than laboratory values. However, field tests tend to be more complicated and therefore costly. In fine-grained soils, in particular, field tests can take a long time because of the slow rate at which liquids such as water move through these soils. In addition, the use of certain liquids (for example, organics) in field tests may not be desirable because of the serious environmental implications. Well-controlled laboratory tests offer the best methods for obtaining K values associated with such liquids.

A laboratory K test was performed to measure the rate at which water will infiltrate a cover constructed from any of the tills. Although the K obtained from the test is only a rough estimate of what a cover constructed from the compacted till will attain in the field, it nevertheless provides important data for calculating potential water fluxes through the cover. For the K tests, till samples were compacted at two percent wet of the optimum water content in a 102 mm diameter split mould using the modified Proctor energy. The specimen was carefully trimmed on the top and sealed with rubber membranes and then assembled in a triaxial cell for testing.

A Geostore Brainard Kilman triaxial panel and cell were used in the test. The sample was initially consolidated to some predetermined stress level and then permeated with sequential increases in hydraulic gradients. The Heath Steele till was permeated with deionized distilled water to 0.58 and 1.25 pore volumes at gradients of 18 and 60, respectively. For a change, the Yukon till was permeated with dilute calcium sulphate solution (0.01 N $CaSO_4.2H_2O$) to 2.43 and 1.61 pore volumes at gradients of 15 and 30, respectively. Dilute calcium sulphate is a standard ASTM reference permeant). A pore volume is the total volume of pore spaces in the sample and is calculated as a product of q/V_T, the ratio of the flow rate (q) to the total sample volume (V_T), and the time of flow, t. Testing a sample to at least one pore volume ensures that all the resident pore water has been displaced by the permeating liquid. This makes it possible to assess the effects, if any, of the permeating liquid on the hydraulic conductivity of the soil.

The results of the K tests obtained on the Heath Steele till are summarized in Figs. 7 and 8, and then also in Table 5. The K value for HS-C decreased only slightly from 2.0 to 1.7 x 10^{-8} cm/s when the hydraulic gradient was increased from 18 to 60. This decrease was due to a decrease in void ratio resulting from increased effective stress at the outflow end of the sample (Table 5). An average effective stress of 24 kPa was applied to the sample at the lower hydraulic gradient of 18. This stress would correspond to that due to the weight of about 80 cm thick capillary barrier and vegetated top soil placed above the compacted till. Thus, a hydraulic conductivity of 2.0 x 10^{-8} cm/s can be used for preliminary flux calculations for till HS-C.

As shown in Fig. 8 for till HS-C, the outflow hydraulic conductivity at a gradient of 60 decreased initially and then increased slowly until the inflow and outflow conductivities equalized at steady state. Fluctuations in laboratory temperature recorded during the tests, presented in Fig. 9, do not show the same trends as the variations in K. Therefore temperature changes alone cannot account for the observed variations in K. The decrease in sample volume observed in the tests is plotted in Fig. 10. The plot shows a substantial decrease in sample volume after 1000 minutes which appears to correspond to the decrease in outflow K.

The K data for the Yukon till is presented in Figs. 11 and 12 for the two hydraulic gradients, 15 and 30, used in the tests. The data are also summarized in Table 6. Inflow and outflow hydraulic conductivities equilibrated at 2 x 10^{-7} cm/s for both gradients of 15 and 30 at 2.6 and 1.7 pore volumes, respectively. The Yukon till had a sand content of 35 percent compared to 26 percent for the Heath Steele till. The higher amount of sand-size material in the Yukon till may have been responsible for its higher hydraulic conductivity. The pore size distributions of the two tills were probably also different.

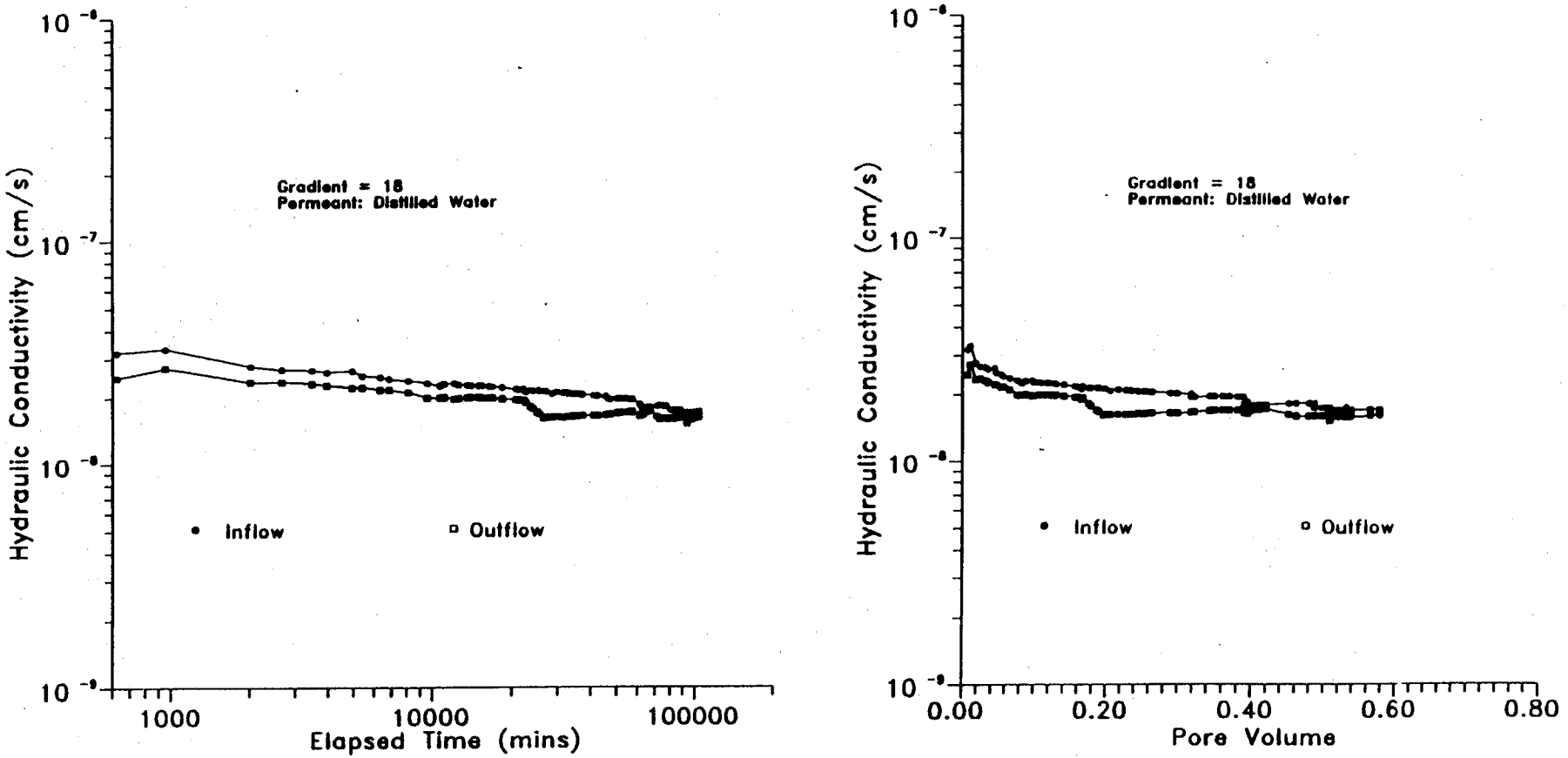

Figure 7 The hydraulic conductivity of compacted till HS-C permeated with distilled water at a hydraulic gradient of 18.

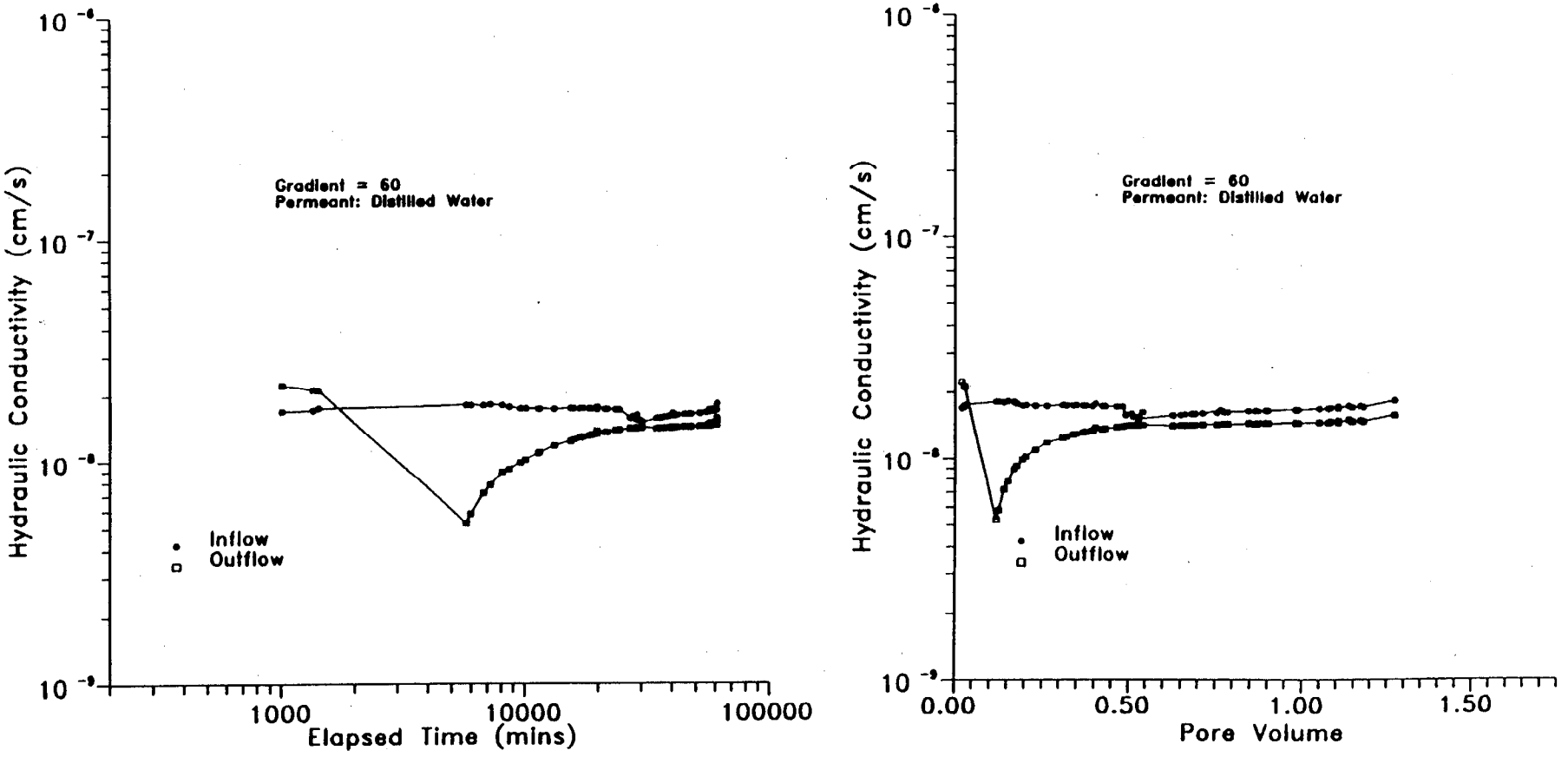

Figure 8 The hydraulic conductivity of compacted till HS-C permeated with distilled water at a hydraulic gradient of 60.

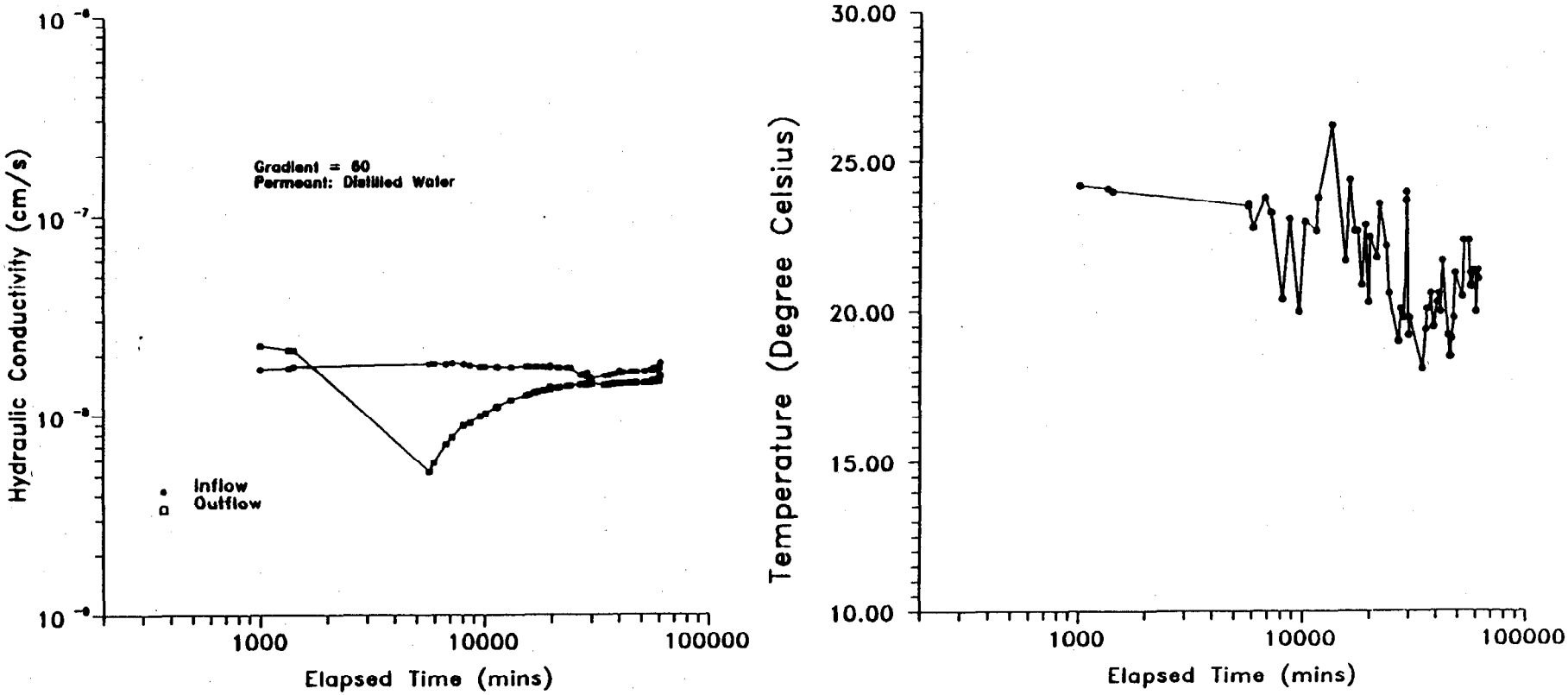

Figure 9 Hydraulic conductivity and laboratory temperature versus time.

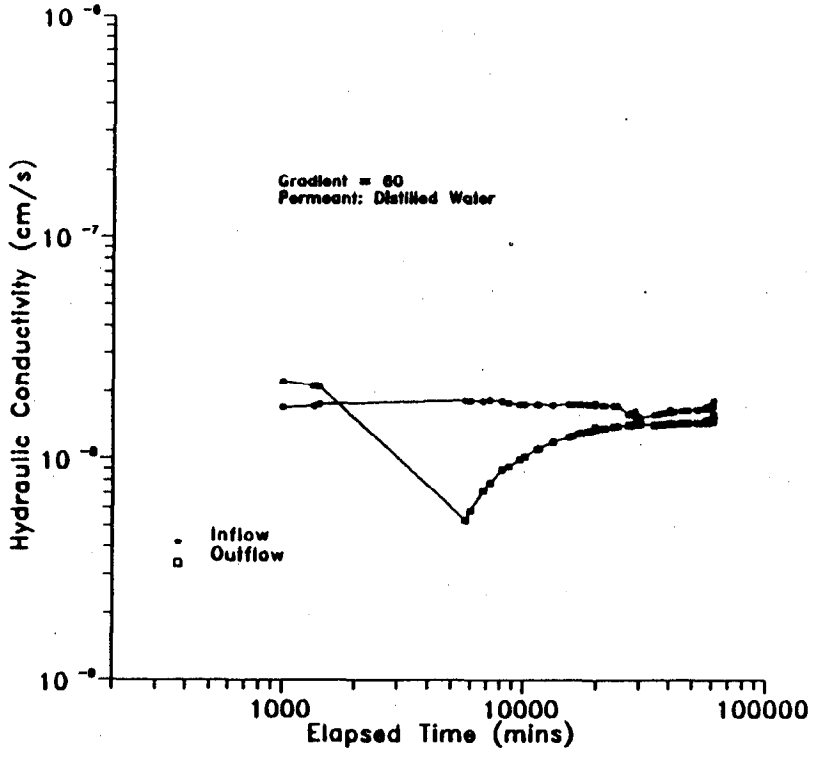

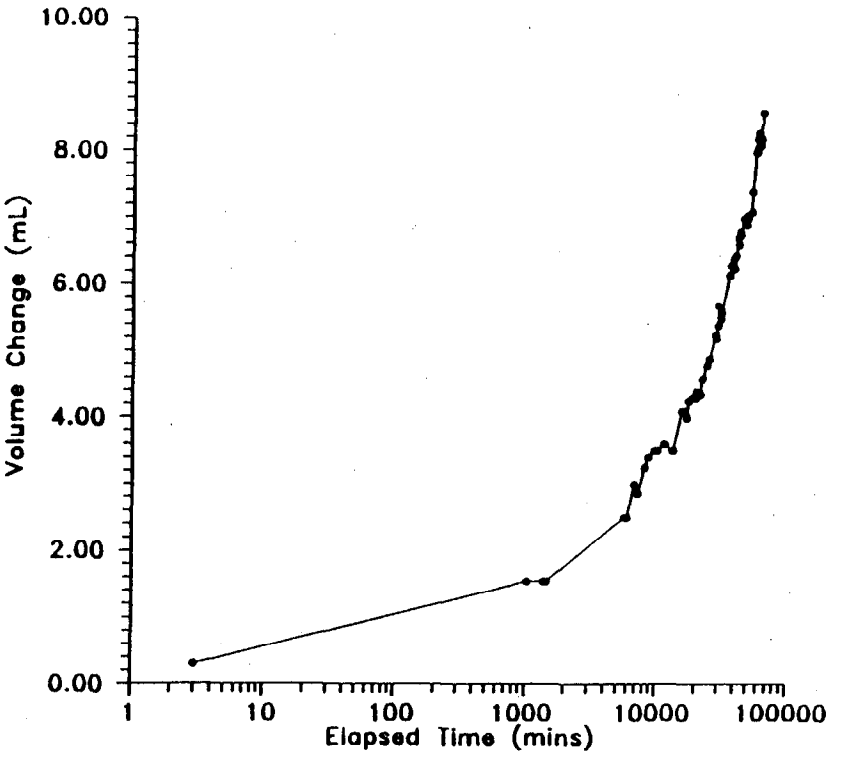

Figure 10 Hydraulic conductivity and change in sample volume versus time.

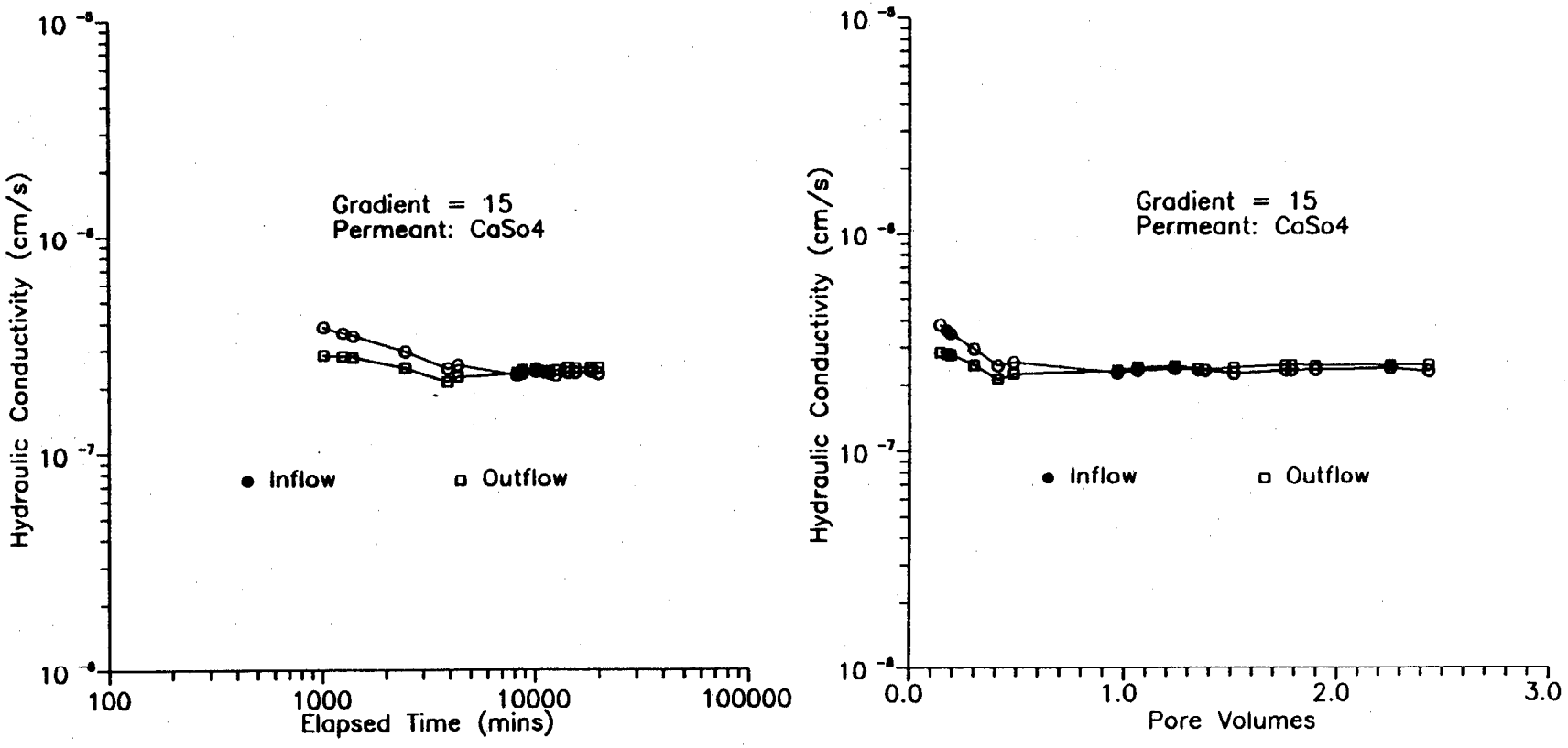

Figure 11 The hydraulic conductivity of compacted Yukon till permeated with 0.01N calcium sulphate solution.

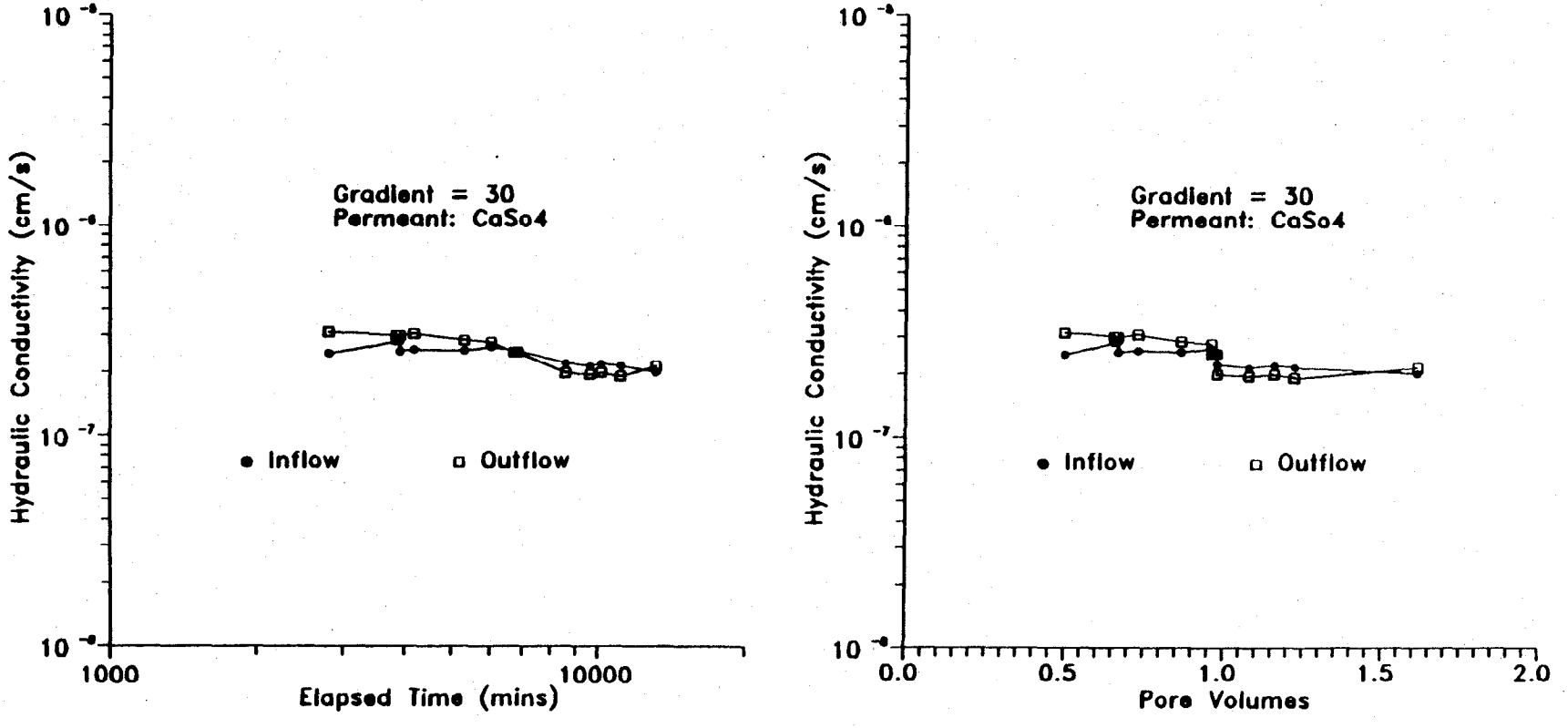

Figure 12 The hydraulic conductivity of compacted Yukon till permeated with 0.01N calcium sulphate solution.

TABLE 5

Heath Steele Waste Rock Covers

DATE STARTED: APRIL 29, 1990

CELL No: 08980

AREA:	81.07 cm^2
WEIGHT OF SAMPLE:	2085.99 gms
HEIGHT OF SAMPLE:	0.1160 M
DIA OF SAMPLE:	0.1017 M
VOLUME OF SAMPLE:	0.0009 M^3

PERMEANT USED: DISTILLED WATER

WATER CONTENT	BEFORE
TARE NO.	A
TARE WEIGHT	192.90
TARE+SOIL WET (gms)	311.87
TARE+SOIL DRY (gms)	298.05
WEIGHT WATER (gms)	13.82
WEIGHT SOIL DRY (gms)	105.15
WATER CONTENT (%)	13.14

INFL PRESS (psi) (kPa)	OUTFL PRESS (psi) (kPa)	CELL PRESS (psi) (kPa)	HYDR GRAD
38.00	35.00	40.00	18.18
261.82	241.15	275.60	

TIMER (mins)	ELPSD TIME (mins)	CELL VOL CHG (mls)	INFL RATE (cm^3/s)	OUTFL RATE (cm^3/s)	INFLO PERM (cm/s)	OUTFL PERM (cm/s)	TEMP CORR'D INFLO PERM (cm/s)	TEMP CORR'D OUTFL PERM (cm/s)	PORE VOL (INF)	PORE VOL (OUT)
75557	0	0.00	0.0000E+00	0.0000E+00	0.0000E+00	0.0000E+00	0.0000E+00	0.0000E+00	0.000	0.000
76178	621	1.45	4.7005E-05	3.6261E-05	3.1892E-08	2.4603E-08	3.0218E-08	2.3311E-08	0.007	0.005
76511	954	2.05	4.8901E-05	4.0169E-05	3.3179E-08	2.7254E-08	2.9174E-08	2.3964E-08	0.011	0.009
77578	2021	2.95	4.0821E-05	3.4636E-05	2.7697E-08	2.3500E-08	2.5819E-08	2.1907E-08	0.019	0.016
78219	2662	3.10	3.9444E-05	3.4748E-05	2.6762E-08	2.3576E-08	2.4113E-08	2.1242E-08	0.025	0.022
79024	3467	3.90	3.9179E-05	3.4131E-05	2.6582E-08	2.3158E-08	2.5070E-08	2.1840E-08	0.032	0.028
79505	3948	3.95	3.8416E-05	3.3561E-05	2.6065E-08	2.2771E-08	2.3860E-08	2.0844E-08	0.036	0.031
80492	4935	4.65	3.8838E-05	3.2759E-05	2.6351E-08	2.2227E-08	2.4230E-08	2.0437E-08	0.045	0.038
80954	5397	4.35	3.6903E-05	3.2734E-05	2.5038E-08	2.2210E-08	2.3128E-08	2.0515E-08	0.047	0.041
81890	6333	5.10	3.6449E-05	3.1975E-05	2.4730E-08	2.1695E-08	2.3432E-08	2.0556E-08	0.054	0.047
82396	6839	4.75	3.5704E-05	3.1927E-05	2.4225E-08	2.1662E-08	2.1730E-08	1.9431E-08	0.057	0.051
83644	8087	5.60	3.5037E-05	3.1121E-05	2.3772E-08	2.1115E-08	2.3280E-08	2.0678E-08	0.066	0.059
85111	9554	4.75	3.4192E-05	2.7214E-05	2.3199E-08	1.8464E-08	2.2719E-08	1.8082E-08	0.077	0.061
86230	10673	6.95	3.3262E-05	2.9358E-05	2.2567E-08	1.9919E-08	2.1534E-08	1.9006E-08	0.083	0.073
86513	10956	6.60	3.3924E-05	2.9436E-05	2.3017E-08	1.9972E-08	2.1707E-08	1.8835E-08	0.087	0.076
86526	10969	6.65	3.3883E-05	2.9401E-05	2.2989E-08	1.9948E-08	2.1532E-08	1.8683E-08	0.087	0.076
86680	11123	6.40	3.3864E-05	2.9594E-05	2.2976E-08	2.0079E-08	2.1924E-08	1.9159E-08	0.088	0.077
87656	12099	7.60	3.4163E-05	2.9066E-05	2.3179E-08	1.9721E-08	2.4948E-08	2.1226E-08	0.097	0.082
88133	12576	7.00	3.3596E-05	2.9289E-05	2.2794E-08	1.9872E-08	2.0724E-08	1.8067E-08	0.099	0.086
89094	13537	7.20	3.3488E-05	2.9364E-05	2.2721E-08	1.9923E-08	2.1038E-08	1.8447E-08	0.106	0.093
89569	14012	7.05	3.3305E-05	2.9499E-05	2.2597E-08	2.0014E-08	2.0873E-08	1.8487E-08	0.109	0.097
90503	14946	7.35	3.3286E-05	2.9495E-05	2.2584E-08	2.0012E-08	2.1600E-08	1.9139E-08	0.117	0.103
90972	15415	7.65	3.3247E-05	2.9463E-05	2.2557E-08	1.9990E-08	2.1405E-08	1.8968E-08	0.120	0.106
91943	16386	8.15	3.3158E-05	2.9344E-05	2.2497E-08	1.9910E-08	2.1721E-08	1.9223E-08	0.127	0.113
92436	16879	7.90	3.2980E-05	2.9376E-05	2.2377E-08	1.9931E-08	2.0345E-08	1.8122E-08	0.130	0.116
93928	18371	8.35	3.2706E-05	2.9123E-05	2.2191E-08	1.9759E-08	2.0176E-08	1.7965E-08	0.141	0.125
96277	20720	9.00	3.2135E-05	2.8797E-05	2.1803E-08	1.9538E-08	2.0562E-08	1.8426E-08	0.156	0.140
96798	21241	8.80	3.1936E-05	2.8758E-05	2.1668E-08	1.9512E-08	2.0340E-08	1.8316E-08	0.159	0.143
97692	22135	9.05	3.2151E-05	2.8575E-05	2.1814E-08	1.9387E-08	2.1674E-08	1.9263E-08	0.167	0.148
97767	22210	9.25	3.1780E-05	2.8553E-05	2.1562E-08	1.9373E-08	2.1017E-08	1.8883E-08	0.165	0.149
98162	22605	9.25	3.1225E-05	2.8054E-05	2.1185E-08	1.9034E-08	1.9980E-08	1.7951E-08	0.165	0.149
99145	23588	9.45	3.1655E-05	2.6885E-05	2.1477E-08	1.8241E-08	2.1443E-08	1.8212E-08	0.175	0.149
99610	24053	9.65	3.1632E-05	2.6365E-05	2.1461E-08	1.7888E-08	2.0672E-08	1.7230E-08	0.178	0.149
100600	25043	9.75	3.1612E-05	2.5323E-05	2.1448E-08	1.7181E-08	2.1678E-08	1.7365E-08	0.186	0.149
101064	25507	9.95	3.1625E-05	2.4862E-05	2.1457E-08	1.6869E-08	2.1423E-08	1.6842E-08	0.189	0.149
102030	26473	10.25	3.1479E-05	2.3955E-05	2.1358E-08	1.6253E-08	2.1272E-08	1.6188E-08	0.195	0.149
102473	26916	10.45	3.1425E-05	2.4056E-05	2.1321E-08	1.6322E-08	2.0249E-08	1.5501E-08	0.198	0.152
103974	28417	10.45	3.0733E-05	2.4106E-05	2.0852E-08	1.6355E-08	2.0719E-08	1.6251E-08	0.205	0.161
105209	29652	11.00	3.1111E-05	2.4141E-05	2.1108E-08	1.6379E-08	2.0973E-08	1.6275E-08	0.216	0.168
106872	31315	11.30	3.0869E-05	2.4057E-05	2.0944E-08	1.6322E-08	2.1430E-08	1.6701E-08	0.227	0.177
106872	31315	11.30	3.0869E-05	2.4057E-05	2.0944E-08	1.6322E-08	2.1378E-08	1.6660E-08	0.227	0.177
107777	32220	11.55	3.0804E-05	2.4131E-05	2.0900E-08	1.6372E-08	2.0900E-08	1.6372E-08	0.233	0.182
108173	32616	11.05	3.0685E-05	2.4247E-05	2.0820E-08	1.6451E-08	1.9681E-08	1.5551E-08	0.235	0.185
109222	33665	11.65	3.0670E-05	2.4234E-05	2.0809E-08	1.6442E-08	2.0428E-08	1.6141E-08	0.242	0.191
109683	34126	11.25	3.0549E-05	2.4322E-05	2.0727E-08	1.6502E-08	1.9456E-08	1.5490E-08	0.244	0.195
110667	35110	11.95	3.0547E-05	2.4305E-05	2.0726E-08	1.6490E-08	2.0056E-08	1.5958E-08	0.251	0.200
111148	35591	11.55	3.0462E-05	2.4398E-05	2.0668E-08	1.6553E-08	1.8334E-08	1.4684E-08	0.254	0.204
112094	36537	11.85	3.0403E-05	2.4427E-05	2.0628E-08	1.6574E-08	1.9500E-08	1.5667E-08	0.260	0.209

TABLE 5 (Continued)

Heath Steele Waste Rock Covers

112562	37005	11.65	3.0334E-05	2.4479E-05	2.0581E-08	1.6608E-08	1.8881E-08	1.5237E-08	0.263	0.212
116434	40877	12.55	3.0029E-05	2.4545E-05	2.0374E-08	1.6654E-08	1.8691E-08	1.5278E-08	0.288	0.235
117865	42308	12.65	2.9919E-05	2.4483E-05	2.0300E-08	1.6611E-08	2.0267E-08	1.6585E-08	0.297	0.243
117876	42319	12.80	2.9912E-05	2.4477E-05	2.0295E-08	1.6607E-08	2.0262E-08	1.6581E-08	0.297	0.243
120860	45303	13.65	2.9744E-05	2.4667E-05	2.0181E-08	1.6736E-08	2.0149E-08	1.6710E-08	0.316	0.262
122214	46657	13.90	2.8881E-05	2.4719E-05	1.9595E-08	1.6772E-08	1.8610E-08	1.5928E-08	0.316	0.270
122707	47150	13.75	2.8915E-05	2.4779E-05	1.9618E-08	1.6812E-08	1.7174E-08	1.4717E-08	0.320	0.274
125567	50010	14.85	2.9061E-05	2.5128E-05	1.9717E-08	1.7049E-08	1.7111E-08	1.4795E-08	0.341	0.295
126542	50985	14.85	2.9077E-05	2.5220E-05	1.9728E-08	1.7111E-08	1.7977E-08	1.5592E-08	0.347	0.301
128091	52534	15.50	2.9108E-05	2.5253E-05	1.9749E-08	1.7134E-08	1.9023E-08	1.6504E-08	0.358	0.311
128455	52898	15.40	2.9081E-05	2.5285E-05	1.9731E-08	1.7155E-08	1.8101E-08	1.5738E-08	0.361	0.313
129482	53925	15.55	2.9037E-05	2.5297E-05	1.9701E-08	1.7164E-08	1.9110E-08	1.6649E-08	0.367	0.320
131252	55695	16.05	2.8922E-05	2.5331E-05	1.9623E-08	1.7187E-08	1.7800E-08	1.5590E-08	0.378	0.331
132338	56781	16.05	2.8868E-05	2.5317E-05	1.9587E-08	1.7177E-08	1.8386E-08	1.6124E-08	0.384	0.337
132659	57102	16.05	2.8852E-05	2.5174E-05	1.9576E-08	1.7080E-08	1.7520E-08	1.5287E-08	0.386	0.337
132669	57112	16.05	2.8847E-05	2.5596E-05	1.9572E-08	1.7366E-08	1.7400E-08	1.5439E-08	0.386	0.343
136589	61032	16.75	2.7417E-05	2.4351E-05	1.8602E-08	1.6522E-08	1.8439E-08	1.6376E-08	0.392	0.348
137092	61535	16.95	2.6936E-05	2.4547E-05	1.8276E-08	1.6655E-08	1.6653E-08	1.5176E-08	0.388	0.354
138043	62486	17.25	2.6553E-05	2.4563E-05	1.8016E-08	1.6665E-08	1.7814E-08	1.6479E-08	0.389	0.360
138510	62953	17.00	2.6329E-05	2.4767E-05	1.7864E-08	1.6804E-08	1.6278E-08	1.5312E-08	0.388	0.365
138537	62980	17.00	2.6318E-05	2.5143E-05	1.7856E-08	1.7059E-08	1.6381E-08	1.5650E-08	0.388	0.371
139481	63924	17.20	2.6399E-05	2.5152E-05	1.7911E-08	1.7065E-08	1.7753E-08	1.6915E-08	0.396	0.377
139968	64411	17.50	2.6458E-05	2.5340E-05	1.7951E-08	1.7193E-08	1.6174E-08	1.5491E-08	0.399	0.383
140936	65379	17.50	2.6550E-05	2.5337E-05	1.8014E-08	1.7191E-08	1.6268E-08	1.5525E-08	0.407	0.388
141409	65852	17.70	2.6587E-05	2.5524E-05	1.8039E-08	1.7318E-08	1.5723E-08	1.5094E-08	0.410	0.394
142363	66806	18.00	2.6657E-05	2.5524E-05	1.8086E-08	1.7318E-08	1.5867E-08	1.5193E-08	0.417	0.400
146670	71113	19.70	2.6917E-05	2.4114E-05	1.8263E-08	1.6361E-08	1.5308E-08	1.3714E-08	0.449	0.402
148121	72564	20.00	2.6999E-05	2.3632E-05	1.8318E-08	1.6034E-08	1.7117E-08	1.4982E-08	0.459	0.402
151006	75449	20.80	2.6983E-05	2.3656E-05	1.8307E-08	1.6050E-08	1.7800E-08	1.5606E-08	0.477	0.418
151487	75930	21.10	2.6966E-05	2.3660E-05	1.8296E-08	1.6053E-08	1.7055E-08	1.4965E-08	0.480	0.421
152451	76894	21.30	2.6931E-05	2.3645E-05	1.8272E-08	1.6043E-08	1.7476E-08	1.5343E-08	0.485	0.426
156006	80449	21.75	2.5741E-05	2.3667E-05	1.7465E-08	1.6058E-08	1.6703E-08	1.5358E-08	0.485	0.446
157480	81923	22.10	2.5756E-05	2.3689E-05	1.7475E-08	1.6073E-08	1.6253E-08	1.4949E-08	0.495	0.455
158203	82646	22.15	2.5752E-05	2.3714E-05	1.7473E-08	1.6089E-08	1.6326E-08	1.5034E-08	0.499	0.459
158655	83098	22.10	2.5753E-05	2.3725E-05	1.7473E-08	1.6097E-08	1.6103E-08	1.4835E-08	0.502	0.462
159644	84087	22.10	2.5747E-05	2.3743E-05	1.7469E-08	1.6109E-08	1.6099E-08	1.4846E-08	0.507	0.468
159646	84089	22.10	2.5747E-05	2.3743E-05	1.7469E-08	1.6109E-08	1.6099E-08	1.4846E-08	0.507	0.468
163035	87478	22.50	2.5854E-05	2.1756E-05	1.7542E-08	1.4761E-08	1.6738E-08	1.4085E-08	0.530	0.446
168281	92724	23.20	2.3349E-05	2.0525E-05	1.5842E-08	1.3926E-08	1.4567E-08	1.2805E-08	0.507	0.446
168515	92958	23.30	2.3290E-05	2.2831E-05	1.5802E-08	1.5491E-08	1.4631E-08	1.4343E-08	0.507	0.497
168759	93202	23.30	2.3319E-05	2.2870E-05	1.5821E-08	1.5517E-08	1.4749E-08	1.4465E-08	0.509	0.500
170200	94643	23.70	2.3404E-05	2.2909E-05	1.5879E-08	1.5543E-08	1.4906E-08	1.4591E-08	0.519	0.508
171440	95883	23.80	2.3449E-05	2.2978E-05	1.5910E-08	1.5590E-08	1.4934E-08	1.4634E-08	0.527	0.516
172630	97073	23.65	2.3496E-05	2.3039E-05	1.5942E-08	1.5632E-08	1.5247E-08	1.4950E-08	0.535	0.524
173145	97588	23.80	2.3329E-05	2.3054E-05	1.5829E-08	1.5642E-08	1.4262E-08	1.4093E-08	0.534	0.527
173149	97592	23.80	2.3499E-05	2.3053E-05	1.5944E-08	1.5641E-08	1.4365E-08	1.4093E-08	0.538	0.527
176932	101375	24.10	2.3732E-05	2.3295E-05	1.6102E-08	1.5805E-08	1.4672E-08	1.4402E-08	0.564	0.553
178785	103228	24.80	2.3847E-05	2.3345E-05	1.6180E-08	1.5839E-08	1.4945E-08	1.4631E-08	0.577	0.565
178785	103228	24.80	2.3847E-05	2.3345E-05	1.6180E-08	1.5839E-08	1.4945E-08	1.4631E-08	0.577	0.565

TABLE 5 (Continued)

Heath Steele Waste Rock Covers

HEATH STEELE WASTE ROCK COVERS 2
DATE STARTED: JULY 19, 1990

CELL No: 08980

AREA:	81.07
WEIGHT OF SAMPLE:	2085.99
HEIGHT OF SAMPLE:	0.1160
DIAMETER OF SAMPLE:	0.1017
VOLUME OF SAMPLE:	0.0009

PERMEANT USED: DISTILLED WATER

WATER CONTENT	BEFORE
TARE NO.	A
TARE WEIGHT	192.90
TARE+SOIL WET (gms)	311.87
TARE+SOIL DRY (gms)	298.05
WEIGHT WATER (gms)	13.82
WEIGHT SOIL DRY (gms)	105.15
WATER CONTENT (%)	13.14

INF PRESS (psi) (kPa)	OFL PRESS (psi) (kPa)	CELL PRESS (psi) (kPa)	HYDR GRAD
38.00	28.00	40.00	60.60
5.52	4.06	5.81	

TIMER (mins)	ELPSD TIME (mins)	CELL VOL CHG (mls)	INFL RATE (cm^3/s)	OUTFL RATE (cm^3/s)	INFLO PERM (10^-7) (cm/s)	OUTFL PERM (10^-7) (cm/s)	TEMP CORR'D INFLO PERM (10^-7) (cm/s)	TEMP CORR'D OUTFL PERM (10^-7) (cm/s)	PORE VOL (INF)	PORE VOL (OUT)
191833	0	0.00	0.0000E+00	0.0000E+00	0.0000E+00	0.0000E+00	0.0000E+00	0.0000E+00	0.000	0.000
191836	3	0.30	5.5556E-04	1.9444E-03	1.1308E-07	3.9578E-07	1.0398E-07	3.6392E-07	0.000	0.001
192837	1004	1.55	8.3831E-05	1.0956E-04	1.7063E-08	2.2301E-08	1.5478E-08	2.0229E-08	0.020	0.026
193180	1347	1.55	8.4756E-05	1.0455E-04	1.7252E-08	2.1281E-08	1.5685E-08	1.9349E-08	0.027	0.033
193180	1347	1.55	8.4756E-05	1.0455E-04	1.7252E-08	2.1281E-08	1.5685E-08	1.9349E-08	0.027	0.033
193250	1417	1.55	8.6450E-05	1.0409E-04	1.7597E-08	2.1188E-08	1.6034E-08	1.9306E-08	0.029	0.035
193250	1417	1.55	8.6450E-05	1.0409E-04	1.7597E-08	2.1188E-08	1.6034E-08	1.9306E-08	0.029	0.035
197538	5705	2.50	8.9249E-05	2.5855E-05	1.8166E-08	5.2626E-09	1.6742E-08	4.8500E-09	0.119	0.035
197538	5705	2.50	8.9249E-05	2.5855E-05	1.8166E-08	5.2626E-09	1.6704E-08	4.8389E-09	0.119	0.035
197809	5976	2.50	8.9246E-05	2.8587E-05	1.8166E-08	5.8187E-09	1.7014E-08	5.4498E-09	0.125	0.040
198564	6731	3.00	8.9016E-05	3.5285E-05	1.8119E-08	7.1820E-09	1.6586E-08	6.5744E-09	0.140	0.056
199017	7184	2.85	8.9899E-05	3.8280E-05	1.8298E-08	7.7916E-09	1.6943E-08	7.2143E-09	0.151	0.064
199901	8068	3.25	8.9138E-05	4.3794E-05	1.8144E-08	8.9141E-09	1.7984E-08	8.8357E-09	0.169	0.083
200453	8620	3.40	8.7490E-05	4.5244E-05	1.7808E-08	9.2091E-09	1.7652E-08	9.1281E-09	0.177	0.091
201412	9579	3.50	8.5865E-05	4.8544E-05	1.7477E-08	9.8808E-09	1.7324E-08	9.7939E-09	0.193	0.109
201895	10062	3.50	8.6050E-05	5.0023E-05	1.7515E-08	1.0182E-08	1.7361E-08	1.0092E-08	0.203	0.118
201895	10062	3.50	8.6050E-05	5.0023E-05	1.7515E-08	1.0182E-08	1.7361E-08	1.0092E-08	0.203	0.118
203150	11317	3.60	8.5785E-05	5.3754E-05	1.7461E-08	1.0941E-08	1.7308E-08	1.0845E-08	0.228	0.143
203319	11486	3.60	8.5684E-05	5.4196E-05	1.7441E-08	1.1031E-08	1.7287E-08	1.0934E-08	0.231	0.146
204973	13140	3.50	8.5363E-05	5.8219E-05	1.7375E-08	1.1850E-08	1.5078E-08	1.0284E-08	0.263	0.179
207177	15344	4.10	8.6027E-05	6.1153E-05	1.7510E-08	1.2447E-08	1.6822E-08	1.1958E-08	0.309	0.220
207177	15344	4.10	8.6027E-05	6.1153E-05	1.7510E-08	1.2447E-08	1.6826E-08	1.1961E-08	0.309	0.220
207692	15859	4.10	8.5913E-05	6.2057E-05	1.7487E-08	1.2631E-08	1.5793E-08	1.1407E-08	0.319	0.231
208616	16783	4.00	8.5900E-05	6.3457E-05	1.7485E-08	1.2916E-08	1.6413E-08	1.2125E-08	0.338	0.250
209092	17259	4.25	8.5945E-05	6.3928E-05	1.7494E-08	1.3012E-08	1.6421E-08	1.2215E-08	0.348	0.259
210082	18249	4.30	8.5758E-05	6.4935E-05	1.7456E-08	1.3217E-08	1.7094E-08	1.2944E-08	0.367	0.278
210536	18703	4.30	8.5548E-05	6.5319E-05	1.7413E-08	1.3295E-08	1.6271E-08	1.2423E-08	0.375	0.286
211481	19648	4.30	8.5250E-05	6.5995E-05	1.7352E-08	1.3433E-08	1.7241E-08	1.3347E-08	0.393	0.304
211481	19648	4.40	8.7201E-05	6.7861E-05	1.7749E-08	1.3813E-08	1.6739E-08	1.3027E-08	0.402	0.313
211481	19648	4.30	8.7201E-05	6.7861E-05	1.7749E-08	1.3813E-08	1.6739E-08	1.3027E-08	0.402	0.313
212960	21127	4.35	8.5041E-05	6.6936E-05	1.7310E-08	1.3625E-08	1.6593E-08	1.3061E-08	0.421	0.331
213442	21609	4.60	8.4995E-05	6.7372E-05	1.7300E-08	1.3713E-08	1.5908E-08	1.2609E-08	0.430	0.341
213442	21609	4.60	8.4995E-05	6.7372E-05	1.7300E-08	1.3713E-08	1.5908E-08	1.2609E-08	0.430	0.341
215164	23331	4.80	8.4758E-05	6.8328E-05	1.7252E-08	1.3908E-08	1.6384E-08	1.3208E-08	0.463	0.374
216045	24212	4.90	8.4566E-05	6.8664E-05	1.7213E-08	1.3976E-08	1.6347E-08	1.3273E-08	0.480	0.390
218710	26877	0.30	7.4196E-05	6.1732E-05	1.5102E-08	1.2565E-08	1.4343E-08	1.1933E-08	0.467	0.389
219228	27395	0.65	7.4162E-05	6.1964E-05	1.5095E-08	1.2612E-08	1.4336E-08	1.1978E-08	0.476	0.398
220183	28350	0.60	7.4192E-05	6.2404E-05	1.5101E-08	1.2702E-08	1.4342E-08	1.2063E-08	0.493	0.415
220479	28646	0.80	7.4181E-05	6.2574E-05	1.5099E-08	1.2737E-08	1.4340E-08	1.2096E-08	0.498	0.420
220481	28648	1.10	7.4176E-05	6.2570E-05	1.5098E-08	1.2736E-08	1.4339E-08	1.2095E-08	0.498	0.420

TABLE 5 (Continued)

Heath Steele Waste Rock Covers

220487	28654	1.10	7.4161E-05	6.2615E-05	1.5095E-08	1.2745E-08	1.4336E-08	1.2104E-08	0.498	0.421
221540	29707	1.10	7.4730E-05	6.3144E-05	1.5211E-08	1.2853E-08	1.4446E-08	1.2206E-08	0.520	0.440
221891	30058	0.90	7.3857E-05	6.3239E-05	1.5033E-08	1.2872E-08	1.4277E-08	1.2225E-08	0.520	0.446
221891	30058	1.00	7.2610E-05	5.9746E-05	1.4779E-08	1.2161E-08	1.4036E-08	1.1549E-08	0.512	0.421
226291	34458	1.00	6.5756E-05	5.3568E-05	1.3384E-08	1.0903E-08	1.2711E-08	1.0355E-08	0.531	0.433
227344	35511	1.55	6.4346E-05	5.2425E-05	1.3097E-08	1.0671E-08	1.2439E-08	1.0134E-08	0.536	0.436
227862	36029	1.70	6.3699E-05	5.1880E-05	1.2966E-08	1.0560E-08	1.2313E-08	1.0029E-08	0.538	0.438
228843	37010	1.70	6.2483E-05	5.0910E-05	1.2718E-08	1.0362E-08	1.2078E-08	9.8412E-09	0.542	0.442
229273	37440	1.80	6.1988E-05	5.0503E-05	1.2617E-08	1.0280E-08	1.1983E-08	9.7626E-09	0.544	0.443

TABLE 6

Yukon Soil

YUKON SOIL: FILE NAME: PYUK6CAS
DATE STARTED: JAN 15TH, 1991

CELL No: SOIL PERMEAMETER CELL

AREA (cm^2):	80.12
WEIGHT OF SAMPLE (gms):	1071.82
HEIGHT OF SAMPLE (m):	0.0650
DIAMETER OF SAMPLE (m):	0.1010
VOLUME OF SAMPLE (m^3):	0.0005

PERMEANT USED: CALCIUM SULPHATE

WATER CONTENT	INITIAL
TARE NO.	34
TARE WEIGHT	53.24
TARE+SOIL WET (gms)	89.07
TARE+SOIL DRY (gms)	83.79
WEIGHT WATER (gms)	5.28
WEIGHT SOIL DRY (gms)	30.55
WATER CONTENT (%)	17.28

INF PRESS (psi) (kPa)	OFL PRESS (psi) (kPa)	CELL PRESS (psi) (kPa)	HYDR GRAD
30.40 209.5	29.00 199.8	40.00 275.6	15.14

TIMER (mins)	ELPSD TIME (mins)	INFL RATE (cm^3/s)	OUTFL RATE (cm^3/s)	INFLO PERM (cm/s)	OUTFL PERM (cm/s)	TEMP CORR'D INFLO PERM (cm/s)	TEMP CORR'D OUTFL PERM (cm/s)	PORE VOL (INF)	PORE VOL (OUT)	CELL CHG (mls)
451146.0	0.0	0.0000E+00	0.0000E+00	0.0000E+00	0.0000E+00			0.000	0.000	0.00
452156.0	1010.0	4.6279E-04	3.4406E-04	3.8145E-07	2.8359E-07	3.6829E-07	2.7381E-07	0.192	0.143	1.80
452391.0	1245.0	4.3484E-04	3.3936E-04	3.5842E-07	2.7972E-07	3.3723E-07	2.6318E-07	0.222	0.174	2.10
452539.0	1393.0	4.2050E-04	3.3561E-04	3.4659E-07	2.7662E-07	3.2462E-07	2.5909E-07	0.241	0.192	2.25
453595.0	2449.0	3.5635E-04	3.0046E-04	2.9372E-07	2.4766E-07	2.7701E-07	2.3357E-07	0.359	0.302	3.00
455025.0	3879.0	2.9896E-04	2.5909E-04	2.4642E-07	2.1355E-07	2.3080E-07	2.0001E-07	0.477	0.413	3.65
455025.0	3879.0	2.9896E-04	2.5909E-04	2.4642E-07	2.1355E-07	2.3080E-07	2.0001E-07	0.477	0.413	3.65
455473.0	4327.0	3.0903E-04	2.7444E-04	2.5472E-07	2.2621E-07	2.3475E-07	2.0847E-07	0.550	0.488	3.85
459373.0	8227.0	2.7760E-04	2.8534E-04	2.2881E-07	2.3519E-07	2.2515E-07	2.3143E-07	0.939	0.965	4.50
459373.0	8227.0	2.7760E-04	2.8534E-04	2.2881E-07	2.3519E-07	2.2515E-07	2.3143E-07	0.939	0.965	4.50
459889.0	8743.0	2.8490E-04	2.9462E-04	2.3483E-07	2.4284E-07	2.2147E-07	2.2902E-07	1.024	1.059	4.40
461201.0	10055.0	2.9068E-04	2.9786E-04	2.3960E-07	2.4551E-07	2.2441E-07	2.2995E-07	1.201	1.231	4.60
462318.0	11172.0	2.8704E-04	2.9135E-04	2.3659E-07	2.4015E-07	2.3338E-07	2.3688E-07	1.318	1.338	4.75
462743.0	11597.0	2.8367E-04	2.8757E-04	2.3381E-07	2.3703E-07	2.3119E-07	2.3438E-07	1.352	1.371	4.75
463651.0	12505.0	2.7561E-04	2.9308E-04	2.2717E-07	2.4157E-07	2.1933E-07	2.3324E-07	1.416	1.506	4.90
463651.0	12505.0	2.7561E-04	2.9308E-04	2.2717E-07	2.4157E-07	2.1933E-07	2.3324E-07	1.416	1.506	4.90
465297.0	14151.0	2.8536E-04	3.0086E-04	2.3521E-07	2.4799E-07	2.0910E-07	2.2046E-07	1.660	1.750	5.20
465542.0	14396.0	2.8544E-04	3.0072E-04	2.3527E-07	2.4787E-07	2.1683E-07	2.2844E-07	1.689	1.779	5.10
465542.0	14396.0	2.8544E-04	3.0072E-04	2.3527E-07	2.4787E-07	2.1683E-07	2.2844E-07	1.689	1.779	5.10
466555.0	15409.0	2.8568E-04	2.9912E-04	2.3547E-07	2.4655E-07	2.2951E-07	2.4031E-07	1.809	1.894	5.10
466555.0	15409.0	2.8568E-04	2.9912E-04	2.3547E-07	2.4655E-07	2.2951E-07	2.4031E-07	1.809	1.894	5.10
469439.0	18293.0	2.8932E-04	2.9957E-04	2.3847E-07	2.4692E-07	2.3077E-07	2.3894E-07	2.175	2.252	5.40
470863.0	19717.0	2.8192E-04	3.0016E-04	2.3238E-07	2.4741E-07	2.1516E-07	2.2908E-07	2.284	2.432	5.55

TABLE 6 (Continued)

Yukon Soil

YUKON SOIL: FILE NAME: PYUK3
DATE STARTED: OCT 18, 1990

CELL No: SOIL PERMEAMETER CELL

AREA:(cm^2)	81.07
WEIGHT OF SAMPLE:(gms)	1490.40
HEIGHT OF SAMPLE:(m)	0.0923
DIAMETER OF SAMPLE:(m)	0.1016
VOLUME OF SAMPLE (TOTAL):	0.0007

PERMEANT USED: CALCIUM SULPHATE SOLUTION (CaSo4)

WATER CONTENT	INITIAL
TARE NO.	A
TARE WEIGHT	154.71
TARE+SOIL WET (gms)	209.63
TARE+SOIL DRY (gms)	201.51
WEIGHT WATER (gms)	8.12
WEIGHT SOIL DRY (gms)	46.80
WATER CONTENT (%)	17.35

INF PRESS (psi) (kPa)	OFL PRESS (psi) (kPa)	CELL PRESS (psi) (kPa)	HYDR GRAD
31.95	28.00	40.00	30.09
220.14	192.92	275.60	

TIMER (mins)	ELPSD TIME (mins)	INFL RATE (cm^3/s)	OUTFL RATE (cm^3/s)	INFLO PERM (cm/s)	OUTFL PERM (cm/s)	TEMP CORR'D INFLO PERM (cm/s)	TEMP CORR'D OUTFL PERM (cm/s)	PORE VOL (INF)	PORE VOL (OUT)	CELL VOL CHG (mls)
324352.0	0.0	0.0000E+00	0.0000E+00	0.0000E+00	0.0000E+00			0.000	0.000	0.00
327151.0	2799.0	6.0170E-04	7.5950E-04	2.4668E-07	3.1137E-07	2.3156E-07	2.9228E-07	0.395	0.498	3.10
327163.0	2811.0	5.9913E-04	7.5626E-04	2.4563E-07	3.1004E-07	2.3057E-07	2.9104E-07	0.395	0.498	3.10
328197.0	3845.0	6.8075E-04	7.2822E-04	2.7909E-07	2.9855E-07	2.6259E-07	2.8090E-07	0.613	0.656	3.60
328271.0	3919.0	6.8704E-04	7.2765E-04	2.8166E-07	2.9831E-07	2.9476E-07	3.1219E-07	0.631	0.668	3.60
328271.0	3919.0	6.1242E-04	7.2765E-04	2.5107E-07	2.9831E-07	2.6275E-07	3.1219E-07	0.563	0.668	3.60
328542.0	4190.0	6.2435E-04	7.4324E-04	2.5597E-07	3.0470E-07	2.4829E-07	2.9556E-07	0.613	0.730	3.80
329659.0	5307.0	6.1931E-04	6.9280E-04	2.5390E-07	2.8402E-07	2.4514E-07	2.7423E-07	0.770	0.862	4.10
329659.0	5307.0	6.1931E-04	6.9280E-04	2.5390E-07	2.8402E-07	2.4514E-07	2.7423E-07	0.770	0.862	4.10
330383.0	6031.0	6.4307E-04	6.7706E-04	2.6364E-07	2.7757E-07	2.5272E-07	2.6608E-07	0.909	0.957	4.30
331069.0	6717.0	6.1879E-04	6.0791E-04	2.5369E-07	2.4922E-07	2.4318E-07	2.3891E-07	0.974	0.957	4.30
331069.0	6717.0	6.1879E-04	6.0791E-04	2.5369E-07	2.4922E-07	2.4435E-07	2.4005E-07	0.974	0.957	5.00
331176.0	6824.0	6.1993E-04	6.0839E-04	2.5415E-07	2.4942E-07	2.4307E-07	2.3855E-07	0.991	0.973	5.00
332906.0	8554.0	5.4117E-04	4.8535E-04	2.2186E-07	1.9898E-07	2.0826E-07	1.8678E-07	1.085	0.973	5.00
333955.0	9603.0	5.2358E-04	4.7693E-04	2.1465E-07	1.9553E-07	1.9782E-07	1.8020E-07	1.178	1.073	5.00
334467.0	10115.0	5.3650E-04	4.8624E-04	2.1995E-07	1.9934E-07	2.0224E-07	1.8330E-07	1.272	1.153	5.00
335449.0	11097.0	5.2496E-04	4.6777E-04	2.1522E-07	1.9177E-07	1.8274E-07	1.6283E-07	1.365	1.217	5.00
335460.0	11108.0	5.2444E-04	4.6731E-04	2.1501E-07	1.9158E-07	1.9073E-07	1.6995E-07	1.365	1.217	5.00
337471.0	13119.0	4.9010E-04	5.2399E-04	2.0093E-07	2.1482E-07	1.8433E-07	1.9707E-07	1.507	1.611	5.00

5.2 Assessment of Hydraulic Behaviour

5.2.1 Hydraulic Properties of Saturated Soil Covers

The use of the capillary barrier concept in the design of soil covers for sulphide tailings has been theoretically investigated by several authors (Magnusson and Rasmuson, 1984; Rasmuson and Eriksson, 1986; Collin, 1987; Nicholson et al, 1989). The capillary barrier is formed at the interface between coarse-grained and fine-grained soils. The concept involves the principles of unsaturated flow between soils of different textures or grain size distributions. If a fine-grained soil overlies a coarse-grained soil and both soils are initially dry, water infiltrating from the surface of the fine layer will not move into the coarse layer until the pressure head in the fine layer approaches zero (that is, the fine-grained soil is at or near saturation). The hydraulic properties which control this phenomenon are the relationships between water content, θ and pressure head, $U(\theta)$ and water content and hydraulic conductivity, $K(\theta)$.

Figure 13 shows moisture storage or moisture characteristic curves for a fine sand, silt and clay, obtained by Ho(1979). The curve for the clay is almost linear while the curves for the silt and sand are highly nonlinear. The differences in the curves demonstrate the effect that soil properties have on the moisture retention characteristics. The shape of the storage curve depends largely upon the grain size and pore size distributions of the soil. The storage curves also indicate that the volume or amount of water retained is a function of the pore water pressure. As the pore-water pressure decreases (that is, becomes more negative) the silt and the fine sand remain saturated until a pressure head of ψ_a, the air-entry value is attained. The air-entry value is the pressure head required to overcome the capillary forces that can be exerted by the largest pore in the soil. The largest pores are the first to drain. As the pressure head becomes negative, progressively smaller pores drain until the residual water content (θ_r) of each soil is attained (Nicholson et al., 1989). As shown in Fig. 13 both the air-entry value and residual water content for the silt are higher than those of the fine sand.

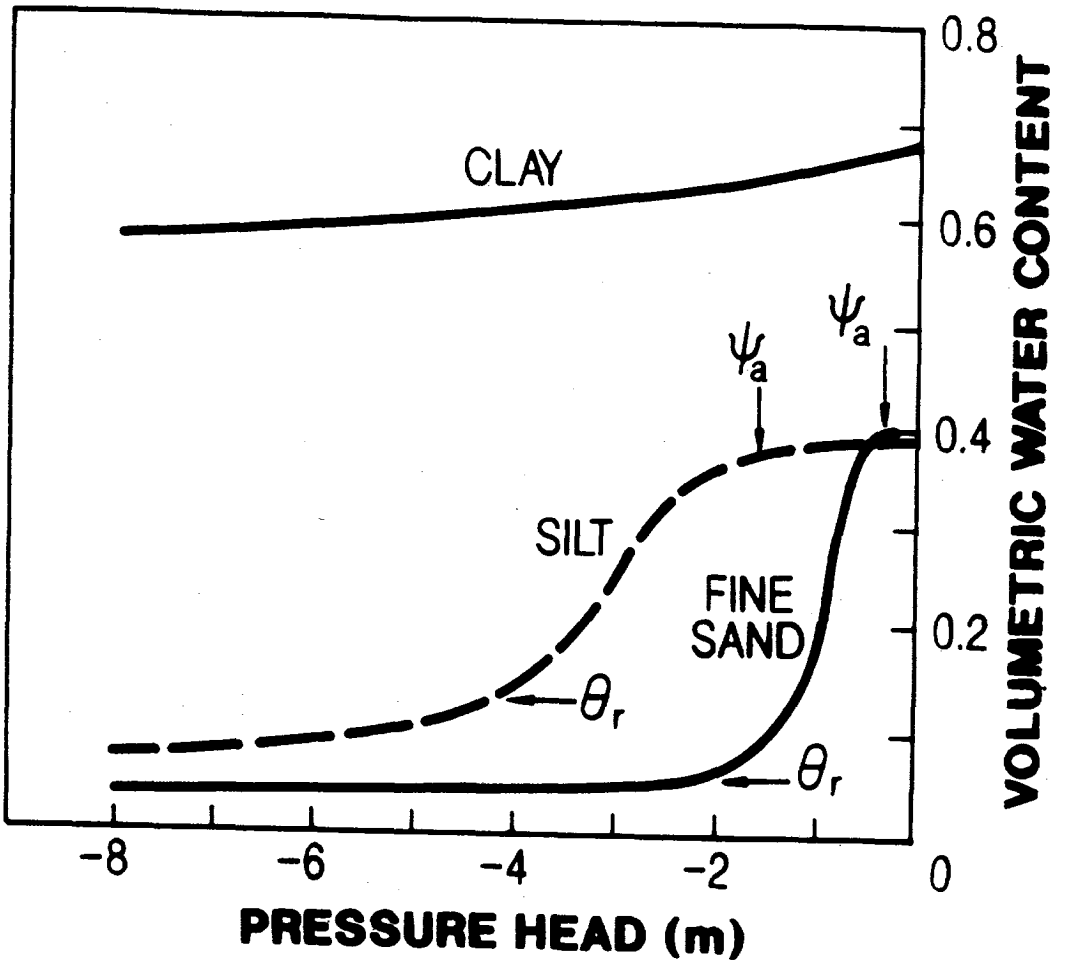

Figure 13 Typical moisture storage curves for soils (adapted from Ho, 1979).

The moisture characteristic curve of a soil is affected by the direction of change of water content and takes different forms according to past history of wetting and drying of the soil. This phenomenon of irreversibility of the moisture content - pore water pressure relationship is called hysteresis (Liakopoulos, 1965; Childs, 1967). Uncertainties associated with the determination of actual moisture characteristic curves for natural soils generally overshadow variations due to hysteresis. Consequently, most analyses of field problems ignore hysteresis.

The hydraulic conductivity, K of an unsaturated soil is a function of its negative pore-water pressure state or magnitude of suction. Generally, K decreases with moisture content since drained or empty pores do not transmit water. The drained pores also obstruct flow and therefore increase the path length of the residual flow column (Childs, 1967). Since drainage or loss of water from the soil pores occurs at the lowest suctions, K decreases sharply during the initial stages of reduction of moisture content.

The hydraulic conductivity function, K(θ) for a particular soil can be established from its moisture characteristic curve since both K and the moisture retention are dependent on the pore water pressure. Several techniques for establishing a K(θ) function are described in the literature (Green and Corey, 1971; Mualem, 1976; Gillham et al., 1976).

The method of Green and Corey (1971) uses the following equation:

$$K(\theta)_l = \frac{K_s}{K_{sc}} \cdot \frac{30\,\gamma^2}{\rho g n} \cdot \frac{e^p}{n^2} \sum_{j=1}^{m} [(2j + 1 - 2l)\, h_j^{-2}] \qquad [17]$$

$$l = 1,2,...m$$

where

$K(\theta)_l$ = calculated conductivity for a specified moisture content or pressure and i denotes the last water content class on the wet end

$\frac{K_s}{K_{sc}}$	=	matching factor (measured saturated conductivity/calculated saturated conductivity)
p	=	parameter that accounts for interaction of pore classes
n	=	total number of pore classes
h_j	=	pressure head for a given class of water-filled pores
ρ,γ, and η	=	density, surface tension and viscosity of water, respectively
g	=	acceleration due to gravity
ϵ	=	porosity

The solution to the Green and Corey (1971) equation is implemented in computer codes such as the PC-SEEP package(Geo-Slope, 1987) and those developed by Collin et al.,(1990) for the analysis of moisture transport in soils.

5.2.2 Column Verification and Modelling

The concept of a capillary barrier involving a coarse-grained soil overlying a fine-grained layer was investigated in a laboratory apparatus at NTC. The apparatus consisted of a 1 m tall Plexiglas column with a 10.8 cm inside diameter. The column was instrumented with specially-designed tensiometer and pressure-transducer systems and electrodes for a TDR (time domain reflectometry) unit. The tensiometers measured the suction developed in the column as it drained while the TDR unit was used to measure the corresponding volumetric water content. The TDR unit used was a Tetronix Model 1502B Time Domain Reflectometer. The principles of the TDR technique for measuring water content are described elsewhere (Topp et al., 1980). Each tensiometer consisted of a 0.5 bar (5 m of water pressure) porous ceramic tip. It was designed as a compromise between the amount of porous ceramic surface area making contact with the soil and impediment to drainage.

An air vent was installed 78 cm above the base of the column, 2 cm below the fine soil/coarse soil interface. A 0.5 bar porous ceramic plate was installed at the base of the column to permit water drainage but prevent air/gas flow. A Tygon tubing line was connected from the base of the column to an Erlenmeyer flask. The flask was used to establish the water table level and to collect the water that drained from the column. A schematic representation of the column is

shown in Fig. 14. The design and instrumentation used were adapted from Sydor (1990). A detailed description of the methods of installation and packing of the soil in the column is found in the above reference in the Waterloo report (Appendix A).

The column was packed with a two layer soil profile consisting of the Yukon till overlying a medium sand layer similar to the Heath Steele sand. The soils were initially saturated and then allowed to drain, keeping the water table at a distance of about 50 cm below the bottom of the column. This was designed to simulate the lowering of the water table in a covered tailings deposit under dry conditions. The water content and pressure head (suction) developed in the draining column were monitored at different times. A photograph of the installed column is shown in Fig. 15.

Figure 16 presents the pressure and moisture profiles observed. The interface between the fine and coarse layer is represented by INT in the figures. The coarse layer drained within 7 days to residual saturation at a suction of -50 cm. At residual saturation, the coarse layer probably attained its minimum hydraulic conductivity and was not able to transmit any more suction. The fine layer did not drain and after 14 days, the pressure profile was observed to be nearly parallel to the static equilibrium line. This meant that the hydraulic gradient across the fine layer was essentially zero so that there was very little flow of water from the fine layer to the underlying coarse layer. The moisture content profile confirmed these observations and showed further that the fine layer remained saturated at a moisture content of nearly 32 percent. The slight decrease in the moisture content at the top of fine layer was attributed to loss of moisture by evaporation.

The column observations described above confirm the results of transient state numerical modelling conducted by Akindunni et al., (1990). These authors showed that a fine layer overlying a coarse layer will remain saturated for 50 days without the need for infiltration. These results suggest that an effective composite soil cover could be designed for tailings decommissioning. The concept is currently being assessed in field applications at the Waite Amulet tailings site near Rouyn, Noranda, Quebec (Yanful and St-Arnaud, 1991). This would provide the opportunity for assessing other factors such as the effects of freeze-thaw and root penetration on cover integrity.

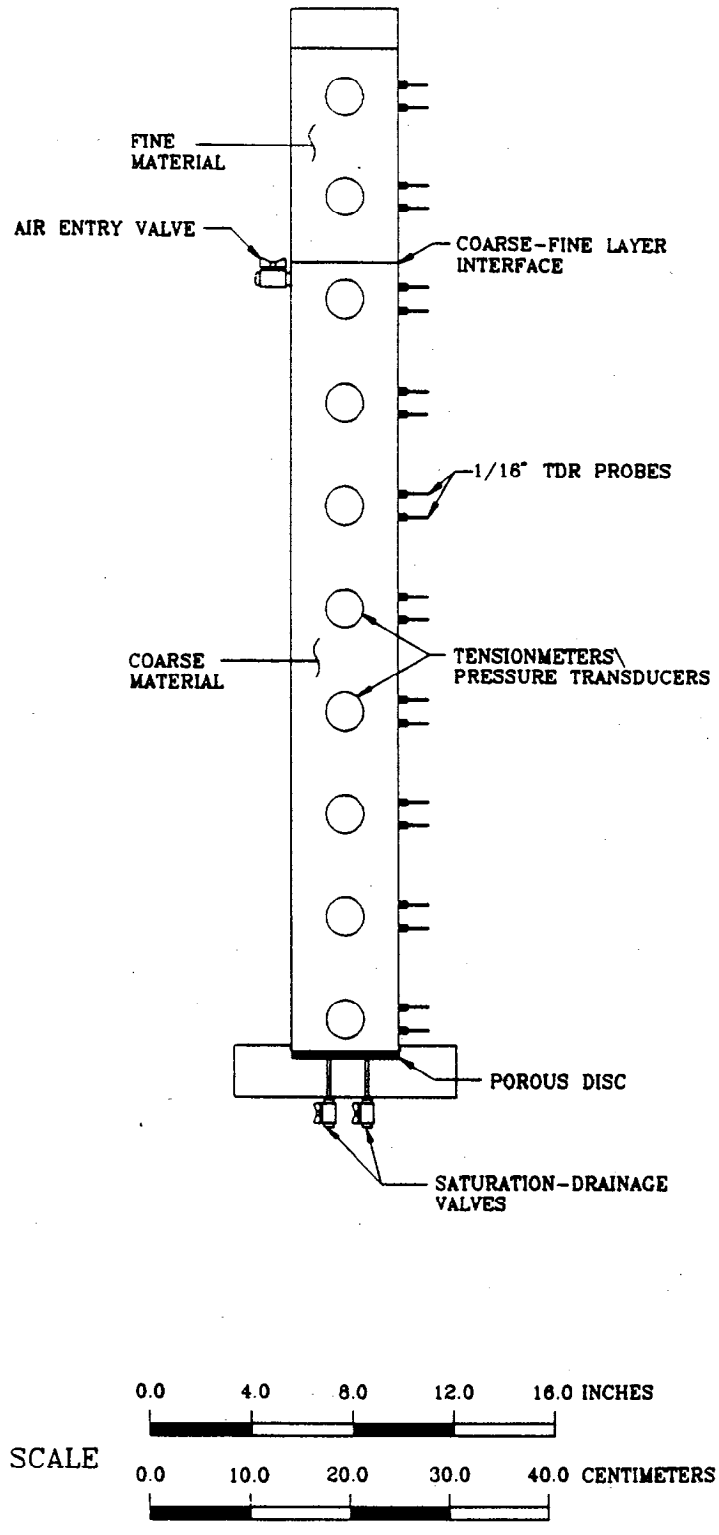

Fig. 14 A schematic representation of the column used for investigating the hydraulics of a two-layer cover system.

Drawn By Keith S. Shikatani

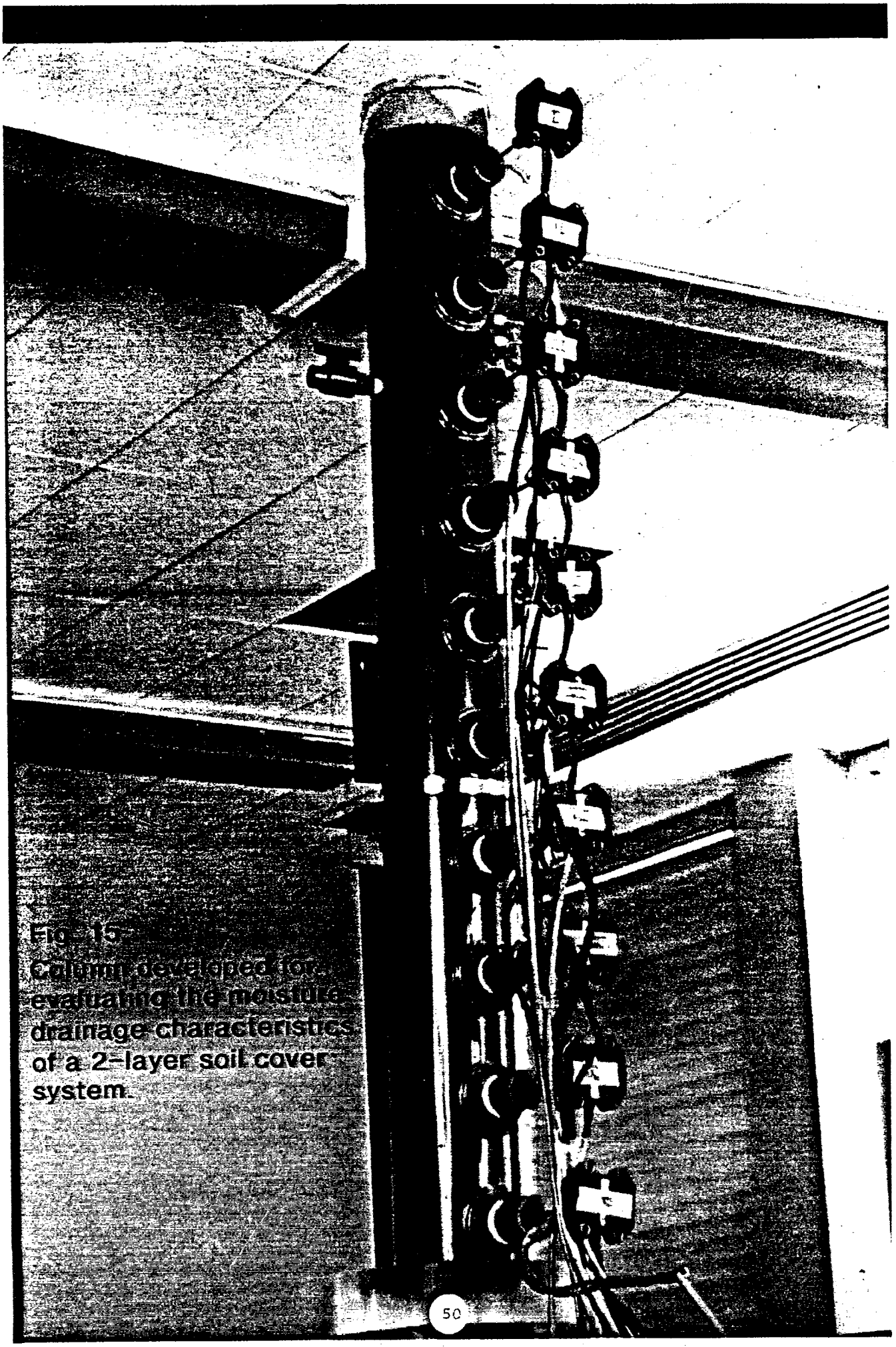

Fig. 15
Column developed for evaluating the moisture drainage characteristics of a 2-layer soil cover system.

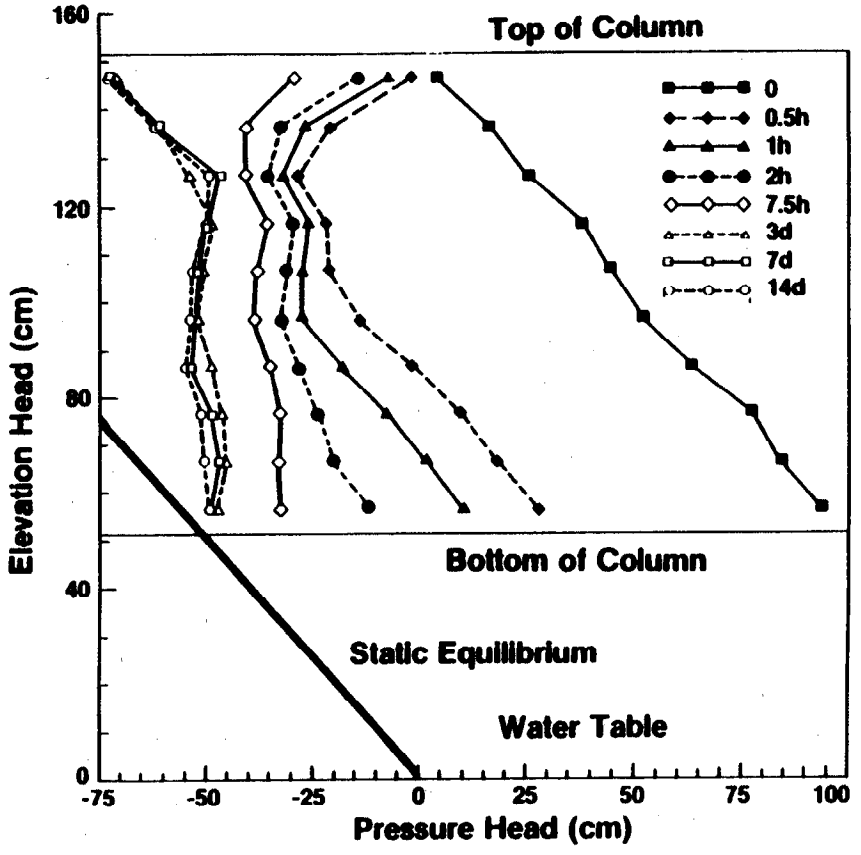

a)

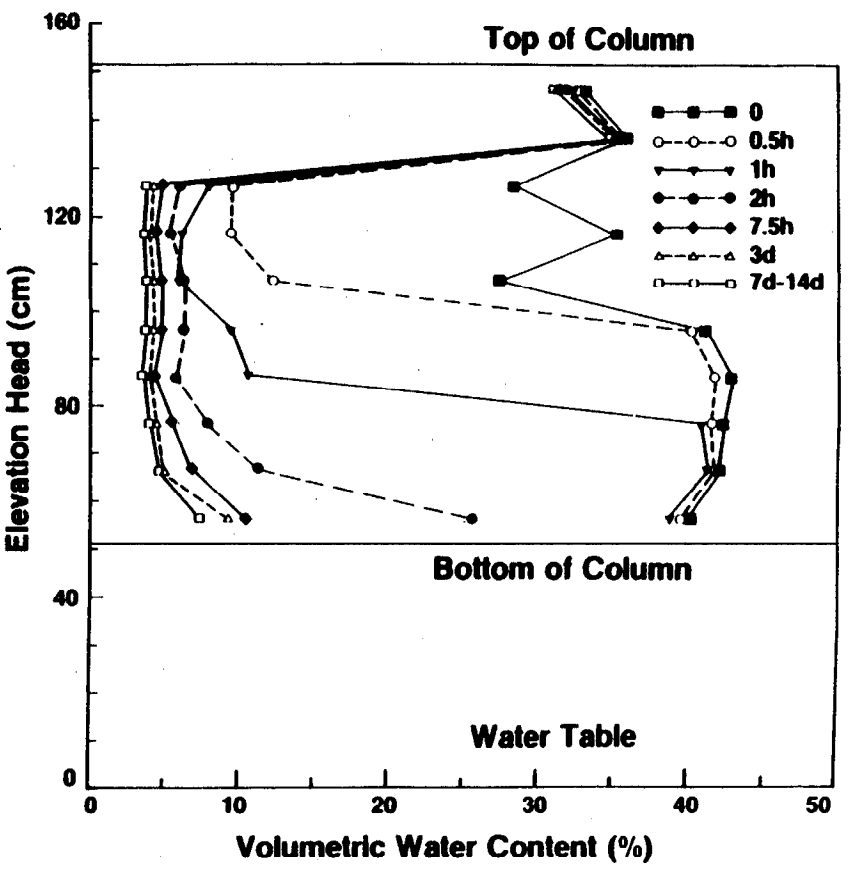

b)

Figure 16 Observed pressure and water content profiles in laboratory column.

The pressure head profiles observed in the column were modelled using a commercially available saturated-unsaturated flow model PC-SEEP, marketed by GEOSLOPE Programming Ltd. of Calgary. The objective of the modelling was to verify whether it was possible to predict the experimental results. If this was possible, then predictions of long-term, worst case scenarios could be made in potential field applications. Two levels of modelling were conducted. Preliminary modelling involving column conceptualization and definition of material properties was conducted at NTC. More detailed modelling, using the material properties measured or defined by NTC, was undertaken under the direction of Dr. L.S. Barbour of the Geotechnical Group at the University of Saskatchewan.

The NTC model did not consider the ceramic plate at the base of the column. Consequently, the predicted drainage was found to be much more rapid than what was observed in the laboratory. Subsequent modelling by the University of Saskatchewan, using the WINDOWS version of PC-SEEP and taking the ceramic base plate into account, indicated that it was possible to obtain a good prediction of the pressures within the column as long as critical aspects of the different porous media in the column are included in the model. The critical features identified in the University of Saskatchewan modelling work were :

a) the release of water from the Yukon till as a result of consolidation under the negative pore pressures released during drainage,

b) the impedance to drainage produced by the presence of the porous stone at the base of the column, and

c) the rapidly decreasing hydraulic conductivity of the sand as it approaches residual saturation.

Details of modelling of the laboratory columns and the properties of the soils used are presented in Appendix B.

5.3 Oxygen Diffusion and Flux Measurements

5.3.1 Laboratory Column Development.

The principal objectives of the diffusion measurements undertaken during the investigation were : a) to develop methods for determining the diffusion coefficient of gaseous oxygen, and b) to develop a methodology for measuring the low oxygen fluxes expected in saturated soil covers. These objectives were achieved by means of a series of laboratory experiments in special plastic columns developed during the study. Two different types of columns were used in the diffusion measurements. The first column consisted of a 50 cm tall clear PVC tubing with an internal diameter of 10 cm. Soil was mixed with water to the desired water content and then compacted directly inside the column to the required density. Prior to placement of material, the interior wall of the column was coated with vacuum grease to prevent side wall leakage of oxygen. Top and base plates were bolted in place to prevent leakage. Figure 17 shows a photograph of the column.

Another column developed in a separate project was used to determine diffusion coefficients. It consisted of a 10 cm internal diameter clear PVC with a height of 20 cm. Soil was placed in the column in the same way as described above. Rubber seals were sandwiched between the ends of the column and the top and base plates. The rubber seals were coated with vacuum grease prior to installation to prevent leakage. Figure 18 shows a schematic representation of the measurement techniques used.

5.3.2 Diffusion Measurements and Computer Modelling

In the first type of column (Fig. 17), oxygen was maintained at a constant concentration of 20.5% (atmospheric value) at the top of the column after purging with oxygen-free nitrogen gas. Oxygen, diffusing through the soil, was allowed to accumulate at the base of the column. Sampling ports with rubber septa were installed at specified points along the height of the column during soil packing. Oxygen concentrations were obtained by sampling the ports at known times, using a Teledyne Model 340 FBS analyzer incorporating a hand-held trigger with a syringe sampler. The analyzer required a sample volume of 2 mL and registered a stable

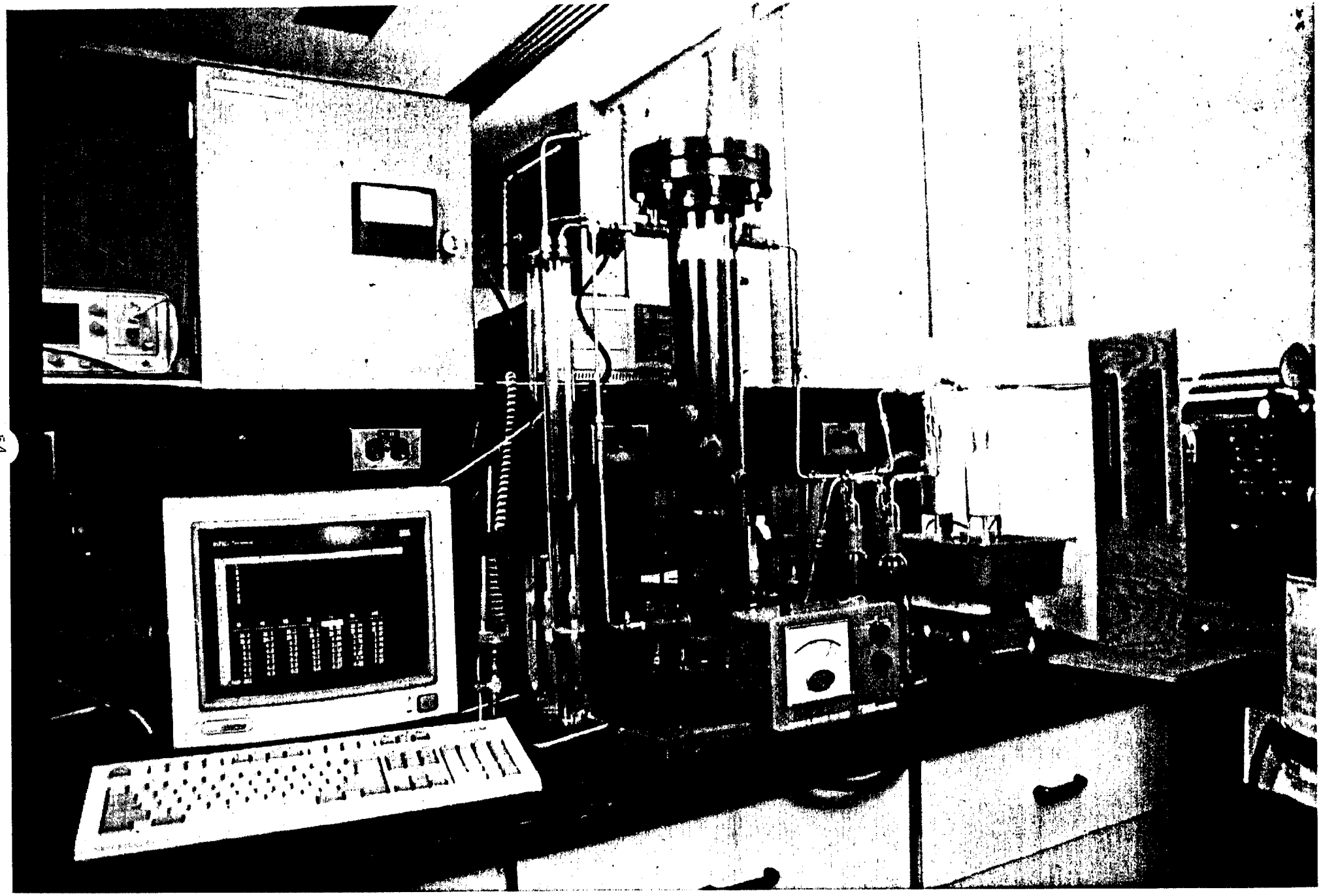

Fig. 17. Column developed for the determination of oxygen diffusion coefficient

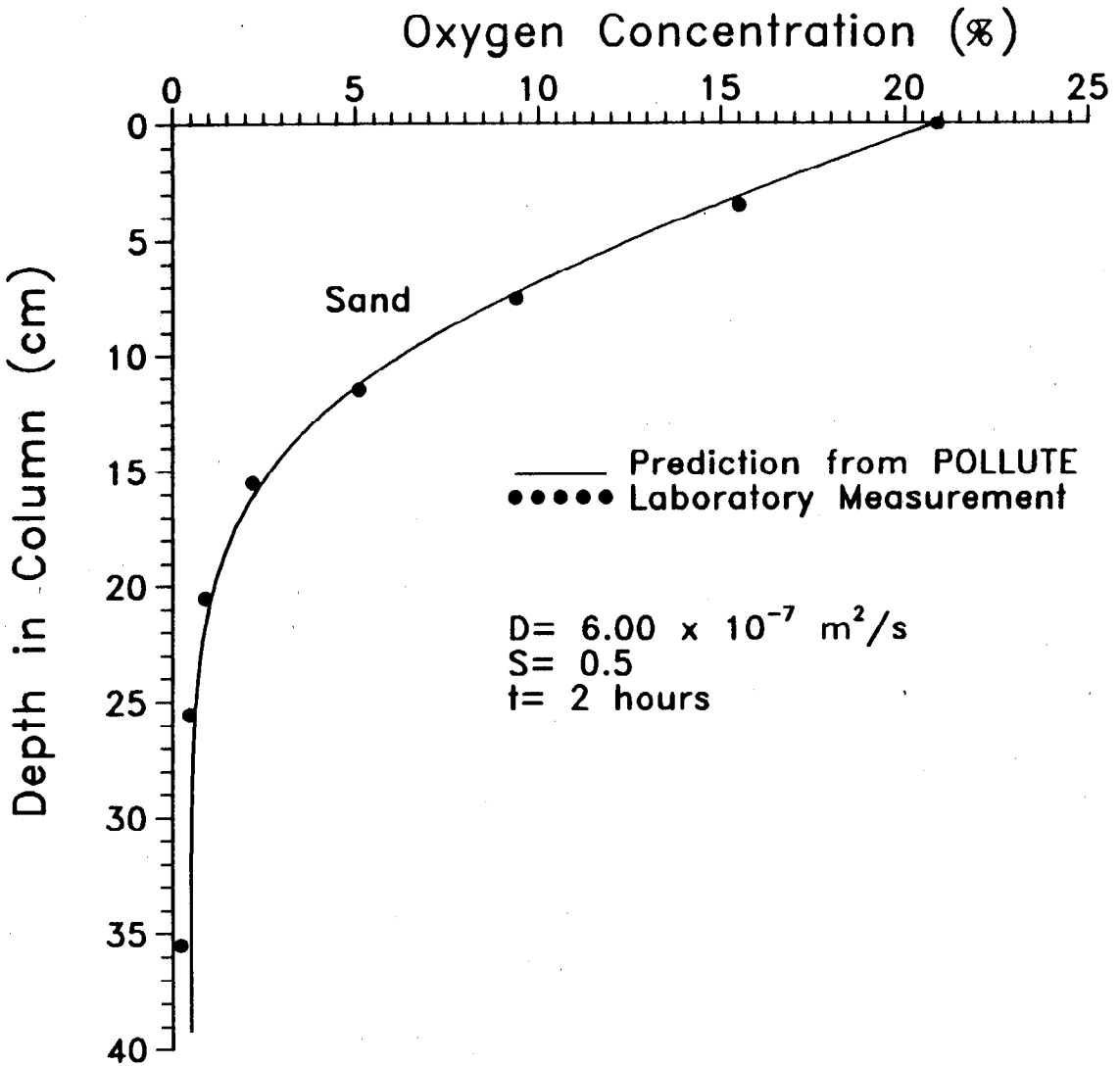

Figure 18 Transient gaseous oxygen profile in diffusion column, Yukon till.

reading within 20 secs. After reading, the sampled gas was released inside the port. The process was repeated twice and the average concentration recorded. The analyzer was calibrated in the atmosphere before sampling of the next port.

Based on the column configurations shown in Fig. 17, the following boundary conditions were used in the simulation of one-dimensional oxygen diffusion through the soil :

$$C\,(\,o,t\,) \;=\; Co,\ for\ all\ t \qquad [18]$$

The base concentration with a zero outflow velocity was calculated using the expression derived by Rowe and Booker (1986):

$$C\,(\tau, z = H_B) \;=\; \int_o^t \frac{f\,(\tau, z = H_B, C)}{\theta_B\, h_B}\, d\tau \qquad [19]$$

where τ is the time variable.

For the second set of diffusion tests, a finite mass of oxygen, initially equal to atmospheric value, was allowed to diffuse into a 10 cm thick soil layer. As in the first type of tests, the column containing the packed soil was purged with nitrogen, prior to the commencement of each test. The residual oxygen concentrations at the top and the base were recorded. These typically ranged from 0.2 to 0.5%. The source concentration (above the soil layer) was continuously monitored with a Teledyne Model 320 P oxygen analyzer with a flow-through sensor. Gas leaving the column was drawn into the sensor by a built-in vacuum pump. The pump was operated at a vacuum equivalent to 2 cm of water during the experiments. A similar analyzer was installed at the base to measure the base concentrations and, also, to ensure that there was no pressure difference between the top and the base.

Several checks were conducted to ensure that the sensor itself did not consume an appreciable amount of oxygen which could affect the change in the source concentration. This was accomplished by monitoring oxygen concentration above a solid polyethylene material finished to the same dimensions as the soil specimens. No measurable change in concentration was observed over the entire lengths of the tests which lasted up to 72 hours. At the end of each diffusion measurement, the soil was weighed again and its gravimetric water content determined. This information was required to calculate both the water-filled and gas-filled porosities of the soil.

In order to obtain diffusion coefficients, the concentration-time data were simulated using the following boundary conditions :

$$C_T(t) = C_o - 1/H_g \int_o^t f_T(t)dt \qquad [20]$$

where

$$f_T(t) = -\theta D_a \left(\frac{\delta C(t)}{\delta z}\right) T \qquad [21]$$

The base was modelled with a zero outflow velocity, as in Equation [12].

The solutions to the diffusion equation incorporating the boundary conditions presented above are implemented in the computer program POLLUTE, developed by Rowe and Booker, 1990.

5.3.2.1 Results

A transient vertical profile of oxygen concentration observed in the 50 cm tall column is presented in Fig. 19. Using the program POLLUTE, the diffusion coefficient required to match the experimental and theoretical oxygen profiles at 50% water saturation was determined to be 6.0×10^{-7} m^2/s.

Figure 20 shows typical oxygen concentrations observed at the top and base of the 20 cm tall column. The data indicate a decrease in the source concentration as oxygen diffuses through the soil and accumulates at the base. At steady state, the oxygen concentration at all depths in the soil was equal so that there was no concentration gradient for further diffusion. Thus the source and base concentrations equalized at equilibrium, as shown in Fig. 20a. The same data have been replotted as mass versus time in Fig. 20b. The gap between the two profiles at equilibrium reflects the mass of oxygen occupying the pore spaces in the soil. From a knowledge of the gas-filled porosity, mass balance calculations were performed to ensure that the soil did not consume or adsorb any oxygen. Diffusion coefficients were determined by fitting theoretical concentration profiles to the experimental data.

Diffusion coefficients determined for the Heath Steele till at different degrees of water saturation are presented in Fig. 21a. The results generally indicated a decrease in diffusion coefficient with increase in water saturation, with greater decreases occurring in the 85 to 95% saturation range. The data also showed some scatter which could be explained by differences in the soil structure during moulding. The diffusion-coefficient water saturation relationship is further illustrated in Fig. 21b, which also shows that the rate of decrease of the source concentration decreases with increase in water saturation. These diffusion coefficients may be too high, especially at high water contents. Oxygen uptake as a result of increased soil microbiological activities at these high water contents may be important. Further testing is in progress to define and estimate biochemical activity factors for the Heath Steele till.

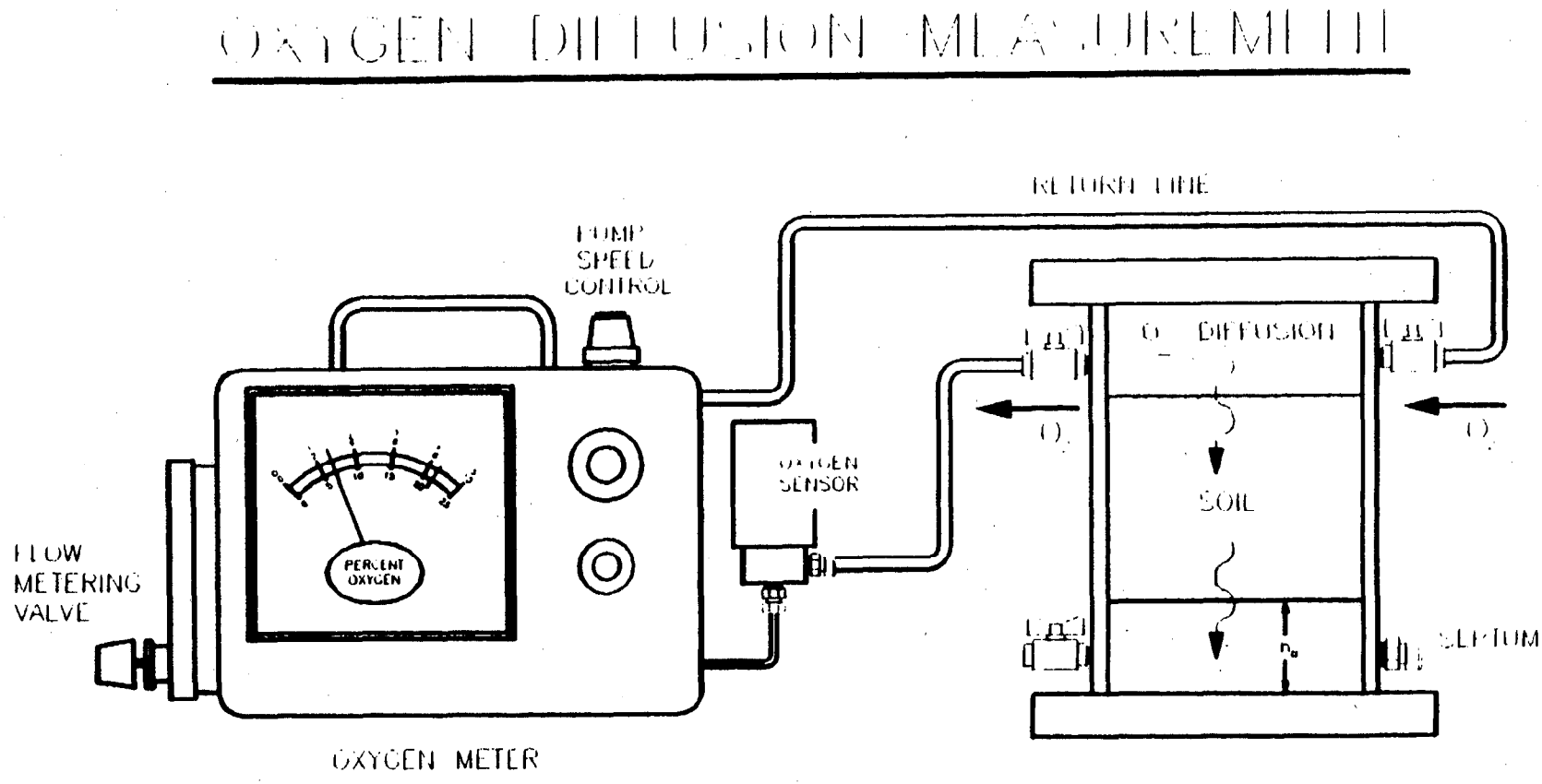

Figure 19 A schematic representation of oxygen diffusion measurement using a finite mass of source oxygen.

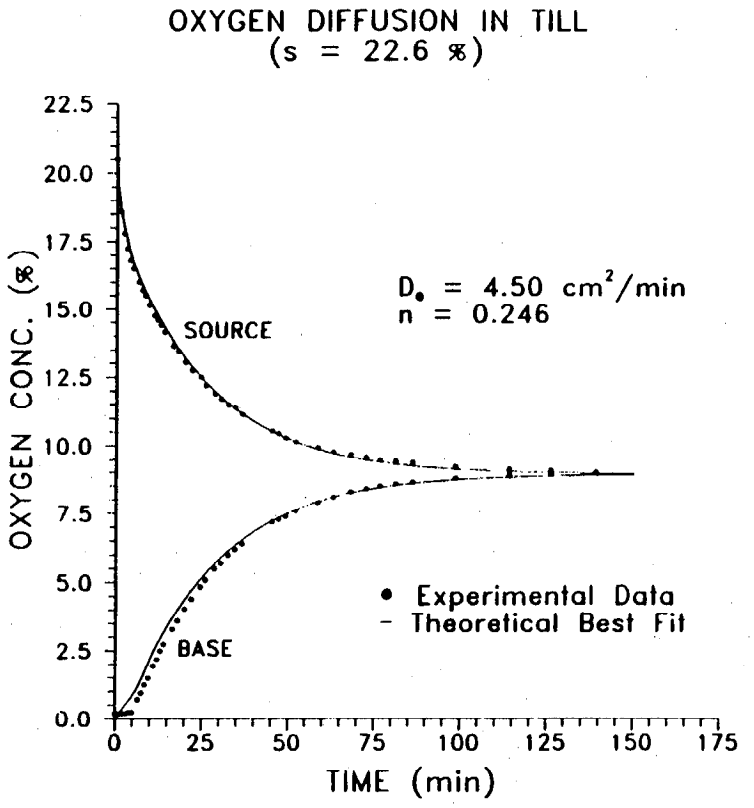

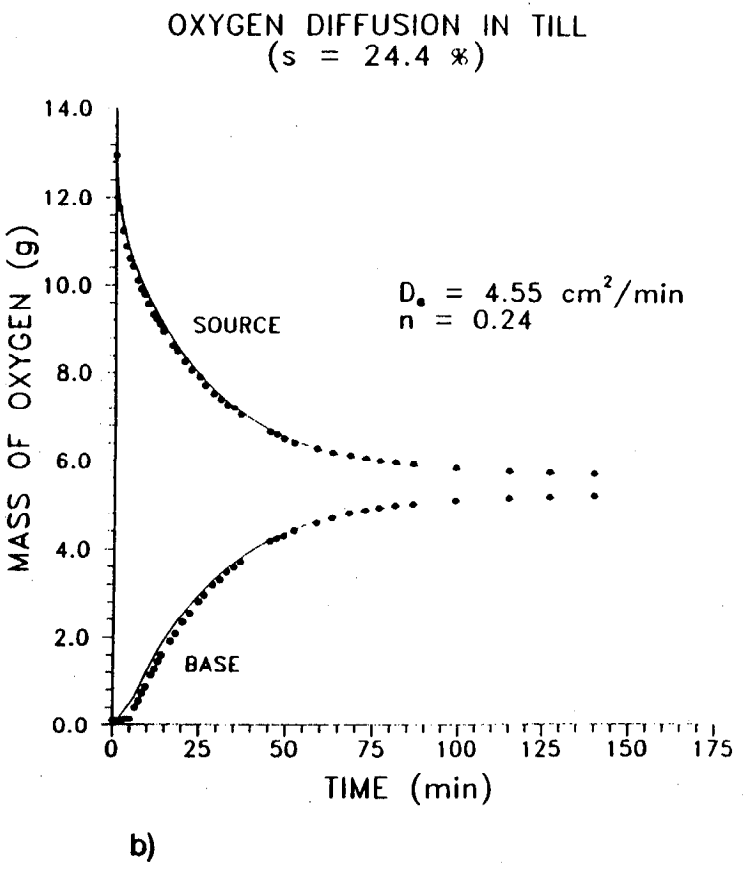

Figure 20 Variation of source and base oxygen concentrations and masses in diffusion cell with time.

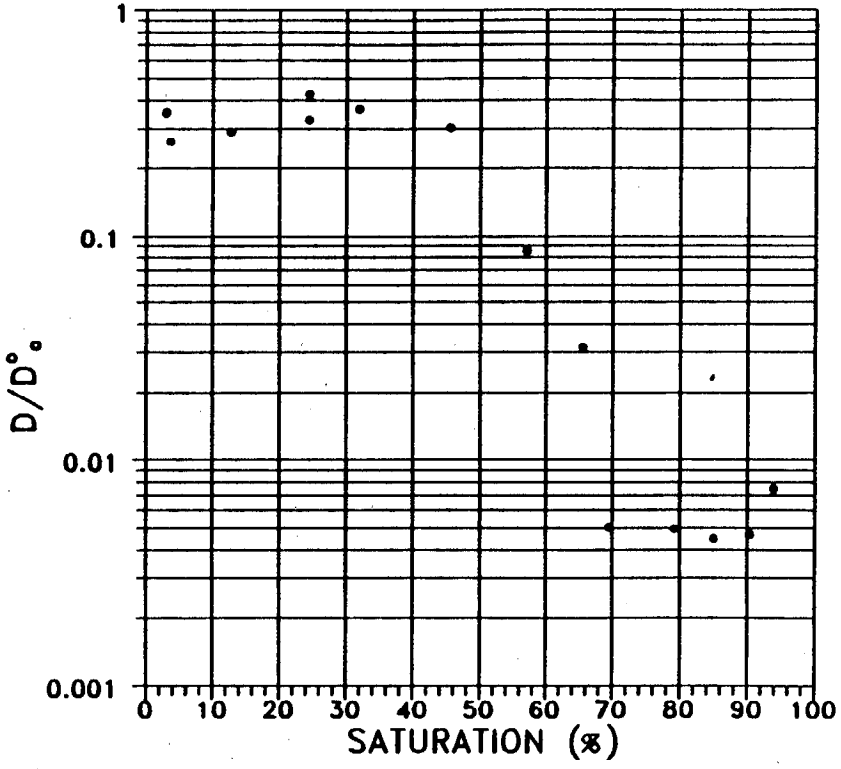

a)

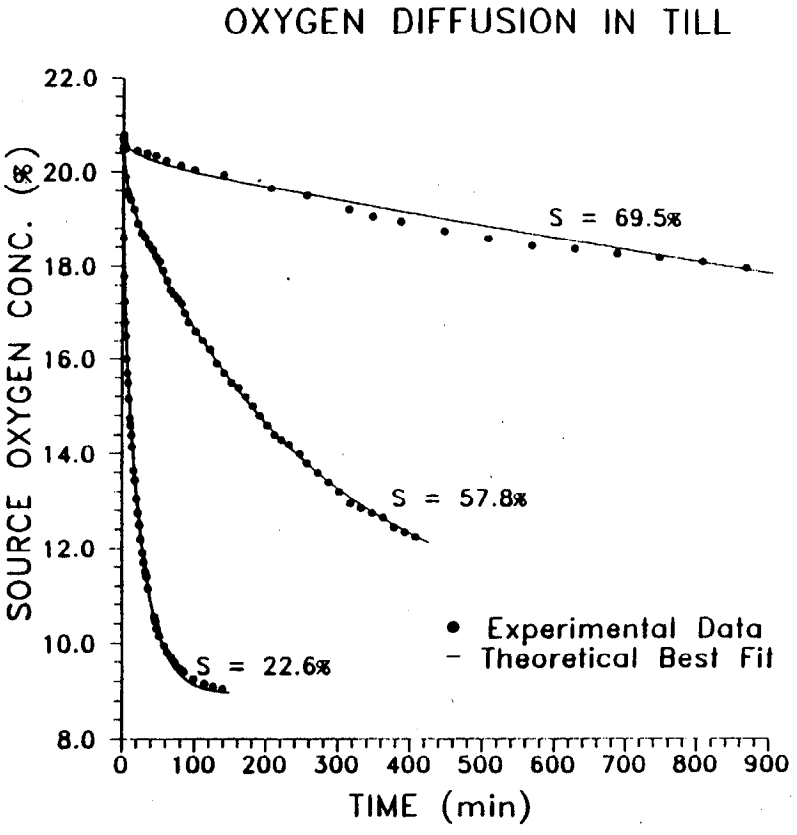

b)

Figure 21 Variation of diffusion coefficient of Heath Steele candidate till, HS-C, with percent moisture saturation.

5.3.3 Demonstration of Low Oxygen Fluxes

5.3.3.1 Investigation of Oxygen Sinks

The demonstration column concept was developed as one aspect of the investigation to verify the reduction of oxygen flux through near-saturated candidate cover materials. The column was intended to allow actual measurements of oxygen flux through a cover layer and hence show that a significant reduction of oxygen flux could be realized by maintaining a high degree of saturation in a fine-grained layer. Such a column was conceptualized to require an oxygen sink to simulate uptake of oxygen by reactive sulphide tailings at the base of a cover. The sink was also required to be quantitative and allow measurement of the uptake of the oxygen over time. The flux of oxygen expected in the column was estimated to be of the order of 8.0×10^{-3} mg/hr and therefore required a very careful and accurate measurement.

Various oxygen sinks were investigated by the University of Waterloo team. The most extensively-studied was a ferrous sulphide slurry. In laboratory experiments, this slurry was tested for changes resulting from oxygen uptake. Initial test runs showed pH decline and increasing specific conductance with time when the slurry was exposed to the atmosphere. The results were consistent with the oxidation reaction. However, subsequent measurements of sulphate concentrations to confirm sulphide oxidation showed a deficit in the reaction stoichiometry. The problem was identified to be the incomplete conversion of all the consumed sulphide to sulphate due to the formation of an intermediate elemental sulphur phase. Consequently, the method was terminated.

An electrode method was reviewed and found to be plausible but would require significant development time and cost. The final option which was pursued and adopted was the analysis of low level oxygen in a gas stream at the base of the column. This concept would involve the flow of oxygen-free gas (nitrogen) at the base of the demonstration column to create a zero concentration boundary. This would be followed by an analysis of the oxygen in the nitrogen caused by diffusion through the soils. This method depended on low level detection of oxygen in the gas phase and it was concluded, after extensive investigation, that the Teledyne Model 360 WAM trace oxygen analyzer would be suitable. This instrument was purchased and

calibrated for actual measurement. However, as explained later, it was found that the use of the nitrogen stream at the base of the column would not provide detectable concentration of oxygen for a long time. The method was therefore modified as described later.

The essential features of the demonstration column are shown in the photograph in Fig. 22. It consisted of a 10 cm diameter (ID) 40 cm tall Plexiglas column with removable (but tightly-fitted) top and base plates (3 and 6 cm thick, respectively). The column was instrumented along its height with a set of 3 mm diameter stainless steel rods for the measurement of volumetric water content by the time domain reflectometry (TDR) technique (Topp et al., 1984). The base plate incorporated a 6 mm thick perforated plastic disc whose purpose was to allow a rapid and efficient mixing of gas reporting to the base of the column.

In the laboratory demonstration work, the column was wet packed with sand HS-D in lifts of approximately 1.5 cm to a final height of 25 cm. A fine mesh polyester screen was then placed over the coarse sand. Lifts of moistened till material (-No. 4 mesh Heath Steele till, HS-C) were next compacted on top of the polyester screen until the desired final height of 6 cm was attained. A PVC perforated disc and standoffs were placed on top of the till layer to make contact with the top plate of the column to prevent uplift of the soil during purging. The column was then purged from the bottom saturation/drainage valve with carbon dioxide (CO_2 gas) which was then allowed to vent out overnight at the air entry port (located a short distance below the sand/till interface). After purging, the column was slowly saturated with de-aired water until ponding occurred on the top surface of the till. Moisture content measurements by TDR were then made, a "water table" location was set and the drainage valve opened. The moisture content was measured over time as the column drained. Figure 23 shows moisture content profiles observed during drainage to 112 days. As shown, the upper till remained essentially saturated to 122 days.

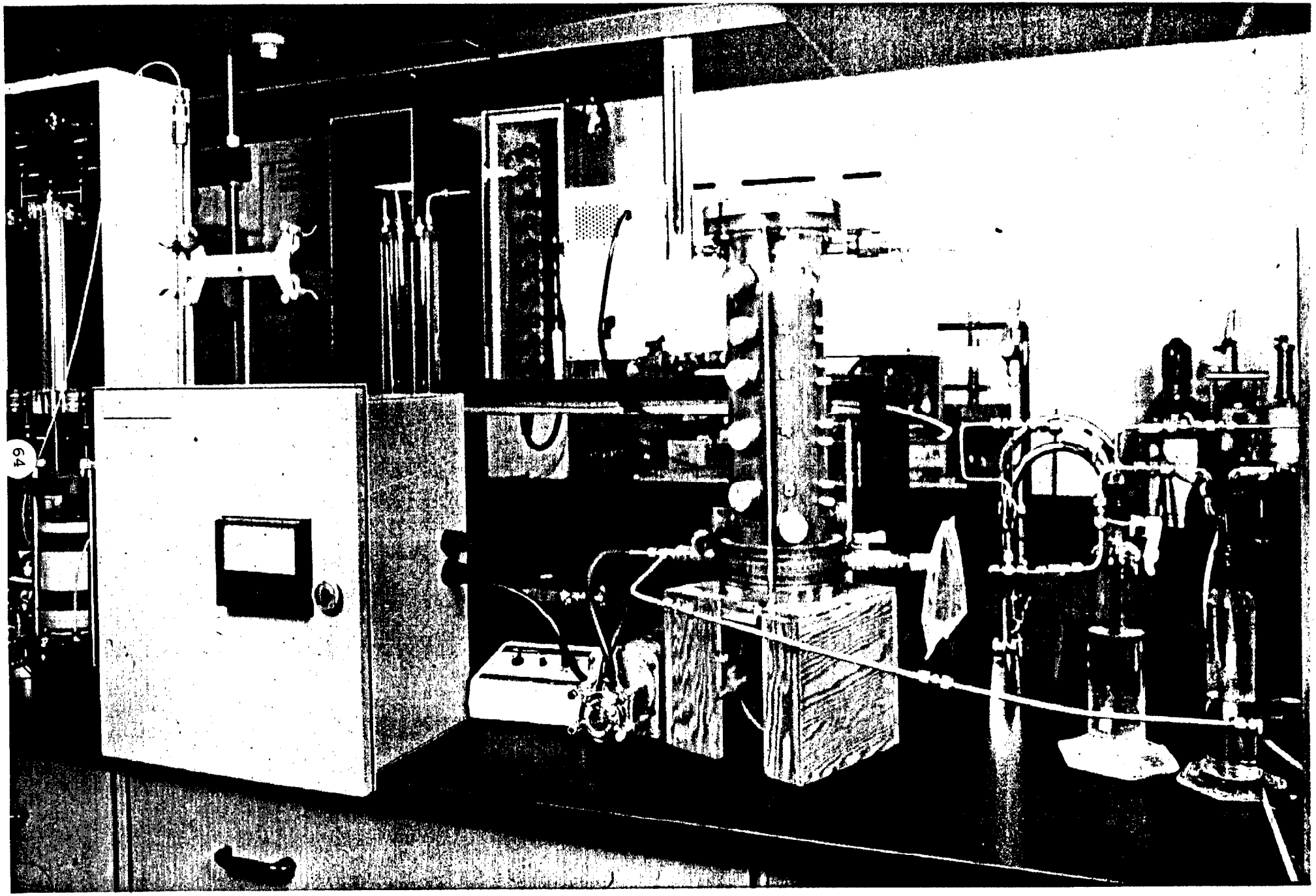

Fig. 22, Demonstration column developed for measuring low oxygen fluxes in saturated soil covers. Trace oxygen analyzer is shown on the left.

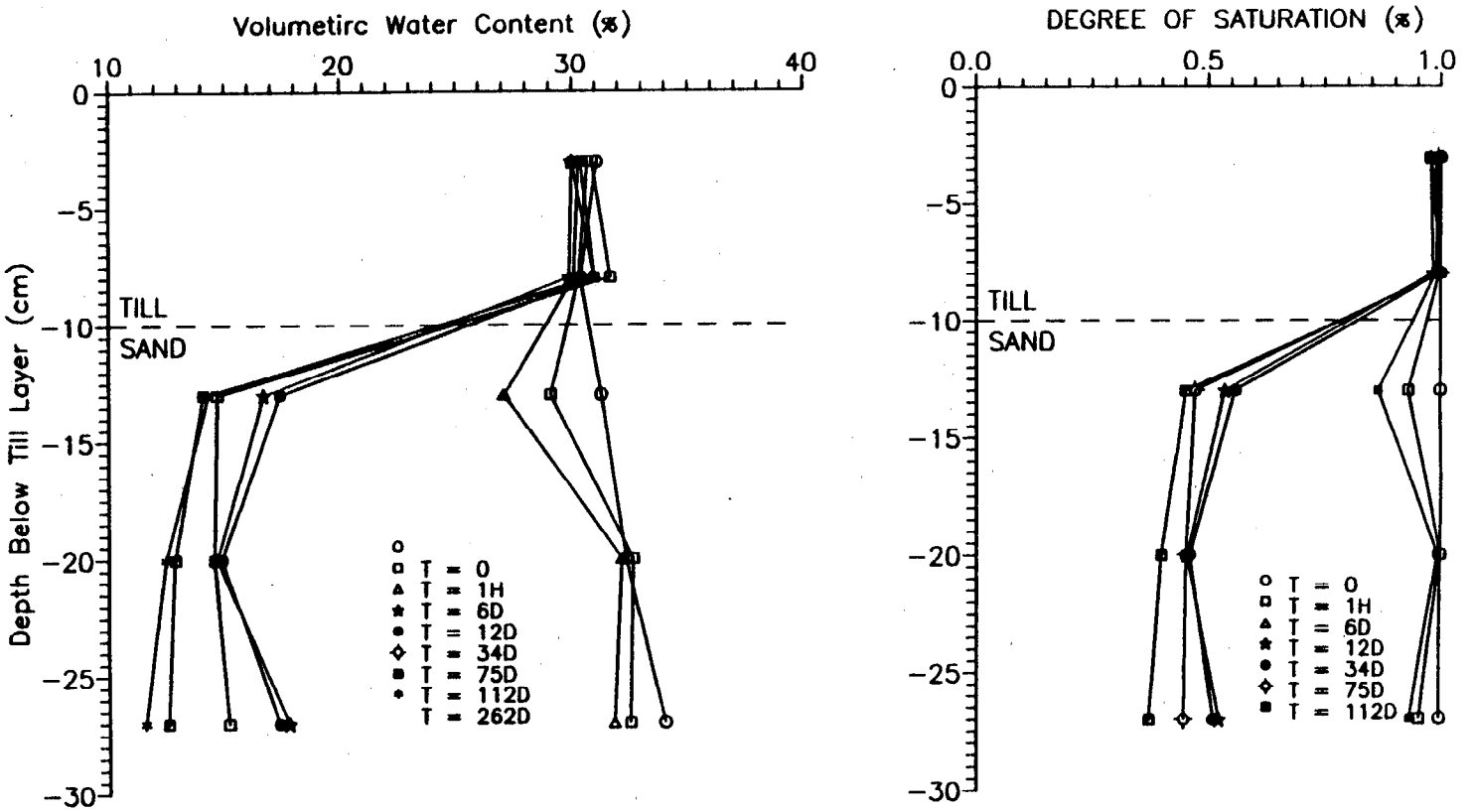

Figure 23 Moisture content profiles in demonstration column.

When the sand had drained to equilibrium, the drainage valve was shut off and the air entry port was closed. Oxygen-free nitrogen was next used to purge the column free of any measurable oxygen. A compressed air source was then introduced to the top of the column to provide constant concentration of gaseous oxygen. The base of the column was continuously flushed with oxygen-free nitrogen gas at a flow rate of about 90 to 100 cm^3/min and a pressure equal to the pressure at the top of the column. Any oxygen that diffused from the top of the column through the soils into the base of the column would be flushed out in the stream of nitrogen gas and the concentration measured on a trace oxygen analyzer (Teledyne Model 306 WAM) with switch selectable ranges up to 100 ppm of oxygen. A minimum gauge pressure of 7 kPa and a maximum of 1000 kPa is required to provide reliable measurement on this analyzer. However, the manufacturer recommends an optimum pressure of 35 kPa. Continuous flushing of oxygen was thought to simulate oxygen sink (similar to the presence of reactive sulphide tailings) at the base of the column.

Computer modelling conducted along with the column installation and testing later showed that the approach described above would extend measurement times to years instead of months. Continuous flushing of nitrogen at the base was therefore eliminated in subsequent modifications of the set up. The final experimental system considered to provide reliable and measurable estimates of oxygen concentrations at the base of the sand was one that incorporates an ultraclean Teflon sampling bag, attached to the base of the column, as shown in the photograph in Fig. 19. The bag is filled with oxygen-free nitrogen and then opened to the base of the column to permit periodic sampling of a known volume of gas (mixture of oxygen and nitrogen) without creating a negative pressure. From computer model predictions involving the use of input values of measured soil diffusion coefficients, water contents and porosities, measurements of oxygen concentrations at pre-determined arrival times can be followed. The flux can then be determined from the concentrations.

6. PREDICTION OF COVER PERFORMANCE

6.1 Development of Oxygen Diffusion Model

As part of the project requirements, a computer-based model was developed for simulating

oxygen transport through cover materials. The model is based on the solution to the transient diffusion equation or Fick's second law (described by Equation [2], Section 2.2), given by Crank (1975) is used. For a single layer cover on sulphide-rich tailings, the following boundary conditions may be applicable:

a) Constant source oxygen concentration, Co.

b) Initial oxygen concentration is zero throughout the cover of thickness L.

c) Oxygen concentration at the base of the cover is assumed to be zero at all times to simulate rapid oxygen consumption by sulphide minerals in the tailings. In other words, the oxygen is consumed as fast as it is transported through the cover.

The solution for the flux at time t, using these boundary conditions is given by Crank (1975) as follows:

$$F(t)=(D\frac{\delta C}{\delta X})_{x=L} = 2C_0\sum_{n=0}^{\infty}(\frac{D}{\pi t})^{1/2}\exp[-\frac{(2n+1)^2L^2}{4Dt}]$$

[22]

The solution for the series is implemented in a computer program developed under the project by the University of Waterloo participants.

The flux of oxygen through a multi-layered cover system was calculated using a steady state diffusion model. The flux is a direct indication of the potential maximum rate of oxidation of sulphide minerals that may occur below a cover. For practical purposes, it is assumed that the time-dependent nature of diffusion in this composite cover system can be ignored. The mass flux F for steady state diffusion is described mathematically by the equation:

$$F = -D \frac{\delta C}{\delta x}$$

[23]

For a multi-layered system, the flux can be equated at the interface for any two adjacent layers with the resulting general equation:

$$(\frac{D_i}{L_i})C_{i+1} + (\frac{D_{i+1}}{L_{i+1}} - \frac{D_i}{L_i})\ C_i + (\frac{D_i+1}{L_i+1})\ C_{i+1} = 0$$

[24]

where i represents the i th layer. Evaluating the fluxes in this manner results in a system of equations (equal to the number of layers minus one) which can then be solved simultaneously.

It is assumed that a constant source oxygen concentration exists at the surface of the cover, equal to atmospheric value, and that the concentration at the base of the deepest layer is zero. The solution of the resulting system of independent equations, using a decomposition matrix routine, is also implemented in the University of Waterloo model mentioned above.

6.2 Oxygen and Acid Fluxes

As already mentioned, the demonstration column can be used for estimating oxygen fluxes. If the diffusion coefficients of the soils are precisely known, the fluxes can be calculated from the computer model. The flux can also be obtained from direct measurements using the apparatus shown in Fig. 22 without the need to precisely know the diffusion coefficients. The oxygen diffusing to the base of the column can be collected in a nitrogen atmosphere (say with the Teflon bag shown in Fig. 22) and then analyzed either on a gas chromatograph or with the trace oxygen analyzer, also shown in the photograph.

Figure 24 shows predictions of the base oxygen concentrations in the demonstration column using diffusion coefficients measured and estimated from empirical equations and the computer program, POLLUTE. The data indicate that attempting to measure the low level of oxygen in a stream of nitrogen (with a flow rate of 100 cm^3/min) is essentially impractical. For no flow conditions, the concentration of oxygen, as expected, is a function of the size of the collection bag.

The column is being tested with the 0.5 L bag. The concentration of oxygen expected at the base is only 80 ppm in 100 days and about 600 ppm in a year. The flux of oxygen through such a composite cover was calculated to be 5.7 x 10^{-5} mg/cm^2/day with POLLUTE and 5.37 x 10^{-5} mg/cm^2/day with the Waterloo model. Parameters used in the models are presented in Table 7.

The overall pyrite oxidation equation can be obtained by adding Equations [3] and [5] to yield :

$$FeS_2(s) + 15/4\ O_2(g) + 7/2\ H_2O\ (l) \rightarrow Fe(OH)_3\ (s) + 2H_2SO_4\ (aq) \qquad [25]$$

This equation implies that 1 mole of gaseous oxygen will oxidize 1 mole of pyrite in the presence of water to produce 0.53 mole of sulphuric acid. Therefore the maximum acid flux predicted from the oxygen flux observed in the demonstration column is 3.45 x 10^{-3} moles/m^2/a or 0.338 g/m^2/a of sulphuric acid (H_2SO_4). In lysimeter tests conducted under a different project at NTC, the maximum acid flux estimated from a tailings deposit without a cover is 1200 g/m^2/a of H_2SO_4. The steady state flux calculated for the uncovered tailings deposit at Waite Amulet using laboratory-measured diffusion coefficients is about 170 g/m^2/a of H_2SO_4.

Figure 25 presents oxygen fluxes computed using the Waterloo model. Two important conclusions can be drawn from the plots: (i) the most beneficial cover will be the one with a very low diffusion coefficient (< 1.0 x $10^{-8}m^2$/s), (ii) for covers with low diffusion coefficients (<2.5 x $10^{-7}m^2$/s), only a thickness of 1m is required to provide the maximum reductions in oxygen fluxes, (iii) a thickness of about 2m is required for a single cover with a higher diffusion coefficient (about 1.0 x$10^{-6}m^2$/s) to provide maximum benefits.

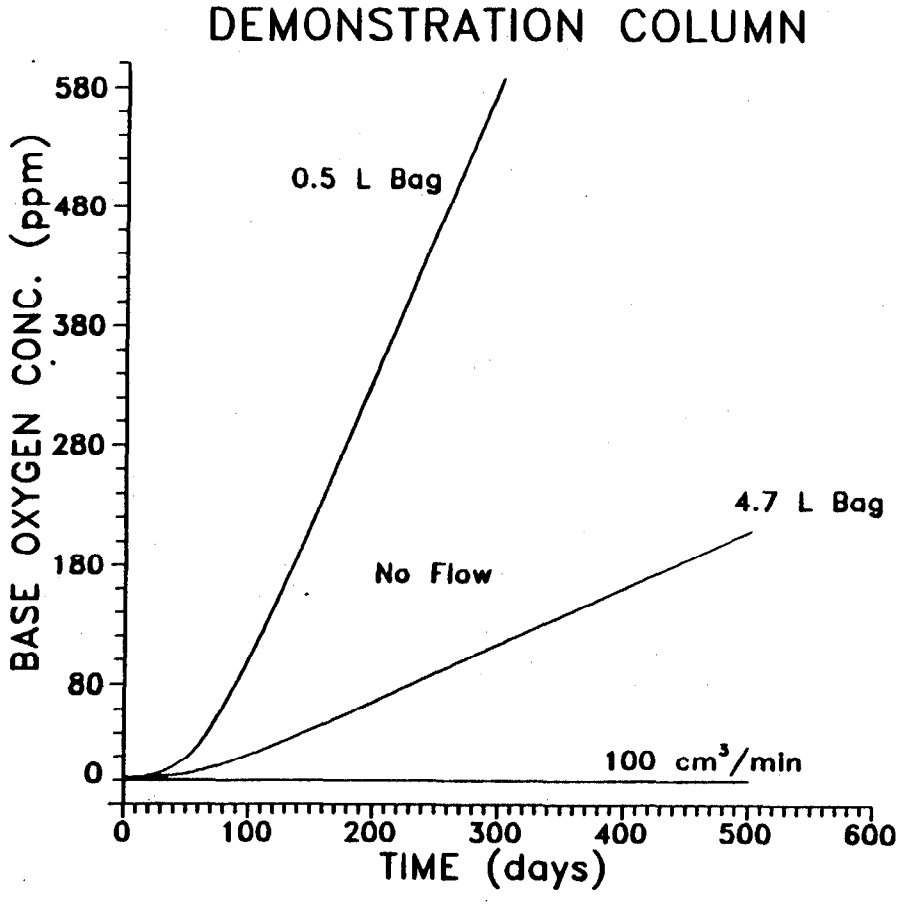

Figure 24 Base oxygen concentrations at different times predicted from demonstration column with POLLUTE.

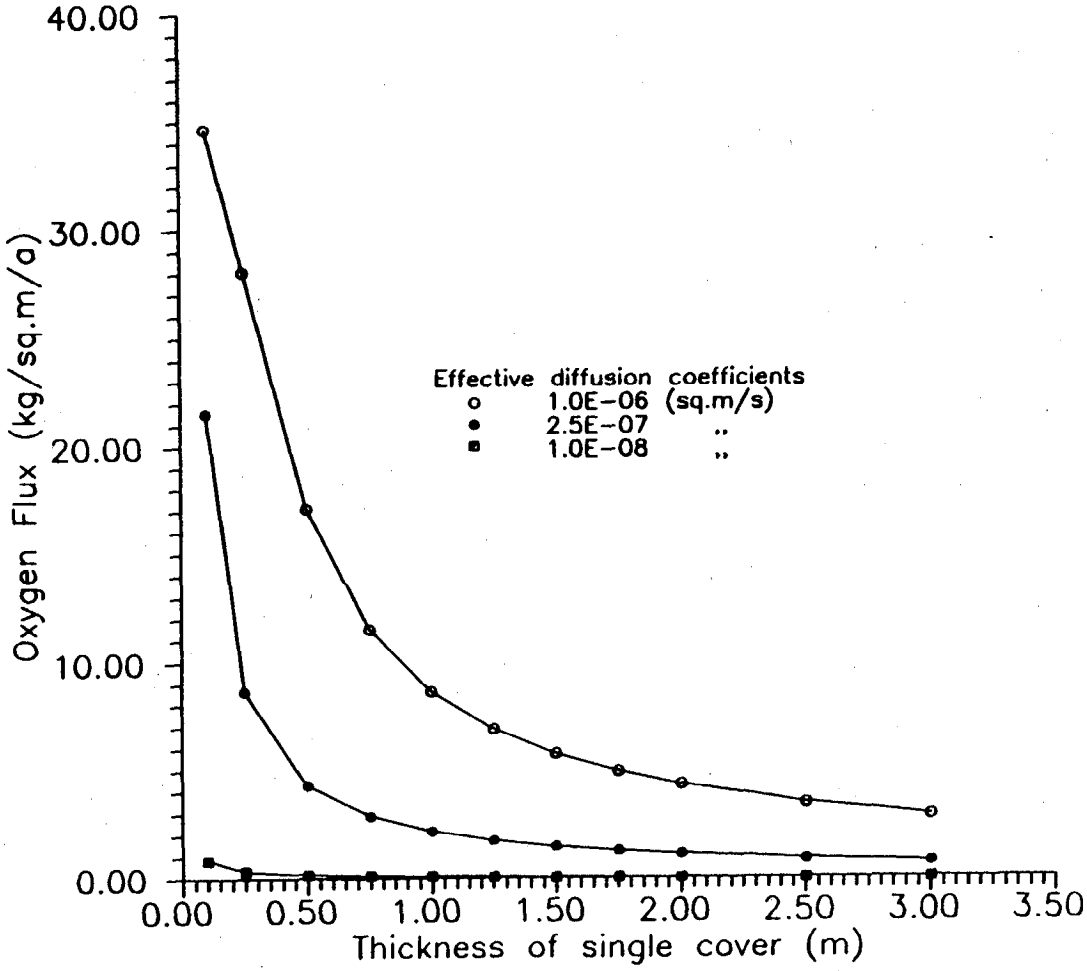

Figure 25 Variation of oxygen flux with cover thickness and diffusion coefficient.

TABLE 7

Parameters used for Modelling of Demonstration Column.

	Till Layer	Sand Layer
Thickness of Soil (cm)	6	25
Air-filled Porosity	0.009	0.198
Diffusion Coefficient (cm^2/day)	0.0864	3344
Water Saturation	0.98	0.50

Boundary Conditions

Top : Constant source (Co = 231,682 ppm)

Base : Fixed outflow velocity (equal to zero)

Initial Concentration : 2.5 ppm

Darcy Velocity : 0

6.3 Cover Design Considerations

A few practical concepts for designing high performance covers can be developed based on the results of this investigation. The initial requirements will be the identification and selection of

suitable materials and knowledge of their diffusion coefficients. From the preceding discussions, it can be stated that the best cover system will be one consisting of soil layers with large contrasts in textures and grain size distributions. Appropriate layering will be required to ensure that, upon drainage of the system, the finest layer will remain saturated. In general, the best material for the fine layer will be one which is able to withstand large suctions without drainage (for example, tills and clays). However, as mentioned shortly in this section, clays with high plasticities may not be suitable because of potential cracking upon freezing. The diffusion coefficient is dependent on the moisture content, which is in turn dependent on the porosity and other physical parameters such as the tortuosity. Diffusion coefficients can be determined using the equipment described in this report. A parallel evaluation of the grain size, moisture drainage and retention characteristics will also be required. Reliable relationships between diffusion coefficient and other more easily measured properties, such as moisture content or saturation, could also be used in place of column measurements. Ongoing work at the University of Waterloo is designed to develop one such relationship. Short-term (weeks) drainage characteristics of any appropriately layered system of materials can be assessed in a laboratory column using methods described in Section 5.2.2. Long-term (months) predictions can be obtained from saturated-unsaturated flow modelling. A few computer programs (for example, PC-SEEP) are available for this purpose.

From the results of evaluation of drainage characteristics, critical moisture contents and porosities can be established for flux calculations. Moisture fluxes from the fine layer into any underlying coarse layers, although small, should be considered and quantified, especially in the region where the hydraulic conductivity - suction curve flattens out. Maximum acid fluxes can then be calculated to give information on cover performance or effectiveness.

An important component of the design evaluation will be an assessment of the freeze-thaw behaviour of potential cover materials. Freeze-thaw evaluation of one of the candidate tills, HS-C, showed a frost heave of 15 to 20 mm on a 100 mm thick sample after only 2 cycles. Scanning electron photomicrographs of the sample taken at the end of the freeze-thaw cycles revealed the formation of ice lenses in the samples. The hydraulic conductivity, K, of the sample, however, did not change significantly after 8 freeze-thaw cycles. The K value increased only slightly from 2.9 to 3.2 x 10^{-7} cm/s. It appeared the sample heaved upon freezing and thawing

without a significant change in the volume of void spaces. Water intake into the sample was about 5 mL at the end of the first freezing cycle, compared to about 16 mL at the end of the second freezing cycle.

The water intake characteristics of the soils noted above support the observation of Konrad (1989) that soil samples compacted at a water content of about 2 percent higher than optimum, unless saturated by a back pressure technique, will absorb water during the first freezing cycle to attain full saturation. This may explain why, in the soil under investigation, the total frost heave during the first freezing cycle was less than the total frost heave at the end of the second cycle. A similar behaviour can be expected in an actual field cover application since the soil will not be fully saturated. It should also be mentioned that freeze-thaw effects vary with soil type. Chamberlain and Gow (1979) found that soils with high plasticity may develop shrinkage cracks during freezing. The development of these cracks will result in changes in internal volume. The amount of shrinkage is a function of the water content and degree of saturation (Penner, 1969). Less plastic soils, such as clayey silts, do not develop shrinkage cracks upon freezing (Konrad, 1989). The soils investigated in the present study are all sandy silts of low plasticity (with clay-sized fraction of only 5 to 14 percent) and are not likely to crack upon freezing.

It would seem that the best materials for a saturated cover will be a silty soil with a clay sized fraction of only about 20 percent. However, the effect of frost heaving has to be evaluated carefully. The depth of frost penetration and the freezing index for the area of application should be taken into account in the design and construction.

7. SUMMARY AND CONCLUSIONS

A contract to develop a laboratory apparatus for evaluating the effectiveness of engineered covers for reactive tailings was awarded to Noranda Technology Centre (NTC) by Supply and Services Canada in 1989. The project was jointly undertaken by NTC and the University of Waterloo in a subcontract with Noranda.

The investigation involved the development of laboratory methodologies through the measurement of pertinent standard material properties, design and construction of columns and

sampling and characterization of candidate cover materials from the vicinities of two active Canadian mine sites. A computer program was developed in the course of the investigation to simulate oxygen diffusion through various cover materials. Another computer program which is commercially available and more versatile than the one developed under the project was adapted to model the experimental schemes investigated. Based on the results of the investigation, the following is concluded :

1) Oxygen transport through fine-grained soil covers on reactive tailings is mainly by molecular diffusion through gas-filled pores. The rate of transport is controlled by the diffusion coefficient.

2) The diffusion coefficient, D_e, of natural soils decreases with increase in the degree of water saturation.

3) The flux of oxygen through covers placed in their nearly saturated states can be expected to be very low and would lead to reduced acid production.

4) Hydraulic conductivities of compacted candidate soils were observed to be of the order of 2×10^{-7} to 2×10^{-8} cm/s at hydraulic gradients of 15 to 60.

5) Any evaluation of potential cover materials should include an assessment of hydraulic behaviour (moisture retention and drainage characteristics). In laboratory column investigations, a saturated candidate till underlain by a medium to coarse-grained sand layer maintained its moisture content up to 100 days. Observed pressure head profiles showed time-dependent drainage to residual saturation. Saturated and unsaturated flow modelling confirmed the laboratory behaviour.

6) A computer-based oxygen diffusion model developed under the project can be used to calculate fluxes for various cover design scenarios.

7) A demonstration column has been developed for measuring the low oxygen fluxes expected in nearly saturated soil covers. The acid flux predicted from the oxygen flux determined in the column was about 0.338 $g/m^2/a$ of H_2SO_4.

8) Freeze-thaw evaluation of candidate soils should be part of any design scheme. For soils with significant silt contents, the depth of frost penetration in an actual field application should be assessed. Soils with very high clay contents may not be suitable because of potential cracking upon freezing.

REFERENCES

Akindunni, F.F., R.W. Gillham, and R.V. Nicholson (1990) Numerical simulations to investigate moisture retention characteristics in the design of oxygen-limiting covers for reactive mine tailings. Submitted to the Canadian Geotechnical Journal.

ASTM D1557-78 (1978) Standard methods for moisture-density relations of soils and soil-aggregate mixtures. In: Soil and Rock; Building Stones; Geotextiles, Vol. 04.08, Annual ASTM Standards, Section 4 Construction, pp. 280-286.

Barbour, S.L. (1987) Role of physicochemical effects on the behaviour of clay soils. Proceedings of the 40th Canadian Geotechnical Conference, Regina, Sask., pp. 323-342.

Bowles, J.E. (1986) Engineering properties of soils and their measurement. McGraw-Hill Book Company, New York.

Chamberlain, E.J., and A.J. Gow (1979) Effect of freezing and thawing on the permeability and structure of soils. Engineering Geology (Amsterdam), 13:73-92.

Childs, E.C. (1967) Soil moisture theory. Advances in hydroscience, pp.73-117.

Collin, M. (1987) Mathematical modelling of water and oxygen transport in layered soil covers for deposits of pyritic mine tailings. Licentiate Treatise. Department of Chemical Engineering, Royal Institute of Technology, Stockholm. 189p.

Collin, M., H. Lindberg, H., and M. Lindgren (1990) Modelling of water and oxygen transport in layered soil covers. Codes for deposits of pyritic mine tailings. Kemakta Consultants Co. Stockholm.

Craig, R.F. (1974) Soil mechanics. 1st edition, Van Nostrand Reinhold Co. Ltd., England.

Crank, J. (1975) The mathematics of diffusion. 2nd. edition. Clarendon Press, Oxford, U.K.

Daniel, J.A., J.R. Harries, A.I.M. Ritchie (1980) Water movement caused by monsoonal rainfall in an overburden dump undergoing pyritic oxidation. pp. 623-629.

Daniel, D.E., D.C. Anderson, and S.S Boynton (1985) Fixed-wall versus flexible-wall permeameters. In: Hydraulic barriers in soil and rock. ASTM Special Technical Publication 874, pp:107-123.

Das, B.M. (1983) Advanced soil mechanics. McGraw-Hill Book Company, New York.

Dreimanis, A. (1962) Quantitative gasometric determination of calcite and dolomite by using Chittick apparatus. Journal of Sedimentary Petrology, 32:520-529.

Fernandez, F., and R.M. Quigley (1985) Hydraulic conductivity of natural clays permeated with simple liquid hydrocarbons. Canadian Geotechnical Journal, 22:205-214.

Filion, M.P. and K. Ferguson (1989) Acid mine drainage research in Canada. Proceedings of the international symposium on tailings and effluent management, Halifax. Tailings and Effluent Management. pp. 61-72.

GEO-SLOPE (1967) PC-SEEP A finite element program for seepage analysis. Users' Manual. GEO-SLOPE Programming Ltd. Calgary, Alberta.

Gillham, R.W., A. Klute, and D.F. Heerman (1976) Hydraulic properties of a porous medium: Measurement and empirical representation. Soil Sci. Soc. Amer. Jour., Vol. 40. pp. 203-207.

Green, R.E., and J.C. Corey (1971) Calculation of hydraulic conductivity: a further evaluation of some predictive methods. Soil Science Soc. Amer. Proc., Vol 35. pp.3-8.

Ho, P.G. (1979) The prediction of hydraulic conductivity from moisture suction relationship. B.Sc. Thesis, University of Saskatchewan, Saskatoon, Canada, 530pp.

Holtz, R.D. and W.D. Kovacs (1981) An introduction to geotechnical engineering. Prentice-Hall, Inc., New Jersey.

Hughes, O.L., R.B. Campbell, J.E. Muller, and J.O. Wheeler (1969) Glacial limits and flow patterns, Yukon Territory, South of 65 Degree North Latitude. Geol Survey Can. Paper 68-34, 9p.

Keele, J. (1910) A reconnaissance across the MacKenzie River, Yukon and N.W.T. Geol. Survey Can. Pub. No. 1097.

Konrad, J.-M. (1989) Effect of freeze-thaw cycles on the freezing characteristics of a clayey silt at various overconsolidation ratios. Canadian Geotechnical Journal, Vol. 26, No. 2, pp. 217-226.

Lai, S-H., J.M. Tiedje, and A.E. Erickson (1976) In-situ measurement of gas diffusion coefficient in soils. Soil Sci. Soc. Amer. J., Vol. 40, pp. 3-6.

Lambe, T.W., (1958) The structure of compacted clay. Journal of the Soil Mechanics and Foundation Division, ASCE, Vol 84, No. SM2, 1654-1 to 1654-34.

Lambe, T.W., and R.V. Whitman, (1979) Soil mechanics. John Wiley and Sons Inc., New York.

Lemon, E.R., and A.E. Erickson (1952) The measurement of oxygen diffusion in the soil with a platinum microelectrode. Soil Sci. Soc. Proc.,pp. 160-163.

Leonards, G.A. and B.K. Ramiah (1959) Time effects in the consolidation of clay. Papers on soils - 1959 Meeting, American society for Testing and Materials, Special Technical Publication No. 254, pp. 116-130.

Liakopoulous, A.C. (1965) Theoretical solution of the unsteady unsaturated flow problems in soils. Bulletin of the International Association of Scientific Hydrology Vol. 10. pp.5-39.

Magnusson, M. and A. Rasmuson, A (1984) Gas diffusion in unsaturated porous media. The National Swedish Environmental Protection Board, Report SNV PM 1843.

Millington, R.J. and R.C. Shearer (1971) Diffusion in aggregated porous media. Soil Science Vol. 111. pp.372-378.

Mitchell, J.K. and J.S. Younger (1967) Abnormalities in hydraulic flow through fine-grained soils. ASTM Special Technical Publication 417, pp. 106-139.

Mitchell J.K. (1976) Fundamentals of soil behaviour. John Wiley & Sons Inc., New York., 422p.

Mualem, Y. (1976) A new model for predicting the hydraulic conductivity of unsaturated porous media. Water Resources Research Vol. 12. pp.513- 522.

Nicholson, R.V., R.W. Gillham, J.A. Cherry, and E.J. Reardon (1989) Reduction of acid generation in mine tailings through the use of moisture-retaining cover layers as oxygen barriers. Canadian Geotechnical Journal, Vol. 16, No. 1, pp. 1-8.

Nielson, K.K., V.C. Rogers, and G.W. Gee (1984) Diffusion of radon through soils: a pore distribution model. Soil Science Society of America Journal 48:482-487.

Olson R.E. and D.E. Daniel (1981) Measurement of the hydraulic conductivity of fine- grained soils. Permeability and groundwater contaminant transport, ASTM Special Technical Publication 746, pp. 18-64.

Papendick, R.I., and J.R. Runkles (1965) Transient-state oxygen diffusion in soil: I. The case when rate of oxygen consumption is constant. Soil Sci. Vol. 100, pp.251-261.

Parizek, R.R. (1985) Exploitation of hydrogeologic systems for abatement of acidic drainages and wetland protection. In: Wetlands Water Management Mined Lands Conference, Pennsylvania State University, October 23-24, pp. 19-53.

Penner, E. (1969) Frost heaving forces in leda clay. Canadian Geotechnical Journal, Vol. 7, pp. 8-16.

Rampton, V.N., R.C. Gauthier, J. Thibault, and A.A. Seaman (1984) Quaternary geology of New Brunswick, Geol. Survey Can. Memoir 416, 77p.

Rasmuson, A. and J.C.Eriksson (1986) Capillary barriers in covers for mine tailings dumps. National Swedish Environmental Protection Board Report 3307.

Reardon, E.J., and P.M. Moddle (1985) Gas diffusion coefficient measurements on uranium mill tailings: Implications to cover layer design. Uranium, 2, pp. 111-131.

Rogers, V.C., K.K. Rich, G.M. Sandquist, and M.L. Mauch (1982) Radon attenuation with earthen covers. RAE-33-14. Annual Report to U.S. Department of Energy UM-TRAP Project Office, Rogers and Associates Engineering Corp., Salt Lake City, Utah.

Rowe, R.K. and J.R. Booker (1990) Pollute V5.0 1-D pollutant migration through a non homogenous soil, User Manual. Geotechnical Research Centre. Faculty of Engineering Science, The University of Western Ontario. Report No.GEOP 90-1.

Silker, W.B. and D.R. Kalkwarf (1983) Radon diffusion in candidate soils for covering uranium mill tailings. NUREG/CR-2924. U.S. Nuclear Regulatory Commission, Washington D.C.

Sydor, R.C. (1990) Moisture control in porous media by selective layering. Unpublished B.A.Sc. Thesis, University of Waterloo, Canada. 66p.

Taylor, D.W. (1948) Fundamentals of soil mechanics. Wiley, New York.

Taylor, S.A. (1949) Oxygen diffusion in porous media as a measure of soil aeration. Soil Sci. Soc. Am. Proc., Vol. 14, pp. 55-61.

Topp, G.C., J.L. Davis, and A.P. Annan (1980) Electromagnetic determination of soil water content: measurement in coaxial transmission lines. Water Resources Research. Vol.16. pp.574-582.

Troeh, F.R., J.D. Jabro, and D. Kirkham (1982) Gaseous diffusion equations of porous materials. Geoderma 27: 239-253.

Van Brakel, J., and P.M. Heertjes (1974) Analysis of diffusion in macroporous media in terms of a porosity, a tortuosity and a constrictivity factor. Int. J. Heat Mass Transfer, Vol. 17. pp.1093-1103.

Yanful, E.K., M.D. Haug, and L.C. Wong (1990) The impact of synthetic leachate on the hydraulic conductivity of a smectitic till underlying a landfill near Saskatoon, Saskatchewan. Canadian Geotechnical Journal 27: 509-519.

Yanful, E.K. and L.C. St-Arnaud (1991) Design, instrumentation and construction of engineered soil covers for reactive tailings management. These proceedings.

Yong, R.N., P. Booninsuk, and A.E. Tucker (1984) A study of frost-heave mechanics of high-clay content soils. Journal of Energy Resources Technology, Vol. 106, December, pp. 502-508.

APPENDIX A

FINAL REPORT

DEVELOPMENT OF A LABORATORY PROCEDURE FOR EVALUATING THE EFFECTIVENESS OF REACTIVE TAILINGS COVERS

SUBMITTED TO:

CENTRE DE TECHNOLOGIE NORANDA
240 BOUL. HYMUS
POINTE CLAIRE, QUEBEC
H9R 1G5

SUBMITTED BY:

UNIVERSITY OF WATERLOO
WATERLOO, ONTARIO
N2L 3G1

PRINCIPAL INVESTIGATORS:
R.W. GILLHAM
R.V. NICHOLSON

27 NOVEMBER 1990

INTRODUCTION

This is the final report of an investigation contracted as a research project to the University of Waterloo by Noranda Technologie in February 1989. Drs. R.W. Gillham and R.V. Nicholson were the Principal Investigators of the project. A copy of the proposal submitted by the University of Waterloo to Noranda is included in Appendix 1.

The primary objective of this investigation was to experimentally verify the role of near-saturated porous granular materials as barriers to oxygen diffusion. This involved the measurement of diffusion coefficients in granular materials near saturation and the demonstration that oxygen flux was subsequently limited by a layer of such material.

The primary objective was only partially achieved. The measurement study is in progress due to long delays resulting from experimental problems. The demonstration study remains incomplete due to the lack of a sufficiently sensitive method to measure low oxygen fluxes that are expected for near-saturated materials.

The major components of the investigation are described in this report with a brief description of the attempted experimental techniques, model development and ongoing work.

BACKGROUND

Reactive sulphide mine wastes that are exposed at the earth's surface can produce acid mine drainage. Oxidation by atmospheric oxygen has been identified as the ultimate cause of the acidification process. A large number of remediation schemes that have been proposed for abatement of AMD are based on the isolation of wastes from oxygen. Flooding and encapsulation of wastes in impermeable materials represent two possible approaches to AMD abatement. Alternatively, fine-grained granular materials such as natural silts or desulphurized tailings may be used as an oxygen barrier with appropriate layering (Nicholson et. al.,1989). The key to the use of a fine-grained layer over the wastes, is the control of the water content that must remain near saturated values even when the water table occurs at depth.

The hydraulics of controlling high water contents by selective textural layering has been discussed by Nicholson et. al. (1989, 1990) and has been demonstrated in the laboratory by Sydor (1990). The results reported by Sydor (1990) confirm the numerical simulation of time-dependent drainage in a layered system described by Akindunni et. al. (1991). Both the laboratory and modelling results suggested that water contents near saturation will be stable for significant periods without further recharge and that under the appropriate conditions, the water content of the cover will be independent of the depth to the water table.

It is well known that water content affects the diffusion of gases in soils. There is an abundance of literature that addresses the dependence of the diffusion coefficient of natural soils on the relative saturation. With few exceptions, however, these studies apply to the movement of gases in moderate- to well-drained soils related to the agricultural concern for root aeration of crop roots. For the most part, empirical models were developed to describe experimental data in soils that exhibited water contents far less than 80 percent of full saturation. So that although it was known that increasing water content leads to lower diffusion coefficients in soils, there was little information on porous materials that approached saturation. In order to apply the concept of moist covers to the abatement of sulphide-mineral oxidation more appropriate models are required. These models must account for the very significant changes in the diffusion coefficient for small differences in the water content in the upper range of saturation.

Very few data are available for diffusion experiments at high water contents. It is recognised that these data are important to verify the appropriate models. The limited number of data and lack of more relevant models for near-saturated porous materials led to the initiation of this investigation.

PURPOSE AND SCOPE OF THE STUDY

The purpose of this investigation was to verify the reduction in oxygen flux for laboratory simulations of granular covers over sulphide tailings. The study was divided into three areas of investigation;

1. Diffusion measurements in granular porous materials as a function of water content in the range of near-saturation;

2. Development of a column to demonstrate the effectiveness of a moist layer in reducing the flux of oxygen.

3. Development of a practical mathematical model to calculate the flux of oxygen through a cover layer.

The diffusion measurements study required the development of a method that would be sufficiently sensitive to detect fluxes on the order of those expected through a water column. This necessitated the use of a transient method in contrast to the steady-state methods used by other investigators for lower water content conditions (e.g. Reardon and Moddle, 1985). Because diffusion was expected to limit mass fluxes to very low levels, it was also necessary to use tracers that have sensitive detection limits. The rationale and a brief chronology of the diffusion measurement study is given in the following sections.

Preliminary concepts of a demonstration column had been presented in a previous report (Siwik et. al., 1988). Although the main components such as an oxygen sink and detectors were identified, no methods had been tested and development of such methods was necessary for this investigation to proceed. In effect, the oxygen sink that would simulate tailings below the cover was the key to the development of a demonstration column. The oxygen sink specifications included a rapid uptake of oxygen from the gas phase and a significant change in a measurable property for low oxygen fluxes. The rationale and a brief chronology of the oxygen sink experiments is given in the following sections.

The purpose of the modelling activity was to develop a model that would perform flux calculations through proposed covers. The description of the model and other documentation is provided in the following sections.

DIFFUSION MEASUREMENTS STUDY

Diffusion Measurements

Rationale

The reduction in diffusivity of any gas through a material is largely the result of specific properties of the material itself, such as air-filled porosity, tortuosity and the extent of blocked pores. Thus, if the ratio D/D_0 is measured for one gas which does not react with the material (where D is the effective diffusion coefficient through the material and D_0 through air), it can be used to approximate the diffusion coefficient of another gas through the same material; in other words:

$$D_b = D_{ob}(D_a/D_{oa})$$

D_b = effective diffusion coefficient of gas B
D_{ob} = diffusion coefficient of gas B in air
D_a = effective diffusion coefficient of gas A
D_{oa} = diffusion coefficient of gas A in air

Reardon and Moddle (1985) developed a sensitive steady-state conducmetric technique whereby D/D_0 values were measured using carbon dioxide as a tracer. It was originally anticipated that this method would be used in the current study.

Principle of the CO_2 method

The granular sample with a known moisture content, is packed into a cylindrical Pyrex sample holder. A gas chamber is attached to one end of the sample holder and a CO_2/N_2 mixture is circulated through this reservoir to maintain a constant CO_2 partial pressure. The other end of the sample holder is connected to a Pyrex reaction vessel containing a NaOH solution. The diffusion cell is then immersed in a constant temperature bath at 25 °C.

As carbon dioxide diffuses through the inert porous material and into the NaOH solution, the electrical conductance of the latter decreases due to the decrease in the highly conductive OH^- ions that are replaced by less conductive HCO_3^- and CO_3^{2-}.

Following the calibration of the drop in electrical conductance as a function of CO_2 intake, the diffusive flux of carbon dioxide can be easily monitored. After an initial period of evaluation, it was determined that this method is appropriate and convenient when the diffusion coefficient of the test material is two orders of magnitude larger than that through water. The diffusion coefficients of gases in water are very low. They are in the order of $1.0 * 10^{-9}$ m^2/s. Therefore, under high degrees of saturation, the transient period of diffusion can be very long. It was estimated that the transient period for the experimental set-up of interest might extend for as long as six to seven weeks. The CO_2 fluxes under these conditions are on the order of $1.0*10^{-8}$ g/min and it is doubtful whether the method is sufficiently sensitive to detect such small fluxes.

Since the Reardon and Moddle technique was judged unsuitable, a new tracer and method were required.

Transient Diffusion Experiments

A transient measurement technique was required to study gaseous diffusion in near-saturated porous materials to achieve reasonable experimental times.

A transient measurement involves the establishment of concentration gradients of a tracer from one end of a sample to another. Before steady-state is established, the material is sampled for the tracer and the observed concentration profile is used to compute the diffusion coefficient of the test material. The diffusion measurements were designed to be made in a cylindrical column, holding the test sample along which samples could be collected at a specified time.

Choice of Tracer

The choice of an appropriate tracer is critical in the context of these experiments. The characteristics of an ideal tracer include the following: 1. low concentration in the atmosphere to avoid contamination of the material, 2. chemically stable, 3. similar physico-chemical properties to oxygen (i.e. low water solubility and diffusion coefficient in the same order of magnitude) and 4. high sensitivity to detection (i.e. very low detection limits).

A literature review was undertaken and four broad groups of gaseous tracers were first examined:

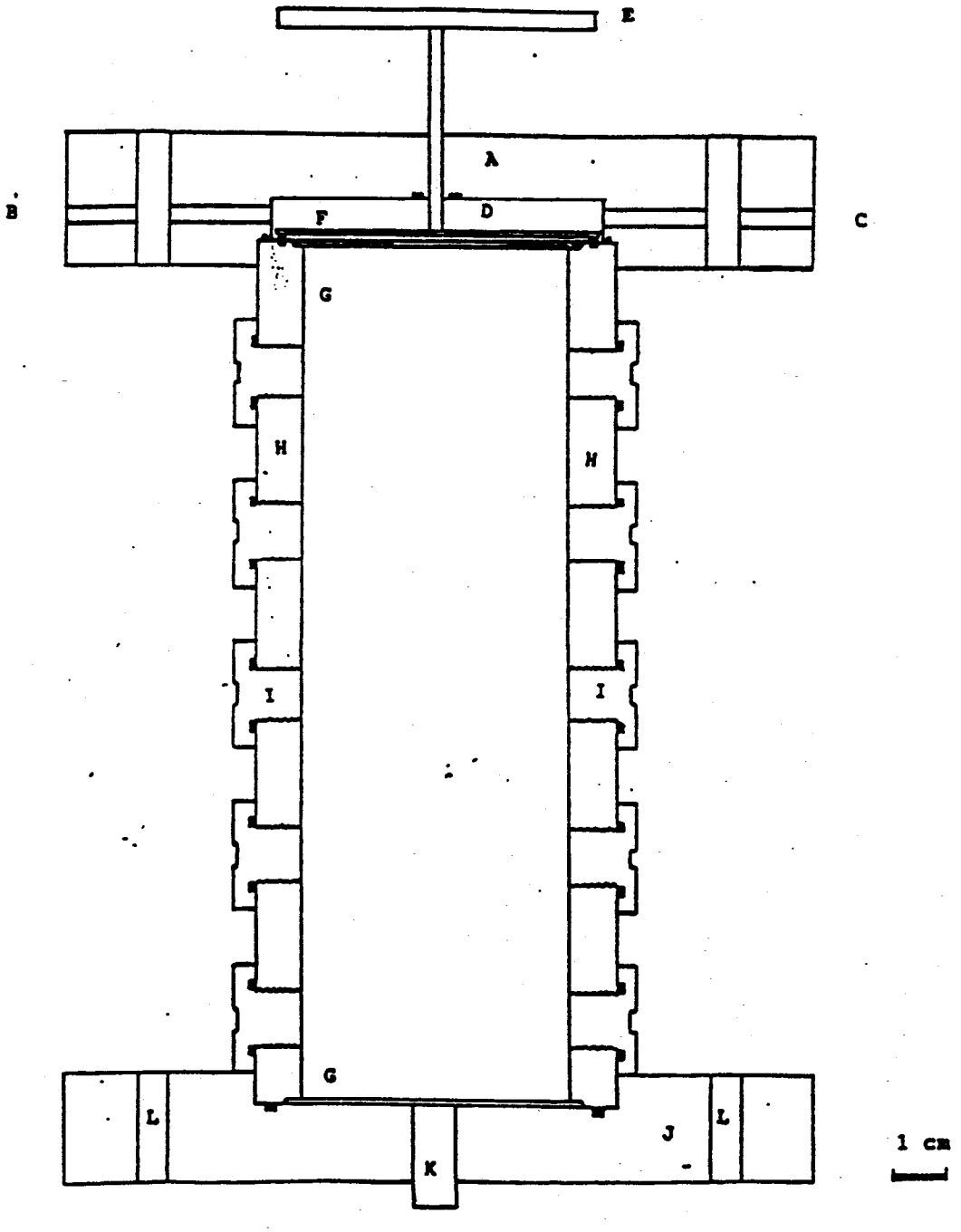

FIGURE 1 Cross-section through the diffusion cell

A) top plate B) gas inlet C) gas outlet
D) head space E) handle F) stainless-steel plate
G) stainless-steel screen H) barrel
I) bolt for sampling port J) bottom plate
K) CO_2 inlet L) rod insertion holes

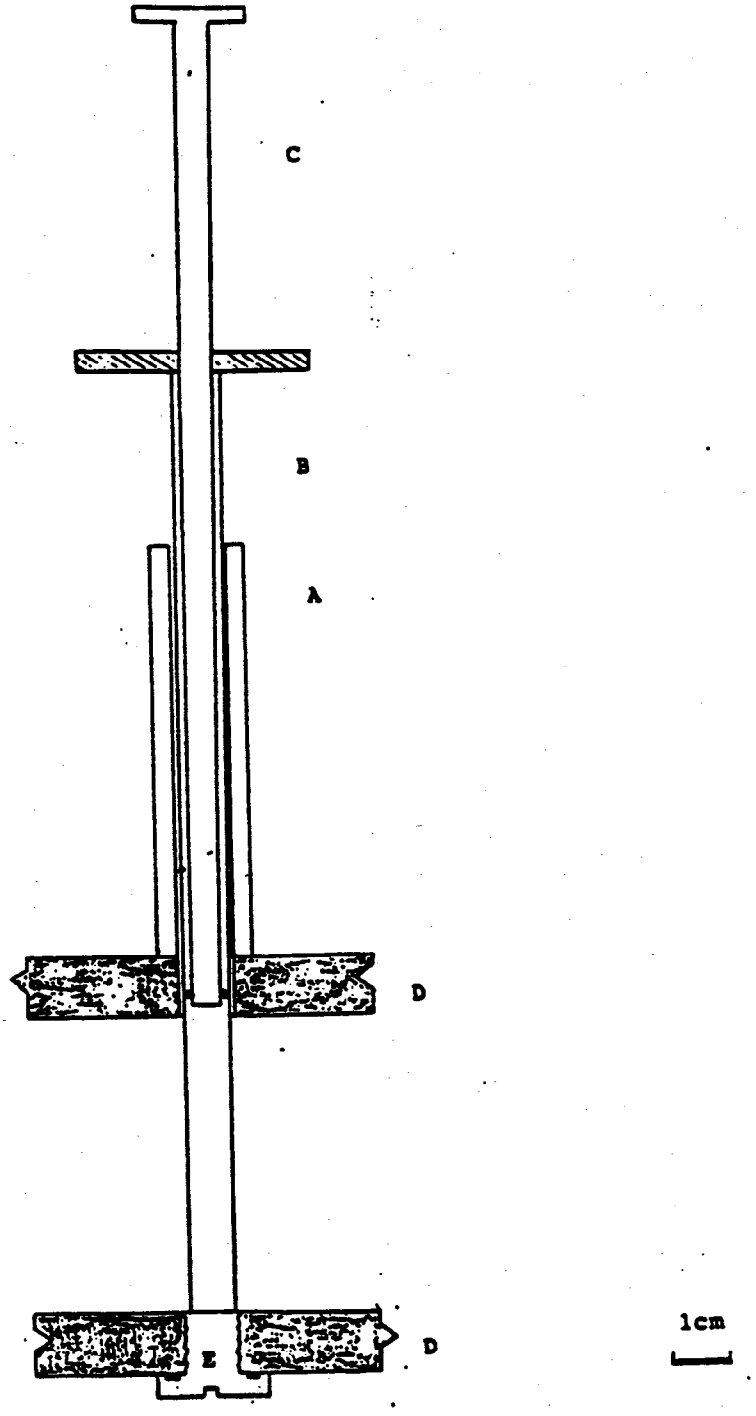

FIGURE 2 Cross-section through the coring equipment.

A) aluminum guide, B) thin wall stainless steel tube
C) plunger equipped with viton o-ring
D) diffusion cell wall
E) bolt

Radioactive gases

Although the analysis for radionuclides is straightforward, the use of such tracers in gaseous form was rejected because of the danger involved in their handling (e.g. accidental breathing due to unexpected leaks).

Stable isotopes

There is a wide variety of stable isotopes, some of which are very close to atmospheric oxygen in terms of their physical-chemical properties. Unfortunately, the cost of the tracers and of the analyses were considered to be unreasonably high and beyond the budget for this project. These analyses and need for sophisticated and costly equipment is not convenient for routine use, although limited research may be appropriate especially if othe methods of measuring low fluxes of oxygen are not found to be useful.

Noble gases

The use of noble gases has several advantages. The concentrations of these gases in the atmosphere are low and they are stable. The physical-chemical properties of argon are close to those of oxygen. Preliminary analytical work showed, however, that the detection limit that we could achieve on our gas chromatographs was not low enough to detect concentrations expected with the low flux of gas through near-saturated materials.

Organic compounds

Consideration was also given to a class of organic liquids known as "solvents". This group of liquid organic compounds is very large and hence different solvents display a wide range of physical-chemical properties. In addition, they can be easily be detected by gas chromatography and the detection limit for these compounds is very low (a few ppb). The solubility of most solvents in water is generally low and the vapour pressure of some of these compounds is fairly high, thus it is easy to produce vapours of these compounds.

Trichloromethane (chloroform) and trichloroethylene (TCE) were selected as tracers for the transient diffusion experiments. They are volatile, making vapour production simple, and analyses of these compounds in the aqueous phase, using a gas chromatograph is straightforward. The water solubility at 25 °C is 7000 and 1100 ppm respectively. A mixture of these two solvents was prepared and air was bubbled through it to generate a gas mixture saturated with

respect to these two tracers.

Diffusion Cell

The proposed testing required a new design for a diffusion cell. The design of the apparatus allows sampling of the aqueous and gaseous phases of the porous medium after a transient gaseous diffusion experiment.

The diffusion cell consist of three major parts (Figure 1). The overall length is 22 centimetres and the dimension of the widest part is 14 centimetres. The zero-flux boundary is first attached to the barrel by friction using a viton O-ring. A thin stainless steel screen prevents the silt material in the barrel from escaping. The base plate contains an access port for CO_2 flushing and for saturating the sample.

The barrel of the cell is 15.5 centimetres long with an I.D. of 5 centimetres. It contains 10 sampling ports distributed at right angles to one another along the length of the cell. During the experiment, Plexiglas bolts equipped with viton o-rings will provide a complete seal between the interior of the barrel and the atmosphere. A second stainless steel screen is secured to the top of the barrel. This holds the porous material in place, below the tracer input end-cap.

The end-cap at the input boundary is equipped with a 5 millimetre deep gas reservoir and a movable plate to isolate the sample from the tracer until the experiment is set to begin. Inlet and outlet holes are drilled on opposite sides of the gas reservoir. When the handle is down, a thin stainless steel plate, attached at the lower end of the vertical handle, rests on a viton o-ring which sits above the top stainless steel screen. This allows flushing of the gas reservoir with the chloroform-TCE vapour until a steady input concentration is achieved. At time zero, the handle is raised. This causes the material to be exposed to the vapour and allows the diffusion process to begin. Note that viton o-rings provide air and water tight seals where required.

Proposed Methods and Materials

After a specified time interval which allows a concentration profile to develop in the sample, the column is cored (Figure 2). While the cell rests on its side a bolt on the side facing up is removed and a thin wall stainless tube is pushed through the silty material until it makes contact with the bolt on the opposite side of the diffusion cell. This second bolt is then removed to allow penetration of the coring device. The material is then extruded from the latter using a stainless steel plunger equipped with a small viton o-ring at the bottom. The material is extruded into a hypovial containing pentane. The pentane acts as a strong sink for the chloroform and TCE present in the aqueous and gaseous phases in the core. The pentane is subsequently analysed for both

compounds. This provides the concentration of the tracers in the column. Coring and soil extraction is performed on the 10 sampling ports.

Construction of the cell was undertaken at a time when inorganic tracers were expected to be used. Thus the initial cell was constructed of Plexiglas. Nevertheless, previous tests had shown Plexiglas to be inert to dissolved concentrations of the organic tracers that were selected, and thus the initial trials proceeded using the Plexiglas cell. These tests showed that at the high concentrations present in the vapour phase, the Plexiglas was seriously degraded. Subsequent to these tests, a second cell has been constructed of stainless steel and brass components. This cell was completed only recently and tests have yet to be initiated.

Porous Materials

During initial testing, it is desirable to use inert porous materials. For this reason, quartz sand and silt mixtures have been selected. A mixture of 70% (dry weight) medium sand and 30% fine silt provides a material that displays the physical properties required for this study (i.e. a heterogeneous grain size distribution and an air entry pressure greater than 15 centimetres of water corresponding to the length of the column).

Vapour Generation System

Several vapour generation systems were evaluated, exhibiting different degrees of success. The system that has proven most convenient consists of 3 glass reservoirs with stainless steel lids that are connected to one another by stainless steel tubing (Figure 3).

Air is bubbled through the reservoir containing de-ionized water. This ensures saturation of the air with water. The humid air is then bubbled through the gas reservoir of the diffusion cell. The gas mixture then passes through the third glass reservoir, which is equipped with a sampling port for analysis, before being recirculated through the system.

Gas Analysis

A considerable period of time was devoted to the analysis of the chloroform-TCE air mixture. Various attempts were made to establish calibration curves for chloroform and TCE. Finally, liquid chloroform and TCE standards (in pentane) were prepared and different alliquots of the standards were injected into several 1-litre amber bottles. After allowing enough time for complete volatilization of the compounds, 500 ml of gas were withdrawn from the bottles with a 1 ml gas-tight syringe

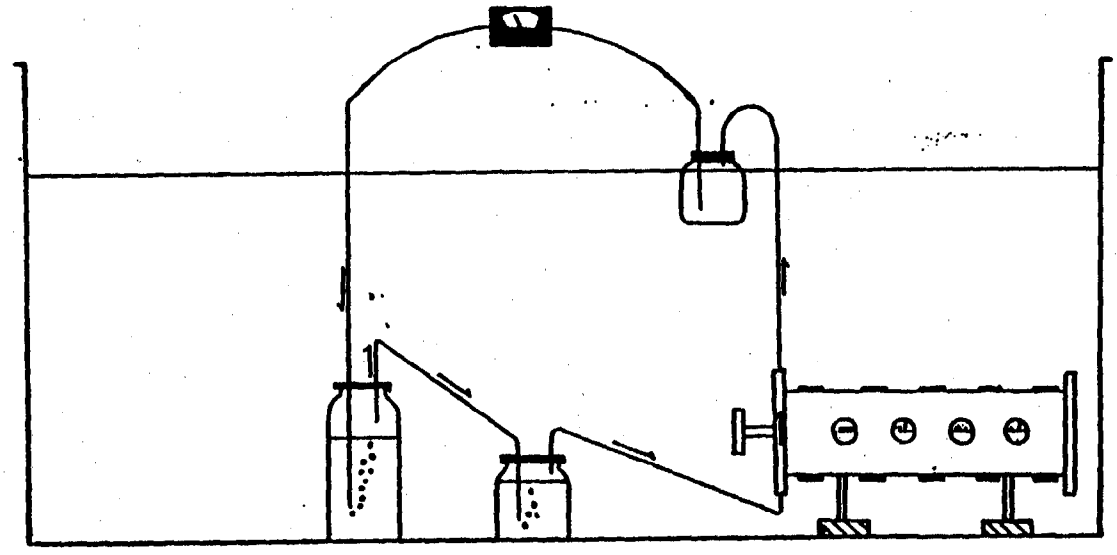

FIGURE 3 Schematic diagram of the experimental set-up. Air is first bubbled through a 500 ml amber bottle partially filled with water and subsequently through a 125 ml amber vial containing a chloroform and TCE mixture. The vapour is then circulated in the headspace of the diffusion cell wich is resting on its side. It is connected to a small gas reservoir required for sampling of the gas phase. The same gas mixture is constantly rejuvinated and recirculated by a small peristaltic pump. The equipment is immersed in a water bath at 25 °C.

(pressure-lock) and subsequently injected into a gas chromatograph through a sampling loop. The peak areas on the chromatograms (GC) were used to produce calibration curves.

The gas reservoir is sampled by withdrawing an aliquot of gas (20 ml) and injecting it in a 1-litre amber bottle. An aliquot of this diluted sample is then injected into the G.C. and the concentrations of both compounds are found by comparison with the calibration curves. Due to the drift of the gas chromatograph, calibration curves must be prepared daily.(see Figure 4)

Sample Preparation

The porous material is oven-dried at 110 °C overnight before packing it in the diffusion cell. The bottom and top plates are removed from the barrel to facilitate handling. The top end of the barrel is temporarily closed by applying masking tape to the top stainless steel screen. The barrel is then weighed. It is subsequently filled through the bottom end with the oven-dried sand-silt mixture by 1 centimetre lifts. The barrel is weighed after the addition of every lift. Each of these is packed tightly using a 2.54 centimetre diameter PVC rod. The surface of the material is "hatched" with a fork prior to the addition of the following lift. This is performed in order to enhance contact between adjacent lifts. The material must be packed tightly in order to avoid horizontal fracturing upon wetting.

Once the material is packed in the barrel, the masking tape is removed and both plates are attached to it. Carbon dioxide is then circulated in the porous medium to remove air from the pores. Because CO_2 is much more water soluble than air, the latter step ensures that all pores become water saturated upon wetting.

To saturate the sample, de-ionized water is de-aired for at least three hours. A piece of five-millimetre diameter Tygon tubing links the erlenmyer containing the DI water to the CO_2 inlet. This tubing is filled with water prior to its insertion in the bottom plate. At this point, the water level in the erlenmyer is brought at the same height as the bottom of the barrel. This causes hydraulic contact with the bottom of the porous material column.

By capillarity, the water rises in the material until all the pores are filled with water along the entire length of the barrel. (Note that the air-entry pressure of the material is < -16.5 centimetre of water.) Although this first step ensures the complete saturation of the material, the erlenmyer is nevertheless slowly elevated by small increments until the water level in it is at the same height as the top of the diffusion cell. The system is then allowed to equilibrate for twenty-four hours, after which the erlenmyer is brought back down to its original level to cause the drainage of any "free-water" if present. The system is allowed to re-equilibrate for forty-eight hours and the cell and

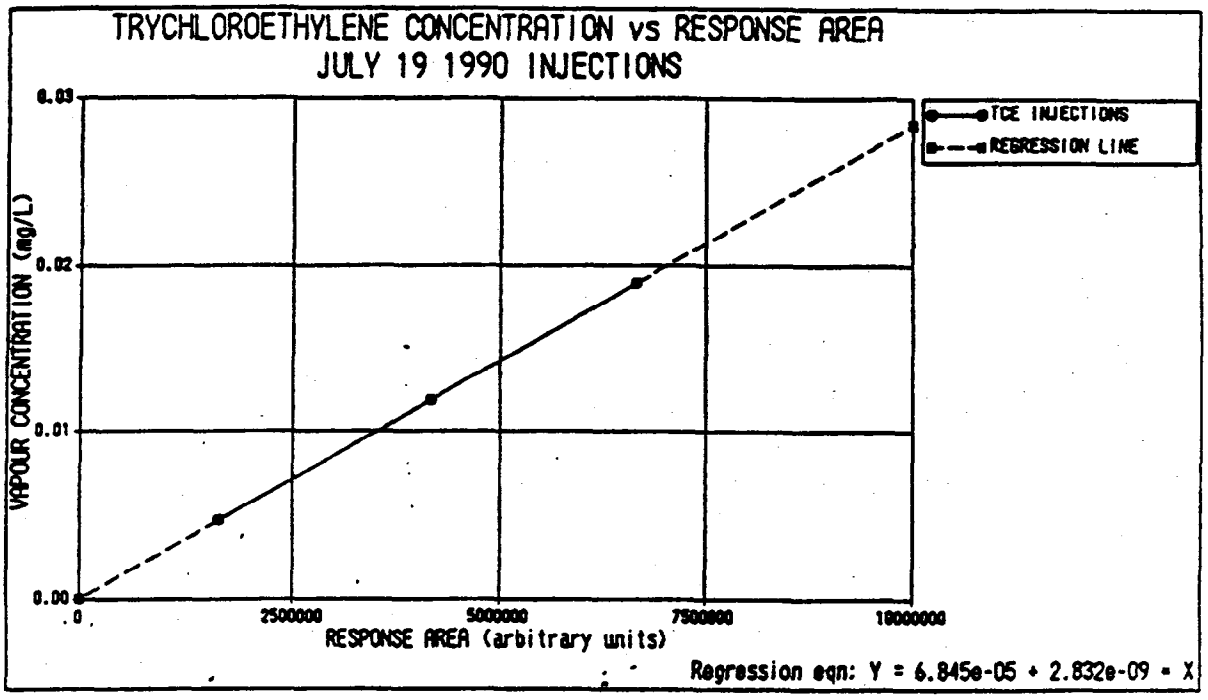

FIGURE 4 Trichloroethylene calibration curve and regression line. The circles represent the injections of the gas samples of known concentration and the squares define the regression line. The response areas obtained from the chromatograms of the gas reservoir analyses are then plotted on the regression line and the TCE concentration is then extrapolated. The same methodology is applied to the chloroform analyses.

Fig 4 was not included in report

the material are then ready for connection in the vapour generation system.

Data Analysis

Following transient diffusion experiments, cores taken through the diffusion cell will be analysed for their chloroform and TCE concentrations. The relative concentration of both compounds (C/C_o) will be plotted against distance from the C_o boundary.

Our goal is to obtain a value for the effective diffusion coefficient of both compounds under the different sets of pre-established conditions of interest. An analytical solution of the diffusion equation can be compared to the data with a least square fit routine, giving a value of D_e.

Once the D_e values are obtained for experiments carried out on different materials at different moisture contents, validation of existing models concerned with the prediction of effective diffusion coefficients as a function of moisture content will be undertaken.

DEMONSTRATION COLUMN STUDY

The purpose of the demonstration column was to show that a moist layer of granular material could indeed significantly reduce the flux of oxygen in a simulated tailings cover experiment. The proposed study included a cylindrical column for the cover layer and the underlying coarse sandy layer. Some form of oxygen sink was required at the base of the column where tailings would normally consume this gas as oxidation of sulphide minerals proceeds. Not only was it necessary to deplete the oxygen but it was also necessary to monitor the rate of gas consumption that would reflect the flux of oxygen through the cover layer. The specific focus of this part of the study was therefore to develop an appropriate methodology for the oxygen sink for use in the demonstration column.

Rationale

Two approaches were originally considered for the design of an oxygen sink, chemical consumption and electrical consumption. The chemical process is based on the oxidation of a substance (reducing agent) by oxygen in the gas phase while monitoring alterations in the system due to the loss of the reducing agent or the increase in the oxidation products. The electrical method is based on the reduction of oxygen at a platinum surface that has a voltage applied across it. Because the chemical methods appeared more straight forward, this approach was examined first. A number of reducing agents were studied for their potential application as a quantitative oxygen sink.

The ideal method would be one which could be monitored in-situ during the experiment. This implies the use of an electrode measurement or other detector that provides a signal. Alternatively, the solution containing the chemical sink could be sampled and analysed at a later time to determine the changes due to oxidation. Methods amenable to electrode measurement were investigated first.

Ferrous Sulphide Slurry

A slurry of amorphous ferrous sulphide was prepared by combining ferrous ammonium sulphate and sodium sulphide. The product is known to be highly reactive with oxygen and is used to maintain anaerobic conditions in biologic experiments. The slurry was first tested by measuring the change in specific conductance of the solution phase in order to monitor the increase in sulphate concentration resulting from oxidation of the sulphide. The electrical conductance increased with time when the slurry was exposed to air but exhibited substantial drift when the system was closed off to air contact. A number of experiments were run with similarly uninterpretable results.

The same method was then used as an oxygen sink but samples were collected over time to analyse for sulphate concentration. Sulphate is the product of oxidation of ferrous sulphide. The preliminary sampling and analysis showed that the residual fine ferrous sulphide particles could not be removed from the water sample even when filtering with a 0.1 micron pore-size filter membrane. The particles that passed through the filter oxidized after sample collection and caused sporadic results for the sulphate concentrations. After a number of attempts to solve these problems, with no success, the ferrous sulphide method was abandoned.

Ferrous Chloride Solution

Ferrous iron oxidizes rapidly in solution when the pH is maintained at a value above approximately 4. The next attempt at the oxygen sink was therefore to use ferrous iron in solution as the reducing agent. The proposed method for monitoring the progress of the oxidation was based on the conversion of ferrous to ferric iron and the redox potential that should increase as the ferric concentrations increase and the ferrous decreases. Even if ferric hydroxide precipitates during the production of ferric iron, the redox potential will increase to reflect the decrease in the more reduced member of the redox couple, and without other interferences, the observed potential can theoretically be used to compute the concentration of the ferrous iron.
A number of experimental runs were attempted, first at high total iron concentrations and pH values of about 6. These conditions produced a precipitate which appeared to be hydromagnetite, even though magnetite is known to be a high temperature mineral. In an attempt to prevent the formation of this solid which is composed of both ferrous and ferric iron, the concentration of

iron was reduced in increments to 1/1000 times the original concentration and the pH was lowered to values close to 4. All such runs resulted in the formation of the solid and no interpretation of the rate of oxidation from the redox data was possible. Sampling and analysis was not attempted because of the unknown loss of both ferrous and ferric iron from solution. This method was also abandoned.

Chromous Sulphate Solution

Chromous ions reduce oxygen in a manner similar to that of ferrous iron. A survey of the literature suggested that the formation of solids would not be significant in the chromous-chromic system. A number of experimental trials were conducted in a manner similar to those with the ferrous chloride. Again it was anticipated that the changes during oxidation could be monitored with the redox potential. These experiments, however exhibited similar results to those using iron. A solid formed during the oxidation process and the electrode potentials were uninterpretable.

Platinum Electrode Reduction

The platinum electrode method was reconsidered after abandoning the chemical methods described above. The process of oxygen reduction at a platinum electrode surface has been applied in other experimental designs. After a more thorough review of the literature and discussions with electro-chemists at both the University of Waterloo and Noranda Technologie, it was concluded that the level of time, effort and resources required to perfect this method for the demonstration would be beyond the those available in the project.

Results

After repeated attempts to develop an oxygen sink without success, the work plan was reevaluated at a joint meeting with Noranda Technologie and the Scientific Authority from Environment Canada. The principle investigators were asked to submit recommendations for further work. Two possibilities were discussed; use of organic vapours in place of oxygen to determine net fluxes through the cover and the use of a highly sensitive oxygen meter to detect oxygen in a constantly flushing stream of nitrogen gas at the base of the column. The organic vapour method was recommended because of the probable difficulties with pressure control and consequent gas advection as an artifact of the gas flow method. An initial proposal for additional funding ($6000) was approved and preliminary work on the organic vapour method was started.

Subsequently, due to timing constraints and limited resources, it

was agreed that work on the organic vapour method be stopped and that the demonstration column work continue at Noranda. Dr. Nicholson met with Noranda personnel in Montreal (mid May 1990), delivered the demonstration column (see Figure 5) prototype with all necessary parts and agreed to meet and provide advice as required and requested by Noranda Technologie.

DIFFUSION MODEL

The completed model is relatively simple but is effective in simulating the process of diffusion through layered materials. Both transient behaviour in a single layer and steady-state behaviour in multi-layered media are considered. A minimum of parameters were used to maintain simplicity. The code was designed in modular form to simplify future modifications.

Rationale

The model developed in this investigation had two purposes. The first was to simulate the time-dependent flux behaviour of oxygen through the cover layer in the demonstration column. Transient calculations are necessary even for thin layers of material in the columns when the water content of the layer approaches saturation. Materials with less moisture, and that exhibit higher diffusion coefficients, may attain steady-state in a reasonable experimental time frame. However, the most effective covers are those with low diffusion coefficients and the time required to approach steady-state would be inappropriately long. The transient model will allow the determination of the diffusion coefficient of the cover by comparing the observed flux over time in the column to the computed values. Although more sophisticated curve-fitting techniques can be applied, the comparison is quick and relatively precise. This type of computation also provides a 'hands-on' familiarity with transient diffusion behaviour. The second purpose was to compute the flux of oxygen through multi-layered media to aid in the design of composite covers for remediation schemes on reactive wastes. For practical purposes, this is a steady-state problem and it is possible to ignore the time-dependent nature of diffusion in the layered media.

Once the diffusion coefficient of a soil or other geologic material is known, the diffusive flux of oxygen through the layer can be computed. The flux is a direct indication of the potential rate of oxidation of sulphide minerals that may occur below a diffusion-barrier layer. The maximum possible flux occurs when the sulphide wastes consume the oxygen at the base of the barrier as fast as it is transported through the upper layer. In that case, the oxygen concentration at the interface between the wastes and the cover approaches zero. The model described here uses this approach. The fluxes calculated in the model can therefore be related to the maximum possible rates of oxidation

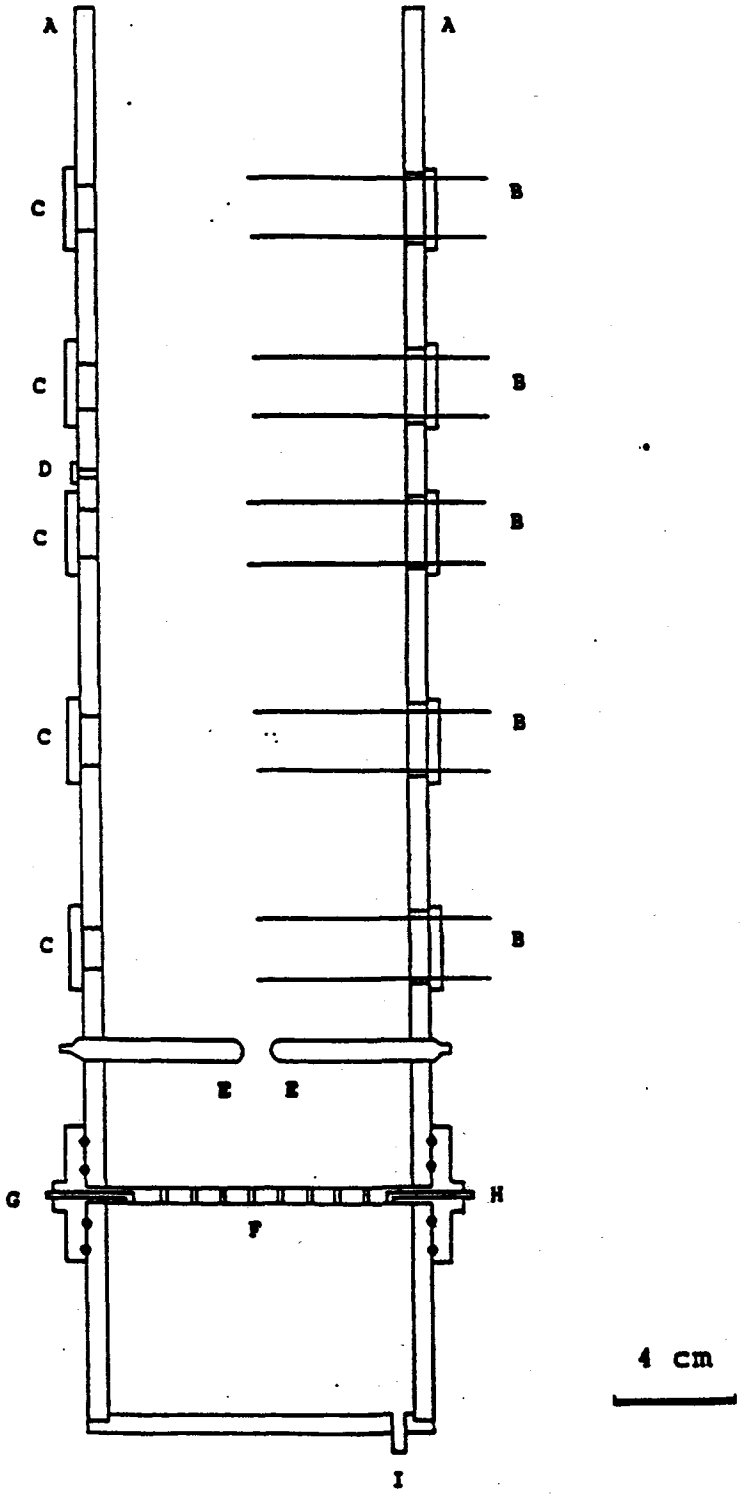

Figure 5

Description of apparatus

A) Wall of experimental column, B) TDR electrodes, C) Tensiometre ports, D) Swage-lock, E) Porous filter candles, F) Perforated plate, G) Gas inlet, H) Gas outlet, I) Flushing port

below the simulated cover.

Components of the Model

The model consists of two separate computations; transient diffusion through a single layer and steady-state diffusion through multi-layered media. The program is interactive and prompts the user for required data after selecting the type of calculation desired. The transient problem is addressed first, with the option to bypass this step and proceed to the steady-state problem. The data are printed to the screen to verify the accuracy of the input.

Transient Diffusion Through a Single Layer

The computation of this process is based on a solution to transient diffusion through a finite slab presented in Crank (1975). The concentration of oxygen at the upper boundary is assumed to be atmospheric (default) but can be set at other values as part of the prompted input to the program. The concentration of oxygen at the base of the layer is assumed to be zero following the rationale presented above.

The equation describing transient diffusion is given as;

$$\frac{\partial C}{\partial t} = D\frac{\partial^2 C}{\partial x^2} \qquad (1)$$

where C is the concentration of the diffusing substance [M/L^3], D is the diffusion coefficient of the medium [L^2/T], x is the distance [L] and t is time [T]. The following boundary and initial conditions apply to this problem.

C=Constant at x=0 (top boundary)
C=0 at x=L (bottom boundary)
C=0 for 0<x<L (throughout the layer)

The solution to this equation with these boundary conditions is given by;

$$F(t) = -\left(D\frac{\partial C}{\partial t}\right)_{x=L} = 2L\sum_{n=0}^{\infty}\left(\frac{D}{\pi t}\right)^{1/2}\exp\left\{\frac{-(2n+1)^2L^2}{4Dt}\right\} \qquad (2)$$

The program requests the following information from the user.

1. Thickness of the layer - this is given in metres.

2. The effective diffusion coefficient of the layer - in m^2/s. This value would be obtained from measurements or other estimates.

3. The total time over which the calculation is to be made - in hours.

4. The name of the listing file for output. This name should be allowable in DOS (ie. up to eight characters with a three character extension after a period)

The oxygen concentration at the surface is requested but the default setting is atmospheric (20.9% by volume).

All values are read in general format but must be supplied with appropriate decimals for real numbers. If exponential input is used, the decimal should be used in the pre-exponential part.

The output file contains the input values, the steady-state flux for comparison (ie. the maximum possible value) and an array containing the time in increments (of one-fiftieth of the total) with the corresponding flux expressed as a total in $kg/m^2/s$ and as a percent of the steady-state flux.

Steady State Diffusion Through a Multi-Layered Sequence

This computation is based on the steady-state diffusion through a finite layer. The layers are stacked one upon the other and can have variable thickness and any specified diffusion coefficient. The concentration profile through the sequence is calculated by equating the flux from each consecutive pair of layers at the interface between them.

Steady-state diffusion is described mathematically by the following equation;

$$F = -D \frac{\partial C}{\partial x} \qquad (3)$$

where F is the mass flux $[M/L^2 T]$ and other parameters are as shown above. The flux can be equated at the interface for any two adjacent layers with the resulting general equation;

$$\left(\frac{D_i}{L_i}\right)C_{i-1} + \left(\frac{D_{i+1}}{L_{i+1}} - \frac{D_i}{L_i}\right)C_i + \left(\frac{D_{i+1}}{L_{i+1}}\right)C_{i+1} = 0 \qquad (4)$$

where the subscript is the notation for any layer. This provides a system of equations (equal to the number of layers minus one) which can be solved simultaneously.

The boundary conditions are represented by a constant concentration at the surface and a concentration of zero at the base of the deepest layer. This results in a system of independent equations (number of layers minus one) which are solved simultaneously using a decomposition matrix routine. The flux is calculated for the top layer only using Fick's first law. This is possible because steady-state is assumed and hence the flux is identical in all layers.The model thus provides the oxygen concentration profile in addition to the flux through the sequence of layers.

The program requests the following information from the user.

1. The number of layers - up to 20 layers can be selected or the program can be easily modified to allow more layers.

2. The thickness and diffusion coefficient for each layer (in metres and m^2/s respectively), one layer per line starting at the top of the sequence.

3. The (DOS compatible) name for the output listing file.

All input data are printed to the screen to insure accuracy.

The output file contains all input data in addition to the total flux of oxygen through the layered sequence and the oxygen concentration profile.

Code Listing and Sample Computation

The code is listed in Appendix 2 along with a problem example illustrating the transient and the steady-state modes of output. The source code and an executable version of the program are provided on the enclosed disk. The program was written in FORTRAN 77 and compiled with MICROSOFT® Fortran. A math co-processor was used to compile the executable version but is not necessary to run the program which can be recompiled easily without it.

RELATED WORK

During this study, two related pieces of research were also being conducted. The first was a laboratory column experiment to investigate the hydraulic behaviour and controls in texturally layered porous media (Sydor, 1990). The second was a modelling study which involved the numerical simulation of time-dependent water drainage in layered porous media (Akindunni et. al., 1991). Both of these studies were based on concepts and preliminary studies of the principal investigators of this project (Nicholson et. al., 1989,1990).

Laboratory Study of Cover Layer Drainage

The original concept of moist covers acting as oxygen barriers is based on the premise that a fine-grained layer will not readily drain to equilibrium when it is located over a coarser material. If drainage is poor or very slow then it is possible that the fine cover will remain nearly saturated for significant periods of time. Until now, to the authors knowledge, this concept has not been demonstrated or the controls investigated. The purpose of the laboratory study was therefore to observe the drainage of an initially saturated two-layered system when the water table was lowered from the surface to some depth below the base of the cover.

The experimental system included monitoring of pressure head and moisture content at closely spaced intervals within the cover and underlying sand periodically over a two week period. The results confirmed the original hypothesis and also showed that the material selection could be based on straightforward measurements of physical properties of the two materials. The complete report is included as Appendix 3.

Numerical Simulation of Cover Layer Drainage

An existing numerical model, which simulates transient flow in one dimension in the vadose zone, was modified to include a change in water table elevation and the subsequent drainage in a layered sequence of porous media. Values for the physical parameters such as hydraulic conductivities and porosities of the cover and base materials are provided as input. The characteristic drainage curves that represent the relationship between pressure head and water content are also required, although only the main drainage curve for each material is necessary. The model then computes the changing conditions over time as the the water table is moved from the cover surface to a specified depth below the cover.

The results again confirmed the original premise that drainage of the upper fine-grained layer occurred very slowly and that it remained fully saturated for periods in excess of 56 days for certain contrasts in grain size between the cover and the underlying material. The results also suggest that the drainage of the cover layer is independent of the depth to the water table. These results are important in that they provide strong evidence that maintaining covers with high water contents is quite feasible and that the choice of materials for the cover can be based on some relatively simple measurements. A copy of the paper by Akindunni et. al.(1991) is included as Appendix 4.

SUMMARY

This study and related work have produced a number of positive and relevant results. The slow diffusion expected in near-saturated materials and which has led to most of the experimental difficulties is a positive attribute of tailings covers. The related work has shown that the hydraulic conditions to prevent drainage of fine-grained covers can be achieved by selecting materials with appropriate properties. Without this slow drainage it would not be appropriate to use covers as diffusion barriers. In addition, the numerical modelling has provided support to the concept and allows simulation of the process without performing costly and time-consuming experiments on all candidate materials.

The attempts to develop an oxygen sink for the demonstration column resulted in failure (and a great deal of frustration). This does not imply that the concept of the diffusion barrier is not valid; on the contrary, it points to the difficulties in measurement when such low fluxes of oxygen are expected. The diffusion measurements in high moisture-content materials is ongoing and will continue outside of the formal subcontract with Noranda Technologie. When results are obtained from these experiments, they will be reported to Noranda.

A model which computes diffusion both for transient conditions in a single layer and steady-state conditions in multi-layered media was developed. The model is appropriate to evaluate the diffusion data when they are obtained from the demonstration column experiments at Noranda and to aid in the design of composite covers.

CONCLUSIONS

The difficulty of developing an oxygen sink was greater than originally anticipated. It may be possible to apply the gas flushing technique to measure the oxygen flux through a cover layer in the demonstration column. However, the resources required to achieve this may be better applied to the initiation of field experiments. The concept of near-saturated covers above the water table has been supported by the related laboratory and modelling studies. It is also known that the diffusion coefficient of moist porous materials is quite low. What remains to be completed is a refinement of the relationship between moisture content and the diffusion coefficient in the near-saturated range. This work is ongoing at Waterloo. Field trials could be used to better evaluate the effects of greater variability of conditions expected at mine sites while using the existing models to evaluate the relative effectiveness of covers in reducing oxygen accessibility in tailings.

REFERENCES

Akindunni, F.F., Gillham, R.W. and Nicholson, R.V., 1991. Numerical simulations to investigate moisture retention characteristics in the design of oxygen-limiting covers for reactive mine tailings. (submitted Can. Geotech. J. June 1990).

Nicholson, R.V., Gillham, R.W., Cherry, J.A., and Reardon, E.J., 1990. Reduction of acid generation in mine tailings through the use of moisture retaining cover layers as oxygen barriers. Reply: Can. Geotech. J. 27 402-403.

Nicholson, R.V., Gillham, R.W. and Reardon, E.J., 1989. Pyrite oxidation in carbonate-buffered solution: 2. Rate control by oxide coatings. Reply: Geochim. Cosmochim. Acta. 54: 395-402.

Nicholson, R.V., Gillham, R.W., Cherry, J.A., and Reardon, E.J., 1989. Reduction of acid generation in mine tailings through the use of moisture retaining cover layers as oxygen barriers. Can. Geotech. J. 26(1): 1-8.

Reardon, E.J. and Moddle, P., 1985. Gas diffusion coefficient measurements on uranium mill tailings: Implications for cover layer design. Uranium. 2: 111-131

Siwik, R.S, Nicholson, R.V. and Smith, J., 1987. Development of a laboratory methodology for evaluating effectiveness of engineered covers for reactive tailings. Report to the National Uranium Tailings Program, DSS 15SQ.23317-6-1737

Sydor, R., 1990. Moisture control in porous media by selective layering. Unpublished B.A.Sc. Thesis, University of Waterloo, Waterloo, Ontario, 66 pp.

APPENDIX 1

UNIVERSITY OF WATERLOO PROPOSAL TO CENTRE DE TECHNOLOGIE NORANDA

APPENDIX B

UNIVERSITY OF WATERLOO

WATERLOO RESEARCH INSTITUTE

Development of a Laboratory Procedure for Evaluating the Effectiveness of Reactive Tailings Covers

WRI AWARD # 1474101

TECHNICAL CONTACT: R.W. Gillham and
R.V. Nicholson
Earth Sciences Department (WCGR)
University of Waterloo

ADMINISTRATION: Barry Hayward
Contracts Manager
Waterloo Research Institute
University of Waterloo

NOVEMBER 16, 1988

Contractual Agreement with the
Centre de Recherche Noranda

for the

Development of a Laboratory Procedure for Evaluating the
Effectiveness of Reactive Tailings Covers

1.0 Introduction

The University of Waterloo proposes to conduct research on the evaluation of properties controlling oxygen transport through moist geologic sediments. This research will be conducted as a subcontract to the Centre de Recherche Noranda. The project will be directed by Drs. R.W. Gillham (WCGR) and R.V. Nicholson (Earth Sciences) utilizing available facilities at the University of Waterloo. Work on the project will be completed by a graduate student (MSc) and a technician selected by Drs. Gillham and Nicholson.

2.0 Technical Scope

This research investigation will comprise laboratory testing and computer modelling to evaluate the characteristic properties that control the diffusion of oxygen through moist unconsolidated geologic sediments. It is anticipated that a specialized laboratory apparatus will be required to conduct the laboratory testing and this device will be constructed and tested as part of the investigation.

2.1 Laboratory Investigation

A procedure and appropriate device will be required to measure the effective diffusion of oxygen through moist sediments. The development of a suitable apparatus will represent a significant time and budget committment in this investigation. Other laboratory testing will also be required, however. This will include but not be limited to the following:

-characteristic moisture drainage curves
-grain size distribution
-moisture content measurements
-porosity measurements
-bulk density and
-permeameter testing (hydraulic conductivity)

It is these and other fundamental parameters and characteristics which will be related to the oxygen diffusion behaviour and used to predict oxygen transport through selected materials.

2.2 Mathematical Modelling

A model will be developed to simulate the diffusive transport of oxygen through moist geologic sediments. The model will be based on time dependent Fickian Diffusion with fundamental measurable properties as the controlling parameters. The model will be verified by comparing results to analytical solutions applying simple limiting conditions. Validation will be performed using the results from the diffusion experiments.

2.3 Testing of Candidate Cover Materials

The investigation by the Waterloo research group is expected to result in the development of a prototype of an oxygen diffusion apparatus. The plans for this device will then be used to construct a few working models at the Centre de Recherche Noranda. The study team at Waterloo will advise on the construction of these devices and on the testing of candidate materials that will be conducted in the Noranda Laboratories. The Waterloo study team will assist Noranda with the acquisition of the fundamental physical data for the candidate materials.

2.4 Anticipated Results

The results of this research project will encompass the following:

1. A prototype experimental apparatus capable of testing the diffusion of oxygen through moist unconsolidated geologic materials.

2. A Computer code to simulate the diffusion of oxygen in materials noted above.

3. Data on the fundamental physical properties and characteristics that control oxygen diffusion in selected test materials.

3.0 Reporting

Reports on progress in this project will be submitted at the end of each phase of work shown in the original proposal to DSS (Table 1 dated October 4, 1988) or approximately on a quarterly basis. A major progress report will be submitted ten (10) months after initiation of the project. A final report will be submitted to the Centre de Recherche Noranda upon completion of the project (expected March 30, 1990). All information on the experimental procedures, data and computer codes, developed during this investigation will be documented in the final report. The report submitted by the University of Waterloo under the conditions of the contract will be self-contained and will be appropriate to include as an appendix to the final report that Noranda intends to submit to the Department of Supply and Services.

4.0 Scheduling

The schedule shown in Table 1 of the original proposal submitted to DSS (dated October 4, 1988) is appropriate for the relative timing of study activities. It is anticipated that the project will be initiated in January 1989. This will shift all activities in Task 1 (Laboratory Studies) by two to three months. The activites in Task 2 (Modelling) should not be significantly affected by the later starting date.

5.0 Budget Summary

The estimated cost of this project is $112,000.00. This includes $90,000.00 in professional time (R.W. Gillham, R.V. Nicholson, 1 graduate student and 1 technician) over the 16 month period of the study. Disbursements are expected to account for $22,000.00. The costs are summarized in Table 1.

The Professional fees are based on the (DSS approved) university rates which include an additional 65% on basic salary and benefits. Time for Drs. R.W. Gillham and R.V. Nicholson is included as Principal Investigators' fees. Disbursements are charged at cost and travel includes a 2% handling charge.

6.0 Method of Payment

Payment will be made not more frequently than once a month in accordance with the following disbursements

Table 1. Summary of costs and personnel allocations for the Covers Assessment Project.

Item Description					
1. Professional Time*	Gillham (Days)	Nicholson (Days)	Graduate (Months)	Tech (Months)	Total
- Laboratory Studies	7	15	8	11	
- Modelling	5	5	4		
(Ben & O/H incl.)		Total Professional Time			90,000

2. Disbursements

- Travel**	2,000
- Equipment Rental (Includes computer time)	6,000
- Supplies/Disbursements (includes equipment fabrication)	10,000
- Chemical Analyses	4,000
Total Disbursements	22,000
Total Estimated Cost	112,000

* includes 65% overhead on base salaries & benefits

** includes 2% overhead on travel costs

Costs are calculated in accordance with Supply and Services Canada Directive #4005 date 31/05/85 covering pricing of research and development contracts with Universities and Colleges.

7.0 Rights and Obligations

All rights, title and interest in and to technical data, intellectual property, patents and trademarks, inventions, acquisitions, shall and are hereby transferred and assigned to Her Majesty. The indemnity provisions set forth in this sub-contract with Noranda, shall be deemed to apply to the aforesaid transfer.

The University shall retain the right to use project results for research and educational purposes and the client shall be furnished with copies of any proposed disclosure relating to this agreement at least ninety (90) days in advance of presentation or publication. If no objection is received within thirty (30) days the University shall be free to proceed. In the event written objection is made, an acceptable version of the proposed disclosure shall be negtotiated, including release date, within the original ninety (90) day notice period.

The University shall be free to publish 12 months after termination of this agreement.

8.0 Contractor

The University of Waterloo, Waterloo Research Institute, 200 University Avenue West, Waterloo, Ontario N2L 3G1 would be named the Contractor. Barry Hayward, Contracts Manager, will be responsible for the administrative support services.

The technical aspects would be discussed with Dr. R.W. Gillham and R.V. Nicholson but any changes to the contract must be made through the Contractor.

APPENDIX 2

Source Code Listing of the Diffusion Model and Examples of Trial Runs

```
C*****************************************************************************
C
C   THIS PROGRAM CALCULATES OXYGEN DIFFUSION IN TWO DISTINCT WAYS.
C
C   (1)  THE TRANSIENT FLUX THROUGH A SINGLE LAYER CAN BE COMPUTED
C   WITH KNOWLEDGE OF THE LAYER THICKNESS, THE EFFECTIVE DIFFUSION
C   COEFFICIENT OF THE LAYER AND THE OXYGEN CONCENTRATION AT THE
C   SURFACE OF THE LAYER. THE CONCENTRATION OF OXYGEN AT THE BASE
C   OF THE LAYER IS ASSUMED TO BE ZERO. THE FLUX IS CALCULATED AS
C   A FUNCTION OF TIME FOR A SPECIFIED RANGE.
C
C   (2)   STEADY STATE DIFFUSION THROUGH A MULTI-LAYERED SYSTEM IS
C   ALSO CALCULATED. UP TO 20 LAYERS CAN BE SELECTED (OR THE PROGRAM
C   CAN BE MODIFIED TO ACCEPT MORE LAYERS). THE THICKNESS AND THE
C   DIFFUSION COEFFICIENT OF EACH LAYER IS SPECIFIED. THE CONCENTRATION

C   OF OXYGEN AT THE TOP BOUNDARY CAN BE SPECIFIED (WITH DEFAULT TO
C   ATMOSPHERIC) AND THE VALUE AT THE LOWER BOUNDARY IS ASSUMED TO BE
C   ZERO. BOTH THE OXYGEN FLUX AND THE CONCENTRATION PROFILE ARE
C   CALCULATED.
C
C                     PROGRAMMED
C                  IN PARTIAL FULFILLMENT OF
C                  A CONTRACT WITH
C
C                  NORANDA TECHNOLOGIE LTD
C                  HYMUS BLVD
C                  POINTE CLAIRE, QUEBEC
C
C                  OCTOBER 01, 1990
C
C                        BY
C
C                  RONALD V. NICHOLSON
C                  DEPARTMENT OF EARTH SCIENCES
C                  UNIVERSITY OF WATERLOO
C                  WATERLOO, ONTARIO
C                  N2L 3G1
C*****************************************************************************
      IMPLICIT REAL*8(A-H,O-Z)
      CHARACTER*32 OUTFIL1,OUTFIL2
      DIMENSION TIME(100),FLUX(100),A(20,3),DE(20),DX(20),W(20),
     &DEPTH(20),PCTO2(20),C(20)
      CHARACTER*60 TITLE
      WRITE(*,3102)
3102  FORMAT(////1X,'GIVE THE TITLE OF THIS PROBLEM ... (UP TO 60',
     &' CHARACTERS)'//)
      READ(*,3103)TITLE
3103  FORMAT(A60)
      WRITE(*,3001)
3001  FORMAT(//1X,'DO YOU WISH TO MAKE A TRANSIENT FLUX CALCULATION',/
     &1X,'FOR ANY ONE LAYER? ... YES=1   NO=0 ...')
      READ(*,3002) K1
3002  FORMAT(I1)
      IF(K1.NE.1)GOTO 501
502   CONTINUE
      WRITE(*,3003)
3003  FORMAT(//1X,'GIVE THE THICKNESS OF THE LAYER IN METRES...')
```

```
      READ(*,3004) TLAYER
3004  FORMAT(G10.3)
      WRITE(*,3005)
3005  FORMAT(//1X,'GIVE THE EFFECTIVE DIFFUSION COEFFICIENT'/
     &1X,'IN SQUARE METRES PER SECOND...')
      READ(*,3006)DEFF
3006  FORMAT(G10.3)
      WRITE(*,3007)
3007  FORMAT(//1X,'GIVE THE TOTAL TIME FOR THE'/
     &1X,'  DIFFUSION PERIOD IN HOURS...')
      READ(*,3008) HTIME
      XTIME=HTIME*3600.
3008  FORMAT(G10.2)
      WRITE(*,3011)
3011  FORMAT(//1X,'GIVE THE OXYGEN CONCENTRATION AT THE UPPER BOUNDARY'
/
     &10X,'IN VOLUME PERCENT ... IF ATMOSPHERIC VALUE IS DESIRED ...'/
     &20X,'PRESS RETURN ...')
      READ(*,3012) CPCT
3012  FORMAT(G10.4)
      IF(CPCT.EQ.0.) CPCT=20.9
      COX=CPCT*1.309E-2
C    *** COX IS IN KG/CU M  GAS PHASE  ***
      WRITE(*,3009)TLAYER,DEFF,HTIME,CPCT
3009  FORMAT(//1X,'THE FOLLOWING DATA WILL BE USED'/
     &1X,' FOR THE TRANSIENT DIFFUSION CALCULATION'//
     &10X,'LAYER THICKNESS = ',F10.2,'   METRES'/
     &10X,'DIFFUSION COEFF = ',E10.3,'   SQ M/S'/
     &10X,'TOTAL TIME      = ',F10.2,'   HOURS'/
     &10X,'OXYGEN CONCN    = ',F10.4,'  %'///)
      WRITE(*,3010)
3010  FORMAT(/1X,'IF THE DATA ARE CORRECT... PRESS RETURN'/
     &1X,'TO REENTER THE DATA TYPE 1 AND RETURN ...')
      READ(*,3002) K2
      IF(K2.NE.0)GOTO 502
      WRITE(*,3014)
3014  FORMAT(//1X,'GIVE OUTPUT LISTING FILENAME FOR'/
     &1X,' THE TRANSIENT CASE...')
      READ(*,3015) OUTFIL1
3015  FORMAT(A32)
      STFLUX=DEFF*COX/TLAYER
      OPEN(6,FILE=OUTFIL1,STATUS='UNKNOWN')
      WRITE(6,3204)TITLE
3204  FORMAT(1X,A60//)
      WRITE(6,3016)TLAYER,DEFF,HTIME,CPCT,STFLUX
3016  FORMAT(//20X,'TRANSIENT DIFFUSION CALCULATIONS FOR THE'/
     &30X,'FOLLOWING CONDITIONS'///
     &10X,'LAYER THICKNESS = ',F10.2,'   METRES'/
     &10X,'DIFFUSION COEFF = ',E10.3,'   SQ M/S'/
     &10X,'TOTAL TIME      = ',F10.2,'   HOURS'/
     &10X,'OXYGEN CONCN    = ',F10.4,'   %'///
     &5X,'THE STEADY STATE FLUX THROUGH THIS LAYER = ',E10.3,
     &' KG/SQ M/S'///
     &5X,'TIME (HOURS)',7X,'FLUX (KG/SQ M/S)',3X,'PCT OF STEADY FLUX')
      CALL TRANSMOD(DEFF,TLAYER,COX,TIME,FLUX,XTIME)
      WRITE(*,3013)
3013  FORMAT(///1X,'TRANSIENT CALCULATIONS ARE COMPLETE...'/
     &1X,'DO YOU WISH TO SOLVE A STEADY STATE LAYERED PROBLEM? ...'/
```

```
     &1X,'IF YES PRESS RETURN ... IF NOT PRESS 1 AND RETURN...'//)
      READ(*,3002) K3
      IF (K3.NE.0) GOTO 503
C
501   CONTINUE
504   WRITE(*,3101)
3101  FORMAT(//1X,'START STEADY STATE MULTI-LAYERED PROBLEM ...'//
     &10X,'GIVE NUMBER OF LAYERS (2...20) ...')
      READ(*,3017)XNLAYER
3017  FORMAT(G10.0)
      NLAYER=INT(XNLAYER)
      DO 30 I=1, NLAYER
      WRITE(*,3018)
3018    FORMAT(/1X,'IN ORDER FROM TOP TO BOTTOM, GIVE THE...'/
     &  20X,'THICKNESS OF THE LAYER (M)... DIFFUSION COEF (SQ M/S)...'/
     &  20X,'ON THE SAME LINE ... SEPARATED BY A COMMA ...'/)
30      READ(*,3019) DX(I), DE(I)
3019  FORMAT(2G10.4)
      WRITE(*,3020)
3020  FORMAT(///1X,'GIVE THE OUTPUT LISTING FILENAME ...'/
     &10X,'FOR THE STEADY-STATE PROBLEM ...')
      READ(*,3015)OUTFIL2
      OPEN(7,FILE=OUTFIL2,STATUS='UNKNOWN')
      WRITE(*,3021)NLAYER
3021  FORMAT(/1X,'THE DATA FOR THIS STEADY STATE PROBLEM',
     &' ARE AS FOLLOWS ...'//
     &10X,'NUMBER OF LAYERS = ',I4,//
     &5X,'LAYER',5X,'THICKNESS (M)',5X,'DIFFUSION COEFF')
      DO 40 I=1,NLAYER
40        WRITE(*,3022) I, DX(I), DE(I)
3022  FORMAT(8X,I3,8X,F10.2,8X,E10.3)
      WRITE(*,3023)
3023  FORMAT(//1X,'IF THESE DATA ARE CORRECT, PRESS RETURN ...'/
     &10X,'TO REENTER DATA PRESS 1 AND RETURN ...')
      READ(*,3002) K4
      IF (K4.NE.0) GOTO 504
C
      C0=0.274
      A(1,1)=0.0
      A(NLAYER,3)=0.0
      W(1)=-C0*(DE(1)/DX(1))
      LC=NLAYER-1
      C(NLAYER)=0.
      DO 10 I=1,NLAYER
            IF (I.EQ.1) THEN
              DEPTH(I)=DX(I)
            ELSE
              DEPTH(I)=DEPTH(I-1)+DX(I)
            ENDIF
10    CONTINUE
      DO 60 I=1,LC
            IF (I.NE.1)  A(I,1)=DE(I)/DX(I)
            A(I,2)=-(DE(I)/DX(I)+DE(I+1)/DX(I+1))
            IF (I.NE.LC) A(I,3)=DE(I+1)/DX(I+1)
            IF(I.NE.1)  W(I)=0.
60    CONTINUE
C
```

```
      CALL MATRIX(A,C,W,LC)
C
      WRITE(7,3105)TITLE
3105  FORMAT(1X,A60//)
      TFLUX=DE(1)*(C0-C(1))/DX(1)
      WRITE(7,1003)NLAYER
1003  FORMAT(/1X,'THE DATA FOR THIS STEADY STATE PROBLEM',
     &' ARE AS FOLLOWS ...'//
     &10X,'NUMBER OF LAYERS = ',I4,//
     &5X,'LAYER',5X,'THICKNESS (M)',5X,'DIFFUSION COEFF')
      DO 70 I=1,NLAYER
70        WRITE(7,1004) I, DX(I), DE(I)
1004  FORMAT(8X,I3,8X,F10.2,8X,E10.3)
      WRITE(7,1001)TFLUX
1001  FORMAT(//5X,'TOTAL OXYGEN FLUX THROUGH THE SURFACE = ',E10.3,
     &'  KG/SQ M/S'///
     &5X,'THE OXYGEN CONCENTRATION PROFILE IS AS FOLLOWS ...',///
     &5X,'DEPTH (M)',5X,'OXYGEN (%)'/)
      WRITE(7,1002)  0.0, 20.9
1002  FORMAT(4X,F10.2,7X,F10.5)
      DO 50 I=1,NLAYER
         PCTO2(I)=C(I)*76.405
50        WRITE(7,1002) DEPTH(I),PCTO2(I)
503   STOP
      END
C
C     ********************************************************************
C
      SUBROUTINE MATRIX (A,C,W,LC)
C
C     TRI DIAGONAL MATRIX SOLVER
C
      INTEGER LC
      REAL*8 C(20),W(20),A(20,3)
C
C     DECOMPOSITION ROUTINE
C
      DO 250 I=2,LC
         A(I,1)=A(I,1)/A(I-1,2)
         A(I,2)=A(I,2)-A(I,1)*A(I-1,3)
 250   CONTINUE
C
C     FORWARD SUBSTITUTION
C
      DO 300 I=2,LC
         W(I)=W(I)-A(I,1)*W(I-1)
 300   CONTINUE
C
C     BACKWARD SUBSTITUTION
C
      C(LC)=W(LC)/A(LC,2)
      DO 350 K=2,LC
         I=LC-K+1
         C(I)=(W(I)-A(I,3)*C(I+1))/A(I,2)
 350   CONTINUE
C
      RETURN
```

```
      END
C
CC    ***************************************************************
C
      SUBROUTINE TRANSMOD (D,TLAYER,COX,TIME,FLUX,XTIME)
C
C   TRANSIENT DIFFUSION THROUGH A FINITE LAYER WITH C=0 AT BOTTOM
C
      IMPLICIT REAL*8(A-H,O-Z)
      DIMENSION TIME(100),FLUX(100),HOURS(100)
      TIME(1)=0.
      FLUX(1)=0.
      DELTIME=XTIME/50.
      PARM1=1.128*COX
      PARM2=TLAYER**2/4.
      STFLUX=D*COX/TLAYER
      DO 20 J=2,51
        TIME(J)=TIME(J-1)+DELTIME
        E1=0.
          DO 10 I=1,21
            II=I-1
10        E1 = E1 + DEXP(-(2.*II+1.)**2*PARM2/(D*TIME(J)))
        FLUX(J)=PARM1 * (D/TIME(J))**0.5 * E1
        PCTFLX=FLUX(J)/STFLUX*100.
        HOURS(J)=TIME(J)/3600.
        WRITE(6,2002) HOURS(J),FLUX(J),PCTFLX
20    CONTINUE
2002  FORMAT(5X,F10.2,10X,E10.3,5X,F10.4)
      RETURN
      END
```

SAMPLE PROBLEM

TRANSIENT DIFFUSION CALCULATIONS FOR THE FOLLOWING CONDITIONS

LAYER THICKNESS =	.10	METRES
DIFFUSION COEFF =	.100E-09	SQ M/S
TOTAL TIME =	45000.00	HOURS
OXYGEN CONCN =	20.9000	%

THE STEADY STATE FLUX THROUGH THIS LAYER = .274E-09 KG/SQ M/S

TIME (HOURS)	FLUX (KG/SQ M/S)	PCT OF STEADY FLUX
900.00	.764E-12	.2793
1800.00	.256E-10	9.3541
2700.00	.756E-10	27.6353
3600.00	.125E-09	45.5247
4500.00	.164E-09	59.8888
5400.00	.193E-09	70.7082
6300.00	.215E-09	78.6742
7200.00	.231E-09	84.4900
8100.00	.243E-09	88.7225
9000.00	.251E-09	91.7989
9900.00	.257E-09	94.0340
10800.00	.262E-09	95.6576
11700.00	.265E-09	96.8368
12600.00	.267E-09	97.6933
13500.00	.269E-09	98.3154
14400.00	.270E-09	98.7673
15300.00	.271E-09	99.0955
16200.00	.272E-09	99.3338
17100.00	.272E-09	99.5070
18000.00	.273E-09	99.6327
18900.00	.273E-09	99.7240
19800.00	.273E-09	99.7904
20700.00	.273E-09	99.8385
21600.00	.273E-09	99.8735
22500.00	.273E-09	99.8990
23400.00	.273E-09	99.9174
24300.00	.273E-09	99.9308
25200.00	.273E-09	99.9406
26100.00	.273E-09	99.9476
27000.00	.273E-09	99.9528
27900.00	.273E-09	99.9565
28800.00	.273E-09	99.9592
29700.00	.273E-09	99.9612
30600.00	.273E-09	99.9626
31500.00	.273E-09	99.9636
32400.00	.273E-09	99.9644
33300.00	.273E-09	99.9649
34200.00	.273E-09	99.9653

35100.00	.273E-09	99.9656
36000.00	.273E-09	99.9658
36900.00	.273E-09	99.9660
37800.00	.273E-09	99.9661
38700.00	.273E-09	99.9662
39600.00	.273E-09	99.9662
40500.00	.273E-09	99.9663
41400.00	.273E-09	99.9663
42300.00	.273E-09	99.9663
43200.00	.273E-09	99.9664
44100.00	.273E-09	99.9664
45000.00	.273E-09	99.9664

SAMPLE PROBLEM

THE DATA FOR THIS STEADY STATE PROBLEM ARE AS FOLLOWS ...

NUMBER OF LAYERS = 4

LAYER	THICKNESS (M)	DIFFUSION COEFF
1	1.00	.100E-06
2	.10	.100E-08
3	1.00	.100E-06
4	.10	.100E-08

TOTAL OXYGEN FLUX THROUGH THE SURFACE = .125E-08 KG/SQ M/S

THE OXYGEN CONCENTRATION PROFILE IS AS FOLLOWS ...

DEPTH (M)	OXYGEN (%)
.00	20.90000
1.00	19.98338
1.10	10.46748
2.10	9.51589
2.20	.00000

APPENDIX 3

Sydor (1990) B.A.Sc. Thesis

MOISTURE CONTROL IN POROUS MEDIA BY SELECTIVE LAYERING

by

Richard C. Sydor

A thesis
presented to the University of Waterloo
in fulfilment of the
thesis requirement for the degree of
Bachelor of Applied Science
in
Geological Engineering

Waterloo, Ontario, Canada, 1990

I hereby declare that I am the sole author of this thesis.

I authorize the University of Waterloo to lend this thesis to other institutions or individuals for the purpose of scholarly research.

Richard C. Sydor

I further authorize the University of Waterloo to reproduce this thesis by photocopying or by other means, in total or in part, at the request of other institutions or individuals for the purpose of scholarly research.

Richard C. Sydor

The University of Waterloo requires the signatures of all persons using or photocopying this thesis. Please sign below, and give address and date.

ABSTRACT

This thesis has application to the reduction of acid generation in mine tailings. The concept entails applying a fine-grained cover material to the surface of the coarser mine tailings. Current conceptual and numerical models suggest that the cover can remain saturated, even with a water table that is located at some distance from the ground surface. The cover can remain saturated because the coarser material below, which drains relatively quickly from full saturation to residual saturation, develops a very low hydraulic conductivity and impedes drainage in the overlying layer. Oxygen diffuses far more slowly in water than in air (approximately four orders of magnitude smaller) and therefore, the saturated cover will significantly reduce the rate of oxygen diffusion into the tailings. The reduced availability of oxygen in the tailings reduces the rate of oxidation by oxygen and hence, decreases the rate of acid generation.

A laboratory soil column experiment was conducted to confirm, in part, the conceptual and numerical models. Specifically, the main objective was to determine if the coarse-grained layer did indeed impede drainage of the overlying fine-grained cover layer.

There was excellent agreement between the experimental results and the results predicted by the conceptual and numerical models. The lower coarse-grained layer, composed of coarse sand, drained rapidly to a value near residual saturation and the pressure head profile became nearly vertical within 24 hours. Saturation and pressure head decreased only very slightly in the column over the following two week period. The pressure head in the coarse-grained layer appeared to be approaching a static condition, which was far from equilibrium, at the end of the experiment. The pressure head transmitted by the coarse layer to the coarse/fine sand interface was approximately equal to the pressure head at which the coarse-grained sand approaches residual saturation. The fine-grained Borden

sand, composing the overlying cover material, remained nearly saturated during the experiment.

The experimental results support the findings of the conceptual and numerical models. All three approaches suggest that the cover can remain saturated if the air-entry value for the fine-grained cover material is greater the sum of the cover thickness plus the suction at which the coarse material approaches residual saturation (all in terms of absolute values).

ACKNOWLEDGEMENTS

The author gratefully acknowledges the numerous technical staff and fellow students, who lent assistance of all forms to this thesis. Special thanks to R.V. Nicholson for providing both technical advice and encouragement.

This work was one aspect of a larger project funded by the Noranda Technology Centre.

TABLE OF CONTENTS

1.0 INTRODUCTION

The mining of ores containing economic minerals, like nickel, zinc, lead, copper, silver, gold, and uranium, produces enormous volumes of tailings during the milling process. In Canada alone, it is estimated that hundreds of millions of tonnes of tailings cover an areal extent of approximately 11 000 ha (Nicholson et al., 1989). These tailings contain sulphides, like pyrite, which readily oxidize, producing acid in the process.

An increase in the acidity of the downward percolating water can have a severe impact on the environment. Acidic water has an increased ability to dissolve solid constituents as it infiltrates through the tailings. As this water enters the subsurface and surface water systems, there is the potential for a severe water quality degradation. Water from these systems may destroy ecosystems or become unsuitable for human consumption or industrial and agricultural applications.

The rate of acid generation is closely related to both the availability of gaseous oxygen and to the rate of oxygen diffusion into the tailings. Unfortunately, the majority of tailings are piled on the earth's surface where there is a virtually unlimited supply of gaseous oxygen. Further, oxygen diffuses quite easily through air. The result is a zone of oxidation in the upper 0.5 to 3 m of the tailings piles, where the acid is produced (Nicholson et al., 1989).

Storing tailings underwater is one possible method for reducing the amount of acid generated. Natural or man-made lakes could be used as storage sites. Relative to air, water has less available oxygen (i.e., dissolved oxygen) and a rate of oxygen diffusion about four orders of magnitude smaller (Nicholson et al., 1989). Considering only the reduction of acid generation, the underwater storage of tailings is better than storing them where they are exposed to air. However, economic, political and other long-term

LIST OF ILLUSTRATIONS

considerations might be prohibitive.

The application of a fine-grained cover layer to the surface of the tailings, which is capable of retaining a high degree of saturation, is an alternative approach to reducing oxygen availability. The cover acts as an oxygen barrier because it greatly reduces the inward diffusional transport of oxygen. With the appropriate selection of a cover material, a high degree of saturation can be maintained, even if the cover is several metres above the water table.

The application of moisture-retaining cover layers to reduce the availability of oxygen in tailings piles has not yet been fully investigated. Recently, Nicholson et al. (1989) developed a theoretical model based on the hydraulic principles and characteristics of partially saturated porous media and Fick's first and second laws, which describe the rate of oxygen diffusion through the cover layer. The model can be used to evaluate the effectiveness of potential cover materials in reducing the oxygen availability. Hydraulically, the model suggests that cover materials, with an appropriate texture, can remain saturated even with a water table that is located at some distance from the ground surface. The cover remains saturated because the coarser material below, drains relatively rapidly to residual saturation. The pressure head in the drained material decreases quickly to approximately the pressure head at which the coarser material approaches residual moisture content. The pressure head does not become substantially more negative than this pressure head. Further, the drained material has a greatly reduced hydraulic conductivity, corresponding to the low moisture content, and impedes further drainage of the system. In essence, the system approaches a static condition, which is far from static equilibrium. Further lowering of the water table should not significantly affect the moisture content of the fine-grained cover layer because the sand can not transmit the pressure head.

Numerical simulation techniques have also been applied to studying moisture retention in cover layers. Akindunni et al. (unpublished) has developed a one dimensional, finite element, saturated-unsaturated flow model to study the drainage through a two-layer profile. The results of the numerical modelling suggest that it is hydraulically possible to maintain full saturation in properly designed cover layers.

The purpose of this investigation was to verify the results of the conceptual and numerical models with experimental results from a laboratory column experiment. Specifically, the main objective was to determine if the coarse-grained layer does indeed impede the drainage of the fine-grained layer.

Water retention in porous media involves the hydraulic principles of capillary forces and flow in unsaturated porous media. When studying the drainage of porous media, it is important to monitor the pressure head and moisture content. Pressure head and moisture content were monitored using pressure transducer-tensiometry and time domain reflectometry, respectively. The next section presents a review of these hydraulic principles and monitoring methods.

2.0 BACKGROUND

2.1 HYDRAULIC PRINCIPLES

2.1.1 Soil Phase Relationships

To describe the hydraulic characteristics of a soil, several terms are used: porosity, volumetric moisture content, and degree of saturation. The porosity, n, is the ratio of the volume of voids to the total unit volume of a soil. The volumetric moisture (or water) content, θ, is the ratio of the volume of water to the total unit volume of a soil. The degree of saturation, S_w, is the ratio of the volume of water to the total volume of voids. The three terms are mathematically defined and inter-related:

$$n = V_v/V_T \quad (1)$$

$$\theta = V_w/V_T \quad (2)$$

$$S_w = V_w/V_v \quad (3)$$

$$\theta = nS_w \quad (4)$$

They are usually reported as a percent or a decimal fraction.

2.1.2 Surface Tension and Capillary Pressure

When a liquid is in contact with a gas, a solid, or another liquid immiscible with the first liquid, free interfacial energy exists between the two substances (Bear, 1972). The interfacial energy arises from the molecular forces of adhesion and cohesion. Adhesion and cohesion are the forces of attraction between molecules of dissimilar and similar substances, respectively (Ghildyal and Tripathi, 1987).

If possible, a surface possessing free energy will contract. The surface of a liquid can be conceptualized as an elastic membrane or skin that attempts to contract. The stretching or

tensile force required to form this skin is called the surface tension, σ (Streeter and Wylie, 1981). Surface tension or interfacial tension is defined as the amount of work that must be done to separate a unit area of two substances. The units of surface tension are force over length, or MT^{-2}.

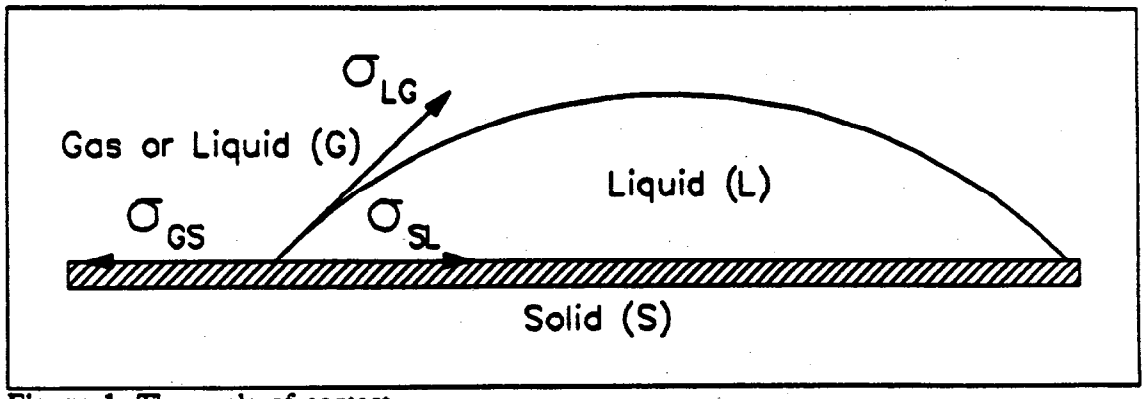

Figure 1: The angle of contact

The angle of contact, α, is defined as the angle between the tangent to the fluid interface (at the point of contact) and the solid surface, measured through the denser fluid (eg., water in an air-water-solid system). Figure 1 shows α for a solid-liquid-gas contact. Its magnitude can be calculated from the equilibrium relationship for the three surface tension vectors: σ_{LG} for liquid-gas, σ_{SL} for solid-liquid, and σ_{GS} for gas-solid surfaces, respectively. This relationship, called Young's equation, is:

$$\sigma_{LG}\cos\alpha + \sigma_{SL} = \sigma_{GS} \qquad (5)$$

or

$$\cos\alpha = (\sigma_{GS} - \sigma_{SL}) / \sigma_{LG} \qquad (6)$$

Young's equation states that cosα is defined as the ratio of the energy released in forming a unit area of interface between a solid S and a liquid L, instead of between a solid S and a fluid G, to the energy required to form a unit area between the liquid L and the fluid G (Bear, 1972). If α is less than 90°, the fluid is said to wet the solid. In this case, the adhesion forces between the liquid and the solid are greater than the liquid's cohesive forces.

As a consequence of the curvature of the liquid surface, the pressure is greater on the concave side of the interface. The pressure difference, called capillary pressure, p_c, can be calculated for the spherical interface shown in Figure 2:

$$2\pi r\sigma = (p_i - p_o)\pi r^2 \qquad (7)$$

or

$$p_c = 2\sigma/r \qquad (8)$$

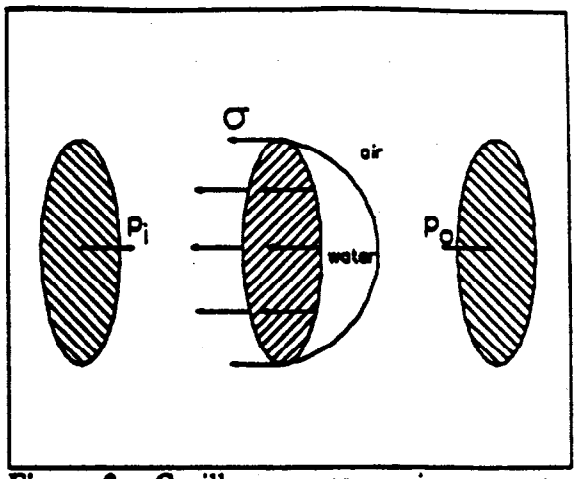

Figure 2: Capillary pressure in a water droplet

This equation states that the capillary pressure, p_c, is directly proportional to the surface tension, σ, and inversely proportional to the radius of curvature, r.

A practical application of equation 8 is to determine the height water will rise in the capillary tube shown in Figure 3. A capillary tube is a hollow open-ended tube with a fine bore. When it is first placed in a container of water, the water level in the tube can be expected to rise only to level A, if surface tension is neglected. Considering surface tension, the water surface in the tube will have a concave upwards spherical meniscus with a pressure difference across it. According to equation 8, the water below the meniscus has a pressure $2\sigma/r$ less than the atmospheric pressure above it. Since the pressure on the water surface at A, outside the tube, is atmospheric (i.e., greater), water will be forced up into the tube. Equilibrium will be established when the hydrostatic pressure, of the column of water in the tube, balances the pressure difference of

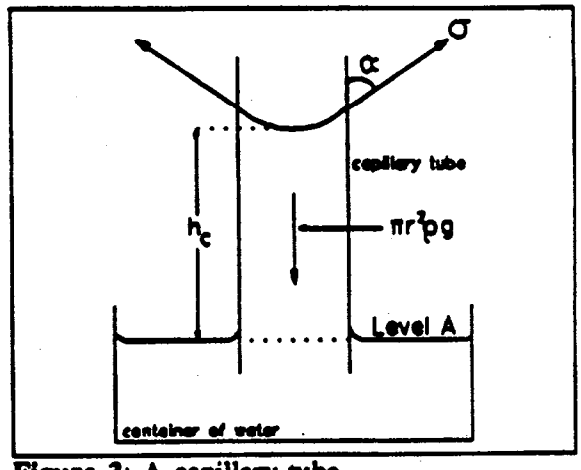

Figure 3: A capillary tube (modified from Bear, 1972)

$2\sigma/r$. At equilibrium, the pressure at level A will be atmospheric both inside and outside the tube. The height of rise, h_c, can be computed from Figure 3:

$$h_c \pi r_2 \rho g = 2\pi r \sigma \cos\alpha \quad (9)$$

or

$$h_c = 2\sigma\cos\alpha / r\rho g \quad (10)$$

Equation 10 is called the capillary rise formula. Using values for water at 20°C, equation 10 becomes:

$$h_c = 0.149/r \ \text{[cm]} \quad (11)$$

Note, $\cos\alpha$ is assumed to be unity because the angle of contact for water and clean glass is very small. For pure water and clean glass, $\cos\alpha$ equals 0° (Bowles, 1979).

A simplified system of capillary tubes, of various bore sizes, can be used to model the distribution of pore sizes in a homogeneous soil at static equilibrium (i.e., no flow). Assuming no flow, the water level in the container will correspond to the water table in the soil section. Both are at atmospheric pressure or zero gauge pressure. The height of the meniscus of the widest capillary tube corresponds to the height of the capillary fringe in the soil section. Above the capillary fringe, the degree of saturation in the soil continues to decrease until a minimum value is attained. This is analogous to successively smaller tubes attaining their respective h_c values. Pressure in the zone above the water table, called the vadose zone, is negative. Below the water table, which is called the saturated zone, pressure is positive.

The minimum saturation value is called, the irreducible water saturation, S_r. This value implies that pores in the soil are sufficiently small in diameter to retain water up to the top of the soil section. In other words, some water remains immobile in the smallest pores in the soil. The irreducible water content, θ_r, corresponds to S_r.

If the soil pores and tubes were initially filled with water and then allowed to drain, each capillary tube would drain to its respective h_c. This indicates that a capillary tube or soil pore will drain if the radius of curvature, of the water meniscus, can not be made sufficiently small to balance the applied negative pressure. The pressure, ψ_a, at the top of the capillary fringe, is called the air entry pressure or bubbling pressure. The air entry pressure is the pressure at which the largest capillary tube, or soil pore, drains of water and fills with air. In a drained capillary tube or soil pore, a film of water will remain along the wall of the tube or the grains forming the pore. This film of water is considered in the S_r and θ_r terms.

Gillham (1984) used the capillary rise formula (equation 10) to correlate the air entry pressure of a soil to the grain size (see Figure 4). The capillary radius, r, was assumed to correspond to the largest pore radius and to twice the grain diameter. The height of rise, h_c, was then interpreted as the ψ_a value. The equation indicates that silts (62 to 4 micron particles) might have ψ_a values ranging from 1 m to 2 m. Similarly, sands (62 μm to 2 mm) might have ψ_a values ranging from 1 cm to 100 cm.

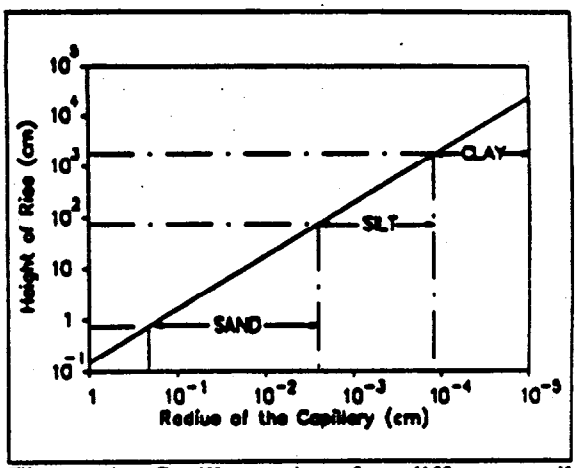

Figure 4: Capillary rise for different soil materials (modified from Gillham, 1984)

In summary, fine-grained materials remain saturated at greater heights above the water table than do coarser grained materials. The theory suggests that drainage, even in fine silts, should occur within two metres of the water table for homogeneous porous media. Layering of porous media results in different behaviour and is discussed in Section 2.2.

2.1.3 Flow

Flow occurs in a water saturated medium from regions with a higher potential to regions with a lower potential. The fluid potential, I, can be expressed as the mechanical energy per unit *mass* of fluid. It is comprised of three terms representing potential, kinetic and elastic energy. The kinetic energy term is usually very small and can be neglected (Freeze and Cherry, 1979). The remaining two terms simplify to:

$$I = g(z+\psi) = gh \qquad (12)$$

where g = the acceleration due to gravity [L/T^2]
h = the hydraulic head [L]
z = the elevation head [L]
ψ = the pressure head [L]

The elevation head, z, is a measure of the gravitational potential energy per unit weight of fluid above an arbitrarily selected datum. The pressure head, ψ, is a measure of the work done on a unit weight of fluid (i.e., elastic energy) to change its pressure from that at the datum to the pressure at the given point in the material. The hydraulic head, h, is the sum of the elevation and pressure heads:

$$h = z + \psi \qquad (13)$$

It is the mechanical energy per unit *weight* of fluid and is a convenient way to represent the fluid potential.

Darcy's law is an empirically derived expression that describes flow in saturated porous media. Figure 5 is a schematic representation of Darcy's law. For one dimensional flow in an isotropic soil, Darcy's law states that the specific discharge, v [L/T], is directly proportional to the hydraulic gradient, (dh/dl):

$$v = -K(dh/dl) \qquad (14)$$

The specific discharge is equal to the fluid flow rate, Q [L^3/T], divided by the cross-sectional area of the porous medium, A [L^2]. The hydraulic gradient is the change in hydraulic head, dh [L], over the length, dl [L]. The constant of proportionality, K [L/T], is

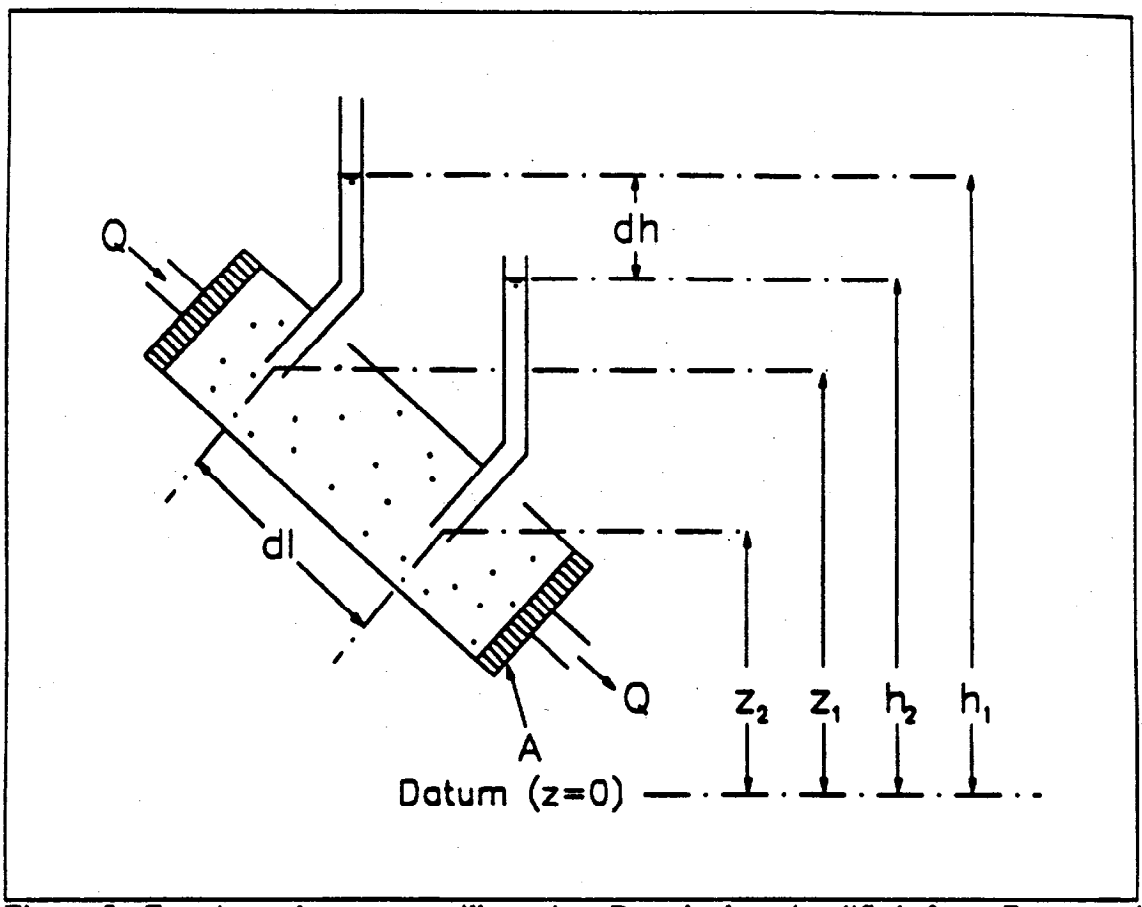

Figure 5: Experimental apparatus illustrating Darcy's law (modified from Freeze and Cherry, 1979)

called the hydraulic conductivity. It is a measure of the ease with which a fluid will flow through a porous medium. As such, it is a function of both the porous medium and the fluid flowing through the medium.

The above form of Darcy's law is applicable for fully saturated porous media. However, for unsaturated flow the effects of hysteresis must be considered. Figure 6 shows typical hysteretic volumetric moisture content-pressure head and hydraulic conductivity-pressure head curves for a soil. The curves are hysteretic because the values of K and θ at a particular ψ can vary depending upon the wetting and drying history of the soil. The envelope curves in Figure 6 are called the main drainage curve and main wetting curve.

The curves inside the envelope, which indicate that only partial draining or wetting occurred before the conditions were reversed, are called scanning curves.

The hysteretic relationships are usually presented as $\theta(\psi)$ and $K(\psi)$ or as $\psi(\theta)$ and $K(\theta)$. In either presentation, moisture content is noticeably hysteretic. However, conflicting opinions exist concerning hysteresis in the $K(\theta)$ relationship. Dane and Weirenga (1975) found $K(\theta)$ to be slightly hysteretic. On the otherhand, Gillham et al. (1976) found no clear indication of hysteresis and used a $K(\theta)$ function of the form:

$$K = a\theta^{n} \qquad (15)$$

where a and n are fitted parameters

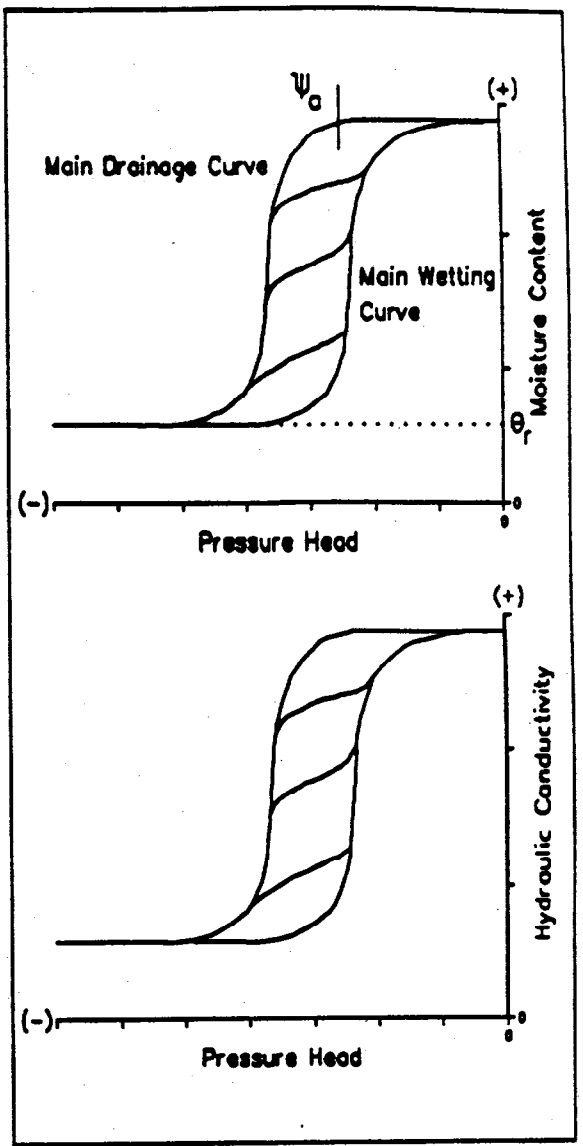

Figure 6: Characteristic curves showing hysteresis
(modified from Freeze and Cherry, 1979)

In their work, both Healy (1989) and Giesel and Renger (1973) chose to ignore hysteresis in $K(\theta)$ and considered it only for the $\theta(\psi)$ relation. Klute and Heerman (1978) considered $K(\theta)$ to not be hysteretic or only marginally hysteretic. Because this study was only concerned with the drainage of the soil column from full saturation, hysteresis in the soil was not particularly important.

provides an excellent indication of a soil material's ability to retain moisture. Potential cover materials should have a ψ_a that is large in magnitude. For this reason, the silt material (ψ_a = -17 cm approx.) used by Barbour (1990) would probably constitute a poor cover material. Nicholson et al. (1990) attributed the low air entry pressure of Barbour's silt to aggregation (i.e., large pore size).

Figure 7 provides insight into how the air entry pressure can be applied to calculate the thickness of the cover that will remain saturated. The figure shows that a soil will start to drain when the pressure head in that soil becomes less than its ψ_a. If the soil is a silt with a ψ_a of -1.7 m, then the silt will remain fully saturated to a height of 1.7 m above the water table. This indicates that the thickness of cover material that will remain fully saturated is:

$$H = \psi_{base} - \psi_a \qquad (18)$$

where H = thickness of the cover
ψ_{base} = pressure head at base of cover
ψ_a = air entry pressure head for the cover material

If a fine-grained cover material was placed over a coarse-grained material and the system allowed to drain from initial saturation, ψ_{base} would correspond to the pressure head at which the residual moisture content is approached in the coarse-grained material, $\psi_{c\,ar}$ (Nicholson et al., 1990). Using the silt and sand from Figure 7, it can be seen that the sand first approaches residual saturation at a pressure head of -90 cm. Using a ψ_a of -170 cm for the silt and equation 18, the thickness of the cover that can remain saturated can be calculated:

$$H = -90 - (-170) = 80 \text{ cm}$$

It is evident from the equation 18 and the above calculation that a maximum contrast in grain size is desired. The smaller the grain size of the fine-grained material, the larger the ψ_a value will be in magnitude. The larger the grain size of the coarse-grained material, the smaller the $\psi_{c\,ar}$ value will be in magnitude. As a result, the thickness of the cover that can remain saturated is maximized and the most effective oxygen barrier is created.

Considering K as a function of ψ or θ, Darcy's law for unsaturated flow can be expressed:

$$v = -K(\psi)(dh/dl) \quad (16)$$

or

$$v = -K(\theta)(dh/dl) \quad (17)$$

When referring to saturated or unsaturated flow over an interval of time, the flow may be considered as equilibrium, steady-state, transient or quasi-equilibrium flow. When water within a soil is at equilibrium, the hydraulic gradient is vertical (i.e. dh/dl=0 or $d\psi/dz=-1$) and all points in the material have an equal hydraulic head; no flow occurs. Steady-state flow occurs when the flow vector (i.e., magnitude and direction) is constant with time at any point in the material. If this flow vector changes with time, transient flow is occurring. Quasi-equilibrium is said to exist if no change is observed in the material, in the period of time of interest. The sensitivity of the measuring instruments and the length of the time interval of interest will greatly affect whether the flow is designated as transient or as quasi-equilibrium.

2.2 LAYERED POROUS MEDIA

Below, the hydraulic principles discussed in Section 2.1 are applied to layered porous media. The discussion will focus on the design considerations for a moisture retaining cover and the transient drainage of a layered soil profile.

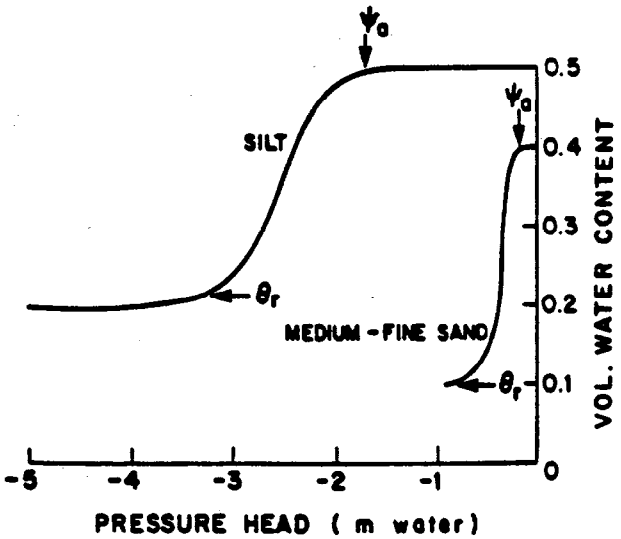

Figure 7: Moisture retention curves for a medium-fine sand and a silt loam (modified from Gillham, 1984)

Moisture retention characteristics for a soil material can be inferred from the shape of the $\theta(\psi)$ profile. Figure 7 shows the $\theta(\psi)$ profiles for a silt loam and a medium-fine sand. For these materials, the magnitude of the air entry pressure, ψ_a, for the silt loam and the sand are approximately 170 cm and 17 cm, respectively. The sand drains very rapidly after its ψ_a is exceeded; the silt drains more gradually. As can be seen, the magnitude of ψ_a

the silt remained fully saturated throughout the simulation. Figure 9 shows that the pressure head profile developed an inflection very early in the experiment. After two hours, the pressure head profile had become nearly vertical in the zone where the coarse sand was drained. Thereafter, the profile became only slightly more negative (i.e., -12 cm to -22 cm). The drainage of the soil section appeared to be approaching a static condition at the residual saturation of the coarse and a pressure head approximately equal to $\psi_{c\,r}$. The authors attributed the slow changes in the saturation and pressure head profiles and hence, the static condition, to the very low hydraulic conductivity of the coarse sand as it approaches residual saturation.

Barbour (1990) conducted similar analyses for layered soil profiles. However, he assumed steady-state flow for a system that is more realistically in a transient flow state. Further, the ψ_a for his fine-grained cover material and the contrast with the underlying material were far too low in magnitude to examine the effectiveness of the moisture cover concept. Both Nicholson et al. (1990) and Akindunni et al. (unpublished) point out these deficiencies in Barbour's analysis.

The transient nature of the system was not considered in the discussion above. The results of the numerical modelling by Akindunni et al. (unpublished) suggest that equation 18 applies for flow that is in a state of quasi-equilibrium. Figures 8 and 9 (from Akindunni et al., unpublished) present saturation and pressure head profiles at various times in the drainage history of a soil profile. The soil profile consisted of 100 cm of Touchet silt loam (ψ_a = -165 cm) overlying 250 cm of coarse sand ($\psi_{c\,ae}$ = -25 cm). At the start of the simulation, the water table was lowered to the datum and the soil section was allowed to drain from saturation. Figure 8 shows that the coarse sand drained very rapidly and approached residual saturation probably within the first day. Thereafter, the saturation in the coarse sand decreased at an increasingly slower rate. However,

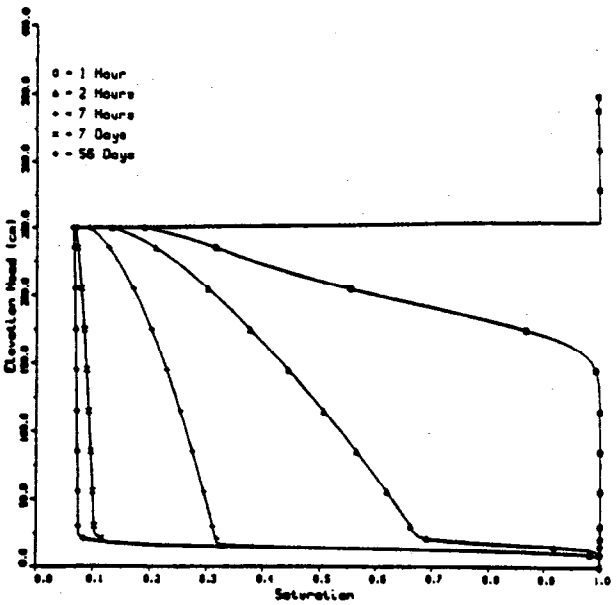

Figure 8: Saturation versus elevation head. Touchet silt loam on coarse sand (from Akindunni et al., unpublished)

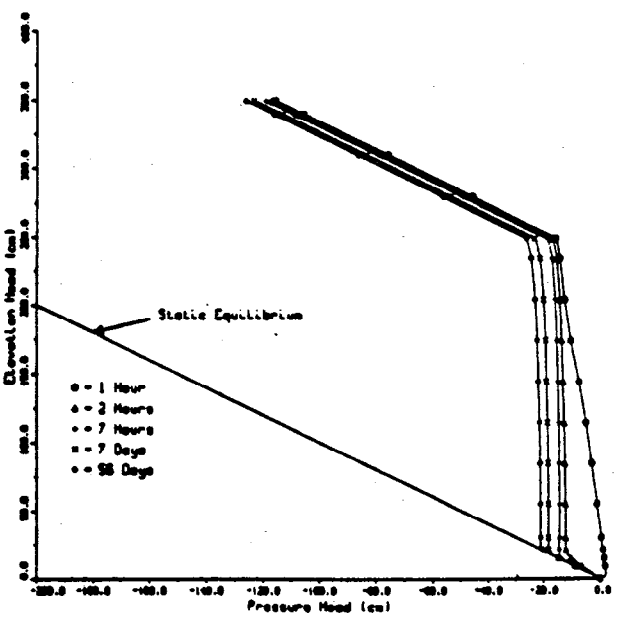

Figure 9: Pressure head versus elevation head. Touchet silt loam on coarse sand (from Akindunni et al., unpublished)

2.3 INSTRUMENTATION

The soil testing conducted required two main types of instrumentation to measure the hydraulic properties of the materials. Each will be discussed separately below.

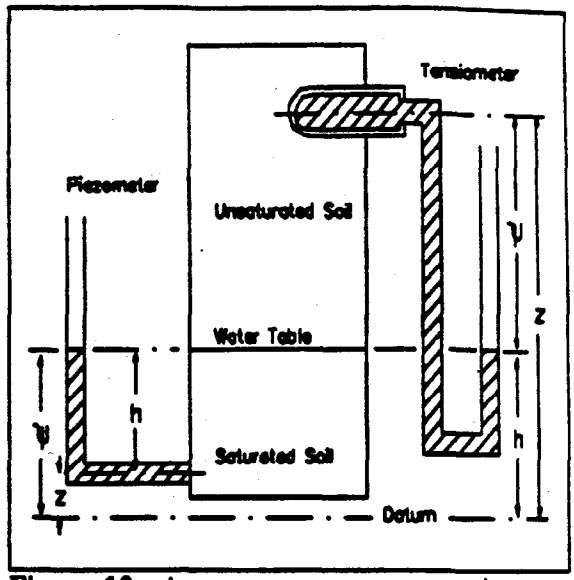

Figure 10: A water manometer tensiometer and piezometer

2.3.1 Pressure Transducer Tensiometry

Fluid pressure in a soil column can be determined using a piezometer for positive pressures or a tensiometer for negative pressures (atmospheric pressure = 0 gauge pressure). Figure 10 shows a simple piezometer and a simple tensiometer. Fluid pressure is read from the height of the water in the manometer tube. Since only tensiometers were used in this study, piezometers will not be discussed further.

Tensiometers have a porous cup on the end that makes contact with the soil. The bubbling pressure of the porous cup must be selected to prevent air from being sucked into the tensiometer. Only water should pass through the porous cup. Further, the cup must have a hydraulic conductivity that permits the rapid equilibration of the tensiometer to pressure changes in the soil water.

The response time of a tensiometer to pressure changes in the soil water is an important consideration. If the response time is too long, the tensiometer may not be able to accurately reflect the pressure changes. The cup's hydraulic conductivity and the tensiometer sensitivity determine the response time (Cassell and Klute, 1986). The

sensitivity is defined as the change of pressure head per unit volume of water in the tensiometer system. It reflects the amount of water that must pass through the porous cup to cause a change in the tensiometer reading. Obviously, tensiometers connected to large diameter tubes will have a lower sensitivity than tensiometers connected to narrower tubes. However, if the tubes become too narrow, capillary rise and temperature effects become significant.

Pressure transducers were used in this study to measure the fluid pressure. Transducers contain a flexible diaphragm in contact with the water from the tensiometer tube. The diaphragm bends slightly to adjust to changes in pressure. Attached to the diaphragm's surface is a strain gauge, which stretches or contracts as the diaphragm bends. The change in electrical resistance of the strain gauge is directly proportional to the change in the fluid pressure. With a calibration curve, the fluid pressure in the soil can be determined from the change in resistance of the strain gauge.

Pressure transducer tensiometers have a much higher gauge sensitivity than manometer-type tensiometers. The former system requires only a very small amount of water to move through the porous cup to adjust to a change in the soil water pressure. Cassell and Klute (1986) gave an example of a pressure transducer with a gauge sensitivity 500 times greater than that of a water manometer with 1.5 mm diameter tubes. The electrical output from transducers permits the use of data collection systems and reduces human error. Further, transducers tend to be more accurate than manometers. However, temperature fluctuations induce errors if the transducer-tensiometer system is not insulated. A second disadvantage is the relatively high cost of pressure transducers when compared to manometers.

The water content can then be calculated from the empirical relationship between K_a and θ (Topp, 1987):

$$\theta = -0.053 + 0.029K_a - 5.5(10^{-4})Ka^2 + 4.3(10^{-6})K_a \quad (21)$$

According to Topp, this relationship has an accuracy of ± 0.02 m^3/m^3 and a precision of ± 0.01 m^3/m^3.

Figure 11 shows an idealized TDR output trace. The travel time of the pulse, t, is shown on the plot. The trace shown is representative of an open circuit because there is an increase in amplitude at the end of the trace. The amplitude decreases at the end of the trace for a short circuit.

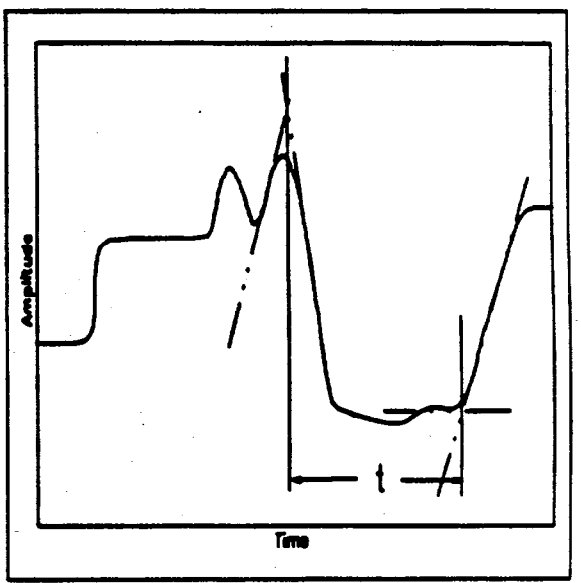

Figure 11: A typical TDR trace (modified from Topp, 1987)

The solid soil particles and the air in the pores have an effect on the propagation velocity. Solid soil particles and air have dielectric constant of 2 to 5 and 1, respectively. In contrast water has a dielectric constant of 80 and hence, governs the propagation velocity (Topp, 1987). A small error results when calculating the water content from the propagation velocity because the influence of the soil and air is not considered in equations 19 to 21. The magnitude of this error increases as the water content decreases.

The TDR electrode essentially measures the water content for a cylinder (Topp, 1987). The long axis of the cylinder is midway between the rods; the diameter is 1.4 times the spacing between the rods; and, the cylinder length is the length of the rods in the soil. As

2.3.2 Time-Domain Reflectometry Measurements

The volumetric water content in a soil can be measured by time-domain reflectometry (TDR). Unlike other methods, the TDR technique is rapid, non-destructive, and non-radioactive (Keng and Topp, 1983). The system consists of a TDR unit connected by coaxial cable to two parallel transmission lines or rods in the soil. An impedance matching transformer, called a balun, connects the unbalanced coaxial cable to the balanced transmission rods.

The TDR determination of water content involves the measurement of the propagation velocity of an electromagnetic (EM) waves (Topp, 1980, 1987). A step voltage pulse or signal is sent from the TDR unit and propagated along the transmission rods. The rods serve as conductors and guide the wave. The soil acts as the dielectric medium and the pulse propagates as a plane wave in the soil. The pulse is reflected from the end of the rods and returns to the TDR unit. The TDR unit records the time interval between sending and receiving the reflected pulse.

The propagation velocity, v, is a function of the soil dielectric constant, K_a. In turn, the dielectric constant is strongly dependent on the water content. An approximate relationship between K_a and v is (Topp, 1987):

$$K_a = (c/v)^2 \qquad (19)$$

where c is the propagation velocity of an EM wave in free space ($3 * 10^8$ m/s). The velocity, v, is calculated from the travel time of the pulse, t, and the length of the transmission rods, *l*:

$$v = 2l/t \qquad (20)$$

where $2l$ is the travel distance of the pulse in the soil.

the spacing is increased, the electrode measures a larger volume and the effects of soil variability are reduced. However, the TDR resolution is reduced.

Two other sources of error are worth noting. Imperfect contact of the rods with the soil can cause an error of unknown magnitude (Topp, 1987). Poor contact may result from soil shrinkage or during the insertion of the rods in the soil. The second error results from the non-parallel alignment of the rods. However, a slight non-parallelism of the rods does not change the path length of the pulse significantly enough to cause an appreciable error (Topp, 1987).

3.0 EXPERIMENT

This study consisted of a laboratory soil column experiment. A fine-grained cover layer was placed over coarse-grained material. The column was permitted to drain from full saturation. Pressure head and moisture content were monitored over the duration of the experiment. The details of the experiment are discussed below.

3.1 MATERIALS

The soil materials were selected to reflect an appropriate contrast in drainage properties. Nicholson et al. (1989 and 1990) suggested that the contrast in grain size or drainage characteristics between the cover and the underlying layer are the controlling factors for the drainage of the cover.

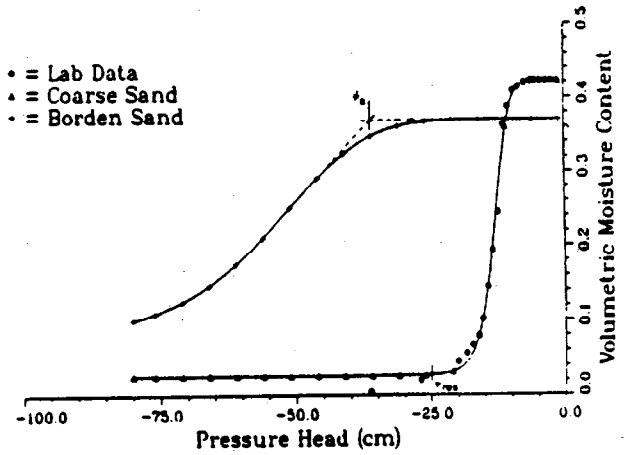

Figure 12: Moisture retention curves. Fine Borden sand on coarse sand
(modified from Akindunni et al., unpublished)

To avoid placement and consolidation problems, fine-grained Borden sand was used to represent the fine-grained cover layer. The moisture retention curve for Borden sand is shown in Figure 12. The curve was determined by Nwankwor (1985) using a methodology similar to the one described in Appendix A. The air entry value for this sand is -37 cm.

A coarse foundry sand was used to represent the coarse-grained layer. Appendix A details the procedure used to determine the moisture retention curve shown in Figure 12. This

sand has an air entry value of approximately -8 cm. Residual saturation is approached at a pressure head of -25 cm. After generating the moisture retention curve, it was discovered that the sand was resin-coated. To remove this coating, the sand was soaked for one day in wash acetone and then rinsed with tap water until the sand no longer smelled like acetone. The rinsed sand was dried in an oven overnight at 60°C.

3.2 METHODOLOGY

The Plexiglas® soil column was one metre in length, with a 10.8 cm (4.25 inches) inside diameter. Tensiometers and TDR electrodes were located at 10 sampling positions, 10 cm apart, along the column. An air vent was installed 78 cm above the base of the column, two centimetres below the coarse/fine sand interface. A 0.5 bar porous ceramic plate was located at the base of the column. A Tygon® tubing line was connected from the base of the column to an erlenmeyer flask. The flask was used to establish the water table level and to collect the water that drained from the column. Figure 13 shows a simple schematic of the column. Appendix B contains a more detailed description of the column, including exact dimensions and material descriptions.

Before packing the column, the porous plate had to be saturated. The porous plate was epoxyed to the Plexiglas® base plate (not shown in Figure 13) and the epoxy was allowed to set overnight. The porous plate was saturated by placing the base plate in an evacuated vacuum chamber. De-aired water was slowly added to the chamber until the porous plate was immersed. The base plate remained immersed in the vacuum chamber for one month. At that time, it was removed and the column was assembled.

To place the sand uniformly in the column, a constant energy Corey packing tool (R. Sri Ranjan, personal communication, 1990) was used. The tool is essentially a long barrelled funnel with two coarse screens. The screens, which are located near the end of the barrel, are separated by three inches and are rotated 45° to each other. For each layer, sand was continuously poured (dry) into the packing tool to create a dense, uniform, single layer of sand. A fine nylon mesh screen was placed at the sand interface to prevent the fine-grained Borden sand from filling pores in the coarse sand. The mesh size was not small enough to prevent dry Borden sand from passing through. However, a smaller mesh size might have interfered with the drainage of the fine-grained layer. Therefore, a 5 mm layer of moist Borden sand was placed on the mesh before the rest of the Borden sand layer was dry-packed. Packing proceeded with the tensiometers in the column.

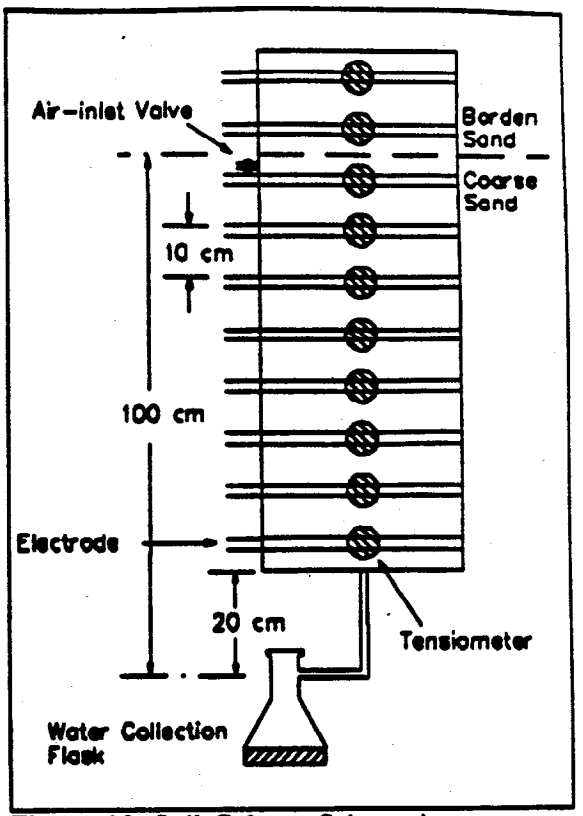

Figure 13: Soil Column Schematic

After the column was packed, the TDR transmission lines were inserted into the column and carbon dioxide gas was slowly passed up the column, through the porous plate. The column was flushed with CO_2 gas for three hours. Then, the column was saturated from the bottom with de-aired, distilled water. To saturate the column, a constant pressure head of about 10 cm was applied (by the de-aired, distilled water) for approximately 12 hours. The column was covered with plastic film to minimize evaporation. The water table in the

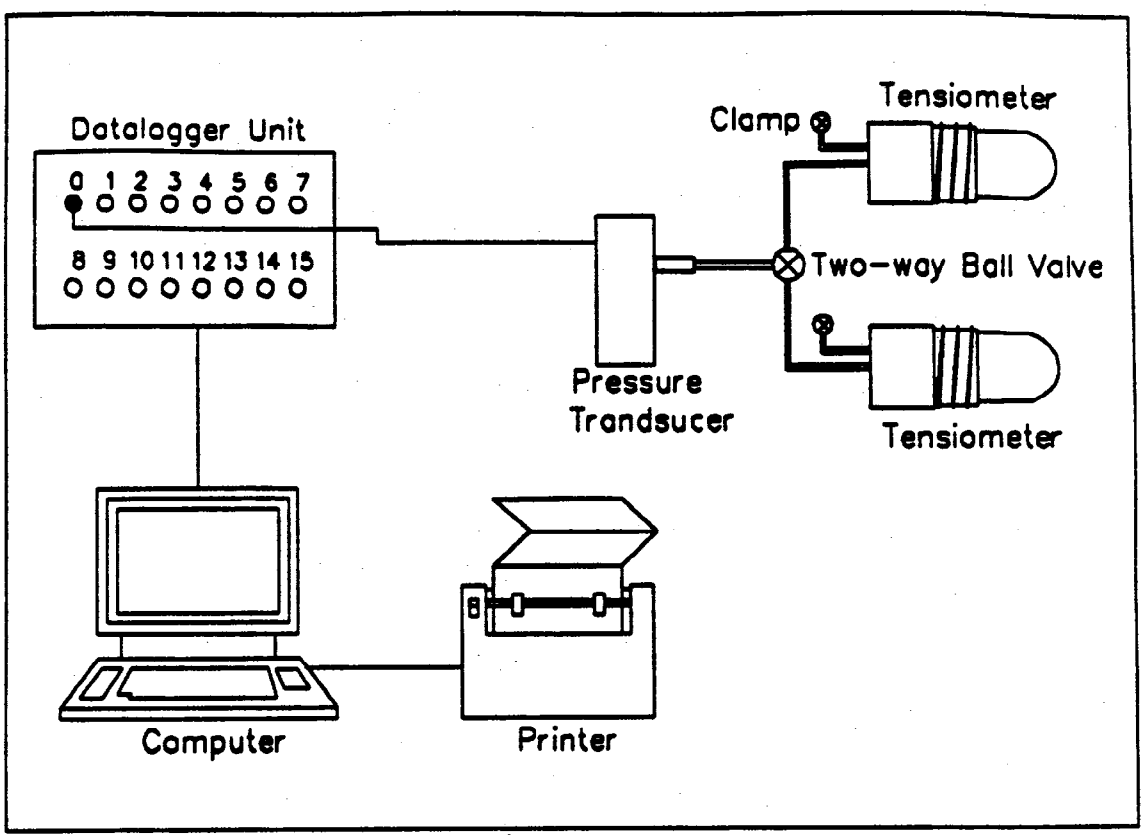

Figure 14: Tensiometer - pressure transducer system components

column was maintained at the top of the Borden Sand until the experiment began. Just before the experiment began, the source of de-aired, distilled water was removed and the Tygon® tubing, at the base of the column, was clamped to prevent premature drainage of the column. Then the Tygon® tubing was connected to the erlenmeyer flask.

Pressure head was measured by connecting pressure transducers to tensiometers. Appendix C details the calibration procedure for the transducers and Appendix D describes the construction and saturation procedures for the tensiometers. To connect the five pressure transducers to the ten tensiometers, five ball valves and poly-tubing were used. Each pressure transducer was located between the two tensiometers to which it was attached, on the column. The electrical leads of the transducers were connected to a data collection system, as shown in Figure 14. The data collection system consisted of a datalogger, a

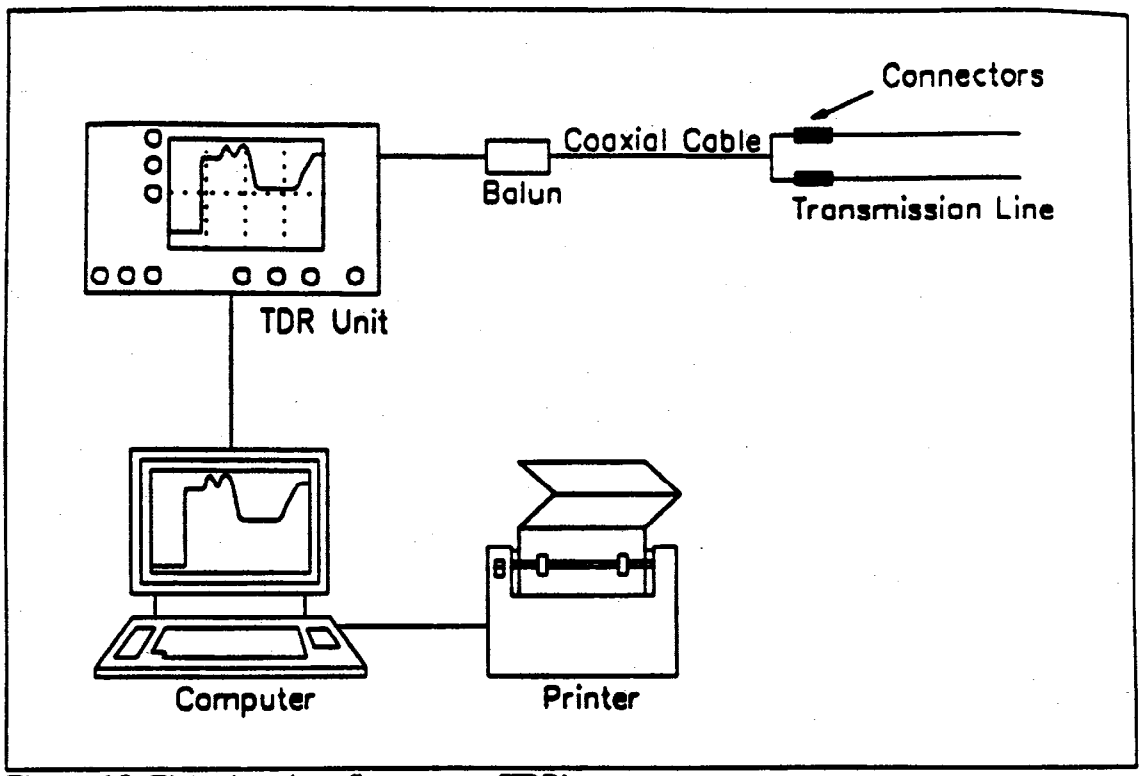

Figure 15: Time domain reflectometry (TDR) system components

computer, and a printer. The datalogger sampled the transducers, converted the analog readings to digital and then sent the digital readings to the computer. The computer controlled when the datalogger sampled the pressure transducers. The computer stored the digital readings from the datalogger in the computer's RAM memory. Periodically, the computer program was interrupted to send the readings to the printer for hardcopy output. The valves were regularly switched to sample all tensiometers. The datalogger was powered by two car batteries and both the computer and printer were plugged into a standard 120 volt A.C wall outlet.

Water content was also monitored. Time domain reflectometry (TDR) electrodes were used to make these measurements. Figure 15 schematically shows the components of the TDR system. Each electrode consisted of two 13.34 cm (5.25 inches) long, 1.6 mm (1/16 inch) diameter steel rods. These rods touched the far end of the column and their long axis was

horizontal. Two centimetres separated the rods in the vertical plane. Swagelok connectors, which were screwed into the column, held the rods in place. A coaxial cable was connected to the ends of the rods extending outside the column. The cable was connected to a balun, which in turn was connected to the TDR unit. The TDR unit, a Tectronix 1502B Time Domain Reflectometer, measured the time delay in the column and displayed the output trace. An IBM® compatible computer, stored these traces in files for analysis at a later time. The coaxial cable was moved from electrode to electrode for each TDR measurement.

As shown in Figure 13, a constant water table 1 m below the fine-coarse sand interface was used for the experiment. To begin the experiment, the clamp was removed from the Tygon® tubing at the bottom of the column and the air inlet valve was opened. Water immediately began to drain from the column and collect in the flask. Pressure transducer sampling occurred every five minutes for the first seven hours of the experiment. Sampling then occurred every 15 minutes for the next five days. Thereafter, a 30 minute sampling rate was used. TDR measurements were made approximately every 30 minutes for the first four hours. Afterwards, hourly measurements were made until after the seventh hour. Daily measurements were then made for the next three days and every second day thereafter. Data were collected over a two week period.

The TDR data were analyzed using WATTDR, a QuickBASIC 4.0 program written by Dave Redman of the University of Waterloo. Details of the TDR analysis are contained in Appendix E.

The analysis of the pressure head data required the use of Lotus 1-2-3 spreadsheets to convert the transducer readings, in millivolts, to pressure heads, in cm. Appendix F contains the raw transducer data and the spreadsheets that were used.

4.0 RESULTS

The results are summarized in Figures 16 to 18. Figure 16 shows the initial moisture content distribution through the column. In the coarse sand, the moisture content was about 0.368, with a high of 0.395 at the bottom and a low of 0.314 at the interface. The Borden sand had a moisture content of 0.360 at the top and 0.322 at the bottom.

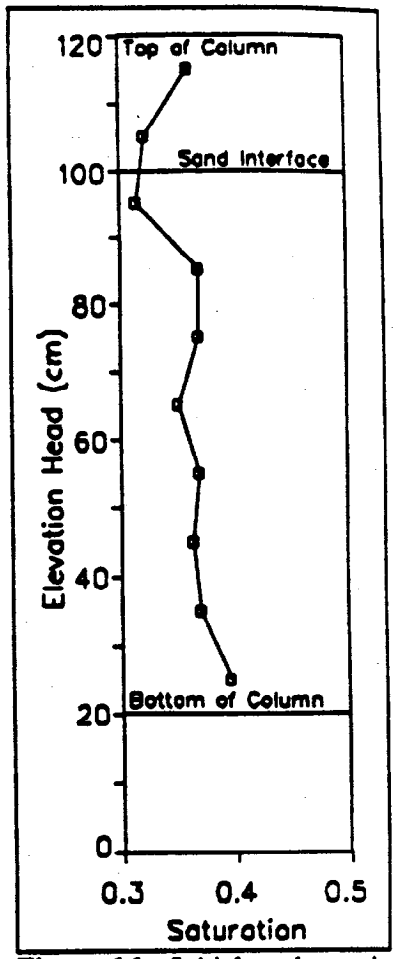

Figure 16: Initial volumetric moisture content profile (t=0)

Figures 17 and 18 show representative profiles of normalized moisture content (i.e., saturation) and pressure head through the column with time. Figure 17 shows that the top of the coarse sand immediately started to drain. After 5 hours, the upper 45 cm of the coarse sand had drained to a saturation of about 12%. After one day, the entire coarse sand layer had drained to about 12%. Thereafter, the saturation decreased slowly to about 10%.

Saturation did not change appreciably in the Borden sand during the first day. By the fifth day, saturation in the bottom of the Borden sand had decreased to 89%, while the top remained essentially saturated. After the fifth day, saturation in the top of the Borden sand started to decrease. At 14 days, the degrees of saturation in the top and bottom of the Borden sand were 77% and 87%, respectively.

Figure 18 shows how drainage affected the pressure head distribution in the column over a two week period. Initially, a linear positive pressure head distribution existed in the

column. This profile was not included in Figure 18 to avoid unnecessary scale changes on the horizontal axis. The pressure head distribution at 15 minutes is the first profile shown. This profile was roughly parallel to the line representing static equilibrium. After 2 hours, pressure head had decreased and the profile had moved towards static equilibrium. The profile was no longer linear in the drained upper 25 cm of the coarse sand. In this drained zone, the pressure head profile was nearly vertical.

As the coarse sand continued to drain, the pressure head profile became increasingly vertical. After the first day, the pressure head profile was nearly vertical throughout the length of the coarse sand. However, the pressure head distribution in the Borden sand, which was still saturated, had not significantly changed. Pressure head decreased slightly in both the coarse and fine sands during the next two weeks. The profiles in the coarse sand remained nearly vertical and laterally shifted approximately 5 cm more towards static equilibrium. In the Borden sand, the profile shifted about 3 cm more towards static equilibrium, while remaining parallel to it. For both sands, the pressure head profiles were still quite distant from static equilibrium. Further, pressure head appeared to be approaching a static condition or a state of quasi-equilibrium.

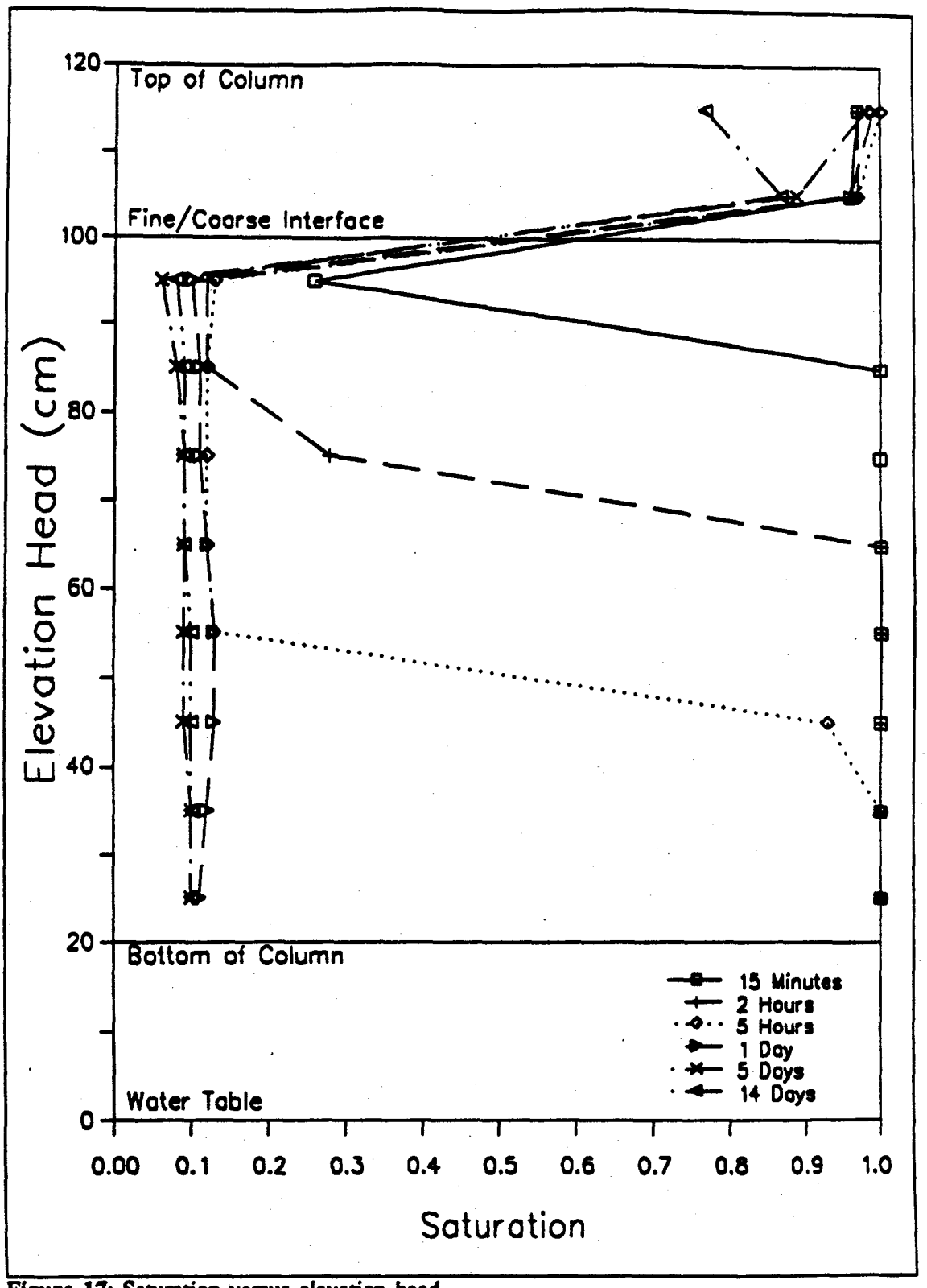

Figure 17: Saturation versus elevation head
Fine Borden sand on coarse sand

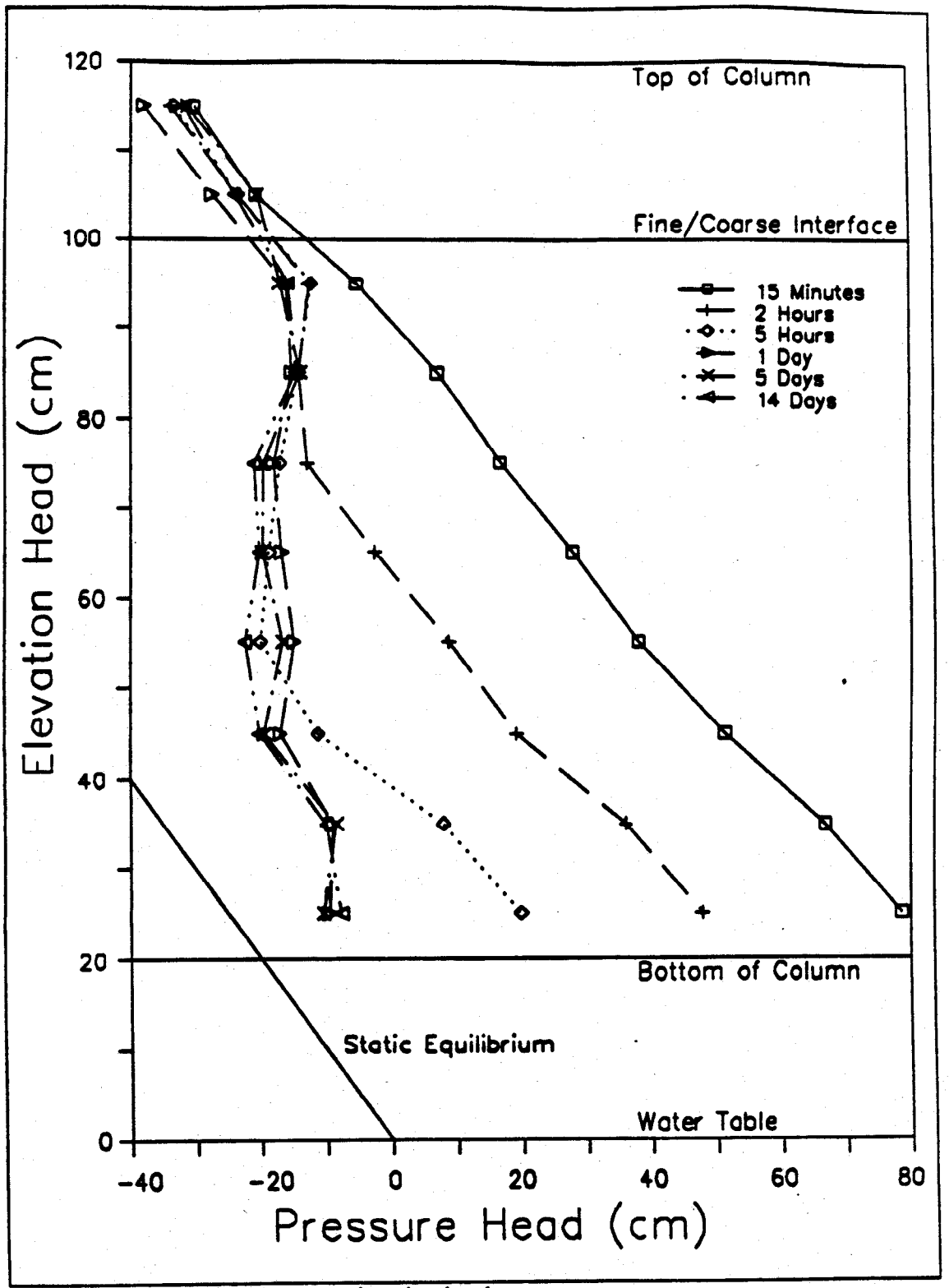

Figure 18: Pressure head versus elevation head
Fine Borden sand on coarse sand

5.0 DISCUSSION

5.1 RESULTS

The saturation profiles showed the anticipated results. In the first day, the coarse layer drained quickly to 12%, which represented the approach to residual saturation. Thereafter, the saturation decreased very slowly in the coarse material to about 10%, which is the residual saturation for the coarse sand. As predicted, the fine-grained Borden sand remained nearly saturated.

The pressure head profiles were also as predicted. The pressure head profile became nearly vertical in the drained zone of the coarse sand. After the first day, the coarse sand was drained and the pressure head profile was nearly vertical throughout the entire coarse sand layer. Thereafter, the pressure profile in the coarse sand moved very slowly towards static equilibrium. Pressure decreased at an increasingly slower rate and the pressure head in the coarse sand appeared to be approaching a static condition. Within experimental error, the pressure head transmitted by the coarse sand to the interface was between -15 cm and -22 cm. This pressure head is very close to the pressure head at which the coarse sand approaches residual saturation in Figure 12 (i.e., -25 cm).

The pressure head profile in the Borden sand did not change significantly during the experiment. Insufficient suction was developed in the Borden sand to cause drainage of the layer as a whole. However, according to equation 18, slight drainage may have occurred at the very top of the layer because the suction at the interface (15 cm to 22 cm) plus thickness of the cover (20 cm) exceeded the air entry value of the sand.

The profiles presented in Figures 17 and 18 are very similar to profiles generated by numerical simulation (see Figures 8 and 9). For example, Akindunni et al. (unpublished) used the same coarse sand in numerical simulations of similar coarse/fine layering of sands. However, the fine-grained cover material was Touchet silt, which has a ψ_a of -165 cm. The simulation results predicted a nearly vertical pressure head profile in the coarse sand. The profile had pressure head values of -18 cm and -22 cm after 7 and 56 days, respectively. The corresponding near vertical saturation profiles for the coarse sand were 0.10 and 0.05, respectively. The numerical simulations suggest that two weeks was an insufficient period of time for the coarse sand to attain the $\psi(\theta_{ms})$ of -25 cm. Overall, there was excellent agreement between the numerical and experimental results.

5.2 ERRORS AND ACCURACY

During the first day, the rate of drainage of the coarse sand was controlled by the low hydraulic conductivity of the porous plate. The plate had a saturated hydraulic conductivity, K_{sat}, of $3.11*10^{-5}$ cm/s. According to Freeze and Cherry (1979), the K_{sat} for coarse sand similar to that used, was between 10^{-1} and 10^{-3} cm/s. By comparing the K_{sat} values, it can be seen that the coarse sand could have drained within minutes with a unit gradient across the layer. As the coarse sand drained, its hydraulic conductivity decreased from K_{sat} to the hydraulic conductivity at residual moisture content, $K(\theta_{ms})$. Similar sands used by Giesel and Renger (1973) and Pickens and Gillham (1980) suggest that the magnitude of $K(\theta_{ms})$ was smaller than the K_{sat} of the porous plate. Therefore, the porous plate should not have inhibited the drainage of the coarse sand after the first day. Indeed, there was no clear indication in Figures 18 and 19 that the porous plate was inhibiting drainage after the first day.

On the second day, the top 3 mm of the Borden sand was observed to be dry. Condensation could be seen on the plastic film covering the top of the column. Therefore, evaporation was responsible for some of the desaturation observed in the top of the Borden sand. Evaporation was also possible in the bottom of the Borden sand layer because the air-inlet valve remained open during the experiment. However, the constant saturation in the bottom half of this layer; the increase in saturation below the interface from Day 5 to Day 14; and, the higher pressure heads just below the interface, indicated that drainage may also have occurred. The exact effects of evaporation and drainage on the desaturation of the fine-grained layer could not be quantified in this experiment.

The TDR saturation data was generally very good. The initial water content measurements (Figure 16) indicated that the Borden sand and the coarse sand had saturated volumetric water contents of 0.36 and 0.368, respectively. The value for the Borden sand was very close to 0.37, which is shown in Figure 12. However, the value for the coarse sand was significantly lower than 0.42, which is also shown in Figure 12. The higher water content for the coarse sand in Figure 12, was attributed to poor packing of the sand specimen that was tested in a 300 ml moisture drainage cup. The initial water content measurements in the column also suggested a slight degree of heterogeneity. Water contents in the coarse layer ranged from 0.314 to 0.395 with a mode of 0.368. Similarly, the two water contents measurements in the Borden sand were 0.322 and 0.360. Non-uniform packing of the sand and incomplete column saturation were most likely responsible for these variations. Poor contact of the transmission lines with the sand and slight deflection of the transmission lines probably contributed marginally to the variations. Interference from the tensiometers and the air-inlet valve did not contribute to the variations because they were located outside the cylindrical zone measured by the TDR electrodes. Overall uncertainty in the volumetric water content was approximately $\pm$ 0.015 or $\pm$ 0.04 when converted to saturation.

In terms of accuracy, the pressure head data was not as good as the TDR data. The calibrations curves, in Appendix C, show that the transducers have decreased sensitivity at pressure head values greater than -60 cm. This low sensitivity of the transducers, poor contact of the tensiometers with the sand, and perhaps, electrical problems in the datalogger (or transducer themselves) resulted in the transducer readings oscillating. Figure 19 presents the first week of pressure head data for Transducer 2, Tensiometer 4. The plot shows typical pressure oscillations, pressure spikes, and periods where data were not collected (long straight lines). The oscillation period varied from three to over twelve hours in length. Consequently, uncertainty in the pressure head was approximately ± 6 cm.

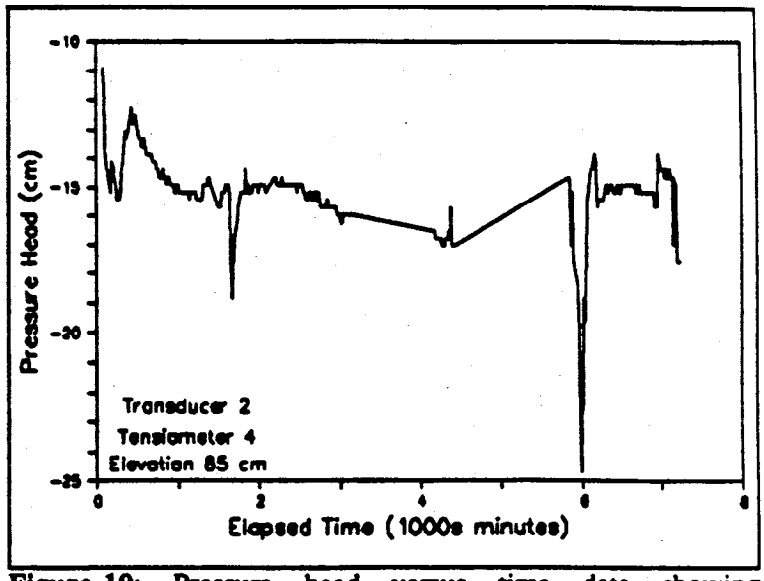

Figure 19: Pressure head versus time data showing oscillations and spikes

Two of the transducers also appeared to read consistently high. The transducers were located at the top and bottom of the coarse sand layer. The pressure head profiles only changed slightly for these transducers, unlike the pressure head for the other transducers. The high pressure heads were attributed to the poor sensitivity of the transducers at low suctions, and to slightly higher water contents in those areas of the column. The influence of each effect could not be quantified.

6.0 CONCLUSIONS

The experimental results agreed well with the results predicted by theoretical and numerical models. The coarse layer drained rapidly to a value near residual saturation and the pressure head profile became nearly vertical. Saturation decreased only slightly once the coarse layer had reached this state. Further, the pressure head profile was moving very slowly towards static equilibrium. However, the profile appeared to be approaching a static condition quite distant from the line representing static equilibrium. The pressure head transmitted to the Borden sand by the coarse layer was approximately equal to the pressure head at which the coarse sand approaches residual saturation.

The fine-grained Borden sand cover remained nearly saturated during the experiment. Slight desaturation occurred because the suction at the top of the layer was slightly exceeded the Borden sand's air-entry value. Overall, the Borden sand remained near saturation because the coarse sand layer was unable to transmit higher suctions to the interface between the layers.

Based on the results of this experiment, it appears that a fine-grained cover can remain fully saturated, with a deep water table, if placed on a coarser material. For the cover to remain saturated, the air-entry value for the fine-grained material must be greater than the thickness of the cover plus the suction at which the coarse material approaches residual saturation (all in terms of absolute values).

7.0 RECOMMENDATIONS

Different soil materials should be tested in the future. A silt cover material overlying a medium-fine sand, which more accurately represents in-situ conditions, should be tested. The water table should be maintained at one depth until the pressure head in the column reaches a static condition. Then, the water table should be lowered further and the resulting effect on the system should be monitored. However, to conduct this experiment, the problems pertaining to the placement of the silt layer and consolidation must first be overcome.

Inserting a coarse-grained layer between the overlying fine-grained cover and the underlying medium-grained material, representing the tailings, might also be tested. The insertion of this coarse layer should permit the water table to be even lower than for the case where it is not inserted.

Future experiments should be conducted over a longer period of time. This would serve to prove or disprove that the pressure head attains a static condition, which is quite distant from static equilibrium.

To quantify errors in the pressure transducers, one transducer should be calibrated over a period, say one week in length. The applied suction should be changed every several hours. This would serve to both check the repeatability of measurements and to characterize any wandering or oscillations in pressure head measurements. The temperature, atmospheric pressure, and humidity should be closely monitored to determine the extent of their influence on the transducer readings.

A similar calibration procedure might be conducted using one transducer connected to two hydraulic lines, each applying a different suction. The effect of the ball valve on transducer stabilization time could then be determined.

Modifications to the current TDR system should be made if future work is to be conducted. Each TDR electrode should be connected to its own coaxial cable. These cables might be connected to a switching unit. This would permit the fully automated collection of data. The computer program, WATTDR, that was used for the analysis of the TDR traces, should be re-programmed to automatically calculate the water contents. At this time, WATTDR requires the operator to fit lines to the traces to determine the time delay of the EM wave.

The pressure transducer-tensiometer system should also be modified for future work. The computer should be re-programmed to permit the storage of data in files, and not in the RAM memory. This would permit the uninterrupted collection of data. Further, the data would exist as computer files, and would not have to be re-entered into the computer, by hand, like the current system requires. Secondly, an A.C. to D.C. power converter could be easily built. This converter would provide a continuous power supply, unlike the car batteries which had to be recharged weekly. Thirdly, the caps for the tensiometers should be machined from rubber stoppers. The threaded tensiometers leaked, were hard to install and made column packing difficult.

Column packing would improve if the tensiometers had rubber stoppers for caps. As the column was packed, the tensiometers could be inserted one at a time, when the level of the granular material approached the level of the tensiometer port (i.e., hole in the column). In this way, the column could be more uniformly packed because the tensiometers would not restrict the movement of the packing tool. Further, tensiometer contact with the granular

material would improve. The transmission lines of the TDR electrodes could be inserted in a similar fashion. This would both improve contact with the granular material and reduce the deflection of the transmission lines in the column.

When packing the fine-grained cover material, a mesh size smaller than the fine-grained material should be used. The thin layer of wet Borden sand that was placed at the interface probably prevented the fine-grained material from attaining full saturation, when the column was saturated.

REFERENCES

1. Akindunni, F., Gillham, R.W., and Nicholson, R.V. unpublished. Numerical simulations to show the importance of moisture retention characteristics in the design of oxygen barriers to reactive mine tailings.

2. Barbour, S.L. 1990. Reduction of acid generation in mine tailings through the use of moisture-retaining cover layers as oxygen barriers: Discussion. Can. Geotech. J., Vol. 26: 1-8.

3. Bear, J. 1979. Hydraulics of groundwater. McGraw Hill, Israel.

4. Bowles, J.E. 1979. Physical and geotechnical properties of soils. McGraw Hill, New York, NY.

5. Cassell, D.K., and Klute, A. 1986. Water potential:tensiometry. Agronomy Monogragh No. 9 (2nd ed.): 563-595.

6. Dane, J.H., and Wierenga, P.J. 1975. Effect of hysteresis on the prediction of infiltration redistribution and drainage of water in a layered soil. J. Hydrology, Vol. 25: 229-242.

7. Freeze, R.A., and Cherry, J.A. 1979. Groundwater. Prentice-Hall, Englewood, NJ.

8. Ghildyal, B.P., and Tripathi, R.P. 1987. Soil physics. Wiley Eastern. New Delhi, India.

9. Giesel , W., and Renger, M. 1973. Numerical treatment of the unsaturated water flow equation: comparison of experimental and computed results. Water Resources Research, Vol. 9, No. 1: 174-177.

10. Gillham, R.W., Klute, A., and Heerman, D.F. 1976. Hydraulic properties of a porous medium: measurement and empirical representation. Soil Sci. Soc. Amer. J., Vol. 43:203-207.

11. Gillham, R.W. 1984. The capillary fringe and its effects on the water-table response. J. Hydrology, Vol. 67: 307-324.

12. Gureghian, A.B., Ward, D.S., and Cleary, R.W. 1979. Simultaneous transport of water and reacting solutes through multilayered soils under transient unsaturated flow conditions. J. Hydrology, Vol. 41: 253-278.

13. Healy, R.W. 1989. Seepage through a hazardous-waste trench cover. J. Hydrology, Vol. 108: 213-234.

14. Keng, J.C.W., and Topp, G.C. 1983. Measuring water content of soil columns in the laboratory: a comparison of gamma ray attenuation and TDR techniques. Can. J. Soil Sci., Vol. 63: 37-43.

15. Klute, A., and Heerman, D.F. 1978. Water movement in uranium mill tailings profiles. U.S. EPA, Technical note ORP/LV-78-8.

16. Nwankwor, G.I. 1985. Delayed Yield Processes and Specific Yield in a Shallow Sand Aquifer. Ph.D. thesis, University of Waterloo, Waterloo, Ont.

17. Nicholson, R.V., Gillham, R.W., Cherry, J.A., and Reardon, E.J. 1989. Reduction of acid generation in mine tailings through the use of moisture-retaining cover layers as oxygen barriers. Can. Geotech. J., Vol. 26: 1-8.

18. Nicholson, R.V., Gillham, R.W., Cherry, J.A., and Reardon, E.J. 1990. Reduction of acid generation in mine tailings through the use of moisture-retaining cover layers as oxygen barriers: Reply to Discussion. Can. Geotech. J., in press.

19. Pickens, J.F., and Gillham, R.W. 1980. Finite element analysis of solute transport under hysteretic unsaturated flow conditions. Water Resources Research, Vol. 16, No. 6: 1071-1078.

20. Rasmuson, A., and Eriksson, J. 1987. Capillary barriers for mine tailings dumps. National Swedish Environmental Protection Board, Report 3307, Solna Sweden.

21. Redman, J.D. 1989. WATTDR user's guide. University of Waterloo, Waterloo, Ontario. unpublished.

22. Redman, J.D. 1990. TDR for determining water content in columns. University of Waterloo, Waterloo, Ontario. unpublished.

23. Streeter, V.L., and Wylie, E.B. 1981. Fluid mechanics. McGraw-Hill Ryerson. Toronto, Ontario.

24. Topp, G.C., Davis, J.L., and Annan, A.P. 1980. Electromagnetic determination of soil water content: measurements in coaxial transmission lines. Water Resources Research, Vol. 16, No. 3: 574-582.

25. Topp, G.C. 1987. The application of time-domain reflectometry (TDR) to soil water content measurement. Proc. of Intel conference on measurement of soil and plant water status, Vol. 1: 85-93.

APPENDIX A: Coarse Sand Moisture Retention Curve Determination

The moisture retention curve for the coarse sand was required to determine the pressure head at which residual saturation was approached. For the desired 20 cm thick fine-grained layer, with an ψ_e of -37 cm, to remain fully saturated, then the pressure head at which residual saturation was approached had to be greater than -17 cm.

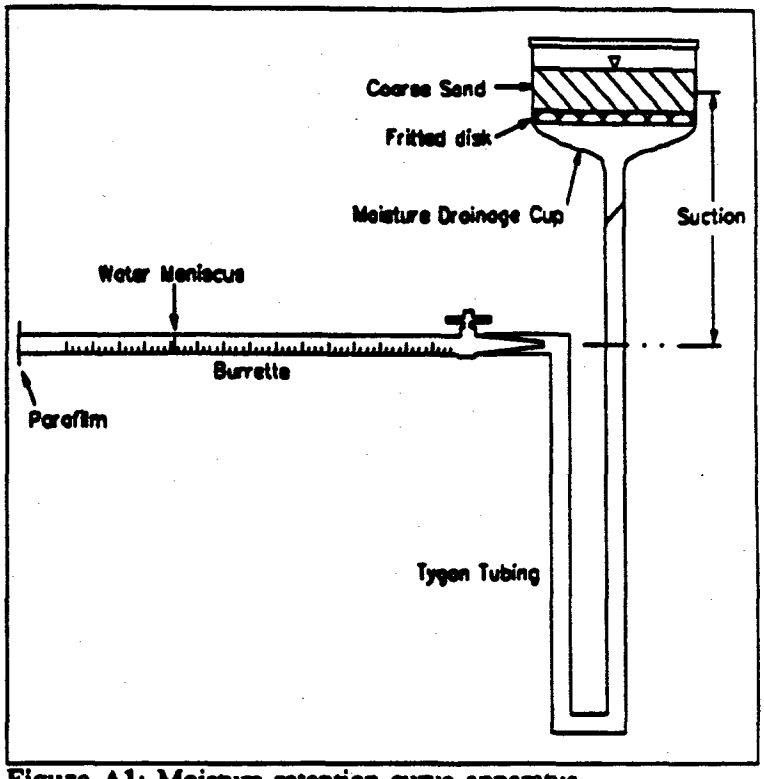

Figure A1: Moisture retention curve apparatus

The retention curve was determined using the apparatus shown in Figure A1. Dry sand was packed in a 300 ml moisture drainage cup to a level that was etched in the glass. Carbon dioxide gas was slowly passed through the porous plate and sand from the bottom for one hour. The porous plate and sand were then slowly saturated from the bottom with de-aired water. The water level in the sand was raised until an unbroken meniscus had almost formed on top of the sand. At this time, it was noted that the surface tension forces at the glass-water-sand interface pushed the sand grains away from the edges of the glass.

The middle of the sand layer was taken as the datum. A horizontal 10 ml burette was positioned at datum level and its valve was opened. Water flowed into the burette and

stabilized. Reading the top of the water meniscus, the water volume was recorded. This reading became the reference water volume.

The burette was lowered in 1 cm decrements and the stabilized water volumes were recorded. The reference water volume was subtracted from each reading to determine the volume of water removed for each increase in suction. When full, the burette was emptied with a syringe and a length of tubing to establish a new reference volume.

After the last reading was measured, the sand was oven dried and weighed. The volume to the etched line on the moisture drainage cup was also measured. The mass of the dry sand was 77.53 g and the volume was 41.2 cm^3. The moisture retention curve was then calculated from this data. The particle density of the sand was assumed to be 2650 kg/m^3. Table A1 contains the experimental data and the calculated pressure head and moisture content data.

The large volume of water removed initially was thought to represent the drainage of the meniscus. It caused a significant error because the calculated volume of water in the voids exceeded the pore volume. To correct this error, the measured volume of water removed was decreased by 0.95 ml, as shown in Table A1. Figure 12 is a plot of the corrected water content versus pressure head.

The smooth curve, shown in Figure 12, was fitted to the corrected data using Van Genuchten's model (see Akindunni et al., unpublished, p.3). Comparison with the lab data indicated that the sand was still draining when measurements were taken. The fitted curve approached residual saturation at a pressure head of -25 cm. This value implied that the overlying fine-grained cover might start to de-saturate in the upper 8 cm of that layer.

TABLE A1: Coarse Sand Moisture Retention Curve Determination

Date of test: Feb. 9, 1990

Mass of sample: 77.53 g
Volume of sample: 41.2 cm3

Height (mm)	Burette Reading (ml)	Comment	Pressure Head (mm)	Water Removed (ml)	Corrected Water Removed (ml)	Water Content	Corrected Water Content
2938	8.275	open burette	0	0	0	0.445	0.422
2925.5	7.7		-12.5	0.575	0	0.431	0.422
2914.5	7.55		-23.5	0.725	0	0.427	0.422
2903.5	7.475		-34.5	0.8	0	0.425	0.422
2893	7.375		-45	0.9	0	0.423	0.422
2883	7.25		-55	1.025	0.075	0.420	0.420
2875.5	7.15		-62.5	1.125	0.175	0.417	0.417
2864	7.025		-74	1.25	0.3	0.414	0.414
2851.5	6.8		-86.5	1.475	0.525	0.409	0.409
2842	6.6		-96	1.675	0.725	0.404	0.404
2832	5.75		-106	2.525	1.575	0.383	0.383
2823	4.75		-115	3.525	2.575	0.359	0.359
2814	6.6	emptied line	-124	8.425	7.475	0.240	0.240
2803	4.5		-135	10.525	9.575	0.189	0.189
2794	2.5		-144	12.525	11.575	0.141	0.141
2784	0.75		-154	14.275	13.325	0.098	0.098
2776	8.6	emptied line	-162	15.225	14.275	0.075	0.075
2765	8.1		-173	15.725	14.775	0.063	0.063
2754	7.65		-184	16.175	15.225	0.052	0.052
2738	7.2		-200	16.625	15.675	0.041	0.041
2668	6.15		-270	17.675	16.725	0.016	0.016
2575	5.5		-363	18.325	17.375	0.000	0.000

APPENDIX B: Column Construction

The Plexiglas® soil column was one metre in length, with a 10.8 cm (4.25 inches) inside diameter and a 12.07 cm (4.75 inches) outside diameter (see Figure B1). Ten holes and twenty holes were drilled in the column for the tensiometers and TDR electrodes, respectively (see Figure 13). The holes for the tensiometers and the electrodes were drilled perpendicularly to each other. All thirty holes were threaded. The centres of the holes for the ten tensiometers were located every 10 cm along the column, starting 5 cm up from the bottom of the column. The holes for the TDR electrodes were centred 1 cm on either side of the centres of the tensiometer holes.

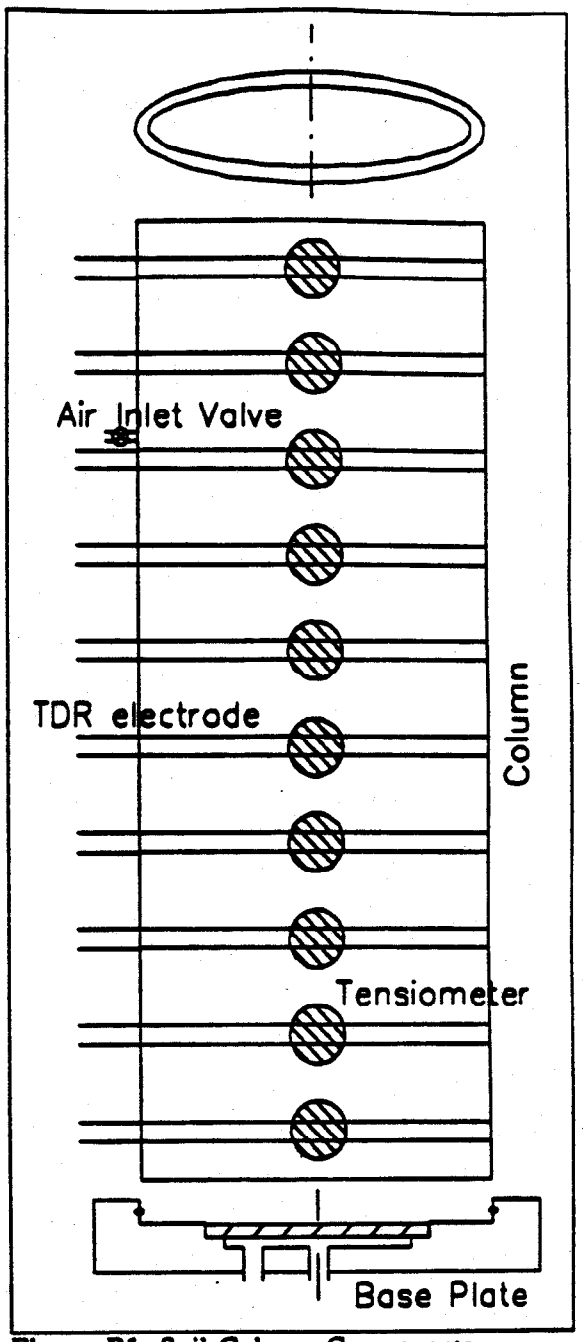

Figure B1: Soil Column Components

The coarse/fine sand interface was located 80 cm up from the bottom of the column. An air-inlet valve was installed 78 cm above the bottom of the column, 2 cm below where the interface was to be located. The long axis of the valve was parallel to the long axis of the TDR electrodes.

The base plate for the column was machined from 3.8 cm (1.5 inches) thick Plexiglas®, which was 15.2 cm (6 inches) in diameter. An O-ring prevented leaks between the base plate and the column. A 0.5 bar porous ceramic plate was recessed into the base plate. The ceramic plate was 76.2 cm in diameter and 7.14 mm thick. It was epoxyed to the base plate. A flushing line and a line to the water column installed in the bottom of the base plate. The flushing line had a two-way valve. The water column consisted of an erlenmeyer flask that was covered with parafilm to prevent evaporation.

APPENDIX C: Pressure Transducer Calibration

Eleven pressure transducers were readily available for the experiment. They had previously been used for one year in the field and then kept in storage. Originally, they were purchased from Honeywell Bull Ltd. in North York, Ontario. Their part number is: 143PC05G. All transducers had a recommended lower operating limit of -3.5 m, except Transducer 1, or Port 0, which had a recommended lower operating limit of -5 m. Of the eleven pressure transducers, only five could be calibrated. The other six transducers either had blown diaphragms or did not yield consistent readings.

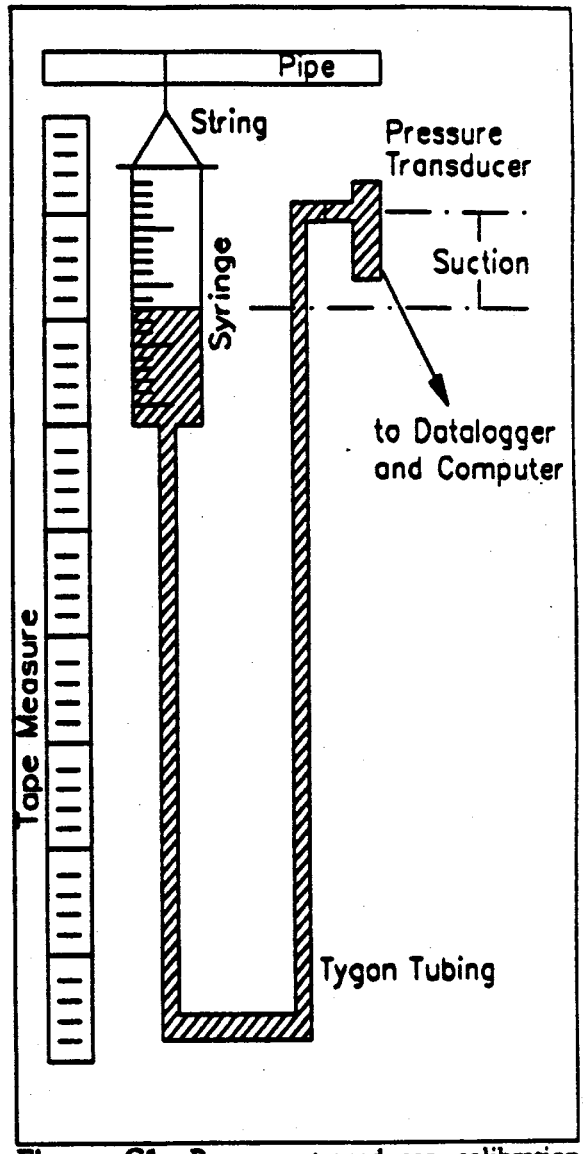

Figure C1: Pressure transducer calibration apparatus

Figure C1 shows the apparatus required to calibrate each pressure transducer. The transducer was plugged into the datalogger unit and the computer was programmed to continuously sample the transducer. The transducer was connected to a 2 m length of Tygon® tubing, which was filled with de-aired water. An open syringe was connected to the other end of the tubing. The open syringe was covered with parafilm to reduce the rate that air was dissolving back into the de-aired water. A small hole was poked in the parafilm to keep the surface of the water,

in the syringe, at atmospheric pressure. The syringe was suspended by a length of string from a pipe near the ceiling of the room. In this way, the elevation of the syringe, relative to the transducer, could be changed. The transducer was clamped in place adjacent to a measuring tape that extended from the floor to the ceiling. The maximum elevation difference that could be easily attained in the room was 210 cm. As a result, the transducer had to be moved once to permit readings over the pressure head range anticipated for the experiment (i.e., +1 m to -2 m).

For the first half of the calibration procedure, the transducer was clamped near the ceiling. The syringe was lowered 2 m relative to the transducer. This suction was applied for approximately 30 minutes. During this time, the transducer was tapped to remove all air bubbles that were trapped in it. The air bubbles were then removed from the length of Tygon® tubing.

When no air bubbles remained, the syringe was raised to the zero suction level and a stabilized transducer reading was recorded in millivolts. The syringe was then lowered in 20 cm decrements and readings were recorded. After measuring a reading corresponding to 210 cm of suction, readings were repeated at suctions of 80 cm and 0 cm to check the repeatability of measurements.

The transducer was clamped at a lower position for the second half of the calibration procedure. The zero suction reading was checked. Then, the transducer was calibrated from +100 cm pressure head to 0 cm in 20 cm decrements. The transducer was discarded if the three readings at 0 cm were not the same to within ±10 mV.

Readings were considered valid and recorded only if the computer displayed the same number over at least three consecutive sampling intervals. Usually, it took five minutes to

get a valid reading. Wander in the readings was attributed largely to the syringe swaying on the string. However, air remaining in the transducer, would have had the same effect on the readings.

After all five transducers were calibrated, third or fourth polynomials were fit to the data (see Table C1). The polynomials were fit using GRAPHER, Version 1.75. Figures C2 to C6 show the calibration curves for these five pressure transducers. The equations for the curves are also shown on these figures. The best fit curves were not included on the plots because they did not differ significantly from the raw curves through the datum points. Comparison of the calculated values and the measured data showed a maximum error of 10 mm. However, the values normally agreed to within 3 mm.

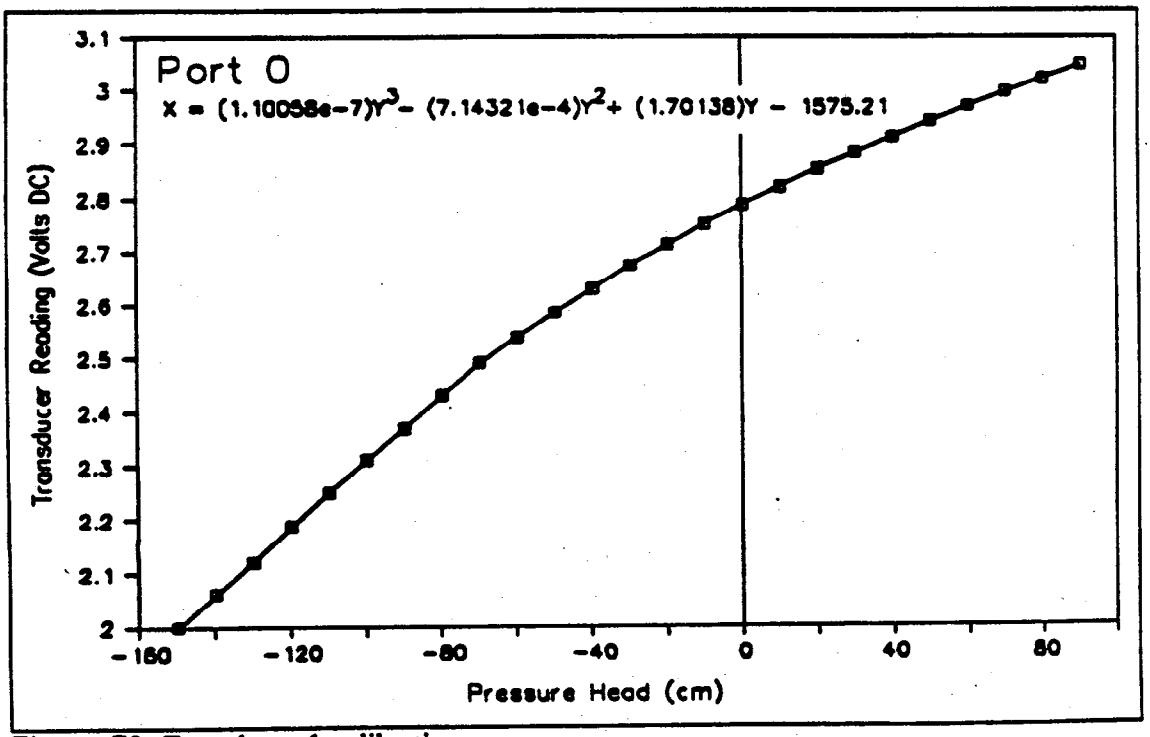

Figure C2: Transducer 1 calibration curve

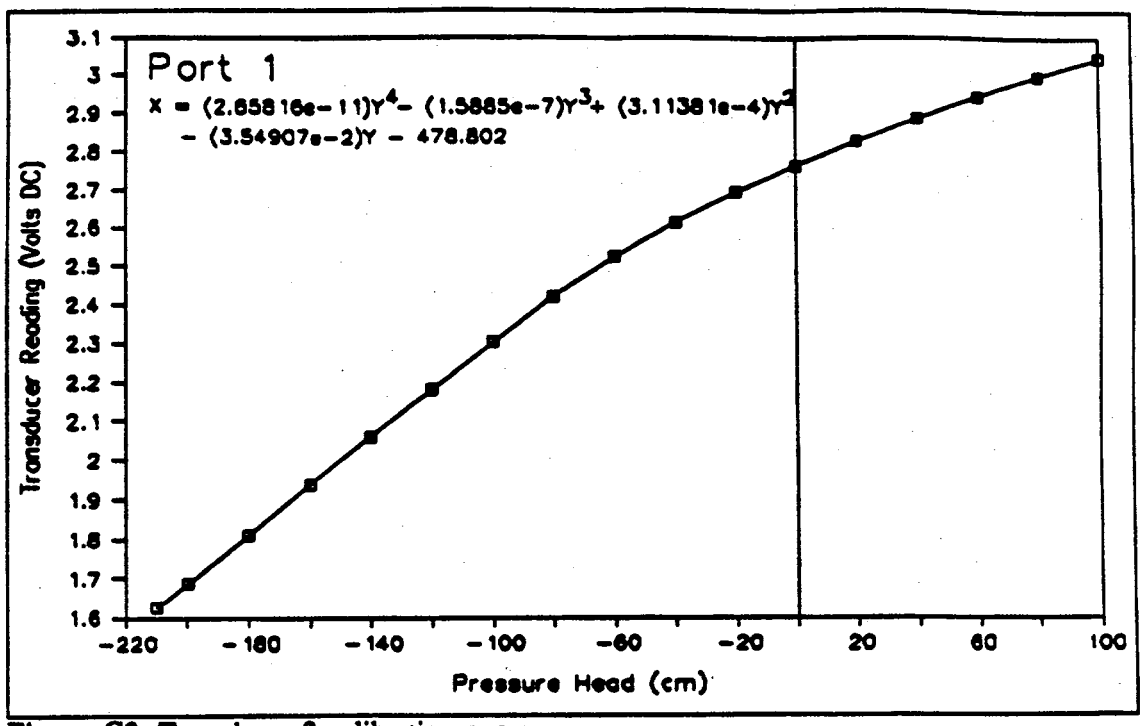

Figure C3: Transducer 2 calibration curve

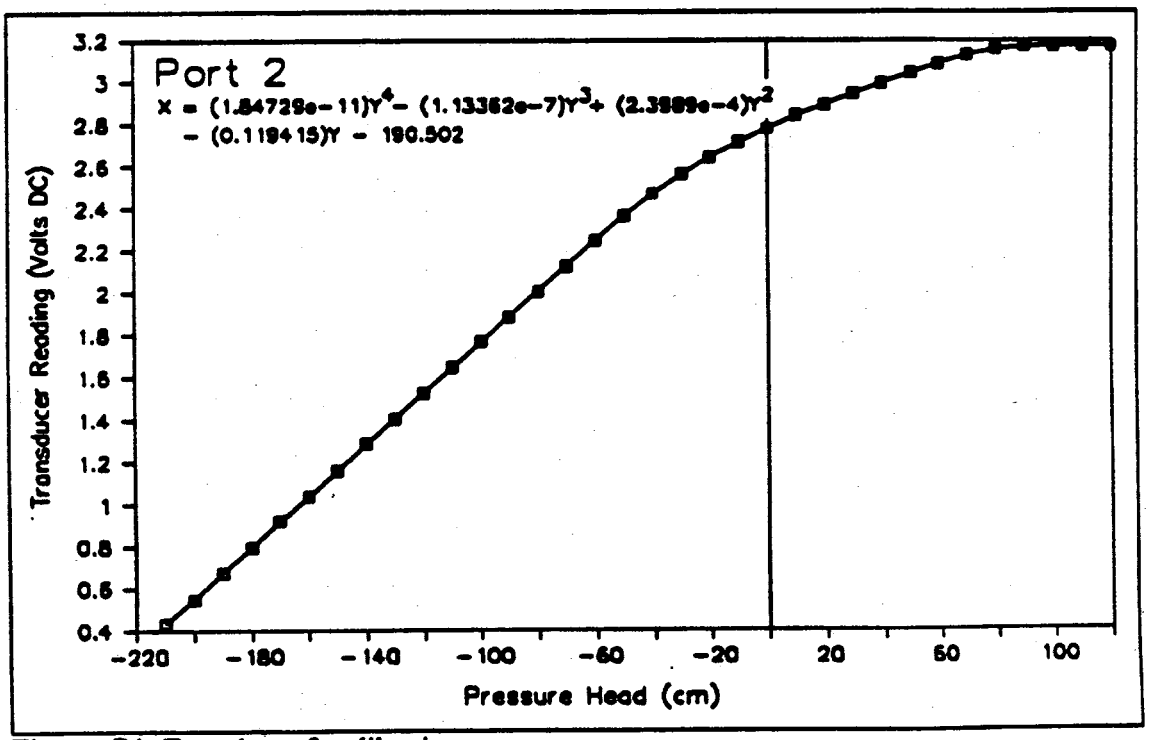

Figure C4: Transducer 3 calibration curve

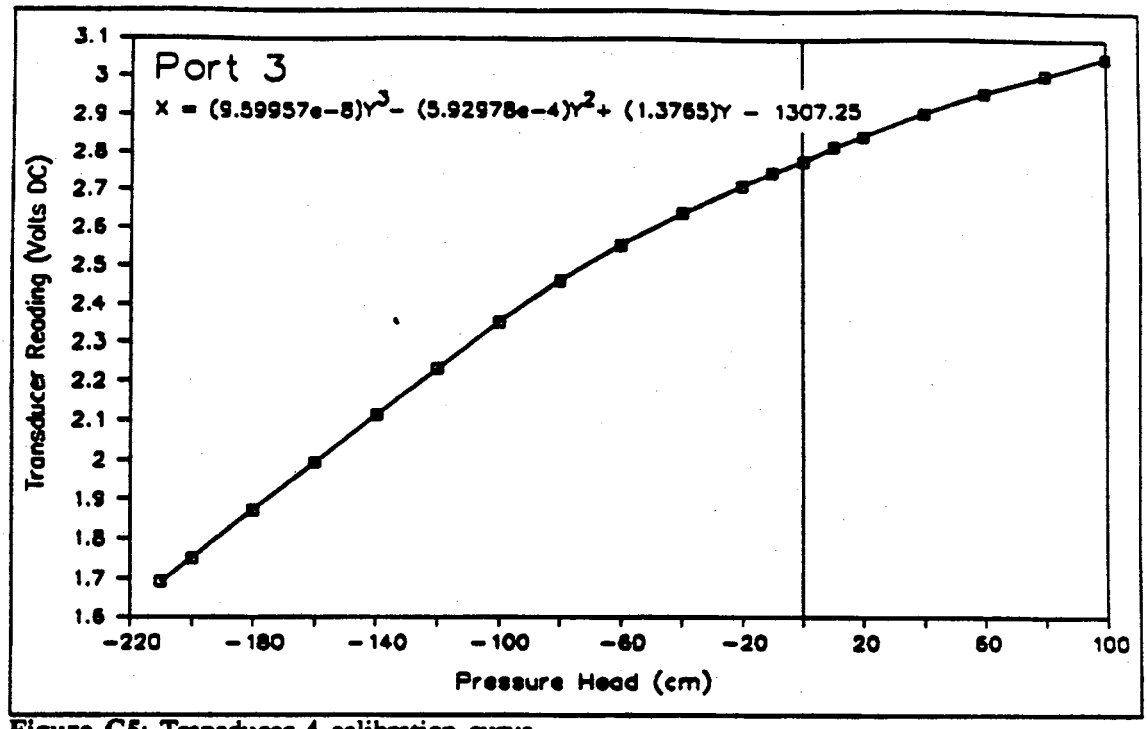

Figure C5: Transducer 4 calibration curve

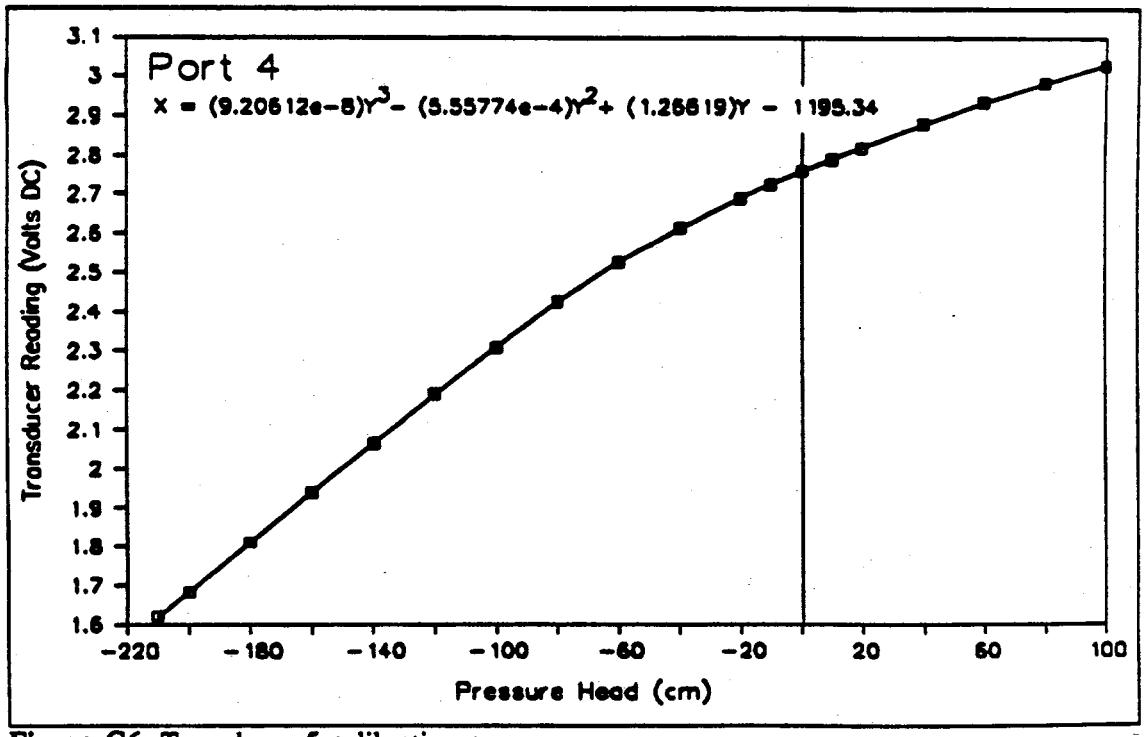

Figure C6: Transducer 5 calibration curve

TABLE C1: Pressure Transducer Calibration Data

PORT 0		PORT 1		PORT 2		PORT 3		PORT 4	
P.H. (cm)	P.T.R (mV DC)	P.H. (cm)	P.T.R (mV DC)	P.H. (cm)	P.T.R (mV DC)	P.H. (cm)	P.T.R (mV DC)	P.H. (cm)	P.T.R (mV DC)
90.5	3048	100	3045	120	3172	100	3052	100	3029
80.5	3023	80	2997	110	3171	80	3006	80	2983
70.5	2998	60	2946	100	3170	60	2958	60	2933
60.5	2971	40	2889	90	3167	40	2905	40	2879
50.5	2943	20	2830	80	3158	20	2845	20	2818
40.5	2913	0	2767	70	3126	10	2817	10	2789
30.5	2883	-20	2697	60	3085	0	2780	0	2758
20.5	2853	-40	2617	50	3042	-10	2749	-10	2724
10.5	2820	-60	2529	40	2995	-20	2714	-20	2688
0.5	2786	-80	2426	30	2945	-40	2641	-40	2611
-9.5	2751	-100	2308	20	2893	-60	2558	-60	2525
-19.5	2712	-120	2184	10	2842	-80	2463	-80	2423
-29.5	2673	-140	2061	0	2779	-100	2356	-100	2308
-39.5	2630	-160	1938	-10	2714	-120	2234	-120	2188
-49.5	2585	-180	1810	-20	2643	-140	2114	-140	2062
-59.5	2539	-200	1688	-30	2561	-160	1993	-160	1940
-69.5	2490	-210	1625	-40	2468	-180	1871	-180	1811
-79.5	2431			-50	2364	-200	1752	-200	1683
-89.5	2370			-60	2246	-210	1691	-210	1619
-99.5	2311			-70	2127				
-109.5	2250			-80	2006				
-119.5	2187			-90	1885				
-129.5	2122			-100	1765				
-139.5	2062			-110	1644				
-149.5	2000			-120	1527				
				-130	1405				
				-140	1285				
				-150	1160				
				-160	1037				
				-170	920				
				-180	798				
				-190	676				
				-200	550				
				-210	433				

Note: 1. Port n corresponds to Transducer (n-1).
2. P.H. = Pressure Head.
3. P.T.R. = Pressure Transducer Reading.

APPENDIX D: Tensiometer Construction and Saturation

The tensiometers, shown in Figure 14, were constructed from 0.5 bar porous ceramic cups and PVC® plastic. The PVC® plastic was machined into caps and threaded. The porous cups were glued to the caps with waterproof 3M® epoxy. Two holes were drilled into the PVC® caps and two lengths of steel tubing, 1/8 inches in diameter, were inserted and epoxyed. The first tube was inserted flush with the end of the cap, while the other tube was inserted almost to the end of the tensiometer.

To saturate the tensiometers, they were stood upright (i.e., porous cup upwards) in an evacuated vacuum chamber and de-aired water was slowly introduced into the chamber. The water level was raised through the length of the tensiometers over a period of approximately four hours. The tensiometers remained immersed in the vacuum chamber for two weeks. Then, they were removed from the chamber and tested for leaks.

Each tensiometer was checked for leaks by covering the porous cup with plastic film and attaching a two metre length of tubing, filled with de-aired water, to the tensiometer. The tubing was held below the tensiometer and applied 2 m of suction to the tensiometer. In all cases the water level in the tubing remained constant, indicating no leaks. The tensiometers were then installed in the column.

APPENDIX E: TDR Data

The TDR measurements were made following the instructions outlined in Redman (unpublished, 1990). The analysis of the TDR traces was performed using WATTDR. Redman (unpublished, 1989) details the procedure for the analysis. Essentially, the time delay for the EM pulse was determined by fitting four straight line segments to each trace, as shown in Figure 11. Table E1 is a record of all water contents determined using the TDR technique. The elapsed times since the start of the experiment were calculated:

elapsed seconds in March to start of experiment, E:

$$E = (D-1)(24*3600)+(H)(3600)+(M)(60)+(S) \quad (21)$$

$$= (2-1)(24*3600)+(13)(3600)+(18)(60)+(20)$$

$$= 134300 \text{ sec.} = 2238.33 \text{ min.}$$

elapsed time since start of experiment, ET:

$$ET = (D-1)(24*3600)+(H)(3600)+(M)(60)+(S)-E \text{ [sec]} \quad (22)$$

The water contents were normalized for each TDR electrode by dividing the water contents by the water content at time zero. The water contents were normalized this way because the variations in water content at time zero could not be quantitatively explained. In other words, the variations in the water content were an combination of sand heterogeneities, incomplete saturation, and variations in transmission line deflection and contact with the sand grains; the influence of each factor could not be quantitatively determined.

Table E2 contains the saturation data for the moisture content profiles shown in Figure 17.

TABLE E1: TDR Water Content Measurements

Probe Length = 109.3 mm = .3596 ft

Elapsed Time (hr)	Water Content 1	Water Content 2	Water Content 3	Water Content 4	Water Content 5	Water Content 6	Water Content 7	Water Content 8	Water Content 9	Water Content 10
0.0	0.36	0.322	0.314	0.368	0.368	0.35	0.368	0.363	0.369	0.395
0.3	0.349	0.306	0.076	0.367	0.366	0.351	0.367	0.362	0.37	0.395
0.8	0.353	0.31	0.044	0.363	0.365	0.35	0.367	0.36	0.369	0.394
1.0	0.346	0.309	0.04	0.129	0.365	0.35	0.365	0.36	0.368	0.395
1.2	0.348	0.304	0.038	0.075	0.365	0.35	0.365	0.361	0.367	0.393
1.5	0.347	0.308	0.037	0.055	0.364	0.348	0.365	0.36	0.368	0.393
1.7	0.352	0.31	0.037	0.049	0.252	0.35	0.366	0.362	0.367	0.392
2.3	0.349	0.312	0.035	0.044	0.058	0.348	0.365	0.366	0.368	0.394
2.5	0.351	0.309	0.035	0.044	0.051	0.194	0.365	0.365	0.367	0.392
3.0	0.356	0.306	0.039	0.044	0.048	0.074	0.366	0.364	0.369	0.393
3.7	0.35	0.306	0.042	0.043	0.045	0.043	0.272	0.365	0.367	0.392
4.0	0.357	0.306	0.041	0.043	0.045	0.041	0.099	0.365	0.368	0.394
5.0	0.363	0.312	0.04	0.044	0.046	0.041	0.047	0.339	0.368	0.393
6.0	0.351	0.31	0.039	0.044	0.045	0.041	0.043	0.068	0.368	0.393
7.0	0.353	0.311	0.038	0.044	0.046	0.04	0.042	0.047	0.366	0.393
24.3	0.355	0.31	0.03	0.039	0.042	0.042	0.046	0.046	0.044	0.044
52.3	0.351	0.303	0.026	0.037	0.04	0.037	0.042	0.045	0.048	0.046
74.3	0.35	0.294	0.026	0.036	0.039	0.037	0.039	0.042	0.046	0.047
120.6	0.352	0.288	0.019	0.03	0.032	0.031	0.033	0.034	0.036	0.04
150.0	0.305	0.274	0.022	0.027	0.032	0.028	0.032	0.032	0.031	0.036
240.0	0.298	0.28	0.025	0.033	0.035	0.033	0.036	0.036	0.037	0.038
288.0	0.295	0.282	0.025	0.031	0.035	0.032	0.035	0.036	0.038	0.04
336.0	0.278	0.28	0.025	0.032	0.034	0.03	0.035	0.036	0.038	0.038

TABLE E2: Saturation Data for Profiles

Elevation Head	15 min	2 hours	5 hours	1 day	5 days	14 days
115	0.97	0.97	1.00	0.99	0.98	0.77
105	0.96	0.97	0.97	0.96	0.89	0.87
95	0.26	0.12	0.13	0.10	0.06	0.08
85	1.00	0.12	0.12	0.11	0.08	0.09
75	1.00	0.28	0.12	0.11	0.09	0.09
65	1.00	1.00	0.12	0.12	0.09	0.09
55	1.00	0.99	0.13	0.13	0.09	0.10
45	1.00	1.00	0.93	0.13	0.09	0.10
35	1.00	1.00	1.00	0.12	0.10	0.10
25	1.00	1.00	1.00	0.11	0.10	0.10

APPENDIX F: Pressure Data

Several LOTUS 1-2-3 spreadsheets were used to convert the pressure transducer readings to pressure head profiles. This appendix presents the spreadsheets and the equations that were used.

Table F1 is a record of the datalogger reset times for the experiment. Each time the datalogger was reset, the time and date was recorded. This permitted the correction of datalogger times to the elapsed time for the experiment. The start time for the experiment was: 13:18:20, Friday, March 2, 1990. Elapsed times since the start of the experiment were calculated using equations 21 and 22 from Appendix E.

Table F2 is the spreadsheet that contained the pressure transducer data. The table is split into two halves. The left half contains all the pressures, in millivolts, for the odd-numbered tensiometers. These tensiometers were the higher tensiometers in the tensiometer pairs (see Figures 13 and 14). Pressures for the lower tensiometers, which were even-numbered, are contained on the right half of the table. The elapsed times for the datum points were calculated in this spreadsheet, given the elapsed time at each datalogger reset (Table F1) and the datalogger times in columns 2 and 9 of this table.

Table F3 is the spreadsheet that converted pressure transducer data to pressure head values, which were subsequently plotted in Figure 18. The transducer readings were converted to pressure head values by applying the appropriate calibration curves, discussed in Appendix C. The calibration curves were first corrected to account for the difference in elevation between the transducers and the tensiometers. For tensiometers 1 to 10, the respective correction, in cm, was: -6.7, +3.3, -6, +4, -5.5, +4.5, -6.8, +3.2, -3.2, and +7.1. The values for the pressure head profiles in Figure 18, are provided in the lower half of the table.

Selecting the transducer readings for Table F3 was not a straightforward procedure for several reasons. For the profile at 15 minutes, the transducer readings for the odd-numbered tensiometers were not available. They were back-calculated for each odd-numbered tensiometer by plotting the available transducer readings (i.e., -26, -21, 24 and 29 min.) and then estimating the transducer readings, at 15 minutes, from the plots. A second difficulty arose when selecting transducer readings just after the valve was switched. The transducer readings were not stable at such times and generally required one to three sampling intervals to stabilize. For example, at the beginning of the experiment, it took one reading (i.e., 5 minutes) for the transducer to stabilize. However, towards the end of the experiment it took three readings (i.e., 135 minutes) for the transducer to stabilize. The stabilized readings were the readings that were recorded. Transducer oscillations constituted a third difficulty. The readings for all of the transducers should have consistently decreased throughout the experiment. However, the readings regularly cycled between increasing intervals and decreasing intervals (see Figure 19). The "wavelength" of the oscillations was random and varied in length from one hour to up to twelve hours. Oscillation amplitude was approximately 1.5 cm of pressure head for all transducers. Transducer readings for Table F3 were selected by choosing values that were representative of the general long-term trend of the data.

TABLE F1: Datalogger Reset Times

Reset Number	Real Time (H:M:S)	Date (D/M/Y)	Datalogger Time (min.)	Elapsed Time (min.)
0	13:17:20	02.03.90	55	-1
1	16:47:20	02.03.90	0	209
2	20:38:00	02.03.90	0	440
3	13:20:20	03.03.90	0	1442
4	14:00:30	03.03.90	0	1482
5	17:48:30	04.03.90	0	3150
6	09:06:00	06.03.90	0	5508
7	14:04:20	07.03.90	0	7246
8	21:38:20	12.03.90	0	14900
9	11:18:20	14.03.90	0	17160
10	14:58:20	16.03.90	0	20260

TABLE F2: Pressure Transducer Data

Nomenclature: E.T. = Elapsed Time. Time elapsed since experiment began.
D.T. = Datalogger Time. Time elapsed since datalogger was re-set.
PT = Pressure Transducer.
T = Tensiometer.

Note: In each pair, the UPPER tensiometers are ODD numbered; the LOWER tensiometers are even numbered.

E.T. (min)	D.T. (min)	PT 1 T 1 (mV)	PT 2 T 3 (mV)	PT 3 T 5 (mV)	PT 4 T 7 (mV)	PT 5 T 9 (mV)	E.T. (min)	D.T. (min)	PT 1 T 2 (mV)	PT 2 T 4 (mV)	PT 3 T 6 (mV)	PT 4 T 8 (mV)	PT 5 T 10 (mV)
-56	0	2863	2943	3149	3072	3106	-16	40	2837	2901	3115	3038	3071
-51	5	2857	2939	3142	3065	3098	-11	45	2844	2909	3114	3036	3070
-46	10	2851	2926	3136	3058	3092	-6	50	2834	2906	3108	3033	3068
-41	15	2848	2923	3131	3054	3087	-1	55	2687	2768	2888	2917	2952
-36	20	2845	2927	3135	3049	3083	4	60	2703	2787	2924	2942	2971
-31	25	2843	2923	3131	3046	3079	9	65	2698	2873	2916	2930	2967
-26	30	2841	2912	3120	3043	3076	14	70	2694	2778	2909	2925	2962
-21	35	2839	2909	3118	3041	3073	19	75	2690	2779	2897	2919	2956
24	80	2692	2761	2888	2914	2950	39	95	2689	2749	2864	2902	2937
29	85	2689	2756	2880	2913	2946	44	100	2688	2744	2855	2898	2933
34	90	2688	2753	2872	2907	2942	49	105	2688	2740	2848	2894	2929
54	110	2686	2744	2841	2889	2924	69	125	2687	2723	2819	2877	2913
59	115	2687	2751	2835	2886	2921	74	130	2685	2718	2809	2872	2908
64	120	2686	2742	2828	2882	2917	79	135	2685	2714	2808	2867	2904
84	140	2685	2739	2792	2862	2899	99	155	2685	2712	2771	2851	2889
89	145	2685	2739	2787	2860	2897	104	160	2684	2704	2766	2848	2886
94	150	2685	2747	2778	2856	2893	109	165	2683	2703	2767	2842	2883
114	170	2683	2736	2752	2836	2880	129	185	2682	2701	2729	2824	2877
119	175	2682	2744	2746	2832	2876	134	190	2681	2701	2722	2821	2865
124	180	2682	2744	2738	2828	2873	139	195	2681	2700	2716	2818	2862
144	200	2681	2734	2716	2815	2859	159	215	2686	2699	2691	2814	2851
149	205	2687	2734	2713	2812	2857	164	220	2752	2698	2686	2811	2849
154	210	2687	2733	2711	2810	2854	169	225	2694	2698	2681	2799	2847
174	230	2692	2735	2716	2795	2846	189	245	2692	2702	2664	2796	2843
179	235	2692	2738	2708	2791	2844	209	0	2688	2701	2643	2778	2831
184	240	2691	2748	2709	2788	2842	214	5	2687	2700	2648	2776	2829
229	20	2684	2747	2709	2765	2822	219	10	2686	2700	2639	2781	2827
234	25	2684	2746	2709	2762	2818	224	15	2685	2699	2637	2779	2824
239	30	2683	2746	2708	2759	2816	244	35	2683	2698	2633	2764	2813
259	50	2684	2744	2709	2750	2807	249	40	2682	2697	2634	2754	2811
264	55	2684	2744	2707	2747	2805	254	45	2686	2697	2633	2752	2809
269	60	2684	2744	2709	2745	2803	274	65	2683	2697	2631	2742	2801
294	85	2683	2745	2718	2738	2794	279	70	2683	2697	2639	2740	2799
299	90	2683	2745	2719	2738	2793	284	75	2683	2697	2631	2738	2797
304	95	2684	2745	2719	2738	2792	289	80	2683	2698	2639	2737	2796
334	125	2683	2746	2714	2740	2786	309	100	2683	2701	2639	2732	2792

A-107

339	130	2683	2746	2714	2749	2785	314	105	2683	2701	2632	2731	2799
344	135	2683	2747	2716	2749	2784	319	110	2684	2702	2633	2729	2798
349	140	2682	2747	2716	2750	2783	324	115	2684	2702	2632	2728	2797
374	165	2683	2747	2718	2750	2777	329	120	2683	2702	2634	2727	2788
379	170	2682	2747	2717	2750	2775	354	145	2683	2706	2635	2722	2782
384	175	2682	2747	2718	2743	2774	359	150	2683	2705	2636	2719	2781
389	180	2682	2747	2719	2743	2773	364	155	2683	2705	2637	2718	2779
414	205	2682	2749	2721	2744	2768	369	160	2682	2705	2637	2717	2778
419	210	2682	2749	2721	2745	2767	394	185	2682	2706	2639	2711	2772
424	215	2682	2749	2722	2745	2766	399	190	2682	2706	2638	2710	2771
429	220	2685	2749	2723	2746	2766	404	195	2682	2706	2639	2709	2770
1447	5	2667	2733	2713	2756	2736	409	200	2682	2707	2638	2709	2769
1452	10	2666	2733	2714	2756	2736	440	0	2677	2709	2643	2709	2763
1457	15	2667	2733	2713	2756	2735	455	15	2684	2707	2643	2708	2760
1462	20	2666	2733	2714	2764	2735	470	30	2675	2708	2643	2707	2756
1467	25	2666	2732	2713	2764	2735	485	45	2674	2708	2643	2706	2752
1472	30	2666	2733	2714	2765	2736	500	60	2682	2707	2644	2706	2749
1477	35	2669	2735	2717	2762	2748	515	75	2681	2706	2643	2705	2745
1482	0	2665	2731	2713	2764	2735	530	90	2674	2705	2644	2705	2742
3165	15	2653	2724	2704	2748	2742	545	105	2673	2705	2645	2704	2738
3180	30	2653	2724	2704	2748	2742	560	120	2673	2704	2644	2704	2736
3195	45	2653	2723	2706	2749	2743	575	135	2681	2704	2646	2704	2733
3210	60	2652	2725	2706	2750	2743	590	150	2681	2705	2645	2704	2730
3225	75	2652	2725	2706	2750	2744	605	165	2681	2704	2646	2703	2727
3240	90	2652	2733	2706	2750	2744	620	180	2672	2703	2646	2703	2725
3255	105	2651	2733	2706	2750	2744	635	195	2672	2703	2646	2703	2723
3270	120	2651	2733	2706	2750	2744	650	210	2671	2703	2655	2703	2720
3285	135	2652	2733	2706	2750	2744	665	225	2671	2703	2648	2703	2718
3300	150	2652	2734	2706	2750	2751	680	240	2671	2703	2655	2703	2716
3315	165	2651	2733	2706	2750	2744	695	255	2670	2702	2655	2703	2714
3330	180	2651	2733	2706	2750	2744	710	270	2670	2702	2648	2712	2712
3345	195	2651	2733	2706	2750	2744	725	285	2669	2702	2648	2704	2710
3360	210	2650	2733	2706	2750	2744	740	300	2669	2701	2648	2704	2707
3375	225	2650	2732	2705	2750	2744	755	315	2669	2701	2648	2704	2704
3390	240	2649	2732	2706	2750	2744	770	330	2668	2700	2648	2712	2703
3405	255	2649	2733	2707	2750	2744	785	345	2668	2700	2649	2712	2702
3420	270	2649	2733	2707	2751	2745	800	360	2668	2700	2649	2712	2701
3435	285	2649	2734	2716	2751	2745	815	375	2669	2701	2650	2712	2700
3450	300	2649	2733	2716	2751	2745	830	390	2668	2700	2651	2713	2699
3465	315	2649	2734	2716	2752	2746	845	405	2668	2700	2650	2713	2698
3480	330	2648	2734	2716	2752	2746	860	420	2668	2699	2650	2714	2698
3495	345	2648	2734	2717	2752	2746	875	435	2668	2700	2652	2714	2697
3510	360	2655	2726	2707	2752	2746	890	450	2668	2700	2652	2715	2697
3525	375	2648	2735	2717	2752	2746	905	465	2668	2700	2652	2715	2697
3540	390	2655	2726	2708	2752	2746	920	480	2667	2699	2651	2715	2696
3555	405	2655	2726	2709	2752	2746	935	495	2667	2699	2652	2715	2696
3570	420	2655	2727	2709	2752	2746	950	510	2667	2699	2663	2716	2696
3585	435	2654	2726	2708	2752	2745	965	525	2666	2698	2653	2716	2696
3600	450	2654	2726	2708	2752	2746	980	540	2666	2698	2653	2716	2696
3615	465	2653	2725	2708	2752	2746	995	555	2666	2699	2654	2717	2696
3630	480	2653	2726	2707	2752	2746	1010	570	2666	2699	2653	2717	2696
3645	495	2653	2726	2707	2752	2746	1025	585	2666	2698	2654	2717	2696

3660	510	2653	2726	2708	2753	2746	1040	600	2666	2698	2654	2717	2696
3675	525	2652	2726	2708	2752	2746	1055	615	2666	2698	2654	2718	2696
3690	540	2653	2726	2708	2752	2746	1070	630	2665	2698	2655	2718	2696
3705	555	2652	2726	2708	2753	2746	1085	645	2664	2698	2655	2718	2695
3720	570	2653	2726	2708	2753	2746	1100	660	2664	2698	2654	2718	2695
3735	585	2653	2726	2708	2753	2746	1115	675	2664	2698	2654	2719	2696
3750	600	2653	2726	2708	2753	2746	1130	690	2671	2698	2655	2719	2696
3765	615	2653	2726	2707	2753	2746	1145	705	2670	2697	2655	2719	2696
3780	630	2653	2726	2707	2753	2746	1160	720	2670	2698	2655	2719	2695
3795	645	2653	2726	2708	2753	2746	1175	735	2670	2698	2655	2719	2696
3810	660	2653	2727	2708	2753	2746	1190	750	2669	2698	2654	2712	2703
3825	675	2653	2726	2708	2753	2746	1205	765	2669	2698	2654	2712	2696
3840	690	2653	2726	2708	2753	2746	1220	780	2669	2698	2654	2712	2703
3855	705	2652	2726	2708	2753	2746	1235	795	2669	2697	2654	2712	2696
3870	720	2652	2726	2708	2753	2746	1250	810	2669	2697	2654	2713	2696
3885	735	2652	2726	2707	2753	2746	1265	825	2670	2697	2654	2713	2696
3900	750	2652	2726	2707	2753	2746	1280	840	2670	2697	2653	2713	2696
3915	765	2651	2726	2707	2753	2746	1295	855	2664	2697	2654	2714	2697
3930	780	2651	2726	2708	2753	2746	1310	870	2664	2698	2655	2715	2697
3945	795	2651	2726	2707	2753	2746	1325	885	2665	2699	2655	2716	2698
3960	810	2651	2726	2707	2753	2746	1340	900	2666	2699	2664	2716	2698
3975	825	2650	2726	2707	2753	2746	1355	915	2666	2699	2655	2716	2698
3990	840	2650	2726	2706	2753	2746	1370	930	2666	2699	2664	2717	2698
4005	855	2650	2726	2707	2753	2746	1385	945	2667	2700	2665	2718	2699
4020	870	2650	2725	2706	2752	2745	1400	960	2667	2700	2655	2718	2699
4035	885	2649	2725	2706	2752	2744	1415	975	2666	2699	2655	2717	2698
4050	900	2651	2727	2706	2752	2745	1442	0	2666	2698	2653	2714	2703
4065	915	2652	2726	2706	2752	2744	1497	15	2665	2696	2651	2716	2694
4080	930	2646	2726	2705	2750	2743	1512	30	2664	2696	2651	2717	2695
4095	945	2648	2726	2705	2750	2742	1527	45	2663	2696	2652	2717	2695
4110	960	2650	2726	2705	2749	2741	1542	60	2671	2696	2651	2718	2696
4125	975	2652	2725	2703	2748	2740	1557	75	2671	2698	2651	2719	2696
4140	990	2654	2725	2703	2748	2739	1572	90	2671	2698	2651	2719	2697
4155	1005	2656	2724	2703	2747	2739	1587	105	2671	2698	2650	2720	2697
4455	1305	2656	2718	2698	2744	2735	1602	120	2670	2699	2651	2720	2697
4470	1320	2665	2718	2698	2751	2734	1617	135	2670	2699	2651	2721	2698
4485	1335	2666	2717	2697	2751	2734	1632	150	2670	2699	2650	2721	2698
4500	1350	2667	2716	2696	2750	2733	1647	165	2669	2698	2650	2729	2698
4515	1365	2665	2715	2696	2750	2733	1662	180	2652	2688	2641	2711	2688
4530	1380	2656	2714	2696	2749	2732	1677	195	2655	2684	2636	2714	2684
4545	1395	2652	2700	2683	2735	2718	1692	210	2651	2689	2640	2711	2688
4560	1410	2639	2697	2680	2732	2715	1707	225	2653	2692	2642	2713	2690
4575	1425	2643	2703	2687	2732	2723	1722	240	2655	2693	2643	2716	2692
4590	1440	2653	2717	2693	2738	2729	1737	255	2656	2694	2644	2717	2694
4605	1455	2654	2715	2696	2751	2733	1752	270	2657	2696	2653	2719	2696
4620	1470	2655	2716	2699	2745	2735	1767	285	2665	2697	2653	2720	2696
4635	1485	2647	2717	2701	2747	2737	1782	300	2666	2698	2654	2721	2697
4650	1500	2646	2719	2702	2749	2739	1797	315	2666	2698	2654	2721	2698
4665	1515	2646	2721	2703	2750	2740	1812	330	2667	2698	2653	2722	2698
4680	1530	2646	2721	2704	2751	2741	1827	345	2667	2698	2653	2722	2699
4695	1545	2646	2722	2705	2752	2750	1842	360	2662	2701	2653	2731	2716
4710	1560	2645	2724	2706	2753	2743	1857	375	2668	2698	2653	2723	2699

4725	1575	2645	2724	2706	2754	2751	1872	390	2668	2699	2653	2723	2699
4740	1590	2645	2724	2705	2753	2751	1887	405	2668	2698	2653	2723	2699
4755	1605	2645	2724	2705	2753	2742	1902	420	2668	2698	2653	2723	2700
4770	1620	2644	2723	2705	2753	2742	1917	435	2668	2698	2653	2723	2700
4785	1635	2645	2724	2705	2752	2742	1932	450	2668	2699	2653	2723	2700
4800	1650	2644	2723	2704	2752	2742	1947	465	2668	2699	2653	2724	2700
4815	1665	2645	2723	2704	2751	2741	1962	480	2668	2699	2652	2723	2700
4830	1680	2645	2722	2704	2751	2741	1977	495	2668	2699	2651	2723	2700
4845	1695	2645	2723	2705	2752	2742	1992	510	2668	2699	2651	2724	2701
4860	1710	2644	2723	2706	2753	2743	2007	525	2668	2698	2652	2724	2701
4875	1725	2644	2724	2706	2754	2751	2022	540	2668	2699	2652	2724	2701
4890	1740	2644	2724	2706	2754	2751	2037	555	2668	2699	2651	2724	2701
4905	1755	2644	2725	2706	2754	2751	2052	570	2668	2699	2652	2724	2701
4920	1770	2652	2725	2707	2755	2744	2067	585	2668	2699	2651	2724	2701
4935	1785	2651	2733	2707	2755	2744	2082	600	2668	2699	2651	2724	2701
4950	1800	2651	2733	2707	2754	2751	2097	615	2668	2698	2650	2724	2701
4965	1815	2651	2725	2707	2755	2744	2202	720	2667	2700	2648	2724	2702
4980	1830	2651	2725	2707	2755	2744	2217	735	2667	2700	2650	2724	2702
4995	1845	2650	2725	2707	2755	2744	2232	750	2667	2699	2649	2724	2702
5010	1860	2650	2725	2707	2755	2744	2247	765	2667	2699	2649	2724	2702
5025	1875	2650	2725	2705	2755	2744	2262	780	2667	2699	2649	2724	2702
5040	1890	2642	2725	2706	2755	2743	2277	795	2667	2699	2649	2724	2702
5055	1905	2641	2725	2706	2754	2743	2292	810	2667	2700	2649	2724	2703
5070	1920	2641	2725	2706	2755	2743	2307	825	2667	2699	2649	2724	2702
5085	1935	2641	2725	2706	2755	2751	2322	840	2667	2699	2649	2724	2703
5100	1950	2641	2725	2706	2755	2744	2337	855	2667	2699	2648	2724	2703
5115	1965	2641	2725	2707	2755	2744	2352	870	2667	2699	2649	2724	2703
5130	1980	2641	2726	2707	2755	2743	2367	885	2666	2699	2639	2724	2703
5145	1995	2641	2725	2706	2754	2743	2382	900	2666	2699	2649	2724	2703
5160	2010	2641	2725	2706	2755	2743	2397	915	2666	2699	2649	2724	2703
5175	2025	2640	2725	2706	2755	2751	2412	930	2666	2699	2648	2724	2704
5190	2040	2641	2725	2706	2755	2743	2427	945	2657	2699	2641	2724	2704
5205	2055	2640	2725	2706	2755	2751	2442	960	2657	2699	2640	2724	2704
5220	2070	2640	2725	2707	2755	2743	2457	975	2657	2699	2640	2724	2704
5235	2085	2640	2725	2706	2755	2751	2472	990	2657	2699	2640	2724	2704
5250	2100	2639	2724	2706	2755	2743	2487	1005	2657	2698	2640	2724	2705
5265	2115	2639	2724	2706	2755	2751	2502	1020	2656	2699	2640	2724	2705
5280	2130	2639	2724	2705	2754	2751	2517	1035	2656	2699	2640	2724	2705
5295	2145	2639	2724	2706	2755	2743	2532	1050	2657	2699	2640	2724	2705
5310	2160	2638	2724	2707	2754	2751	2547	1065	2657	2699	2640	2724	2704
5325	2175	2638	2724	2706	2755	2742	2562	1080	2657	2698	2640	2723	2704
5340	2190	2638	2724	2707	2754	2751	2577	1095	2657	2698	2640	2723	2704
5355	2205	2638	2724	2706	2754	2742	2592	1110	2657	2697	2639	2722	2704
5370	2220	2637	2724	2707	2754	2742	2607	1125	2657	2697	2639	2722	2704
5385	2235	2637	2723	2706	2754	2750	2622	1140	2657	2697	2640	2722	2704
5400	2250	2636	2723	2706	2754	2750	2637	1155	2657	2698	2640	2723	2704
5415	2265	2636	2723	2705	2754	2742	2652	1170	2657	2698	2640	2723	2705
5430	2280	2636	2723	2705	2754	2742	2667	1185	2657	2697	2639	2723	2705
5445	2295	2636	2723	2705	2754	2742	2682	1200	2656	2697	2639	2722	2705
5460	2310	2635	2723	2705	2754	2742	2697	1215	2657	2698	2640	2723	2705
5475	2325	2635	2723	2705	2753	2741	2712	1230	2656	2697	2640	2722	2705
5508	0	2637	2731	2702	2749	2745	2727	1245	2656	2697	2639	2722	2705

5523	15	2639	2723	2701	2748	2736	2742	1260	2657	2698	2640	2722	2705
5538	30	2650	2723	2701	2748	2735	2757	1275	2657	2697	2640	2721	2704
5553	45	2654	2724	2701	2748	2735	2772	1290	2657	2696	2638	2722	2705
5568	60	2648	2731	2701	2747	2734	2787	1305	2657	2696	2639	2721	2705
5583	75	2651	2722	2706	2747	2734	2802	1320	2657	2696	2639	2721	2704
5598	90	2652	2720	2702	2746	2734	2817	1335	2658	2696	2639	2721	2705
5613	105	2653	2720	2703	2747	2735	2832	1350	2658	2696	2638	2721	2705
5628	120	2654	2733	2730	2749	2734	2847	1365	2658	2697	2639	2721	2705
5643	135	2654	2723	2721	2748	2734	2862	1380	2657	2697	2639	2721	2705
5658	150	2654	2719	2700	2746	2733	2877	1395	2658	2696	2639	2721	2705
5673	165	2656	2723	2724	2747	2733	2892	1410	2658	2696	2640	2721	2705
5688	180	2656	2721	2716	2747	2733	2907	1425	2658	2696	2639	2720	2705
5703	195	2656	2721	2716	2746	2732	2922	1440	2658	2696	2639	2720	2705
5718	210	2664	2720	2713	2746	2732	2937	1455	2658	2696	2638	2720	2705
5733	225	2656	2719	2712	2745	2732	2952	1470	2657	2696	2639	2720	2705
5748	240	2656	2719	2717	2745	2732	2967	1485	2658	2696	2638	2720	2705
5763	255	2656	2717	2718	2745	2732	2982	1500	2656	2695	2638	2719	2704
5778	270	2656	2718	2712	2745	2732	2997	1515	2657	2695	2637	2719	2705
5793	285	2664	2718	2718	2745	2732	3012	1530	2656	2695	2637	2719	2705
5808	300	2656	2718	2719	2745	2732	3027	1545	2657	2694	2637	2719	2705
5823	315	2665	2719	2714	2746	2732	3042	1560	2656	2694	2636	2719	2705
5838	330	2656	2718	2717	2745	2731	3057	1575	2656	2695	2637	2719	2705
7276	30	2703	2715	2703	2750	2728	3072	1590	2656	2695	2637	2719	2705
7306	60	2702	2715	2696	2750	2735	3087	1605	2656	2695	2637	2719	2706
7336	90	2692	2714	2694	2740	2726	3102	1620	2655	2695	2637	2719	2706
7366	120	2690	2712	2692	2738	2725	3117	1635	2655	2695	2637	2719	2706
7396	150	2689	2710	2691	2736	2724	3150	0	2654	2695	2636	2718	2704
7426	180	2673	2694	2675	2718	2707	4170	1020	2658	2693	2635	2713	2704
7456	210	2670	2690	2675	2718	2708	4185	1035	2659	2693	2634	2713	2704
7486	240	2681	2705	2688	2732	2721	4200	1050	2660	2692	2634	2712	2704
7516	270	2685	2712	2702	2747	2728	4215	1065	2660	2692	2634	2712	2704
7546	300	2687	2715	2696	2750	2732	4230	1080	2660	2692	2633	2712	2704
7576	330	2689	2718	2700	2745	2735	4245	1095	2668	2692	2634	2719	2703
7606	360	2690	2718	2701	2746	2737	4260	1110	2667	2692	2634	2719	2703
7636	390	2691	2722	2702	2747	2738	4275	1125	2667	2691	2633	2719	2703
7666	420	2690	2722	2703	2748	2739	4290	1140	2667	2691	2634	2718	2703
7696	450	2691	2723	2703	2749	2738	4305	1155	2659	2691	2633	2719	2704
7726	480	2691	2725	2703	2750	2740	4320	1170	2659	2692	2633	2719	2704
7756	510	2691	2725	2704	2750	2740	4335	1185	2658	2692	2633	2719	2704
7786	540	2691	2726	2704	2749	2740	4350	1200	2658	2692	2634	2712	2705
7816	570	2691	2726	2704	2749	2739	4365	1215	2658	2693	2634	2719	2704
7846	600	2691	2727	2704	2749	2739	4380	1230	2657	2692	2634	2719	2703
7876	630	2691	2727	2703	2749	2739	4395	1245	2659	2696	2688	2719	2704
7906	660	2691	2726	2703	2748	2738	4410	1260	2657	2691	2633	2719	2703
7936	690	2692	2728	2702	2748	2738	4425	1275	2665	2691	2632	2718	2703
7966	720	2692	2727	2703	2748	2738	4440	1290	2664	2691	2633	2718	2702
7996	750	2692	2727	2703	2748	2738	5853	345	2664	2700	2655	2708	2698
8026	780	2692	2727	2703	2748	2738	5868	360	2664	2700	2649	2715	2697
8056	810	2692	2727	2703	2748	2738	5883	375	2664	2691	2650	2714	2696
8086	840	2692	2727	2703	2748	2738	5898	390	2655	2698	2652	2706	2696
8116	870	2691	2727	2703	2748	2738	5913	405	2654	2689	2645	2705	2695
8146	900	2692	2728	2702	2748	2738	5928	420	2654	2688	2646	2704	2694

A-111

8176	930	2691	2727	2702	2748	2738	5943	435	2652	2687	2644	2703	2693
8206	960	2691	2727	2703	2748	2738	5958	450	2651	2686	2642	2702	2692
8236	990	2691	2728	2703	2748	2738	5973	465	2647	2681	2624	2699	2690
8266	1020	2691	2728	2703	2748	2738	5988	480	2636	2661	2607	2686	2669
8296	1050	2692	2728	2702	2748	2738	6003	495	2627	2669	2606	2686	2670
8326	1080	2691	2728	2702	2748	2738	6018	510	2631	2670	2613	2686	2678
8356	1110	2690	2728	2703	2747	2746	6033	525	2635	2684	2617	2692	2684
8386	1140	2700	2730	2701	2745	2735	6048	540	2637	2681	2622	2698	2690
8416	1170	2703	2732	2718	2745	2734	6063	555	2637	2688	2625	2703	2694
8446	1200	2703	2728	2699	2750	2732	6078	570	2638	2697	2636	2713	2696
8476	1230	2697	2728	2717	2744	2733	6093	585	2637	2698	2637	2714	2698
8506	1260	2697	2735	2715	2751	2732	6108	600	2637	2700	2638	2716	2699
8536	1290	2697	2735	2718	2751	2732	6123	615	2637	2701	2632	2717	2700
8566	1320	2697	2735	2715	2749	2731	6138	630	2637	2701	2632	2717	2700
8596	1350	2696	2731	2703	2747	2729	6153	645	2636	2702	2633	2718	2702
8626	1380	2696	2731	2703	2747	2730	6168	660	2637	2703	2633	2719	2702
8656	1410	2696	2731	2703	2749	2732	6183	675	2636	2702	2633	2719	2702
8686	1440	2699	2735	2713	2744	2732	6198	690	2635	2696	2634	2712	2703
8716	1470	2696	2733	2696	2748	2731	6213	705	2634	2697	2634	2713	2704
8746	1500	2696	2733	2696	2748	2730	6228	720	2634	2697	2634	2713	2704
8776	1530	2703	2732	2695	2738	2728	6243	735	2634	2697	2635	2714	2713
8806	1560	2694	2721	2693	2737	2727	6258	750	2633	2697	2635	2714	2713
8836	1590	2692	2719	2693	2736	2726	6273	765	2632	2697	2634	2715	2714
8866	1620	2680	2715	2682	2724	2714	6288	780	2632	2698	2635	2715	2714
8896	1650	2687	2707	2682	2726	2717	6303	795	2632	2698	2635	2715	2714
8926	1680	2685	2716	2690	2736	2726	6318	810	2632	2699	2636	2716	2707
8956	1710	2688	2723	2696	2750	2732	6333	825	2632	2699	2636	2716	2715
8986	1740	2689	2733	2698	2751	2734	6348	840	2631	2698	2636	2716	2707
9016	1770	2689	2735	2699	2744	2734	6363	855	2631	2699	2636	2716	2707
9046	1800	2690	2728	2699	2746	2736	6378	870	2631	2699	2636	2716	2706
9076	1830	2691	2730	2700	2747	2737	6393	885	2631	2699	2637	2716	2707
9106	1860	2691	2730	2701	2747	2745	6408	900	2631	2698	2636	2716	2706
9136	1890	2692	2732	2701	2747	2737	6423	915	2630	2698	2635	2716	2706
9166	1920	2692	2732	2701	2747	2737	6438	930	2630	2698	2636	2716	2707
9196	1950	2692	2732	2701	2747	2737	6453	945	2630	2699	2637	2716	2707
9226	1980	2692	2732	2701	2747	2737	6468	960	2630	2699	2636	2716	2707
9256	2010	2692	2732	2701	2746	2736	6483	975	2629	2698	2636	2716	2707
9286	2040	2692	2732	2700	2746	2736	6498	990	2671	2698	2637	2717	2707
9316	2070	2691	2730	2700	2747	2745	6513	1005	2684	2699	2637	2717	2707
9346	2100	2690	2730	2701	2747	2737	6528	1020	2686	2699	2637	2717	2707
9376	2130	2691	2732	2700	2747	2737	6543	1035	2687	2699	2637	2717	2707
9406	2160	2692	2733	2702	2747	2737	6558	1050	2688	2699	2637	2717	2707
9436	2190	2692	2734	2702	2748	2737	6573	1065	2688	2699	2637	2717	2707
9466	2220	2692	2733	2701	2748	2737	6588	1080	2688	2699	2637	2717	2707
9496	2250	2693	2734	2702	2748	2737	6603	1095	2689	2699	2637	2717	2707
9526	2280	2693	2734	2701	2748	2737	6618	1110	2689	2699	2638	2717	2707
9556	2310	2692	2733	2701	2748	2737	6633	1125	2689	2699	2638	2717	2707
9586	2340	2691	2732	2701	2747	2737	6648	1140	2689	2699	2637	2717	2707
9616	2370	2691	2733	2701	2748	2738	6663	1155	2690	2699	2637	2717	2707
9646	2400	2691	2733	2700	2748	2738	6678	1170	2690	2698	2637	2717	2707
9676	2430	2691	2733	2701	2748	2738	6693	1185	2690	2699	2637	2717	2707
9706	2460	2691	2734	2702	2749	2739	6708	1200	2690	2698	2637	2717	2706

A-112

9736	2490	2691	2733	2701	2748	2738	6723	1215	2690	2699	2637	2717	2707
9766	2520	2691	2733	2701	2749	2739	6738	1230	2690	2698	2637	2716	2706
9796	2550	2691	2734	2700	2749	2739	6753	1245	2690	2698	2637	2716	2706
9826	2580	2691	2736	2701	2746	2736	6768	1260	2690	2698	2637	2716	2706
9856	2610	2700	2735	2699	2744	2733	6783	1275	2690	2698	2637	2716	2706
9886	2640	2700	2731	2696	2750	2731	6798	1290	2690	2698	2636	2717	2706
9916	2670	2701	2731	2703	2749	2731	6813	1305	2690	2698	2636	2716	2706
9946	2700	2702	2730	2696	2748	2730	6828	1320	2691	2698	2637	2716	2706
9976	2730	2703	2729	2703	2749	2731	6843	1335	2690	2698	2636	2716	2705
10006	2760	2703	2729	2703	2750	2732	6858	1350	2690	2698	2636	2716	2705
10036	2790	2703	2729	2696	2751	2733	6873	1365	2690	2698	2635	2716	2705
10066	2820	2703	2731	2697	2751	2732	6888	1380	2689	2698	2635	2716	2705
10096	2850	2696	2731	2696	2751	2733	6903	1395	2690	2698	2635	2716	2705
10126	2880	2697	2732	2697	2744	2733	6918	1410	2690	2696	2636	2715	2704
10156	2910	2698	2733	2698	2744	2733	6933	1425	2690	2697	2636	2714	2703
10186	2940	2697	2730	2697	2745	2734	6948	1440	2698	2696	2635	2713	2702
14900	0	2733	2752	2670	2796	2751	6963	1455	2698	2703	2636	2712	2700
17205	45	2701	2747	2706	2741	2744	6978	1470	2700	2702	2635	2719	2700
17250	90	2702	2745	2705	2739	2742	6993	1485	2700	2701	2635	2718	2699
17295	135	2701	2743	2701	2736	2739	7008	1500	2702	2701	2635	2718	2699
17340	180	2698	2737	2697	2731	2735	7023	1515	2702	2701	2633	2717	2698
17385	225	2696	2733	2695	2728	2732	7038	1530	2702	2700	2634	2717	2698
17430	270	2694	2731	2693	2726	2729	7053	1545	2703	2701	2633	2717	2698
17475	315	2694	2729	2692	2725	2729	7068	1560	2703	2700	2632	2717	2698
17520	360	2694	2729	2692	2726	2729	7083	1575	2703	2700	2633	2717	2698
17565	405	2694	2729	2692	2727	2730	7098	1590	2696	2701	2634	2717	2698
17610	450	2696	2731	2693	2728	2732	7113	1605	2696	2700	2633	2717	2698
17655	495	2695	2729	2694	2728	2732	7128	1620	2696	2700	2633	2716	2697
17700	540	2693	2728	2693	2728	2732	7143	1635	2703	2691	2632	2716	2697
17745	585	2693	2730	2693	2729	2733	7158	1650	2703	2700	2632	2715	2696
17790	630	2694	2732	2693	2729	2733	7173	1665	2696	2699	2632	2715	2696
17835	675	2694	2732	2694	2729	2733	7188	1680	2695	2689	2631	2706	2696
17880	720	2695	2733	2693	2729	2733	7203	1695	2703	2689	2638	2705	2695
17925	765	2697	2734	2695	2730	2734	7246	0	2695	2689	2631	2705	2695
17970	810	2697	2733	2694	2730	2734	14945	45	2692	2708	2641	2718	2711
18015	855	2697	2733	2695	2731	2735	14990	90	2687	2702	2637	2708	2706
18060	900	2698	2735	2694	2731	2735	15035	135	2684	2700	2635	2705	2705
18105	945	2698	2736	2697	2732	2736	15080	180	2683	2700	2634	2703	2704
18150	990	2699	2737	2696	2733	2737	15125	225	2682	2699	2634	2702	2703
18195	1035	2699	2737	2698	2734	2738	15170	270	2682	2699	2634	2701	2703
18240	1080	2699	2737	2697	2734	2739	15215	315	2681	2699	2634	2700	2702
18285	1125	2698	2737	2697	2735	2739	15260	360	2681	2699	2634	2700	2703
18330	1170	2698	2737	2697	2735	2739	15305	405	2681	2699	2634	2701	2703
18375	1215	2696	2736	2696	2734	2739	15350	450	2681	2699	2634	2700	2703
18420	1260	2695	2737	2696	2734	2738	15395	495	2681	2699	2636	2700	2703
18465	1305	2693	2737	2695	2731	2735	15440	540	2681	2698	2634	2700	2703
18510	1350	2691	2735	2695	2729	2733	15485	585	2682	2700	2636	2703	2706
18555	1395	2689	2732	2691	2726	2730	15530	630	2683	2701	2635	2703	2706
18600	1440	2688	2730	2690	2724	2728	15575	675	2683	2700	2636	2702	2704
18645	1485	2687	2728	2689	2722	2726	15620	720	2683	2698	2636	2698	2701
18690	1530	2686	2727	2686	2720	2724	15665	765	2684	2695	2633	2695	2698
18735	1575	2686	2727	2688	2722	2725	15710	810	2686	2695	2633	2694	2697

18780	1620	2686	2728	2688	2721	2725	15755	855	2688	2695	2634	2694	2696
18825	1665	2685	2727	2686	2719	2723	15800	900	2687	2694	2633	2694	2697
18870	1710	2685	2726	2685	2717	2721	15845	945	2688	2694	2632	2693	2696
18915	1755	2685	2724	2682	2716	2719	15890	990	2688	2693	2633	2691	2693
18960	1800	2684	2721	2680	2714	2718	15935	1035	2686	2690	2630	2688	2691
19005	1845	2685	2721	2681	2716	2720	15980	1080	2684	2688	2628	2686	2689
19050	1890	2687	2724	2685	2720	2724	16025	1125	2682	2687	2628	2685	2688
19095	1935	2687	2725	2686	2722	2726	16070	1170	2679	2684	2626	2683	2686
19140	1980	2688	2727	2687	2723	2727	16115	1215	2675	2681	2620	2681	2684
19185	2025	2688	2729	2688	2724	2728	16160	1260	2680	2689	2624	2690	2694
19230	2070	2688	2730	2688	2724	2728	16205	1305	2683	2695	2628	2696	2701
19275	2115	2689	2730	2689	2725	2729	16250	1350	2686	2701	2632	2702	27060
19320	2160	2688	2731	2689	2725	2729	16295	1395	2687	2703	2635	2704	2708
19365	2205	2689	2732	2690	2726	2730	16340	1440	2687	2705	2635	2706	2710
19410	2250	2689	2733	2691	2727	2731	16385	1485	2686	2705	2635	2706	2711
19455	2295	2689	2733	2690	2727	2731	16430	1530	2688	2707	2636	2707	2712
19500	2340	2689	2733	2691	2728	2732	16475	1575	2690	2709	2639	2711	2716
19545	2385	2690	2735	2693	2729	2733	16520	1620	2691	2712	2640	2715	2720
19590	2430	2690	2735	2693	2729	2733	16565	1665	2692	2714	2642	2717	2722
19635	2475	2690	2736	2695	2730	2734	16610	1710	2692	2714	2643	2717	2722
19680	2520	2691	2737	2695	2731	2735	16655	1755	2697	2714	2643	2717	2721
19725	2565	2691	2737	2694	2731	2735	16700	1800	2695	2714	2643	2716	2721
19770	2610	2691	2736	2694	2732	2736	16745	1845	2695	2713	2641	2717	2721
19815	2655	2690	2736	2694	2732	2736	16790	1890	2694	2714	2642	2717	2722
19860	2700	2689	2737	2694	2732	2736	16835	1935	2694	2715	2642	2718	2722
19905	2745	2688	2738	2694	2731	2734	16880	1980	2695	2715	2642	2718	2723
19950	2790	2688	2738	2693	2730	2733	16925	2025	2694	2715	2643	2718	2722
19995	2835	2688	2736	2692	2729	2732	16970	2070	2697	2717	2645	2717	2721
20040	2880	2689	2738	2693	2729	2732	17015	2115	2700	2716	2646	2715	2718
20085	2925	2689	2736	2692	2728	2731	17060	2160	2700	2714	2646	2712	2715
20130	2970	2689	2734	2692	2728	2732	17105	2205	2700	2711	2644	2709	2711
20175	3015	2688	2735	2693	2729	2733	17150	2250	2699	2708	2644	2705	2707
20220	3060	2689	2738	2693	2729	2732	17160	0	2697	2705	2642	2702	2705
							22960	2700	2681	2705	2628	2702	2705

TABLE F3: Pressure Head Profiles

Pressure Transducer Data

DEPTH (cm)	15 min	2 hour	5 hour	1 day	5 day	14 day
5	2696	2682	2684	2665	2692	2690
15	2694	2683	2683	2667	2695	2681
25	2770	2744	2745	2732	2728	2733
35	2778	2702	2701	2698	2703	2700
45	2904	2746	2719	2713	2703	2693
55	2909	2748	2639	2653	2631	2628
65	2916	2832	2738	2756	2750	2730
75	2925	2833	2734	2714	2705	2702
85	2958	2876	2792	2736	2738	2733
95	2962	2880	2797	2698	2695	2705

Pressure Head Values

DEPTH (cm)	15 min	2 hour	5 hour	1 day	5 day	14 day
5	-30.3	-33.8	-33.3	-37.9	-31.3	-31.8
15	-20.8	-23.5	-23.5	-27.4	-20.6	-24.0
25	-5.2	-12.6	-12.3	-16.0	-17.1	-15.7
35	7.2	-14.1	-14.4	-15.2	-13.9	-14.6
45	16.8	-12.8	-17.1	-18.0	-19.5	-21.0
55	27.9	-2.5	-18.7	-16.8	-19.8	-20.2
65	37.9	8.8	-20.1	-14.9	-16.7	-22.4
75	51.2	19.1	-11.3	-17.0	-19.5	-20.3
85	66.7	36.0	7.9	-9.1	-8.5	-10.0
95	78.6	47.7	19.8	-9.6	-10.5	-7.7

Note: 1. "DEPTH" is the depth below the top of the column to the tensiometer.

2. The polynomials for the calibration curves were used to calculate the pressure head values after they were corrected to account for the difference in elevation between the transducers and the tensiometers.

APPENDIX 4

AKINDUNNI ET AL (1991)

Numerical Simulations to Investigate Moisture Retention Characteristics in the Design of Oxygen–Limiting Covers for Reactive Mine Tailings

by

Festus F. Akindunni, R.W. Gillham and R.V. Nicholson

Waterloo Center for Groundwater Research

University of Waterloo, Ontario

Canada N2L 3G1

DRAFT

Summitted to

Canadian Geotechnical Journal

May, 1990

Introduction

Nicholson *et al.* (1989) discussed the hydraulic principles involved in the use of fine–textured materials as protective covers for reactive mine tailings. Using schematics and assuming static flow conditions, they demonstrated how fine–textured materials could remain at high moisture content above relatively coarser granular materials, even when the water table is at some arbitrary depth, far from the ground surface. The authors concluded that such a layered system would effectively reduce the influx of oxygen, thereby inhibiting oxidation of the underlying sulphide–bearing tailings. They showed that a necessary requirement to maintain cover material in a fully saturated state after prolonged drainage is that the magnitude of the air entry value (AEV) be greater or equal to the sum of the cover thickness and the magnitude of the pressure head at which the underlying coarse layer approaches the residual moisture content.

Discussing the paper, Barbour (1990) used steady–state flow relationships to analyse a two–layer system. He concluded that the analysis of Nicholson *et al.* (1989) placed unnecessary restrictions on the moisture retention characteristics of the cover material. The analysis also indicated that for the cover material selected, an appreciable flux of water (in the form of infiltration) would be required in order for the design to be effective. Although Nicholson *et al.* (1990) clarified the concerns raised by Barbour (1990), they also indicated the limitations of the static (Nicholson *et al.*, 1989 and 1990) and steady–state (Barbour, 1990) approaches to the analysis of the problem. It was further indicated that a transient analysis was necessary to fully demonstrate the anticipated behaviour. The objective of this paper is to use a transient numerical model to further elucidate the concepts presented by Nicholson *et al.* (1989 and 1990).

Methodology

A one–dimensional, finite element, saturated–unsaturated flow model (Abdul, 1985) was applied to the problem of drainage through a two–layer vertical profile. The program was originally developed for two dimensional, homogeneous, anisotropic, variably saturated and hysteretic flow in compressible porous media. The governing equation applicable to this study is somewhat simpler, and is of the form

$$K_s k_r(\psi) \frac{\partial}{\partial z}\left(\frac{\partial \psi}{\partial z} + 1\right) = (C(\psi) + S(\psi) S_s) \frac{\partial \psi}{\partial t} \qquad (1)$$

where

K_s = saturated hydraulic conductivity $[LT^{-1}]$

k_r = relative hydraulic conductivity, [/] $\quad 0 \leq k_r \leq 1$

C = specific moisture capacity $[L^{-1}]$

S = degree of saturation (normalized moisture content) [/]

S_s = specific storage $[L^{-1}]$

ψ = pressure head $[L]$

z = coordinate in the vertical direction $[L]$

t = time $[T]$

To accomodate layering, the original version of the program was modified to allow for variation of soil properties with location. The effect of specific storage is considered to be negligible in this study. However, to be consistent with the form of equation 1 its value for each material was estimated from the relationship

$$S_s = \rho g(a + bn) \qquad (2)$$

where

ρ = density of water

g = acceleration due to gravity

a = compressibility of the soil material

b = compressibility of water

n = porosity

Freeze and Cherry (1979) gave the value for b, and estimates of a for different materials. Values of compressibility used in this study were 4.4×10^{-10}, 3.3×10^{-8}, and 1×10^{-7} m^2/N for water, sand and silt respectively.

Three sets of simulations were conducted, involving five different porous media. These included:-

1. The 'silt' and 'sand' used by Barbour (1990)
2. Touchet silt loam overlying Crab Creek sand (Brooks and Corey, 1964), and
3. Touchet silt loam overlying a coarse sand.

Moisture retention characteristics of the different materials are shown in Figure 1. The relative hydraulic conductivity for each porous medium was calculated from the corresponding moisture retention curve using the method of Mualem (1976) as suggested by van Genuchten (1980), such that the moisture content (θ) at any arbitrary pressure head was given by

$$\theta(\psi) = \left\{(\theta_s - \theta_r)\left(\frac{1}{1+(\alpha \mid \psi \mid)^q}\right)^p\right\} + \theta_r \qquad (3)$$

and

$$k_r(\psi) = \frac{\left\{1-(\alpha \mid \psi \mid)^{q-1}\left[1+(\alpha \mid \psi \mid)^q\right]^{-p}\right\}^2}{\left[1+(\alpha \mid \psi \mid)^q\right]^{\frac{p}{2}}} \qquad (4)$$

where

θ_r = the residual moisture content

θ_s = saturated moisture content

α, q = curve fitting parameters (α has a dimension L^{-1}), and

$$p = 1 - \frac{1}{q} \qquad (0 < p < 1,\ q > 1) \tag{5}$$

Table 1 contains a summary of the hydraulic and the curve–fitting parameters for each material. In equations 1 and 4, the hydraulic conductivity at a specified pressure head (or moisture content) is assumed to be the product of the hydraulic conductivity at saturation and the relative hydraulic conductivity, such that the relative hydraulic conductivity attains unity as the moisture content approaches its saturated value and becomes zero at residual moisture content.

Each layered system consists of 2.5 metres of the coarse–grained material underlying 1 metre of a finer cover material. A choice of this geometry was a delibrate attempt to be consistent with the system discussed by Barbour (1990) and Nicholson *et al.* (1990). Furthermore, Nicholson *et al.* (1989) had shown that the effectiveness factor of a cover material as a barrier to influx of oxygen increases appreciably within the first metre of cover thickness, beyond which it does not change much. Other simulations (not shown here), with more than 2.5 metres of underlying coarse material, gave results that are consistent with the discussion that follows.

The initial condition considered the entire profile to be saturated, with the water table at the surface. The boundary conditions include zero–flux across the top boundary and a time–dependent pressure head at the bottom which, in effect, lowered the water table linearly from the top of the profile to the bottom over the first one hour of the simulation period. This boundary was used to relax the constraint on the numerical model caused by large and sudden changes in the boundary condition. Within the time frame of the simulations (56 days), this

boundary condition is physically equivalent to an "instantaneous" lowering of the water table to the base of the profile. Variations in pressure head, total hydraulic head and degree of saturation were tabulated for specified elevations over a period of 56 days.

Results and Discussion

The results are summarized in Figures 2 to 4. Because the water table was initially at the top of the column, an increasingly positive (hydrostatic) pressure head profile would extend below the surface. To reduce the z–axes and because late–time data are of greatest relevance, only times corresponding to negative pressure head profiles are shown. The graphs are plotted for selected times to show the general trends of the hydraulic response.

The pressure head profiles for the three pairs of soil materials (Figure 2 a, b and c) changed rapidly during early time and, in all cases, appear to be approaching a static condition by 14 days. Relatively small changes occurred between 14 days and the conclusion of the simulations at 56 days. The final profiles are very similar for all pairs of soil materials. In particular, within the cover layer, which remains saturated or at a relatively high moisture content, the pressure head approaches the 1:1 hydraulic equilibrium condition. For a distance below the cover the pressure head is almost constant and is close to the pressure head at which the moisture content approaches the residual value for the respective coarse–layer materials (Figure 1). At greater depth, as the water table is approached, the pressure head profile again approaches the 1:1 hydrostatic condition. While the final profiles appear to be approaching a static condition, they are far from the static equilibrium condition indicated on each graph. This is a consequence of the low value of relative hydraulic conductivity when moisture content approaches the

residual value.

The results of these simulations can be extended to address the situation that might lead to a zero pressure head (i.e. atmospheric) at the interface. The pressure head at the interface between the medium–size material and the cover changed from about –0.4m at one hour to about –0.65m at 56 days (Figure 2b). For the case of a coarse underlying material, the pressure head at which the residual saturation is first approached is about –0.1m (Figure 1). Furthermore, the pressure head at the interface dropped only marginally throughout the duration of the simulation (Figure 2c), keeping the interface pressure head at values more positive than –0.3m at 56 days. One can envision coarser materials with less negative pressure head values at residual saturation, resulting in an interface pressure head that could practically be zero. It is therefore suggested that a condition of "drip" surface at the interface would be an end–member of the continuous spectrum, satisfied only by a very coarse (or gravelly) underlying material.

The changes in saturation for the three cases simulated are given in Figure 3. For the materials considered by Barbour (1990), the degree of saturation in the sand declines more rapidly than in the silt (Figure 3a). Nevertheless, even at a time of 2 hours, the entire cover layer was at a water content less than saturation, which would substantially reduce the cover's effectiveness as an oxygen barrier. Thus, while Barbour (1990) showed that the moisture content could be increased by application of a constant flux, under natural conditions, the cover material considered by Barbour (1990) would be an ineffective barrier after only a few hours of redistribution and drainage following precipitation events.

The saturation profiles for the Touchet silt over Crab Creek sand are substantially different (Figure 3b). In particular, while the sand drained rapidly, the silt re-

mained fully saturated over its entire thickness for almost the entire duration of simulation. This observation is readily explained by reference to the pressure head profiles. The maximum negative pressure head at the bottom of the silt layer is about −0.65m, corresponding to the pressure head at which the underlying sand approaches its residual moisture content value (Figure 1). The maximum negative pressure head of about −1.65m occurs at the surface of the cover reflecting an equilibrium pressure head distribution in the cover. Thus at no point in the cover layer does the pressure head significantly exceed the AEV of the Touchet silt material (−1.65m, Figure 1). The silt therefore remains saturated. For the case of Touchet silt overlying coarse sand, the silt remained fully saturated over its entire thickness throughout the duration of the simulation (Figure 3c). In this case, the maximum negative pressure at the base of the silt layer is only about −0.25m which again corresponds to the pressure head at which the coarse sand approaches the residual moisture content (Figure 1).

The hydraulic head profiles for each soil pair are shown in Figure 4. For both cases where the Touchet silt is the cover material (Figures 4 b and c), there is a negligible hydraulic gradient across the cover layer throughout the duration of simulation. This is consistent with the static equilibrium pressure head profiles discussed previously. Clearly if there is no hydraulic gradient across the cover layer, there can be no flow of water across the layer. In the absence of a surface flux, as assumed in the present simulations, this implies that there is no drainage of the surface layer. This is consistent with the fact that the magnitude of the pressure head did not exceed the AEV of the silt. In contrast to the cover layer, the value of hydraulic gradient in the underlying material is close to unity at all times in the zones at residual saturation. Hence drainage would proceed at the rate of the prevailing hydraulic conductivity within the drained zone, diminishing with time

as the degree of saturation decreases. At late time, the profiles become almost static, though far from equilibrium, as a result of slow drainage caused by the very low values of hydraulic conductivity. The materials analysed by Barbour (1990) exhibit profiles across the cover layer that are significantly different from other pairs of material simulated, particularly at early time when the hydraulic gradient is appreciable (Figure 4 a) while saturation is high (Figure 2 a). Under these circumstances, the relative hydraulic conductivity (k_r) would have a significant magnitude and drainage of the cover would be inevitable.

Conclusion

Based on the moisture retention characteristics of selected materials, the numerical simulations demonstrated that it is hydraulically possible to maintain a fully saturated layer of fine–texture material above a coarse material even though the water table may be far from the ground surface. Neglecting water losses by evapotranspiration and for an appropriate choice of cover material with an appropriate thickness, no infiltration would be necessary to maintain a fully saturated cover layer. Two fundamental characteristics are important in assessing what thickness of a particular material can be maintained fully saturated. The first is the AEV of the cover layer. The second characteristic is the pressure head at which the underlying material approaches residual saturation, in as much as this determines the pressure head at the interface. The thickness of the cover layer that would remain saturated after prolonged drainage and redistribution would be the difference in the magnitude of AEV of the cover material and the magnitude of the pressure head at the interface.

It is recognised that these simiulations do not address all of the practical design considerations for fine–grained covers. In particular, hysteretic effects caused by

alternate cycles of wetting and drying conditions, reduced moisture content caused by evapotranspiration, and the effects of freezing and thawing on the integrity of the cover are important questions that need to be addressed. Further laboratory and modelling studies are in progress to better define the limitations of the concept. Preliminary results of the laboratory experiments show trends that are consistent with the discussion above.

References

1. Abdul, A.S., Experimental and numerical studies of the effect of the capillary fringe on streamflow generation, Ph.D. Thesis, Earth Sciences Dept., University of Waterloo, 1985.

2. Barbour, S.L., Reduction of acid generation in mine tailings through the use of moisture retaining cover layers as oxygen barriers: Discussion, *Canadian Geotechnical Journal*, 1990.

3. Brooks, R.H., and A.T. Corey, Hydraulic properties of porous medium, *Hydrology Paper #3,Colorado State University*, **3**, 1–27, 1964.

4. Freeze, R.A., and J.A. Cherry, Groundwater, Prentice Hall, 1979.

5. Mualem, Y., A new model for predicting the hydraulic conductivity of unsaturated porous media, *Water Resources Research*, **12** (3), 513–522, 1976.

6. Nicholson R.V., R.W. Gillham, J.A. Cherry and E.J. Reardon, Reduction of acid generation in mine tailings through the use of moisture retaining cover layers as oxygen barriers, *Canadian Geotechnical Journal*, **26**, 1–8, 1989.

7. Nicholson R.V., R.W. Gillham, J.A. Cherry and E.J. Reardon, Reply to discussion by S. Lee Barbour of: Reduction of acid generation in mine tailings through the use of moisture retaining cover layers as oxygen barriers. *Canadian Geotechnical Journal*, 1990.

8. van Genuchten, M. Th., A Closed-form equation for predicting the hydraulic conductivity of unsaturated soils, *Soil Sci. Soc. Amer.*, **44**, 892–898, 1980.

Material	AEV (cm)	θ_r	θ_s	K_{sat} (cm/min)	α (cm^{-1})	q
* Silt	10.0	0.074	0.381	0.045	0.028	3.60
* Sand	8.0	0.095	0.322	0.331	0.050	4.05
Touchet Silt	165.0	0.18	0.485	0.035	0.004	7.05
Crab Creek Sand	24.0	0.141	0.448	0.431	0.029	10.21
Coarse Sand	8.0	0.026	0.422	7.80	0.077	9.74

* As presented by Barbour (1990)

α, and q are curve fitting parameters in the van Genuchten (1980) model, and all other parameters are measurable properties of the porous media.

Table 1: Summary of the hydraulic and curve–fitting parameters for the selected materials

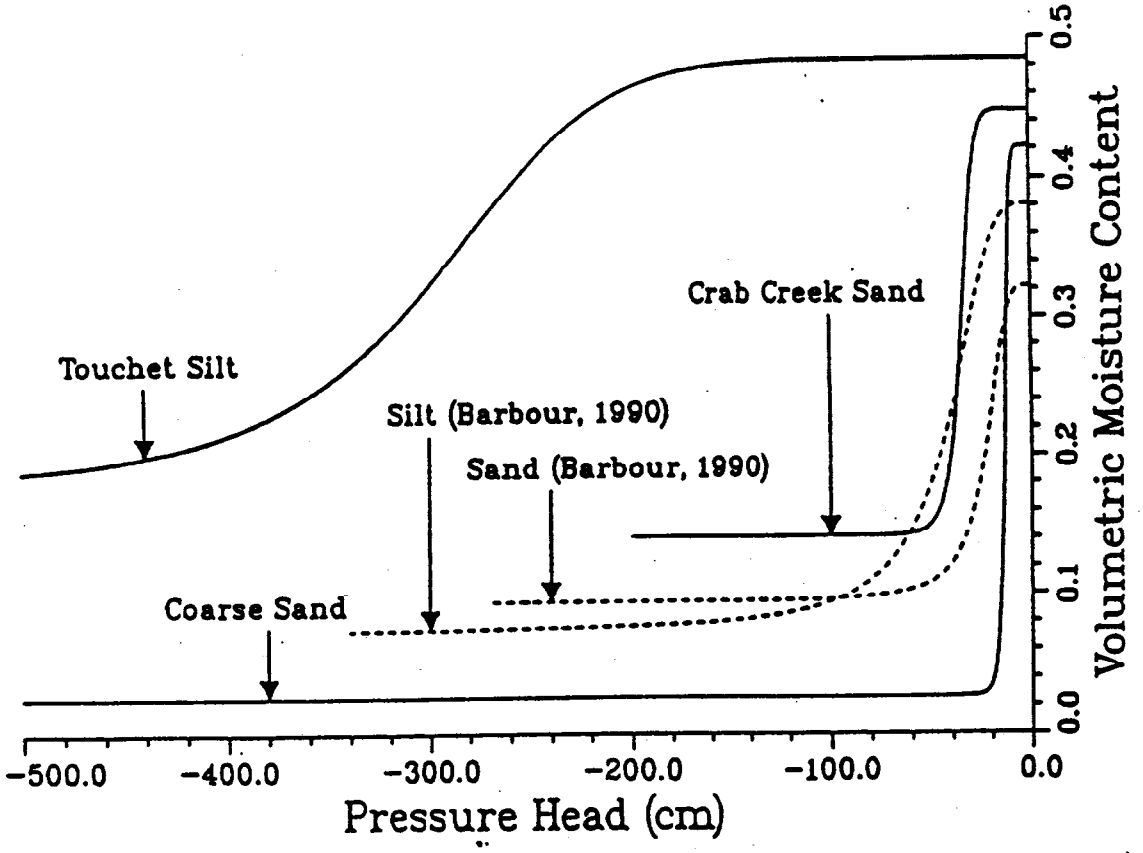

Figure 1: Moisture retention characteristics of the selected materials

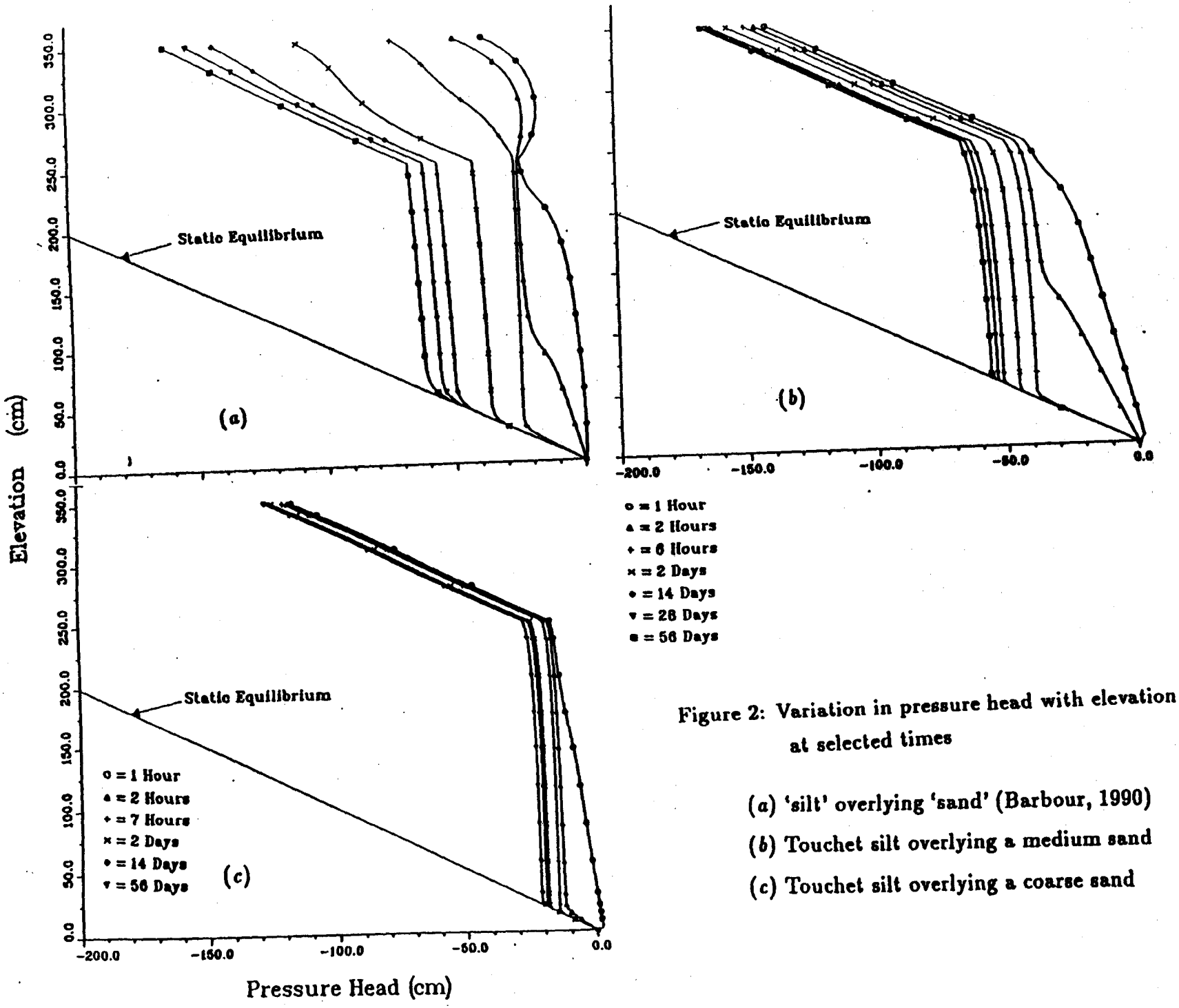

Figure 2: Variation in pressure head with elevation at selected times

(*a*) 'silt' overlying 'sand' (Barbour, 1990)

(*b*) Touchet silt overlying a medium sand

(*c*) Touchet silt overlying a coarse sand

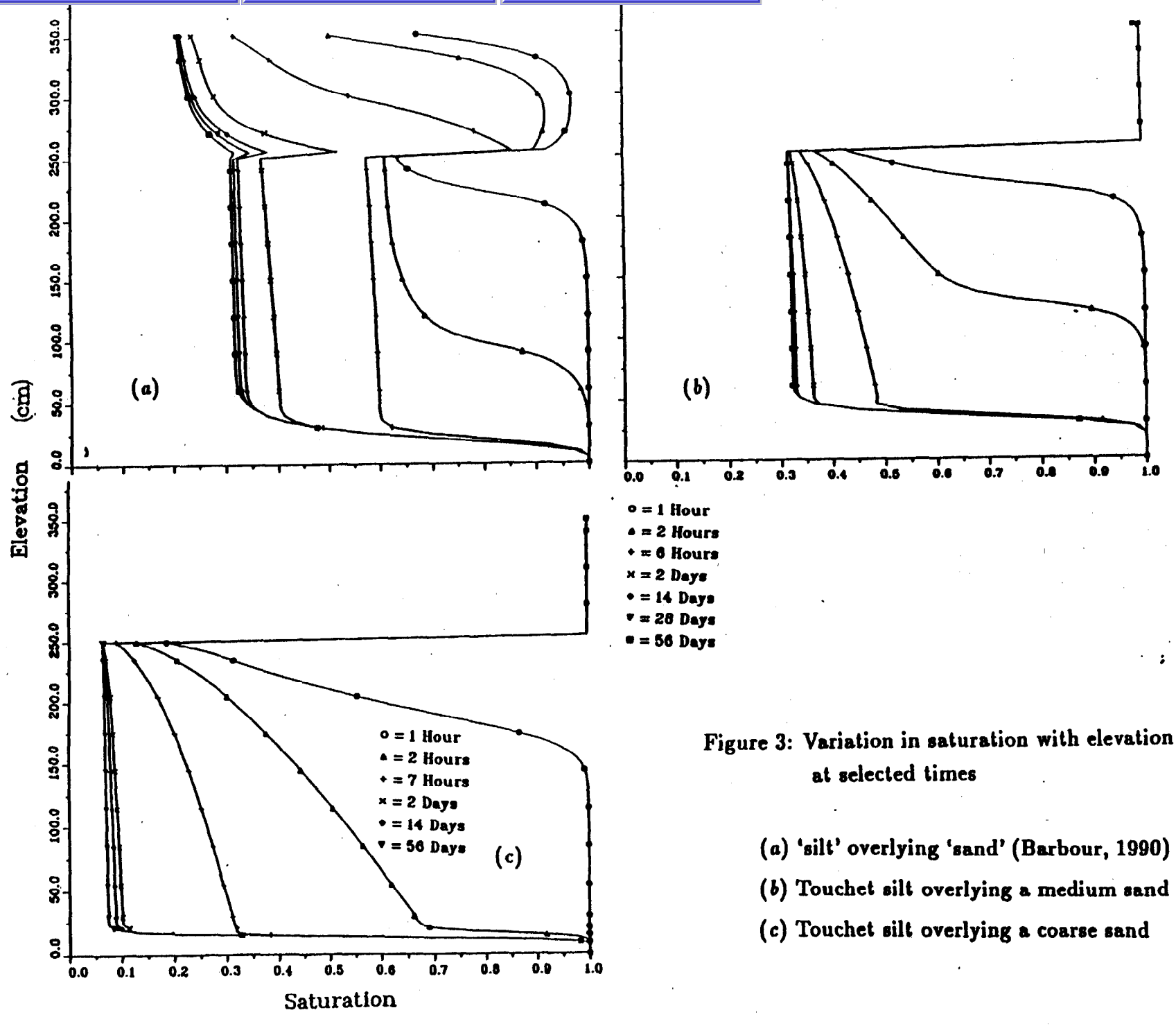

Figure 3: Variation in saturation with elevation at selected times

(*a*) 'silt' overlying 'sand' (Barbour, 1990)

(*b*) Touchet silt overlying a medium sand

(*c*) Touchet silt overlying a coarse sand

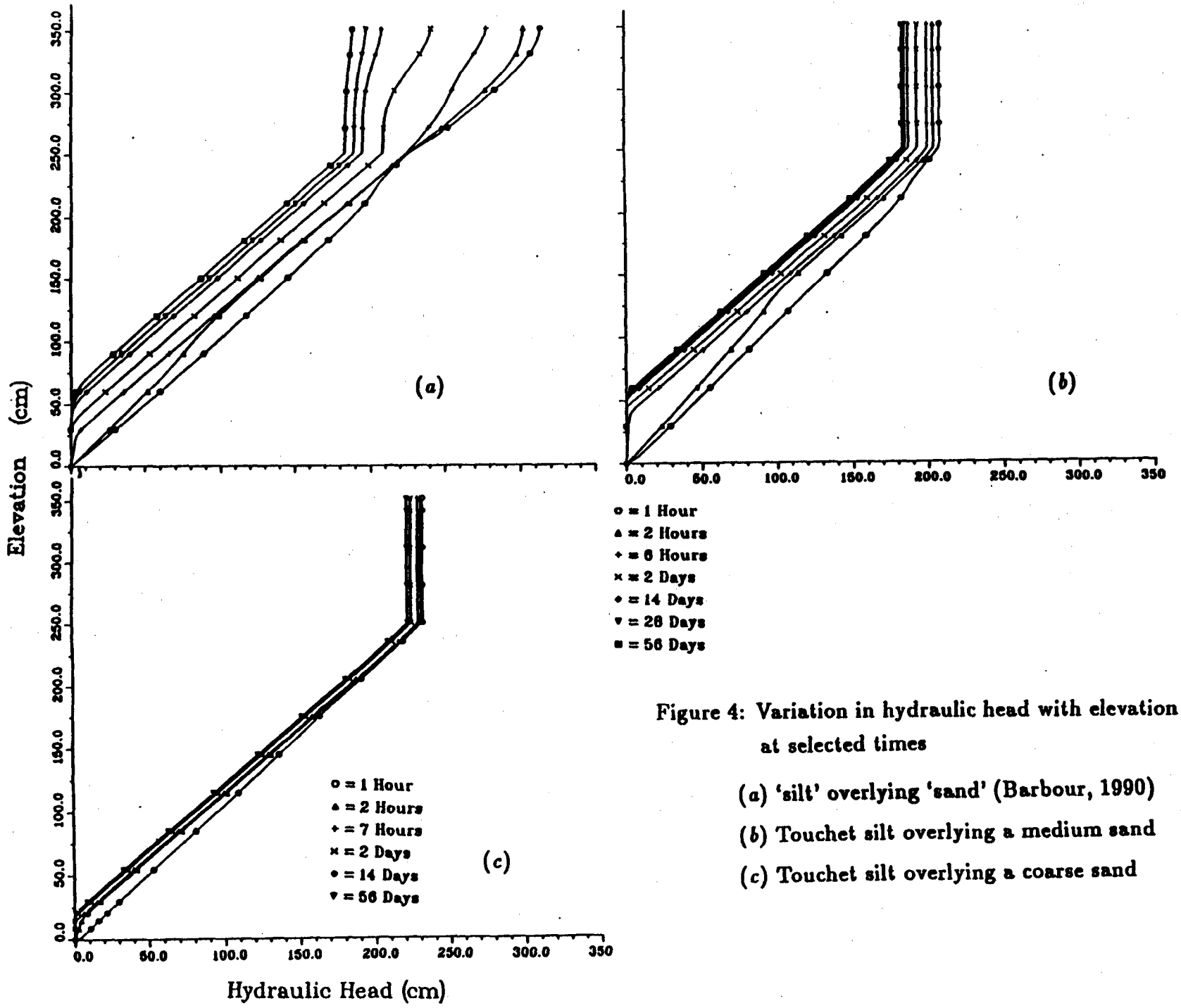

Figure 4: Variation in hydraulic head with elevation at selected times

(*a*) 'silt' overlying 'sand' (Barbour, 1990)

(*b*) Touchet silt overlying a medium sand

(*c*) Touchet silt overlying a coarse sand

REPORT ON THE MODELLING AND ANALYSES OF DRAINAGE FROM A LAYERED LABORATORY SOIL COLUMN

Prepared for
Centre de Technologie Noranda
Noranda Technology Centre

by
S. Lee Barbour and Brenda E. Bews
Geotechnical Group
Department of Civil Engineering
University of Saskatchewan

November 1991

TABLE OF CONTENTS

1.0 INTRODUCTION

In a letter dated April 12, 1991, Noranda Technology Centre (NTC) asked the Geotechnical Group at the University of Saskatchewan to provide technical assistance to NTC personnel in modelling the drainage from a laboratory column of a layered cover system. On July 23, 1991, NTC provided the Geotechnical Group with a set of data and the results of preliminary modelling which had been undertaken by NTC. Some difficulties had been encountered in the simulation and the University of Saskatchewan was asked if they would review the work and attempt to simulate the behavior of the laboratory column during drainage. The letters of April 12 and July 23, 1991 are included in Appendix A.

This report provides a summary of these modelling efforts. Section 2 contains a brief description of the laboratory column study. Section 3 summarizes the modelling which had been completed by NTC up to the end of July, 1991. Section 4 summarizes the results of the modelling undertaken by the University of Saskatchewan. Final conclusions and recommendations regarding this study are provided in Section 5.

2.0 DESCRIPTION OF THE LABORATORY DRAINAGE COLUMN

A complete written description of the column drainage test was not provided by NTC. The following description is our understanding of the construction, testing and monitoring of the column. Much of this information has been obtained through discussions with NTC personnel and consequently some details may be lacking.

2.1 Column Construction

It is understood that the layered soil column was constructed in order to observe the behavior of a clay cover placed over sandy tailings. The column was prepared in a plastic pipe approximately 1 meter in length. A 1/2 bar ceramic porous stone was placed at the base of the column, followed by approximately 72 cm of compacted sand and then 28 cm of compacted clay. The column was prepared in a fully saturated condition and hydrostatic conditions were then established with the water table at the top of the column. The column was instrumented with a set of 10 tensiometers spaced evenly along the length of the column. There is some question as to whether there was a tensiometer at the very top of the column.

Drainage was initiated by lowering an outlet tube connected to the base of the column to an elevation 0.5 meters below the base of the column. Provision was made to keep the top of the column at atmospheric pressure conditions; however, evaporation from the top of the column was prevented. During drainage of the column, periodic measurements of

pressure along the column were made. It is assumed that the total volume of water drained from the column with time was also measured.

2.2 Soil Types

The three materials used in the column construction were the porous stone, a compacted Yukon Clay, and the Heath-Steele Sand. The moisture characteristic curves for the clay and sand, as provided by NTC, are illustrated in Figures 1 and 2.

The air entry value for the clay appears to be approximately 20 kPa of suction. The maximum negative water pressure that could have developed at the top of the column after drainage was approximately 15 kPa, consequently, it was considered unlikely that the clay would drain. However, it is important to note that because of the soft nature of this clay significant changes in water content could still occur as a result of consolidation under the negative pore water pressures that developed during drainage.

The sand has a very low air entry value (less than 2 kPa of suction), consequently, drainage of the sand was likely. The suction at which the sand reaches a residual water content is approximately 4 kPa. Under a fully drained, hydrostatic condition, the average suction in the sand would be approximately 9 kPa and consequently, it should be expected that a significant portion of the sand column would have approached the residual water content. This is important in that the critical hydraulic conductivity values controlling drainage of the column at long times will be those developed near the residual water content.

The hydraulic conductivity functions predicted for the clay and sand, using the technique proposed by Green and Corey (1971) are shown in Figures 3 and 4. This technique is fairly reliable for water contents above the residual water content; however, the predicted flattening of the hydraulic conductivity function as the soil approaches the residual saturation is questionable. It is likely that in fact the hydraulic conductivity decreases more rapidly in this zone as the liquid phase within the soil becomes discontinuous.

The saturated hydraulic conductivity of the three materials; clay, sand and porous stone, are 3.6×10^{-06}, 4.0×10^{-02}, and 3.1×10^{-05} cm/s, respectively. The value of hydraulic conductivity for the porous stone was obtained from the manufacturer's literature. We understand that the saturated hydraulic conductivity of the other two materials had been measured by NTC.

2.3 Laboratory Observations

Figures 5 and 6 illustrate the profiles of pressure head, and the computed hydraulic head within the laboratory column at various times. The original data provided by NTC (Appendix A) was referenced to an elevation datum of 0.5 metres at the column base. The data shown in Figures 5 and 6 was provided by Noranda and it is based on an elevation equal to zero datum at the base of the column.

There are a number of significant observations which can be made from these figures. First, it is apparent from the observed data that drainage of the sand took place. The gradients in the clay layer indicate that some release of water from the clay also occurred. particularly at early times. Secondly, it is interesting that near the base of the column, the gradient in the sand was extremely flat, even though the hydraulic head in the sand was well above the boundary condition value of -0.5 m. This indicates that the porous stone at the base of the column produced an impeded drainage condition. Finally, after approximately 3 days, it is apparent that nearly stagnant conditions developed, even though the gradients measured in the sand were still quite significant. Since there was little change in pressure between the 3 day and 7 day readings, there could not have been any significant release of water. The gradients indicate that the hydraulic conductivity of the sand must have been extremely low. This might be expected because the average suction in the sand was approximately 5 kPa, the same suction at which the sand approaches the residual water content.

These three features of the observed pressure and hydraulic head changes within the column - the release of water from the clay, the impedance of the porous stone, and the low hydraulic conductivity of the sand as it approached its residual water content - are critical features which must be duplicated in any modelling study.

3.0 NTC SIMULATION MODEL

This section provides only a brief summary of the modelling completed by NTC to the end of July 1991. This summary is based solely upon correspondence and telephone conversations with NTC personnel since no detailed summary of this work was available at the time. The PC-SEEP, saturated-unsaturated flow model marketed by GEOSLOPE Programming Ltd. of Calgary was used for these simulations.

3.1 Description of the NTC Model

The NTC model was a two layer soil system consisting of 28 cm of Yukon Clay over 128 cm of Heathe-Steele Sand. The porous stone was not included in the model. The entire height of the model used was 1.5 metres. It is not clear why this was done. It may have been used so that the elevation, pressure and hydraulic head data would coincide at zero. This is not necessary and it would have been better to simulate the actual column height and boundary conditions.

The mesh used by NTC is shown in Figure 7. The zones of finer element spacing were used to provide greater spatial discretization at the base of the clay and at the base of the sand; zones in which rapid changes in head and pressure are likely to occur.

The initial head within the column was taken to be 1.5 metres. The drop in head from 1.5 to 0.5 metres at the lower boundary of the model at a time equal to zero was "ramped" over the first hour of the simulation. This was done in order to prevent instability in the solution arising from an abrupt change in the boundary condition.

3.2 Results of the NTC Model

The plots of pressure head and total head within the column as obtained from the NTC model are shown in Figures 8 and 9. It is readily apparent that the drainage predicted by this model is much more rapid than that observed in the laboratory. In addition, the three characteristic features of the observed data described in Section 2.3 are not reproduced. The gradient within the clay remains flat, the gradients within the sand drop quickly and reach a hydrostatic condition, and there is no apparent impedance at the base of the column.

4.0 UNIVERSITY OF SASKATCHEWAN SIMULATION MODEL

The saturated-unsaturated flow model used for the University of Saskatchewan modelling was the SEEP/W saturated-unsaturated flow model, recently released by GEOSLOPE Programming Ltd. of Calgary. This model is a WINDOWS version of the older PC-SEEP model and it includes a number of significant improvements in areas such as mesh generation, convergence schemes, boundary conditions, and material properties.

The University of Saskatchewan modelling was undertaken in two stages. In the first stage, an attempt was made to duplicate the model results obtained by NTC in order to confirm that both models were providing similar answers for the same mesh and material property data base. The modelling results obtained by the University of Saskatchewan proved to be an exact match of those obtained by NTC.

In the second stage, efforts were made to re-configure the finite element mesh, boundary conditions, and material parameters in order to more accurately reflect the conditions developed in the laboratory column. A sensitivity study was then undertaken in order to highlight the effects that variations in material parameters have on the simulation results. Although a unique set of parameters can not be determined by back-analyses, a good fit to the experimental results was obtained with only minor modifications to the original parameter data set.

4.1 Description of the Model - Mesh Design and Boundary Conditions

In order to incorporate the effects of the impedance caused by the porous stone, a three layer model consisting of a 0.5 cm porous stone, 72 cm of sand, and 28 cm of clay was developed. Each element is 1 cm high, has 8 nodes, and has nine points of interpolation. The mesh developed for the simulation is illustrated in Figure 10.

A zero elevation datum was assigned to the base of the column; consequently, the initial head throughout the column was 1 metre. The boundary condition at the base of the column was "ramped" from 1.0 metres to 0 metres over 2 minutes. This time was established by trial and error as a minimum and realistic time for the development of the lower boundary condition without causing numerical instability.

The total simulation of 7 days was run in three stages with each stage using the predicted head from the previous stage as initial conditions. This procedure allowed the simulation to be broken down into a series of smaller simulations in which appropriate time steps could be assigned over each time interval. The first stage included the boundary condition ramping and ran from 0 to 2 minutes. The second stage of the simulation ran from 2 minutes to 2.2 hours, and the final stage ran from 2.2 hours to 7 days. In the data files included with this report, these stages are referred to by the number designations 8, 9, and 10, respectively.

4.2 Overview of the Simulation Cases

A series of 27 different simulation runs were made in order to investigate the response of the model to changes in the following material parameters:

(i) the water content versus suction relationship for the clay,

(ii) the saturated hydraulic conductivity of the clay,

(iii) the hydraulic conductivity relationship for the sand, and,

(iv) the hydraulic conductivity of the porous stone.

These parameters control the three characteristic features of the laboratory model as described previously in Section 2.3. Several additional runs were also made to investigate the effectiveness of changing the parameters controlling the convergence scheme used in the simulation. Table 1 provides a summary of the parameters used for each of the different cases. The pressure head and hydraulic head profiles through the column for each simulation are provided in Appendix B.

In Cases A through H, the magnitude of the hydraulic conductivity of the clay, sand and porous stone were varied. For cases I through K the steepness of the hydraulic conductivity relationship for the sand was adjusted so that the hydraulic conductivity dropped more dramatically as the sand approached its residual water content (Figure 4). For Cases L and M, the saturated hydraulic conductivity and the water content relationship for the clay (Figure 11) were varied. In Case N, a hydraulic conductivity relationship for the sand (Figure 4) as predicted by the technique proposed by Laliberte et al (1968) was used. Case O was used as a check on the stability of the solution if the model parameter KFAC was varied. This parameter limits the change in hydraulic conductivity of an element during one iteration by the value of KFAC times one log cycle of hydraulic conductivity.

Cases P through S were a series of simulations based on the hydraulic conductivity relationship for the sand used in Case K (Figure 4). In each case, the saturated hydraulic conductivity of the clay, the water content relationship for the clay, or the hydraulic conductivity of the porous stone were varied. Cases T through W were similar to Cases P through S except that the hydraulic conductivity relationship for the sand was the same as that used in Case J. Case X illustrated the combined effect of all the adjustments made in Cases T through W. Case Y combined the decrease in the hydraulic conductivity of the clay in Case V with the decrease in the hydraulic conductivity of the stone in Case W. Case Z used a tighter KFAC value in an attempt to remove some of the obvious numerical instability that was present in Case Y. The final Case AA, used a slightly lower hydraulic conductivity for the porous stone. A disk containing the initial data files for these cases is enclosed with this report.

4.3 Discussion of Simulation Results

It is apparent from even the original data set (Case A) that many of the critical features of the laboratory observations, as well as the general shape of the pressure changes, could be reproduced. Slight gradients developed in the clay, slower time dependant changes in pressure occurred throughout the sand, with impedance at the base of the column. The only feature that was not reproduced was the stagnation of the pressure changes at later times.

Cases B through H illustrate that by fairly minor changes in the hydraulic conductivity of the clay, sand and porous stone many of the above features could be accentuated. None of these changes; however, had any significant influence on the stagnation of pressure

changes at long times. Cases I through K illustrated that this feature could only be reproduced if the hydraulic conductivity relationship for the sand was decreased rapidly as the water content of the sand approaches its residual value.

The refinements used in the remaining cases illustrated that a very good match to the observed pressure heads within the column could be obtained with only minor adjustments to the soil parameters, providing that the appropriate hydraulic conductivity relationship for the sand was utilized.

It is evident in the simulation results that problems with numerical stability develop as the hydraulic conductivity relationship for the sand is steepened. The use of the KFAC parameter appeared to be quite effective in controlling this problem. Figure 12 provides a comparison of the convergence of the head vector with iteration number for a time step in which convergence was quite problematic. Case Y used a KFAC value of 1.0, while Case Z used a KFAC value of 0.1. The lower KFAC value produces stable convergence. The stability of the solution is also evident in the pressure head and hydraulic head profiles for these cases shown in Appendix B.

The "best" simulated match to the actual column observations was provided by simulation Case AA. Figure 13 provides a comparison of the laboratory observations with the simulation results. The comparison is quite good over most of the profile. The heads at the top of the clay appear to be a little different. There is some question as to whether the pressure head at the top of the column was actually measured. It is more likely that the hydraulic heads at the top of the clay begin to flatten near the top of the column as the water flux decreases.

5.0 CONCLUSIONS AND RECOMMENDATIONS

Modelling of the laboratory column has illustrated that it is possible to obtain a good prediction of the pressures within the column as long as critical aspects of each media type are included in the model. These features include:

(i) The release of water from the clay as a result of consolidation under the negative pore pressures that develop during drainage.

(ii) The impedance produced by the presence of the porous stone at the base of the column.

(iii) The rapidly decreasing hydraulic conductivity of the sand as it approaches it's residual water content.

The final simulation Case AA illustrated that a good match can be obtained with only slight alterations to the original data set provided by NTC. In Case AA the following adjustments to the original data set were made:

(i) The hydraulic conductivity function for the sand was steepened near the residual water content.

(ii) The hydraulic conductivity of the clay was reduced by a factor of 2.

(iii) The hydraulic conductivity of the porous stone was reduced by a factor of 2.7 from its catalogue value.

The use of a steeper function for the hydraulic conductivity near the residual water content has already been explained. The reduction in the saturated hydraulic conductivity of the clay is not particularly severe. One would expect some reduction in the hydraulic conductivity of the clay in the column from that measured in separate tests, either due to consolidation or possibly due to incomplete saturation during construction. The reduction in the hydraulic conductivity of the porous stone may appear quite significant; however, it is important to keep in mind that the original estimate of the hydraulic conductivity was based on a catalogue value. No hydraulic conductivity testing of the porous stone used in the laboratory column has been undertaken.

Some suggestions for further work would include the following:

(i) A more complete match of the laboratory observations could be attempted. In particular, adjustments to the water content and hydraulic conductivity relationships for the clay could be tried; however, some evaluation of the accuracy of the pressure readings within the clay should be made before effort is expended in a "curve fitting" exercise.

(ii) Checking any "calibration" using the cumulative flux through the base of the column, as predicted by the model, against the total drainage volumes measured in the laboratory, would be useful.

(iii) Direct measurements of the hydraulic conductivity of the porous stone should be made.

(iv) Direct measurements of the hydraulic conductivity of the clay cover in an "as compacted" condition could be undertaken.

(v) Laboratory techniques to verify and investigate the hydraulic conductivity relationship for the sand at water contents near the residual water content should be developed. Some work in this area is just beginning at the University of Saskatchewan.

(vi) Further sensitivity studies could be undertaken on the impact that the level of spatial and temporal discretization have on the model results.

(vii) More formalized sensitivity studies could be undertaken on the role that variations in soil properties have on the model results.

REFERENCES

GEO-SLOPE Programming Ltd. 1987. PC-SEEP A Finite Element Program for Seepage Analyses. GEO-SLOPE Programming Ltd., Calgary, Alberta, Canada.

GEO-SLOPE International Ltd. 1991. SEEP/W A Finite Element Program for Seepage Analyses. GEO-SLOPE International Ltd, Calgary, Alberta, Canada.

Green, R.E. and Corey, J.C. 1971. Calculation of hydraulic conductivity: A further evaluation of some predictive methods. Soil Science of America Proceedings, 35, pp. 3-8.

Laliberte, G.E., Brooks, R.H., and Corey, A.T. 1968. Permeability calculated from desaturation data. ASCE Journal of Irrigation and Drainage Division, pp. 57-71.

Table 1 - Simulation Cases

Case	Saturated Hydraulic Conductivity (m/day)			Hydraulic Conductivity Relationship - Sand	Water Content Relationship - Clay
	Clay	Sand	Stone		
(bold print indicates that the value is different than the original data set)					
Orig	3.11e-03	3.45e+01	2.68e-02	Fig 4 - Original Fnc	Fig 1 - Original Fnc
A	3.11e-03	**1.72e+01e**	2.68e-02	Fig 4 - Original Fnc	Fig 1 - Original Fnc
B	3.11e-03	**3.45e+00**	2.68e-02	Fig 4 - Original Fnc	Fig 1 - Original Fnc
C	3.11e-03	3.45e+01	**2.68e-03**	Fig 4 - Original Fnc	Fig 1 - Original Fnc
D	3.11e-03	3.45e+01	**1.34e-02**	Fig 4 - Original Fnc	Fig 1 - Original Fnc
E	3.11e-03	**1.72e+01**	**1.34e-02**	Fig 4 - Original Fnc	Fig 1 - Original Fnc
F	3.11e-03	**1.72e+01**	**6.70e-03**	Fig 4 - Original Fnc	Fig 1 - Original Fnc
G	3.11e-03	**1.72e+01**	**1.34e-02**	Fig 4 - Original Fnc	Fig 1 - Original Fnc
H	**1.55e-03**	**1.72e+01**	**1.34e-02**	Fig 4 - Original Fnc	Fig 1 - Original Fnc
I	3.11e-03	**1.72e+01**	**1.34e-02**	**Fig 4 - Steep Fnc I**	Fig 1 - Original Fnc
J	3.11e-03	**1.72e+01**	**1.34e-02**	**Fig 4 - Steep Fnc J**	Fig 1 - Original Fnc
K	3.11e-03	**1.72e+01**	**1.34e-02**	**Fig 4 - Steep Fnc K**	Fig 1 - Original Fnc
L	3.11e-03	**1.72e+01**	**1.34e-02**	Fig 4 - Original Fnc	**Fig 11 - Steep Fnc**
M	**1.55e-03**	**1.72e+01**	**1.34e-02**	Fig 4 - Original Fnc	Fig 1 - Original Fnc
N	3.11e-03	**1.72e+01**	**1.34e-02**	**Fig 4 - Case N Fnc**	Fig 1 - Original Fnc
O*	3.11e-03	**1.72e+01**	**1.34e-02**	Fig 4 - Original Fnc	Fig 1 - Original Fnc
P	3.11e-03	3.45e+01	2.68e-02	**Fig 4 - Steep Fnc K**	Fig 1 - Original Fnc
Q	3.11e-03	3.45e+01	2.68e-02	**Fig 4 - Steep Fnc K**	**Fig 11 - Steep Fnc**
R	**1.55e-03**	3.45e+01	2.68e-02	**Fig 4 - Steep Fnc K**	Fig 1 - Original Fnc
S	3.11e-03	3.45e+01	**1.34e-02**	**Fig 4 - Steep Fnc K**	Fig 1 - Original Fnc
T	3.11e-03	3.45e+01	2.68e-02	**Fig 4 - Steep Fnc I**	Fig 1 - Original Fnc
U	3.11e-03	3.45e+01	2.68e-02	**Fig 4 - Steep Fnc I**	**Fig 11 - Steep Fnc**
V	**1.55e-03**	3.45e+01	2.68e-02	**Fig 4 - Steep Fnc I**	Fig 1 - Original Fnc
W	3.11e-03	3.45e+01	**1.34e-02**	**Fig 4 - Steep Fnc I**	Fig 1 - Original Fnc
X	**1.55e-03**	3.45e+01	**1.34e-02**	**Fig 4 - Steep Fnc I**	**Fig 11 - Steep Fnc**
Y	**1.55e-03**	3.45e+01	**1.34e-02**	**Fig 4 - Steep Fnc I**	Fig 1 - Original Fnc
Z*	**1.55e-03**	3.45e+01	**1.34e-02**	**Fig 4 - Steep Fnc I**	Fig 1 - Original Fnc
AA* - **Final Simulation**					
	1.55e-03	3.45e+01	**1.00e-02**	**Fig 4 - Steep Fnc I**	Fig 1 - Original Fnc

(* - KFAC equal to 0.1, all other cases KFAC = 1.0)

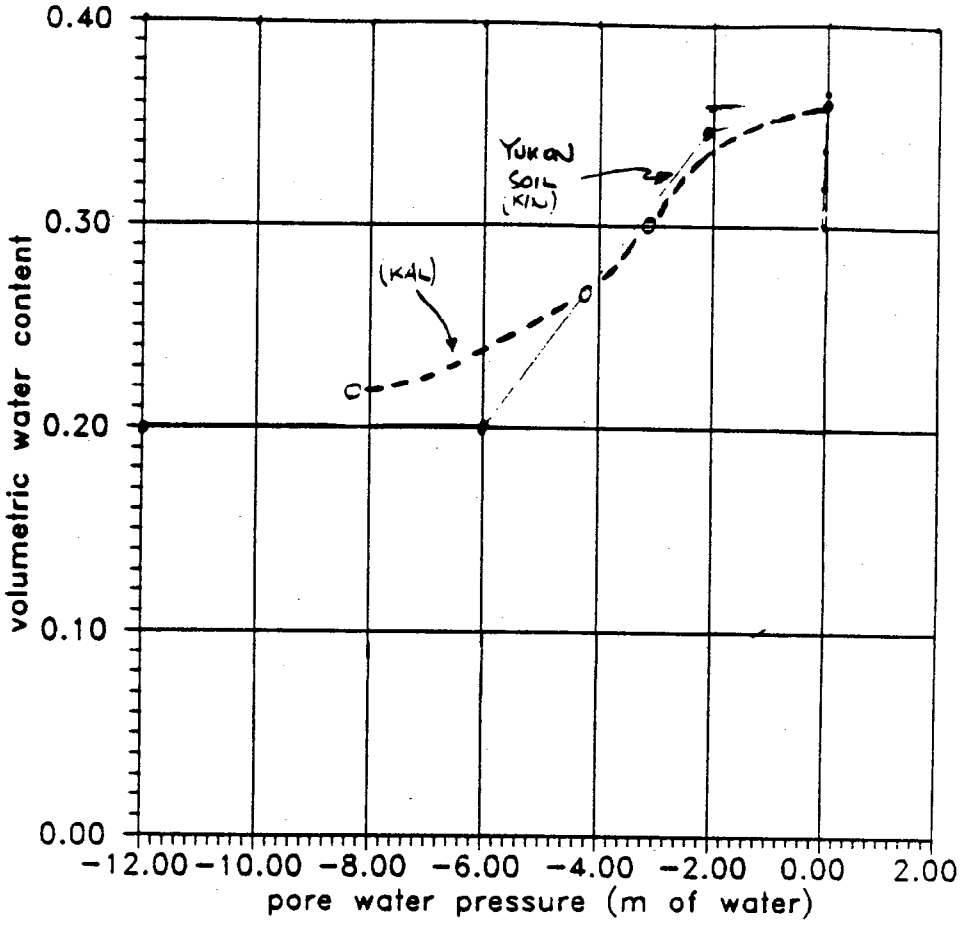

Figure 1 Volumetric water content versus matric suction relationship for the Yukon Clay as provided by NTC

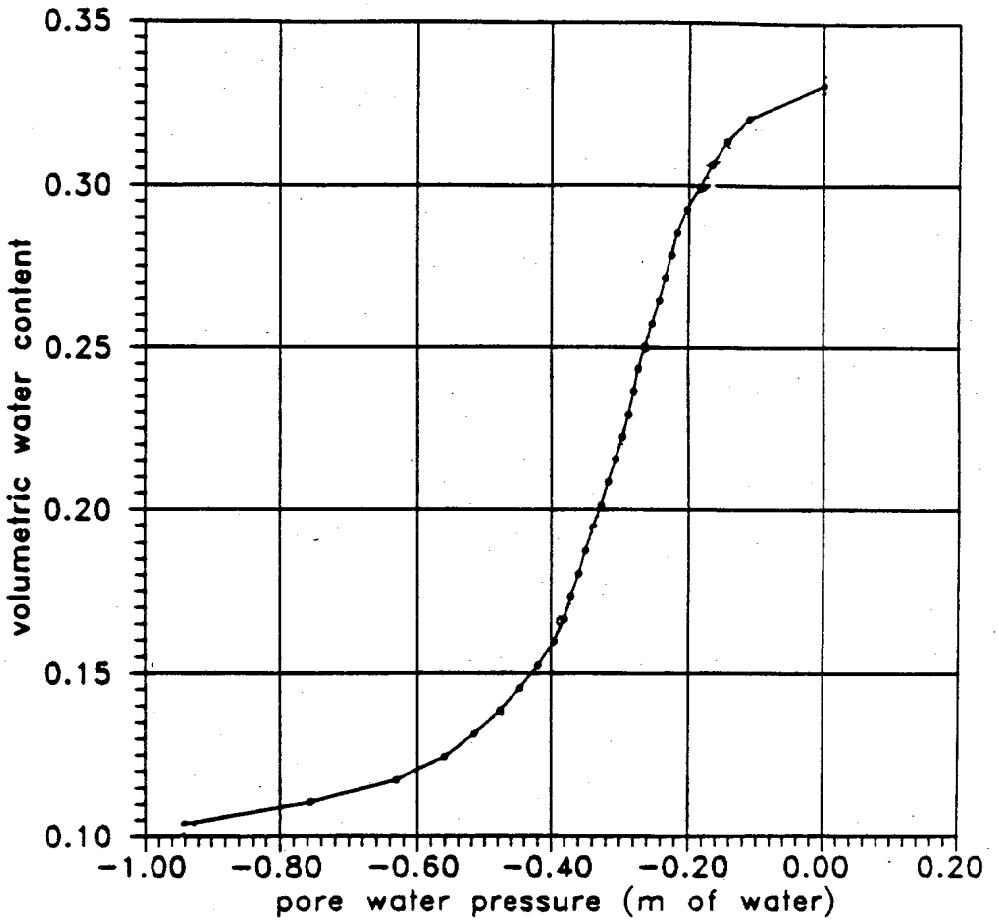

Figure 2 Volumetric water content versus matric suction relationship for the Heath-Steele Sand as provided by NTC

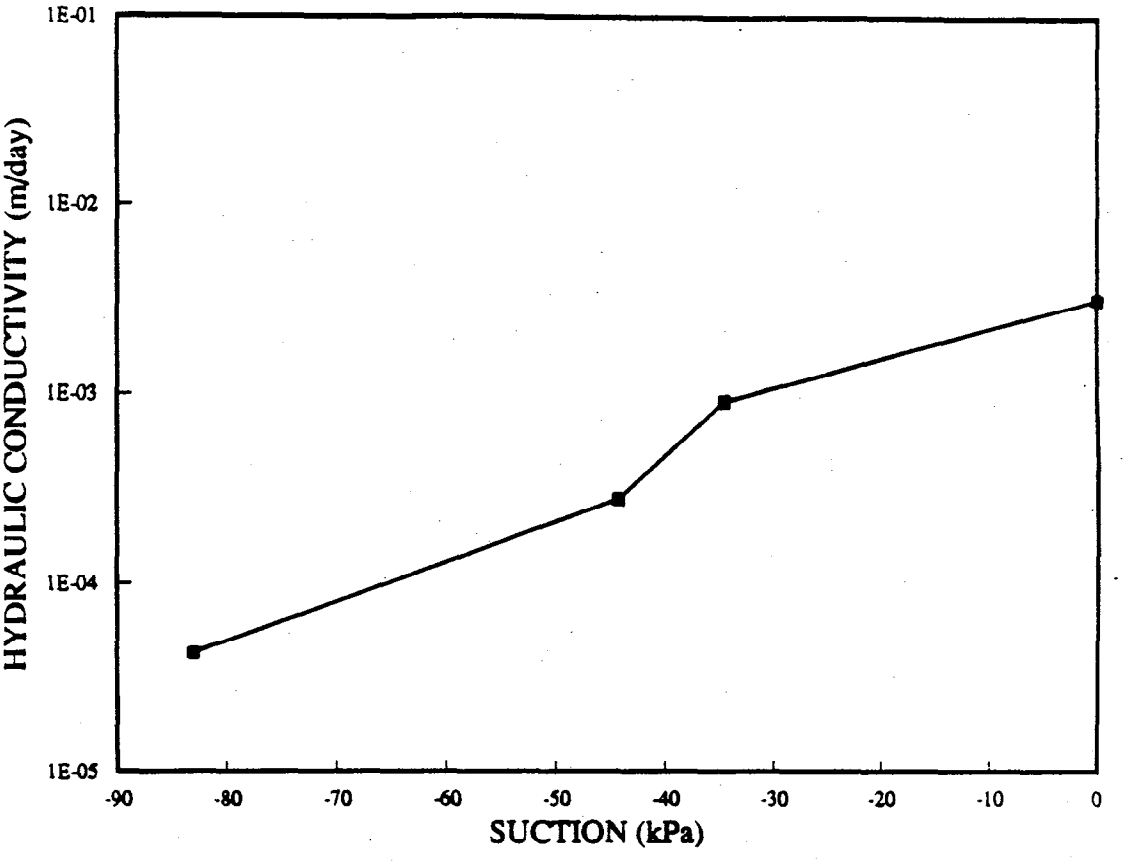

Figure 3 Hydraulic conductivity versus matric suction relationship for the Yukon Clay

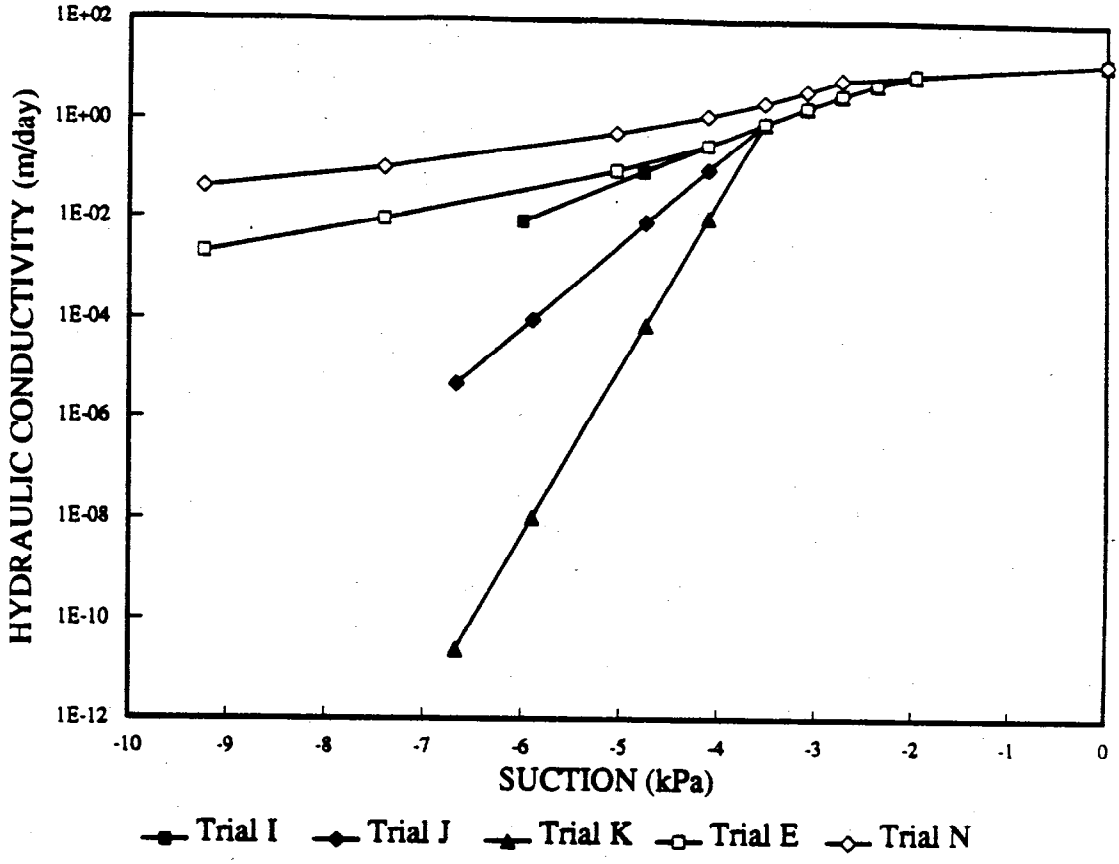

Figure 4 Hydraulic conductivity versus suction relationships for the Heath-Steele Sand. (Data points only - all functions smoothed by spline interpolation in the model)

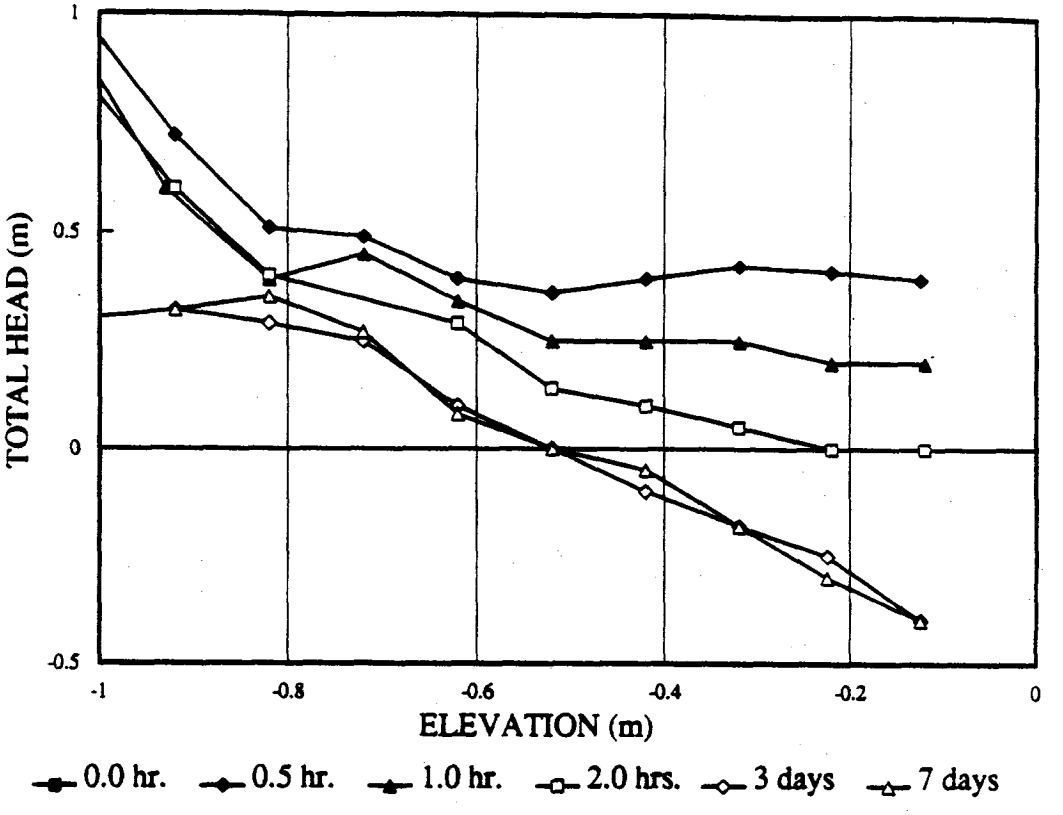

Figure 5 Hydraulic head profile within laboratory column at different times

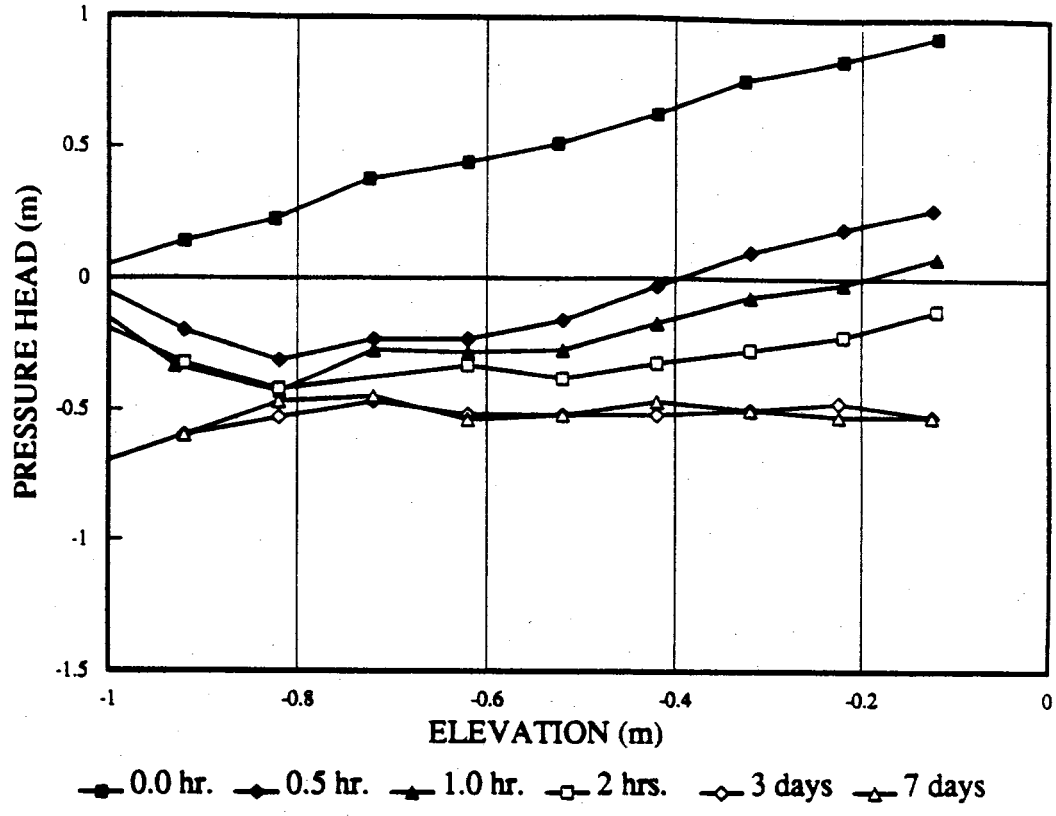

Figure 6 Observed pressure head profiles within laboratory column at different times

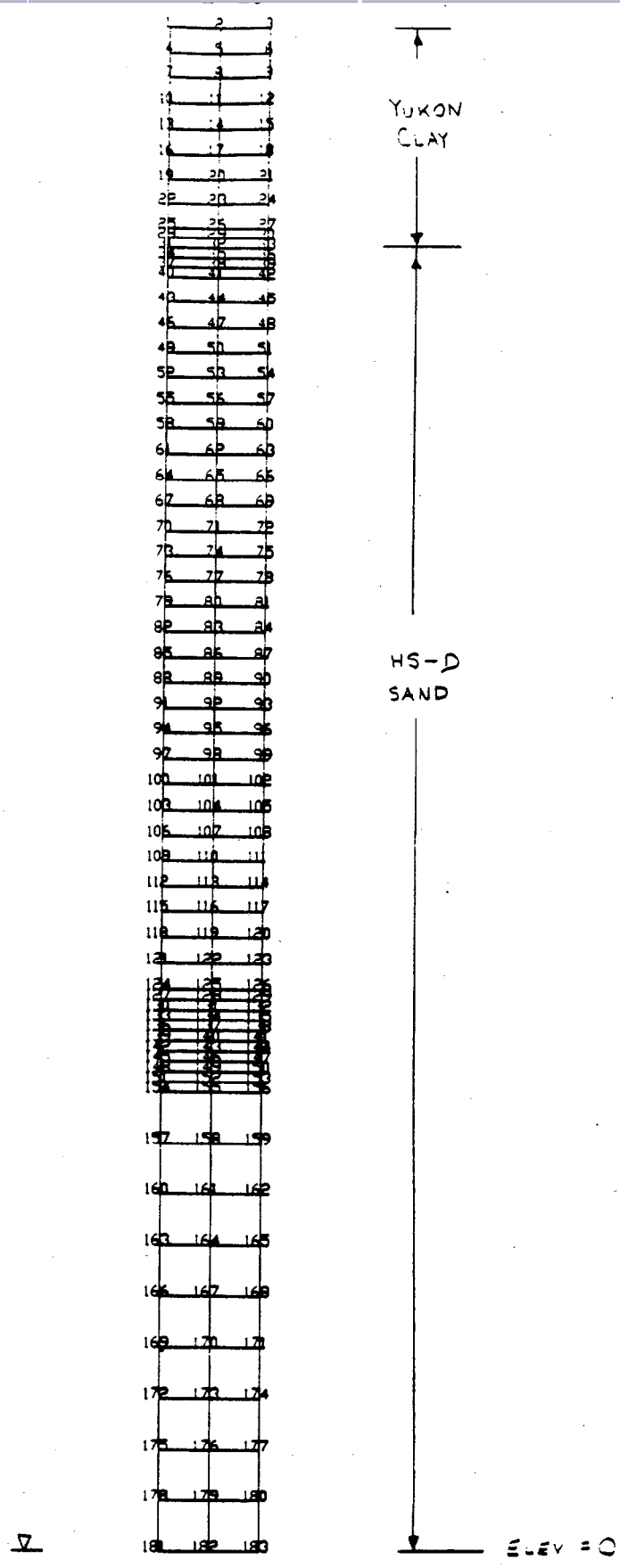

Figure 7 Finite element mesh for the NTC model.

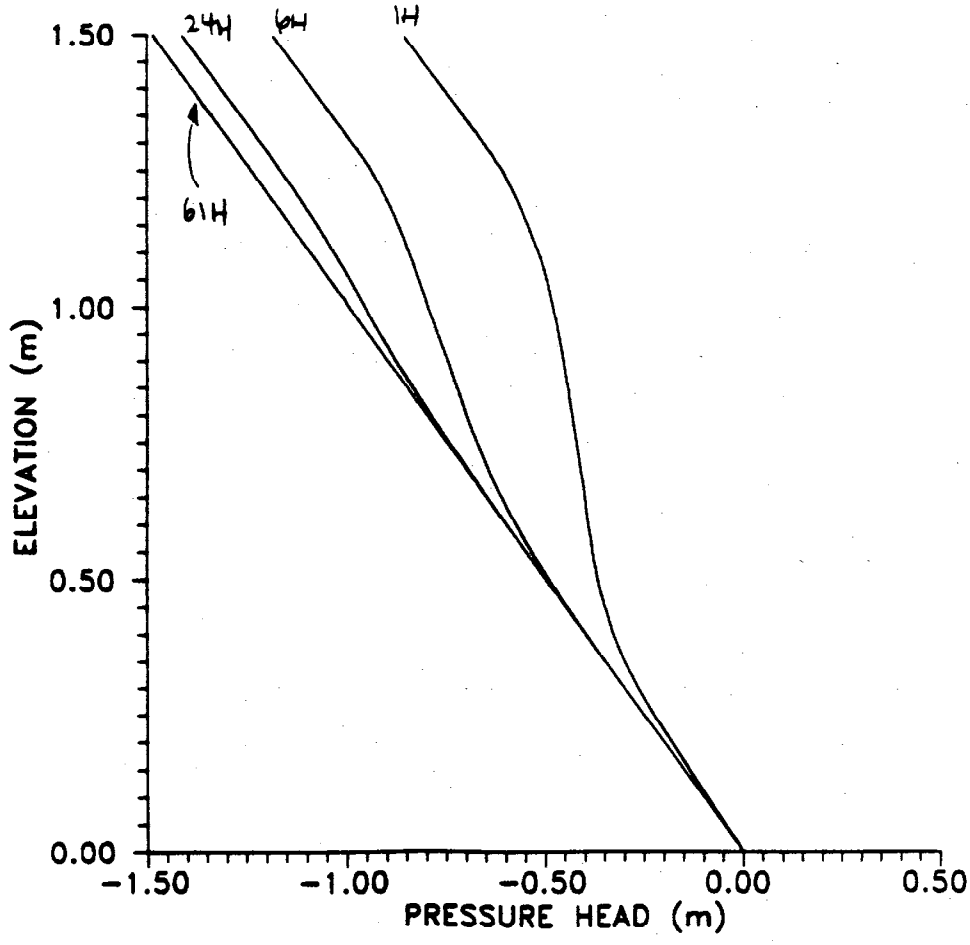

Figure 8 Simulated pressure head profiles from the NTC model

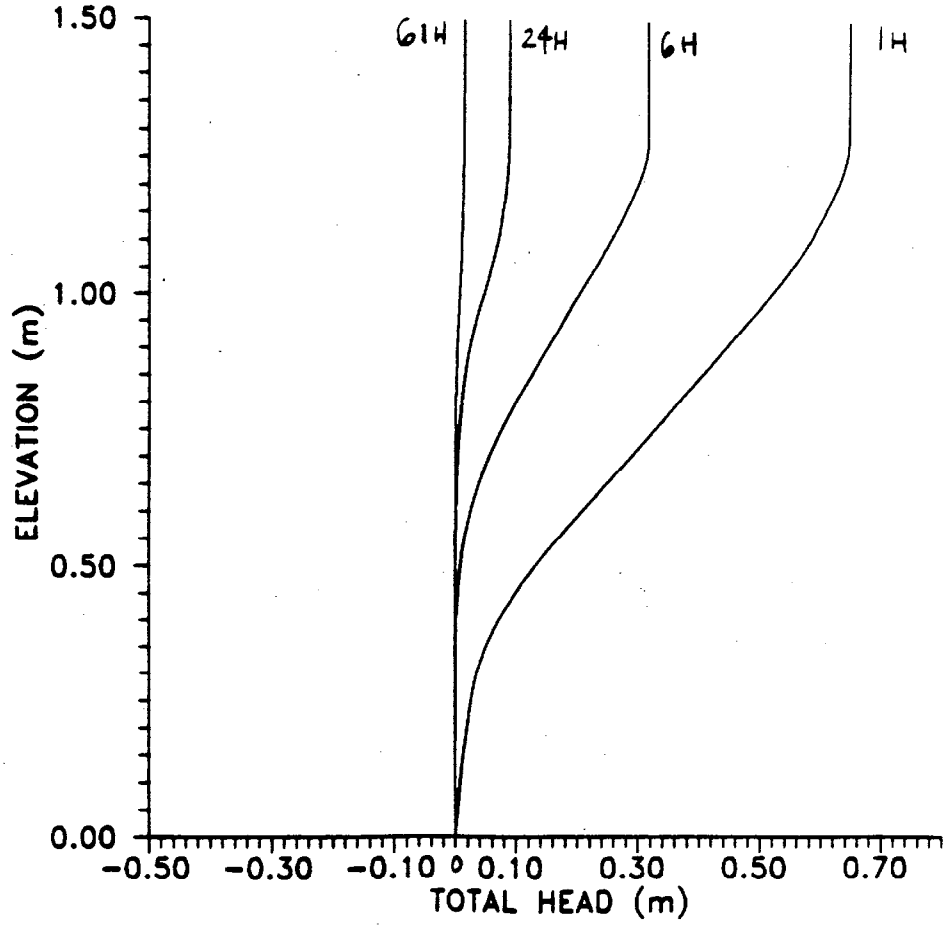

Figure 9 Simulated hydraulic head profiles from the NTC model

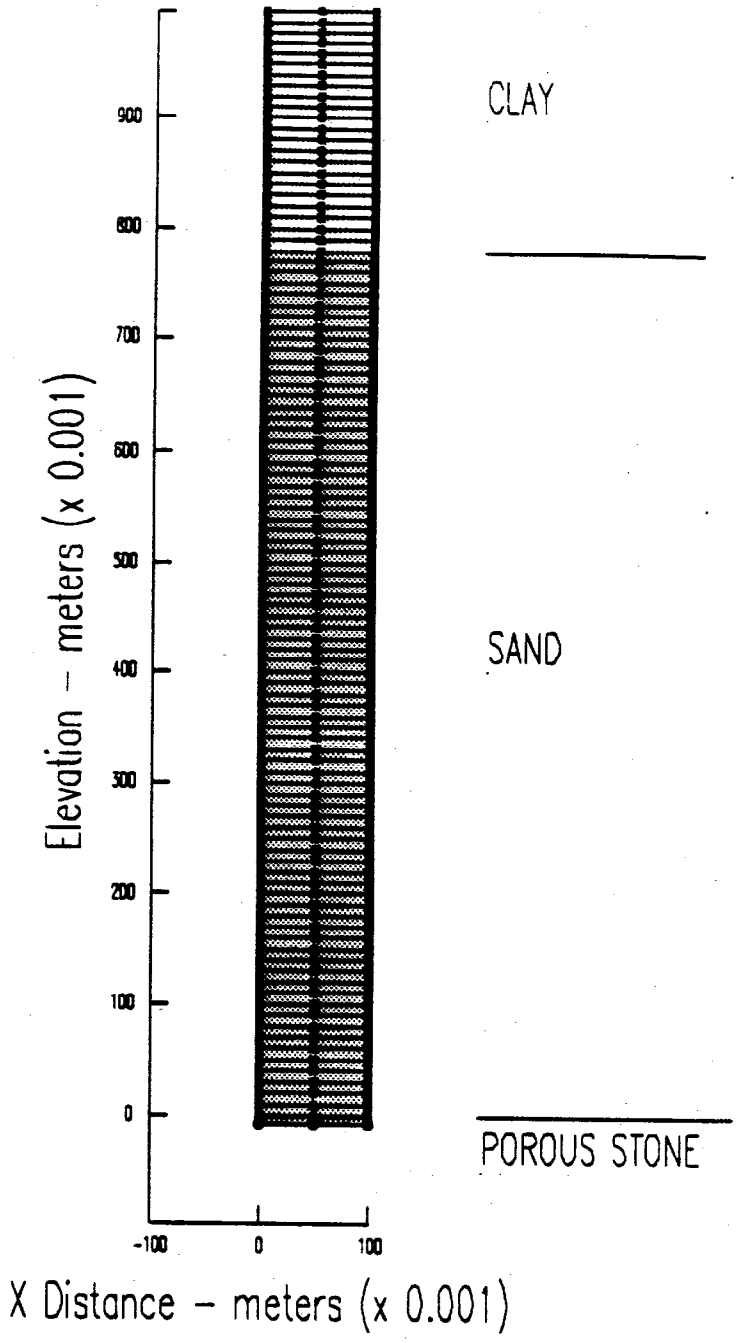

Figure 10 Finite element mesh used for the University of Saskatchewan model.

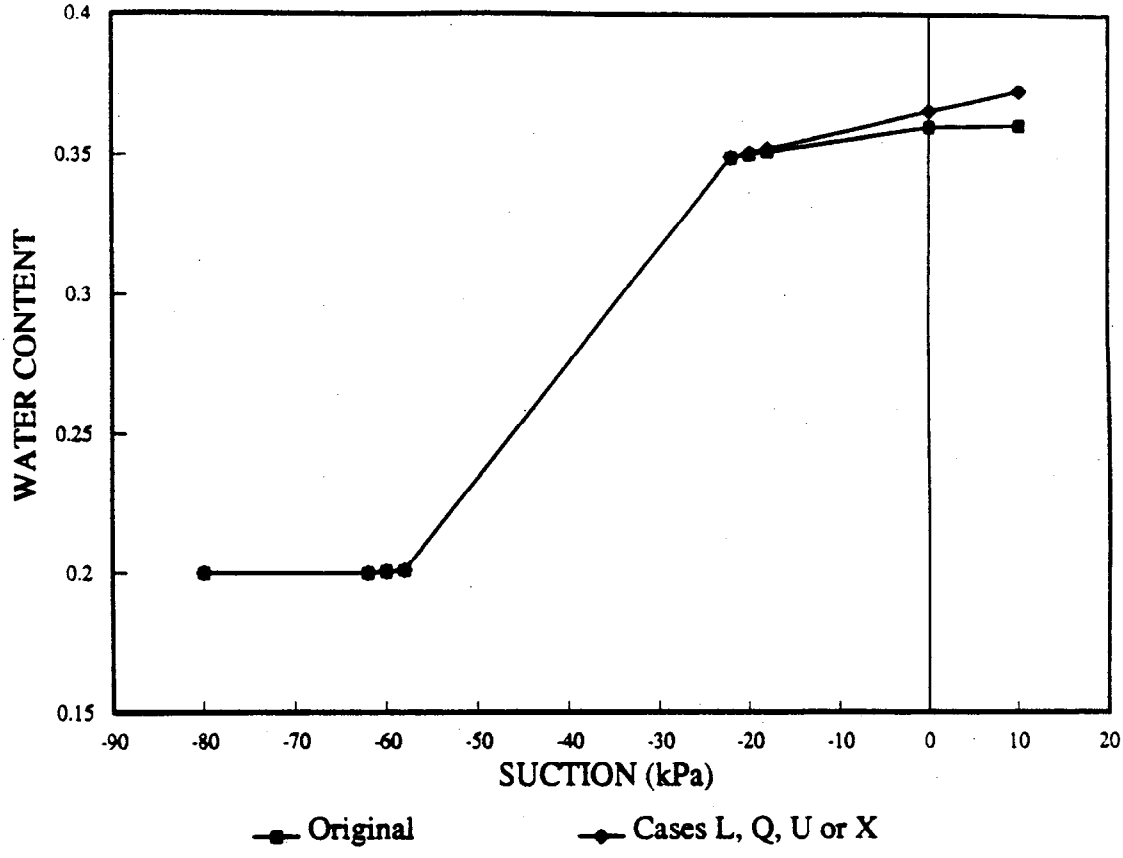

Figure 11 Volumetric water content relationships for the Yukon Clay as used in the model simulations. (Data points only - all functions smoothed by spline interpolation in the model)

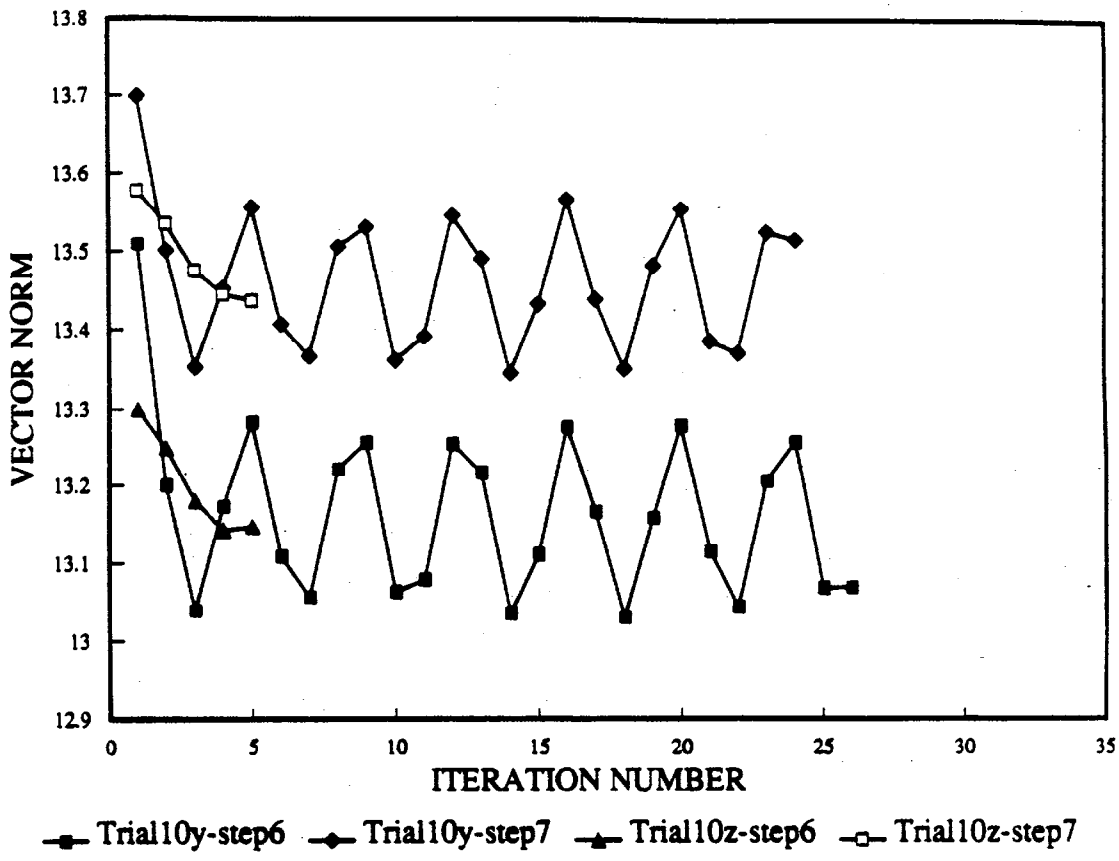

Figure 12 The effect of KFAC on the convergence of time steps 6 and 7 in trial simulations 10Y and 10Z.

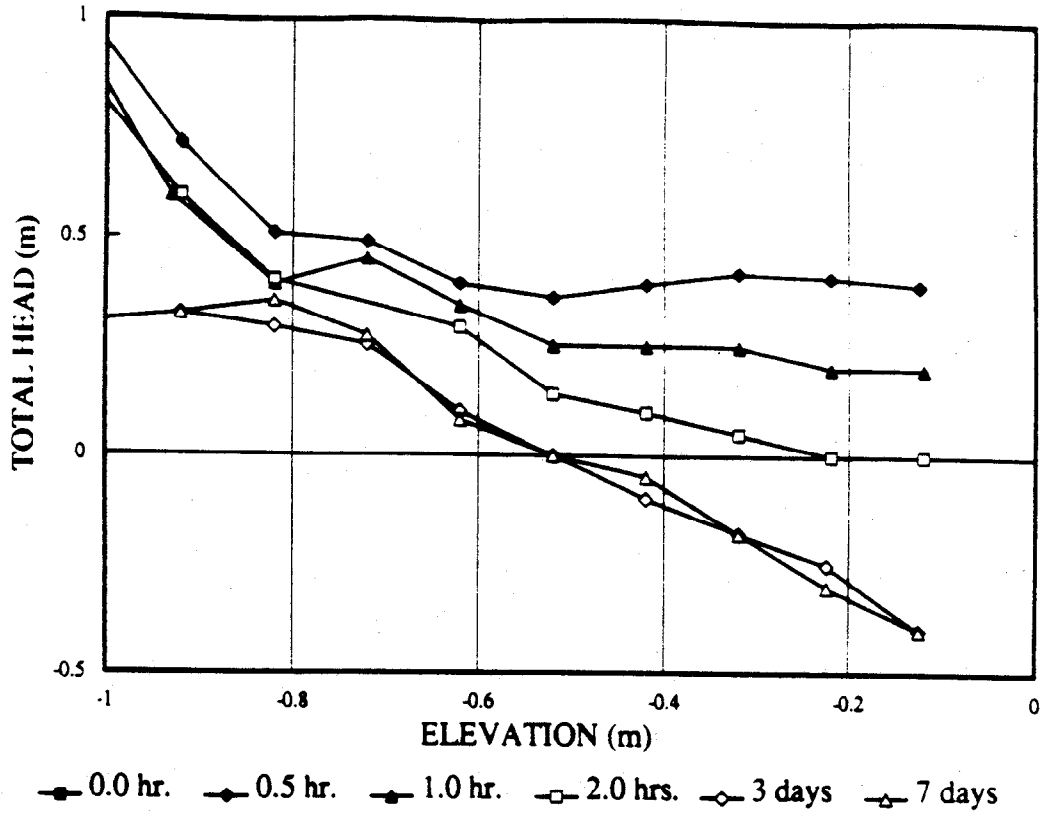
TOTAL HEAD (m)
1
0.5
0
-0.5
-1
-0.8
-0.6
-0.4
-0.2
0
ELEVATION (m)
0.0 hr.
0.5 hr.
1.0 hr.
2.0 hrs.
3 days
7 days

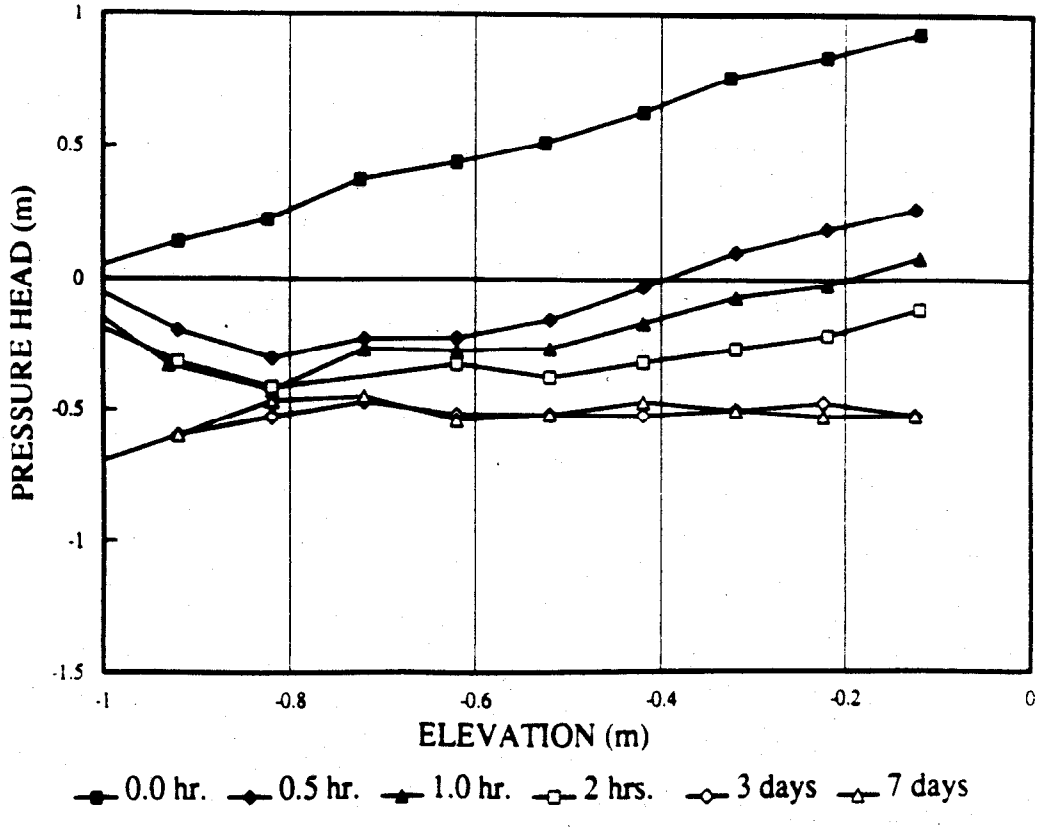
PRESSURE HEAD (m)
1
0.5
0
-0.5
-1
-1.5
-1
-0.8
-0.6
-0.4
-0.2
0
ELEVATION (m)
0.0 hr.
0.5 hr.
1.0 hr.
2 hrs.
3 days
7 days

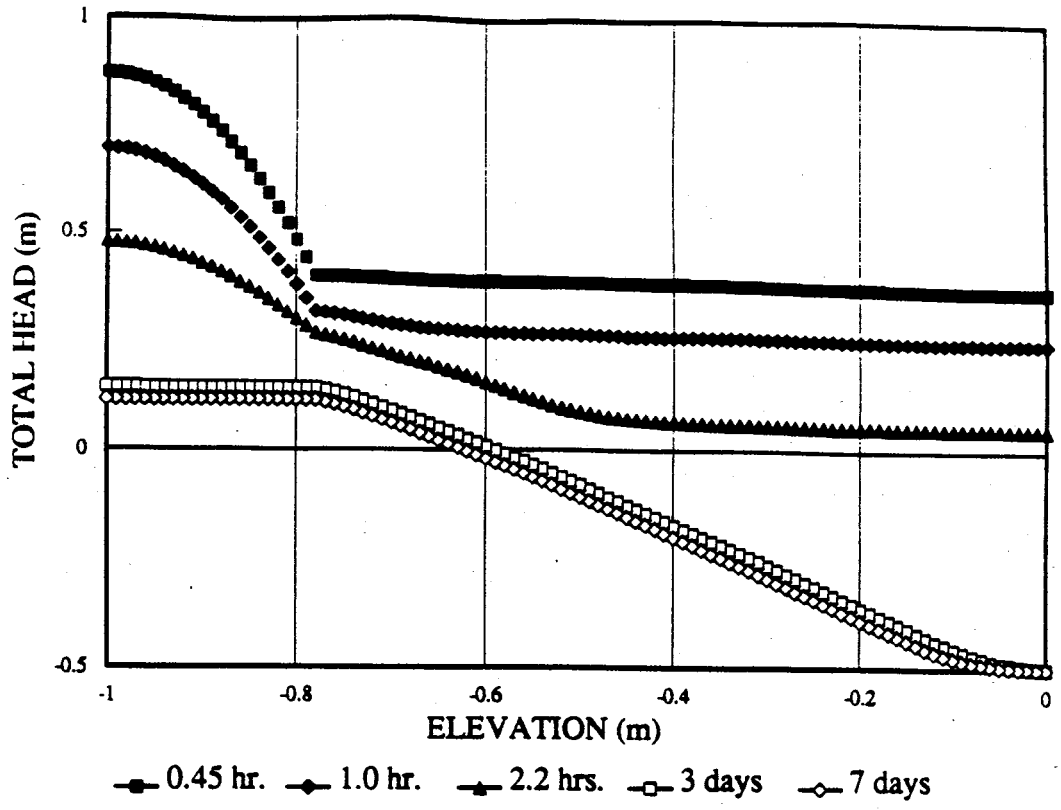

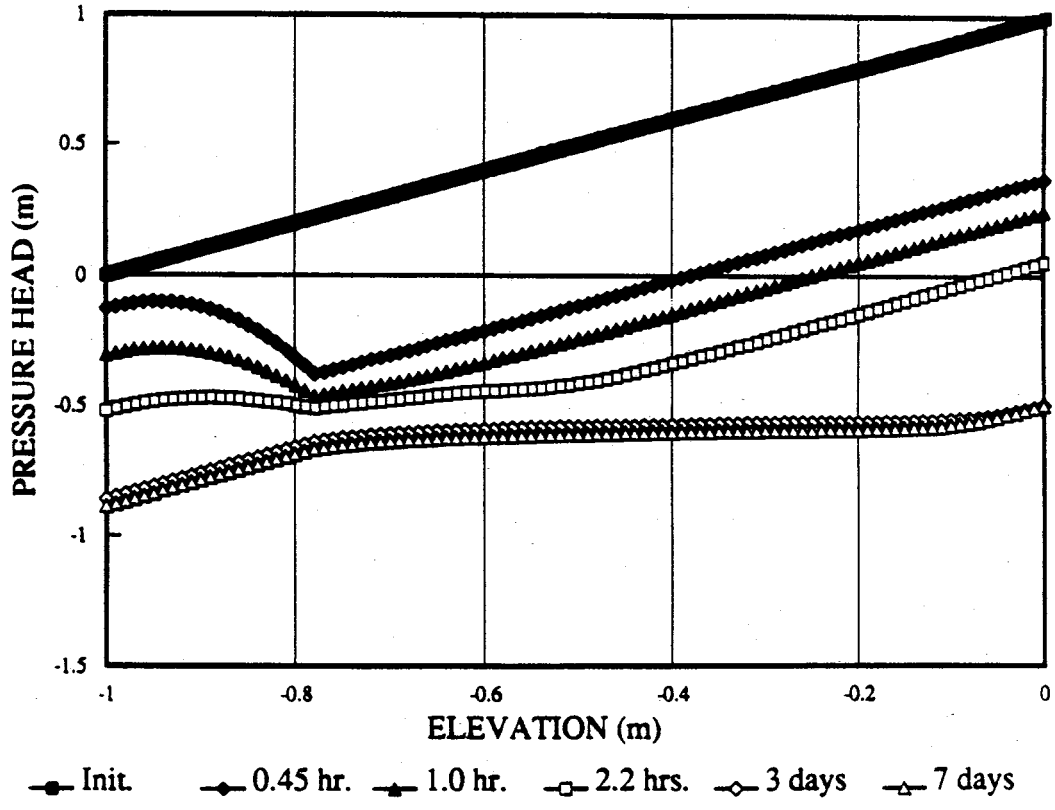

Figure 13 Hydraulic head and pressure head profiles for simulation case AA
a) overlay of laboratory observations
b) Case AA simulation results.

APPENDIX A

CORRESPONDENCE

Centre de technologie Noranda

noranda

July 23, 1991

Dr. L. Barbour
Department of Civil Engineering
University of Saskatchewan
Saskatoon, Saskatchewan
S7N 0W0

Dear Lee:

As we discussed before, we are trying to reproduce the results of the transient drainage of our lab columns using PC-SEEP. I included in this package a diskette with datafiles:

COLUMN7.SEP:	Transient run, times 0 to 1 day initial heads 1.5 m bottom boundary condition changing from h = 1.5 m to 0 m MAXKDIF set to 0.100
COLUMN7L.SEP	times 1-2.5 days solution from COLUMN7.SEP used as initial condition bottom boundary h = 0 (constant)
COLUMN4.SEP	Included only as reference smaller grid contains SOIL data from KCAL fitted results instead of matched results used in COLUMN7 run

Also included are:

- Grid with comments on soils and boundary condition
- STORAGE curve for top soil (Yukon clay)
- STORAGE and SOIL curves for bottom soil (HS-D, or Heath Steele D sand)
- Grainsize distribution curves for both soils
- Elevation vs Total Head plot at selected times using results of COLUMN7 and COLUMN7L
- Elevation vs Pressure Head plot for same times

- Elevation vs Total head plot for Laboratory column

Comments and questions:

1) I have looked at new example 12 in the PC-SEEP manual, which does a simulation of the steady state solution by Kisch. Is it essential to vary the MAXKDIF parameter and perform the run in three steps? If so, it should also be done for the transient run.

2) I have not performed the sensitivity analysis on the hydraulic conductivity of the bottom sand. This would seem to be an interesting task for a student to start on.

3) Our resulting plots resemble those of Akidunni (1990); however, the curves shift much faster to smaller head values, indicating that drainage occurs faster.

As Ernest indicated to you on the phone, we would like you to perform runs and tell us what you think about it.

Regards,

CENTRE DE TECHNOLOGIE NORANDA

Luc St-Arnaud, P.Eng, M.Sc.
HYDROGEOTECHNICAL GROUP

Encl.

APPENDIX B

HYDRAULIC HEAD AND PRESSURE HEAD PROFILES

- SIMULATION CASES A THROUGH AA

Observed Total Head Profiles

in Laboratory Column (from Noranda Data)

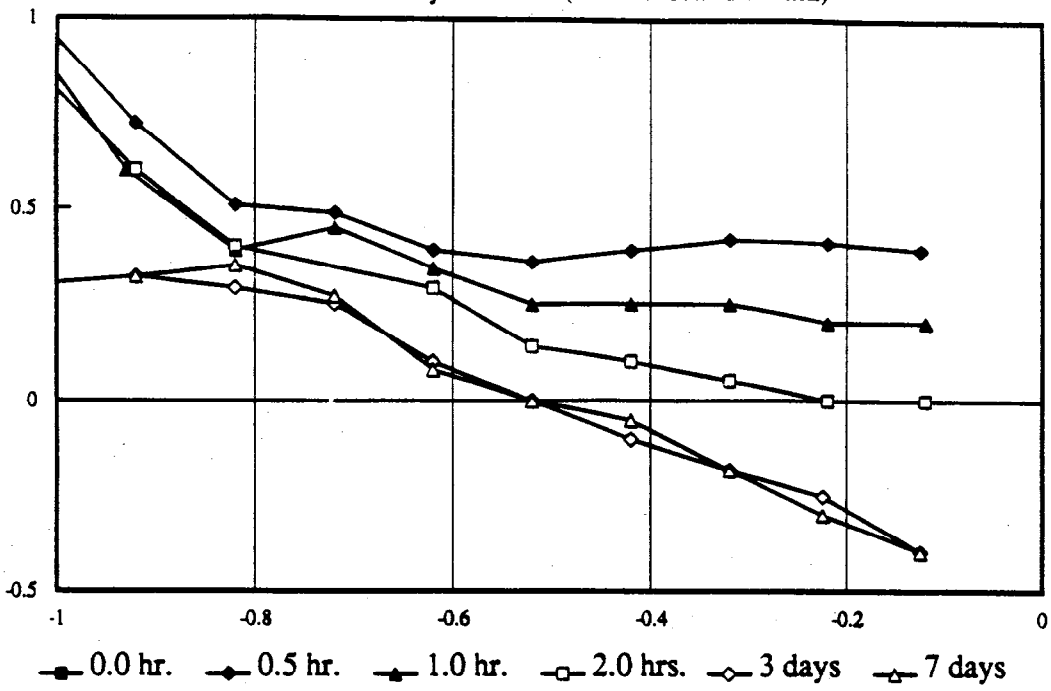

Observed Pressure Head Profiles

in Laboratory Column (from Noranda Data)

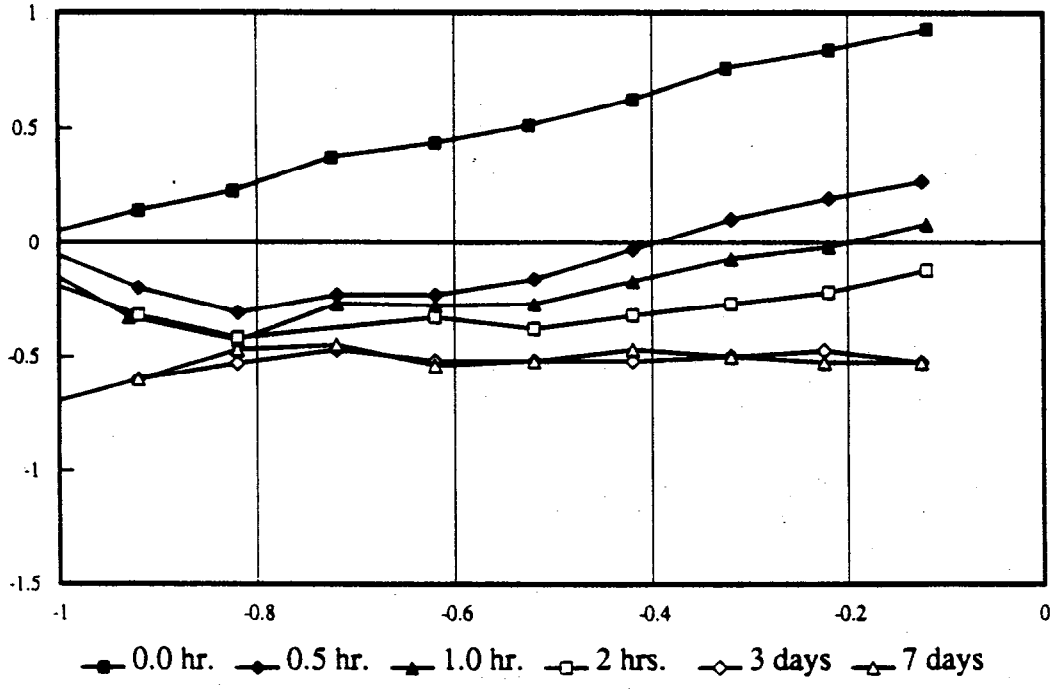

Simulation of Original Data Set

Total Head (m) vs. Elevation (m)

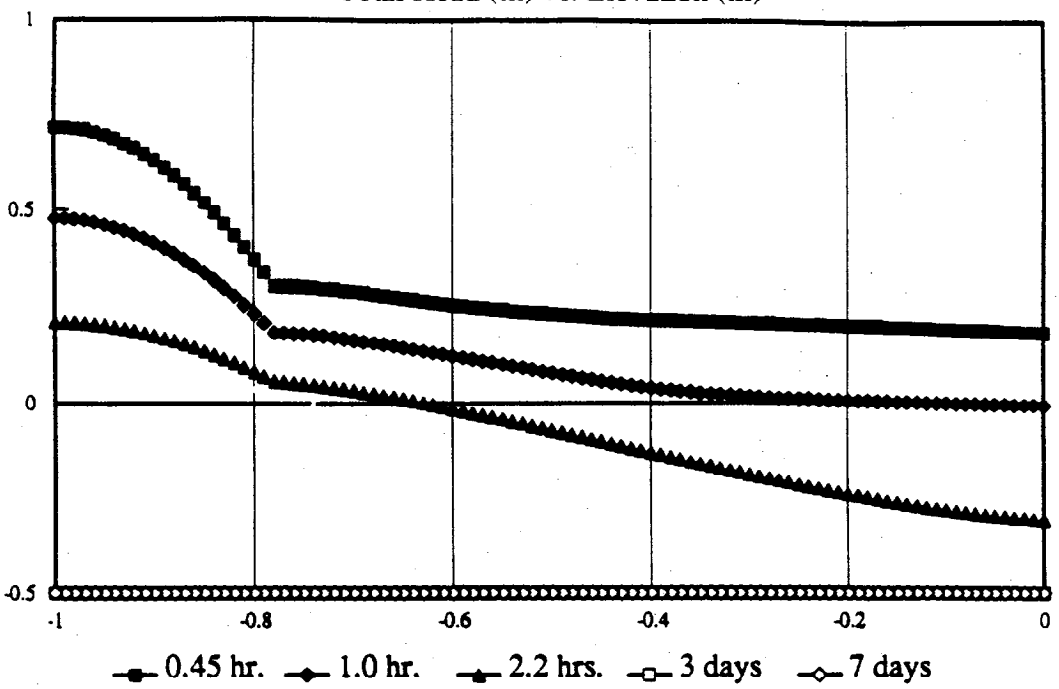

Simulation of Original Data Set

Pressure Head (m) vs. Elevation (m)

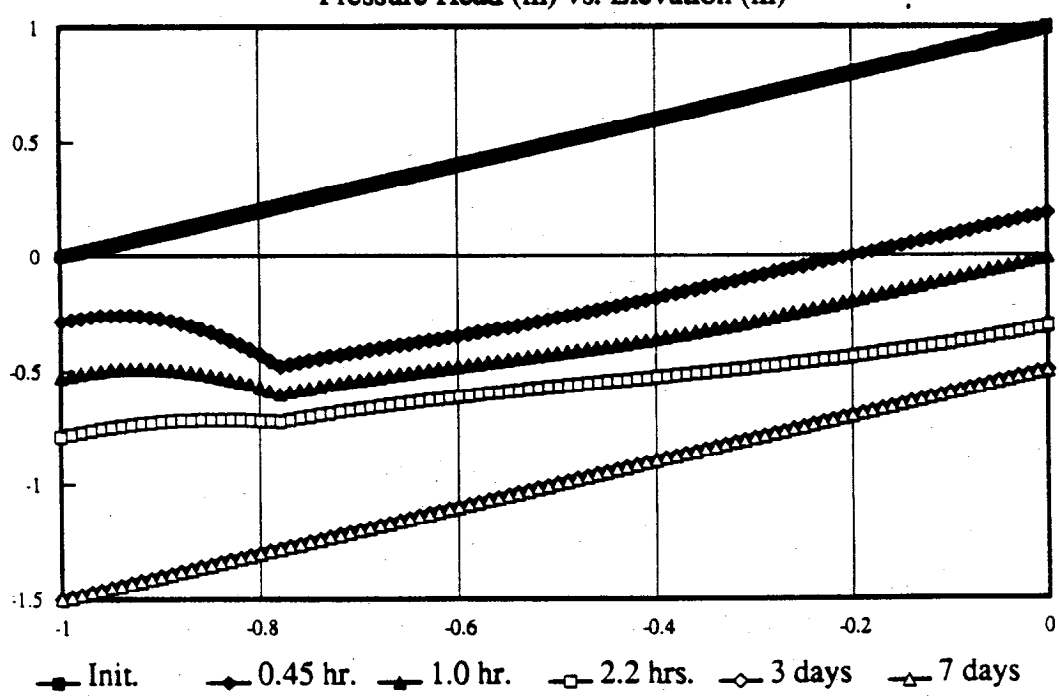

TRIAL 8-10A / NORANDA

Total Head (m) vs. Elevation (m)

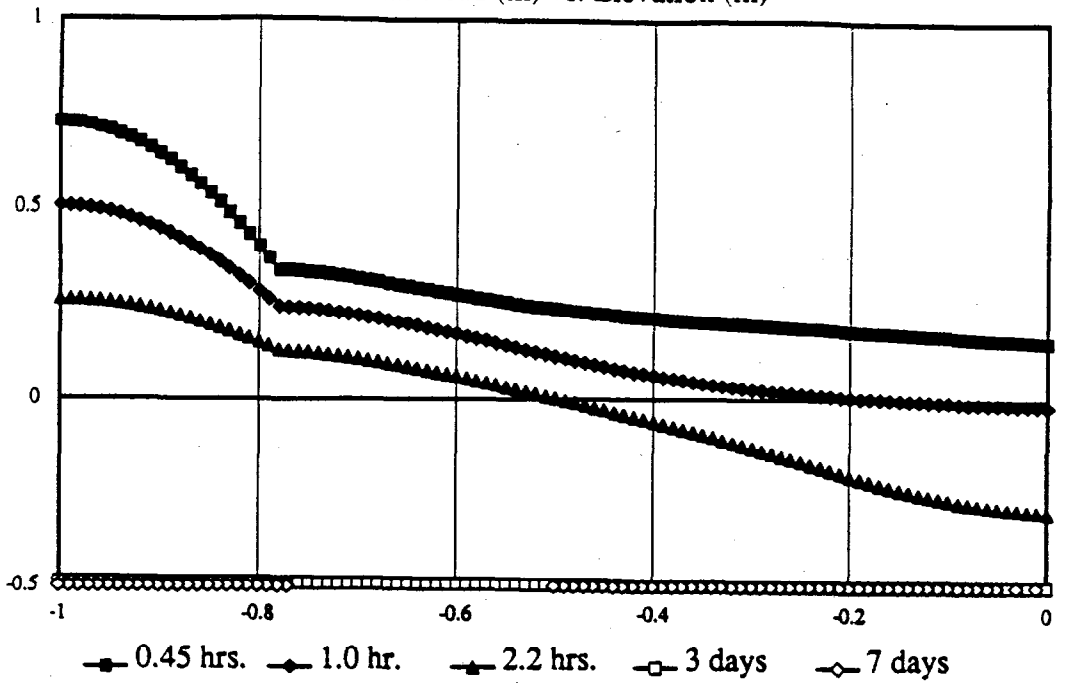

TRIAL 8-10A / NORANDA

Pressure Head (m) vs. Elevation (m)

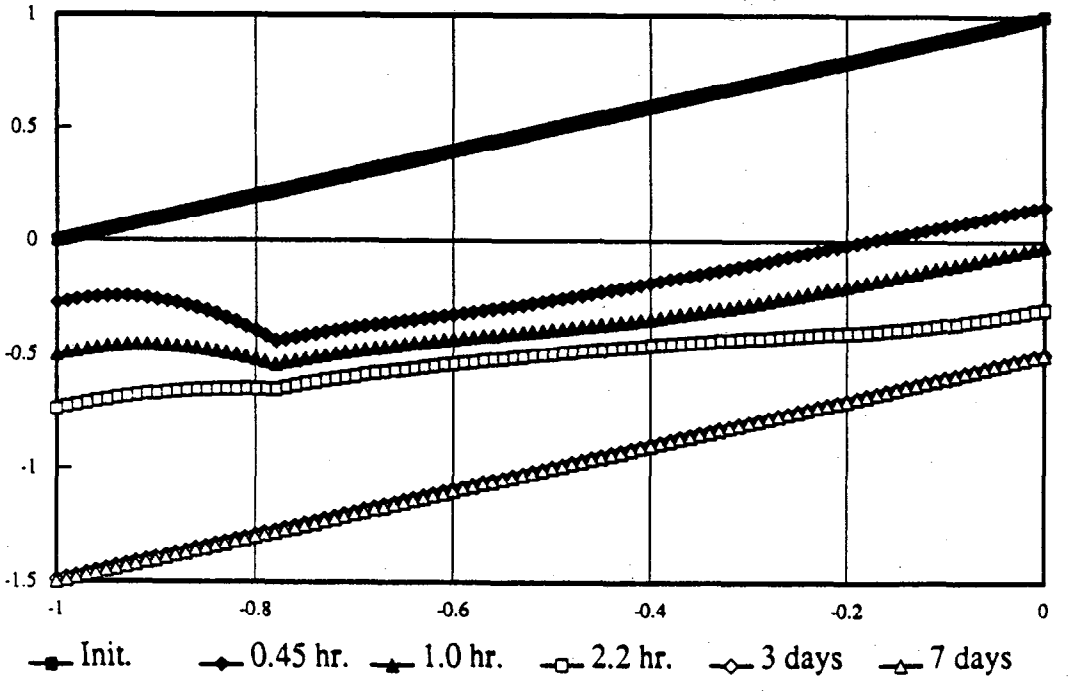

TRIAL 8-10B / NORANDA

Total Head (m) vs. Elevation (m)

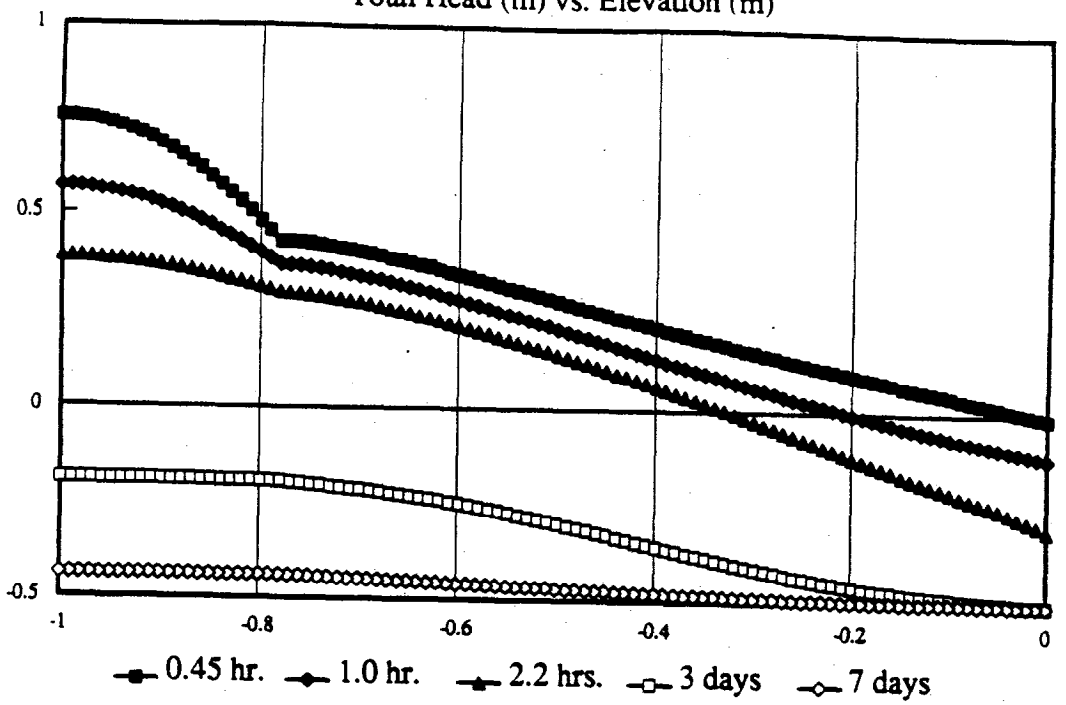

TRIAL 8-10B / NORANDA

Pressure Head (m) vs. Elevation (m)

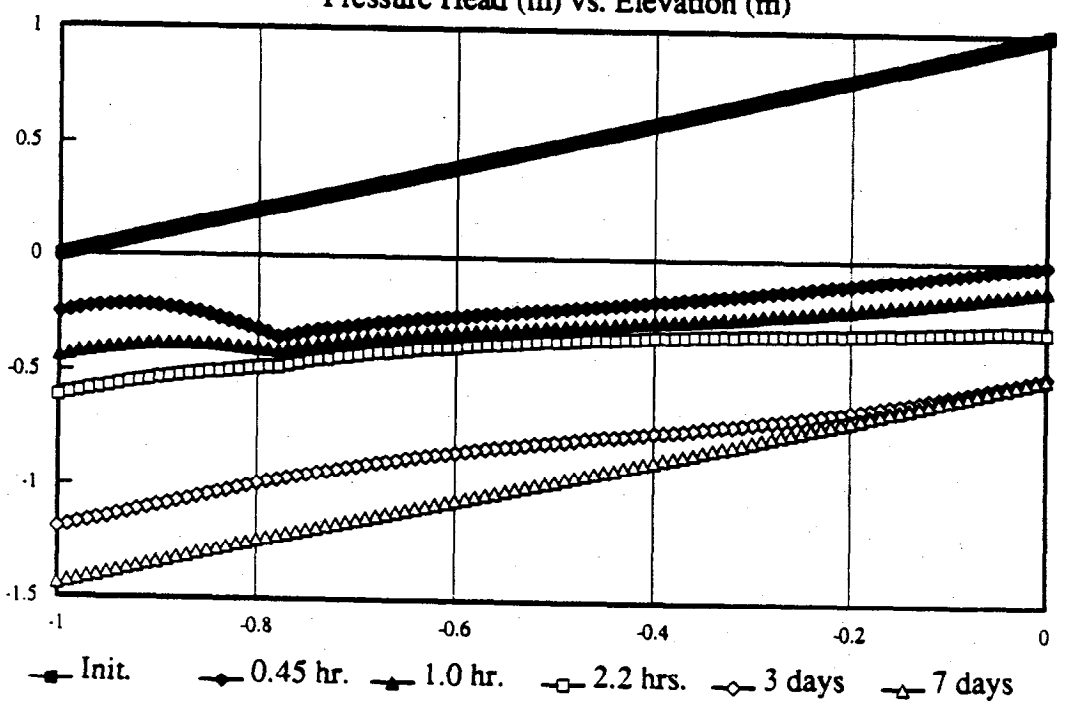

TRIAL 8-10C / NORANDA

Total Head (m) vs. Elevation (m)

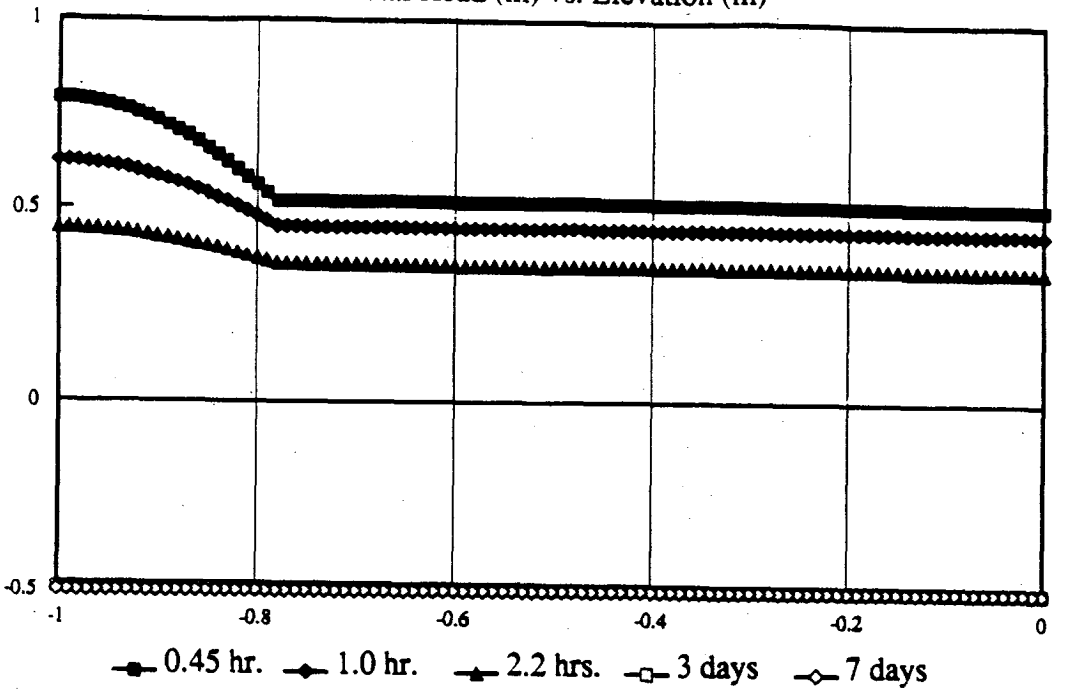

TRIAL 8-10C / NORANDA

Pressure Head (m) vs. Elevation (m)

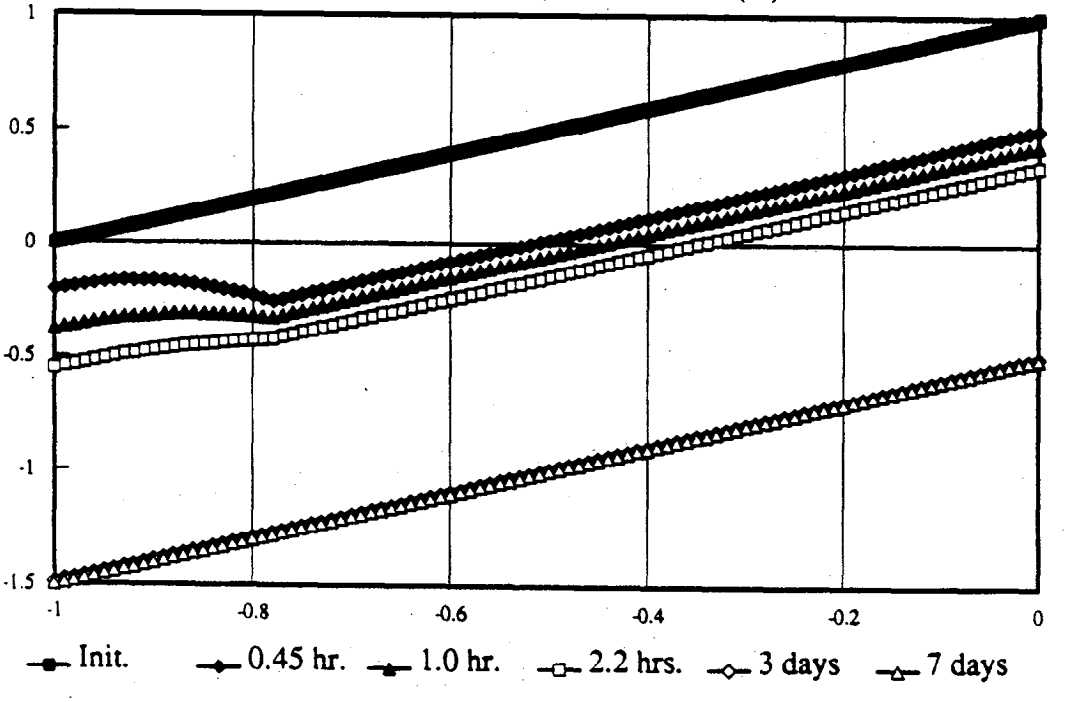

TRIAL 8-10D / NORANDA

Total Head (m) vs. Elevation (m)

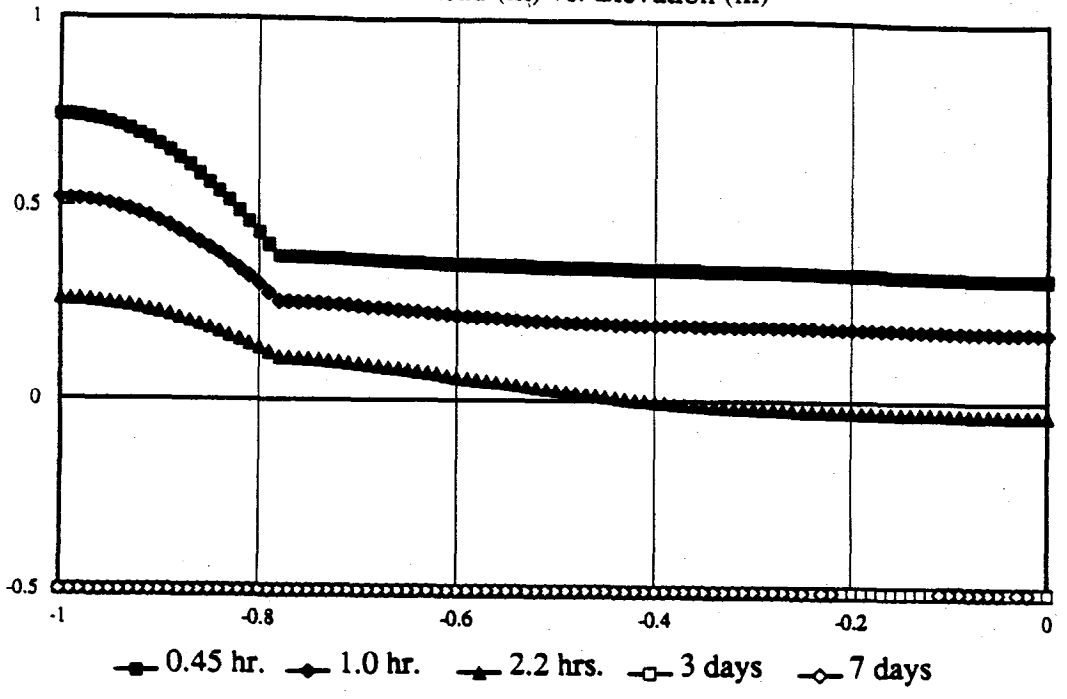

TRIAL 8-10D / NORANDA

Pressure Head (m) vs. Elevation (m)

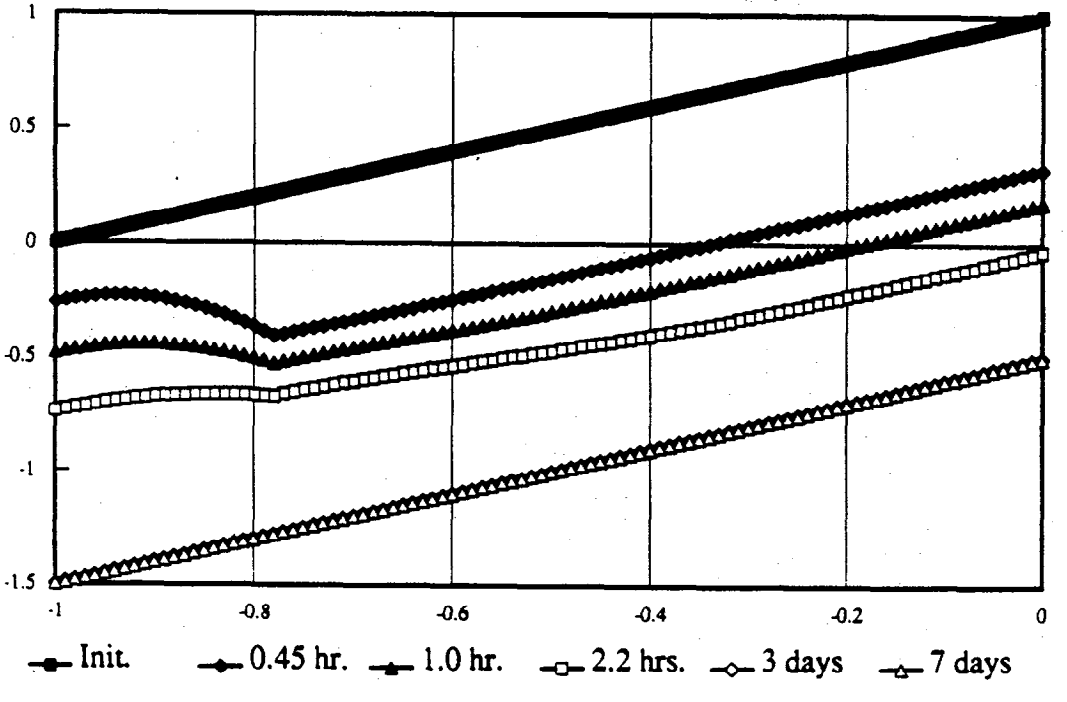

TRIAL 8-10E / NORANDA

Total Head (m) vs. Elevation (m)

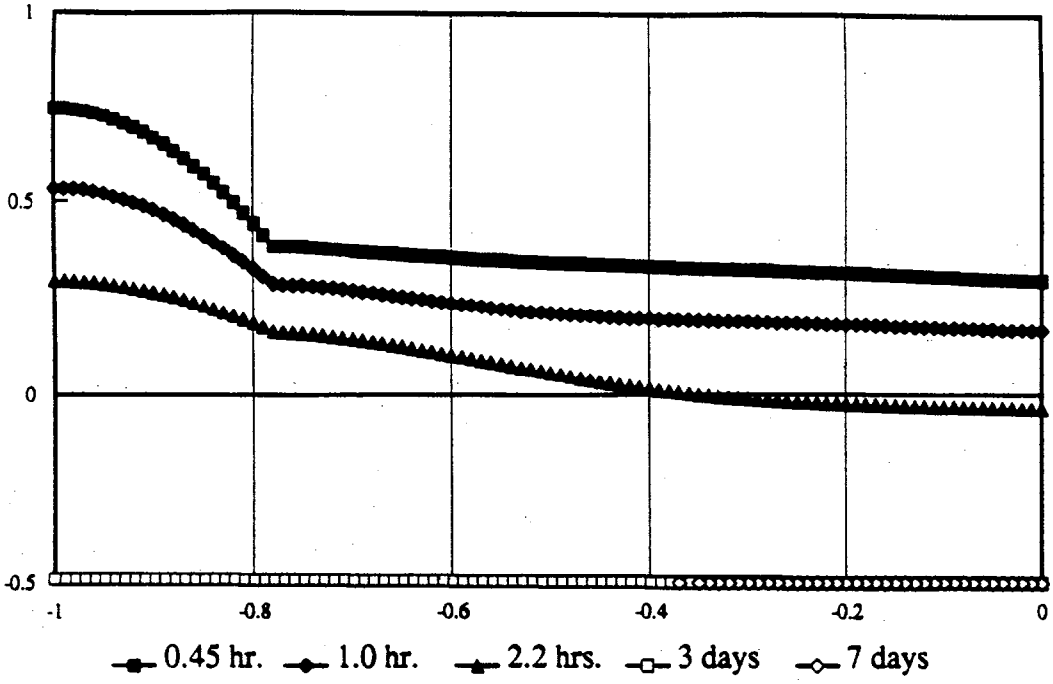

TRIAL 8-10E / NORANDA

Pressure Head (m) vs. Elevation (m)

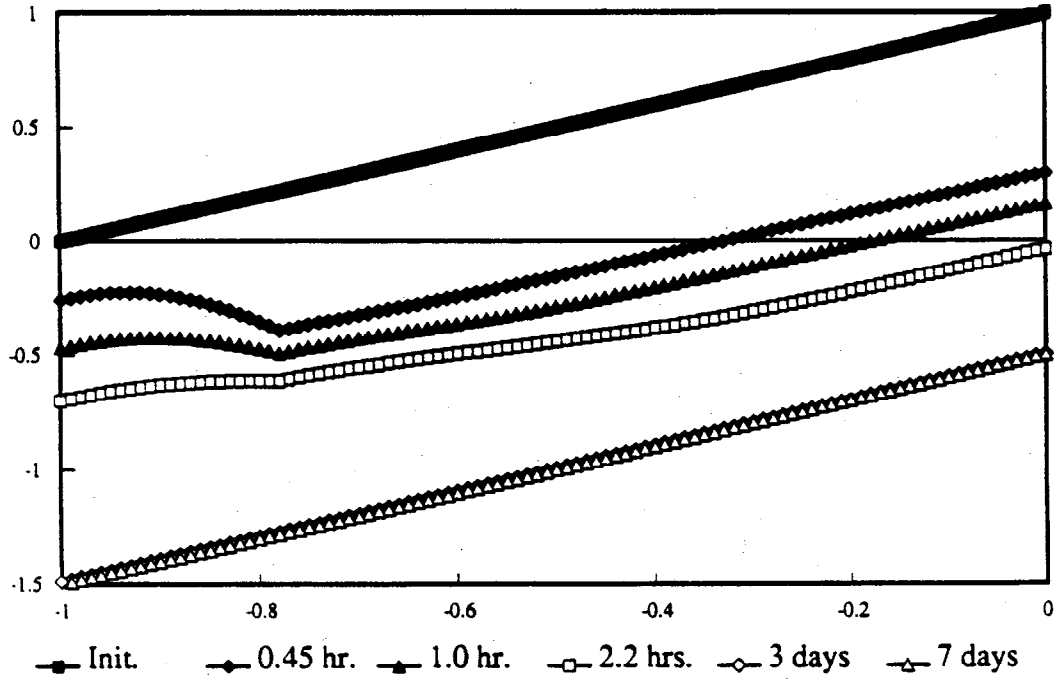

TRIAL 8-10F / NORANDA

Total Head (m) vs. Elevation (m)

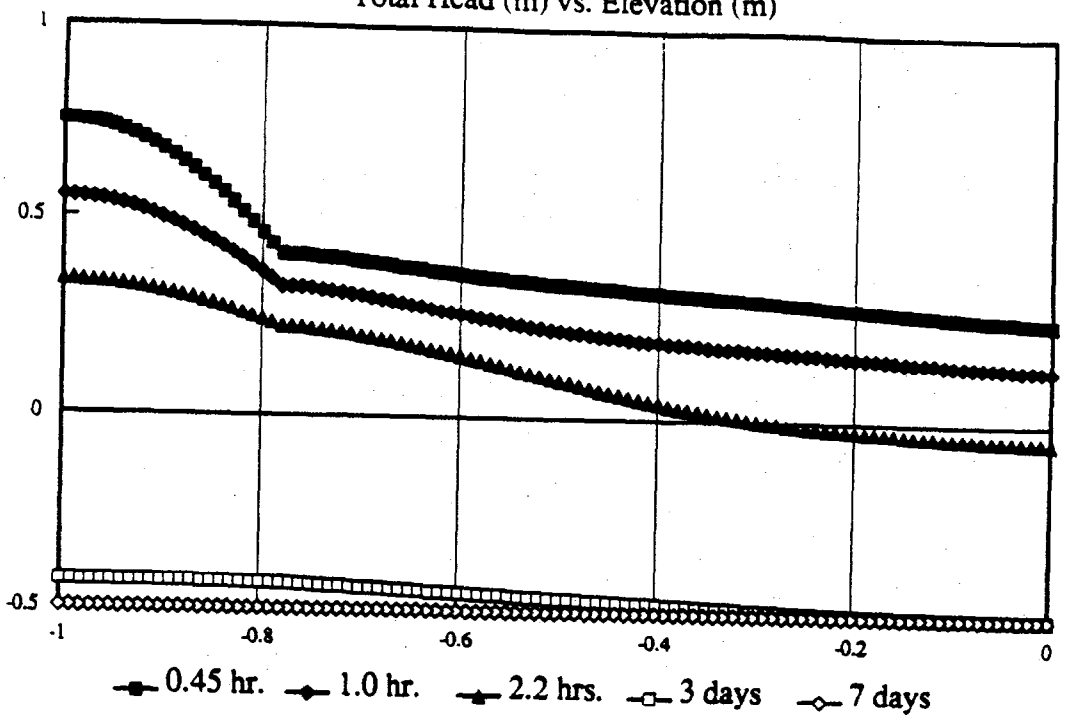

TRIAL 8-10F / NORANDA

Pressure Head (m) vs. Elevation (m)

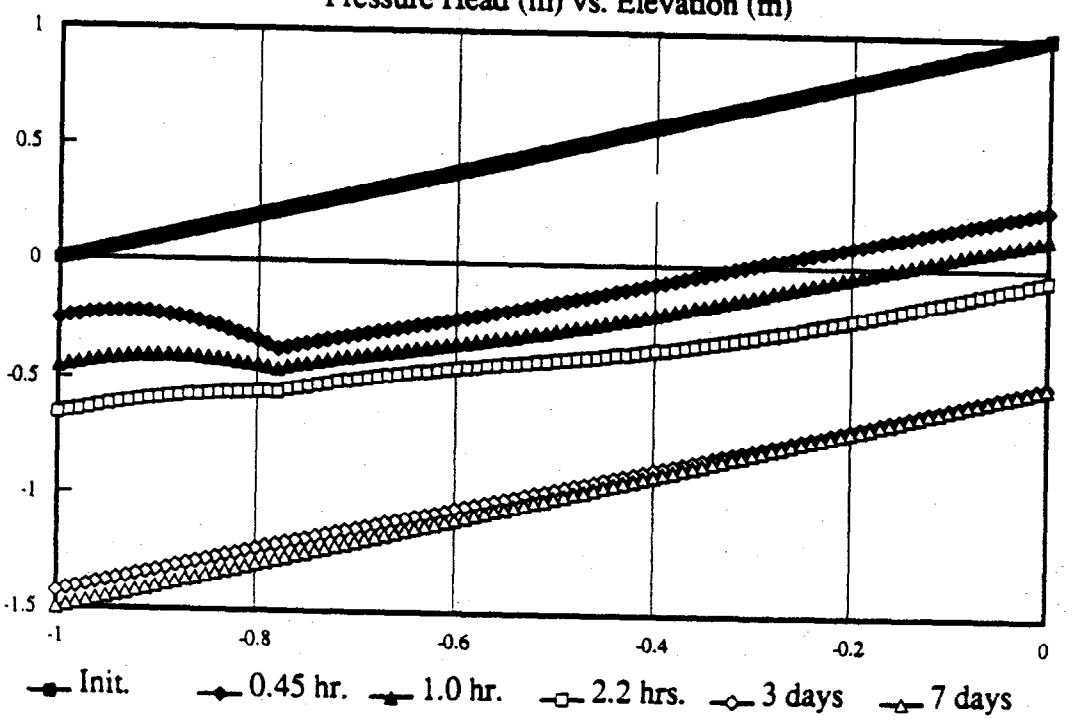

TRIAL 8-10G / NORANDA

Total Head (m) vs. Elevation (m)

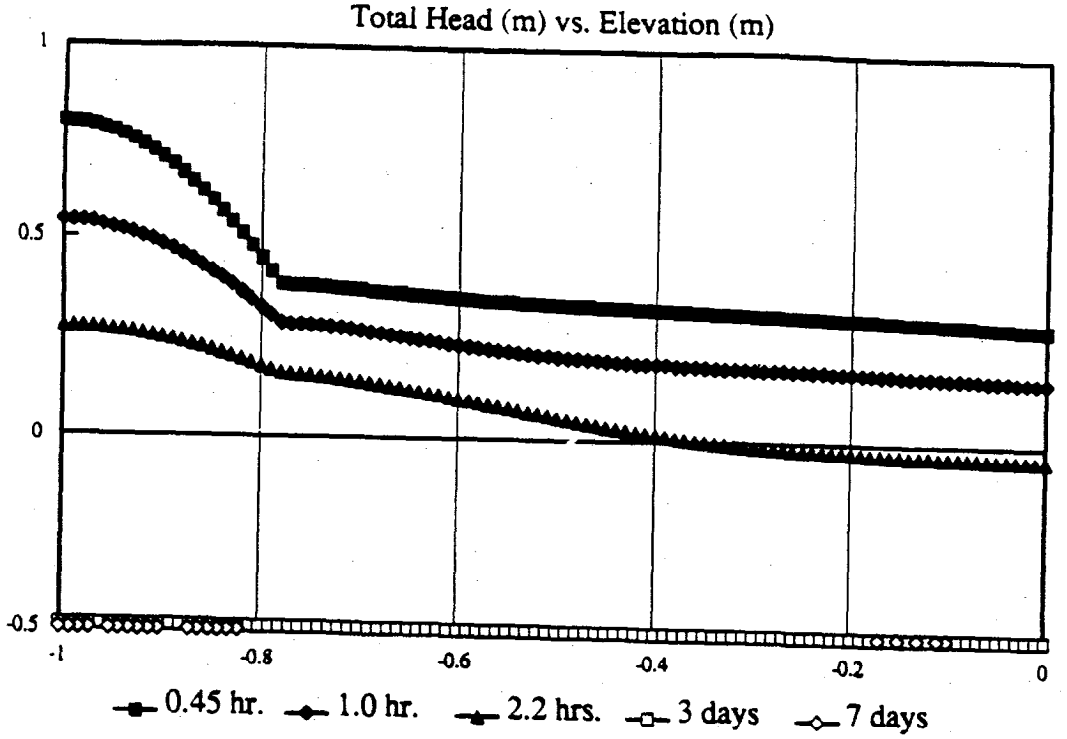

TRIAL 8-10G / NORANDA

Pressure Head (m) vs. Elevation (m)

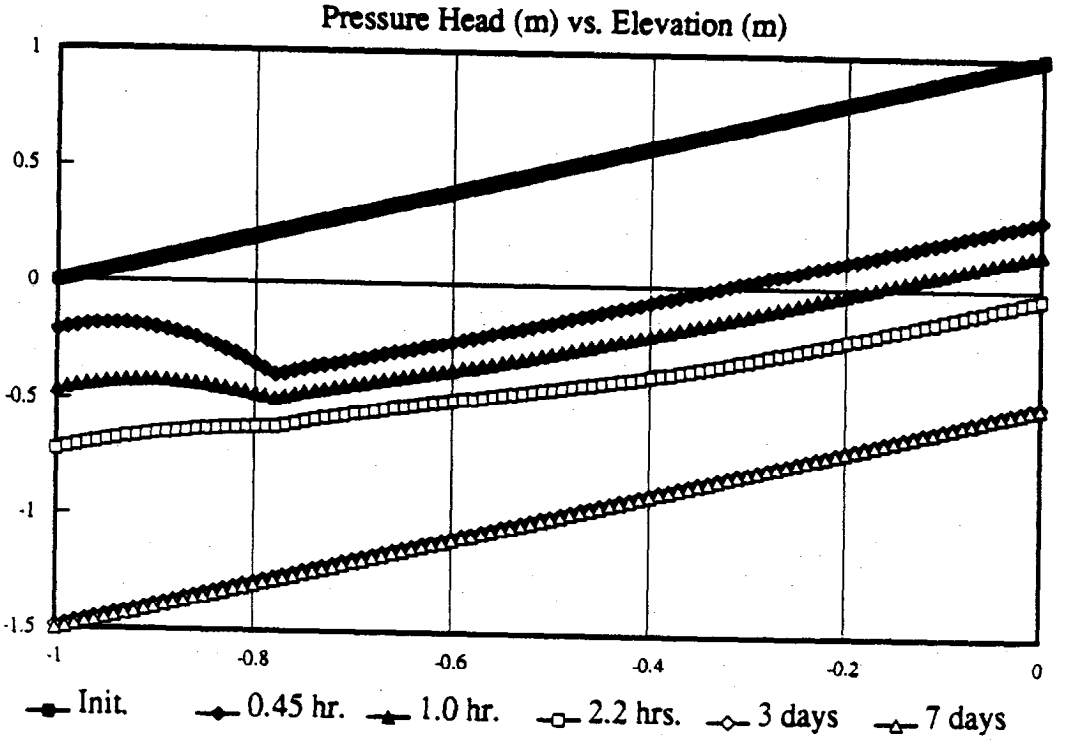

TRIAL 8-10H / NORANDA

Total Head (m) vs. Elevation (m)

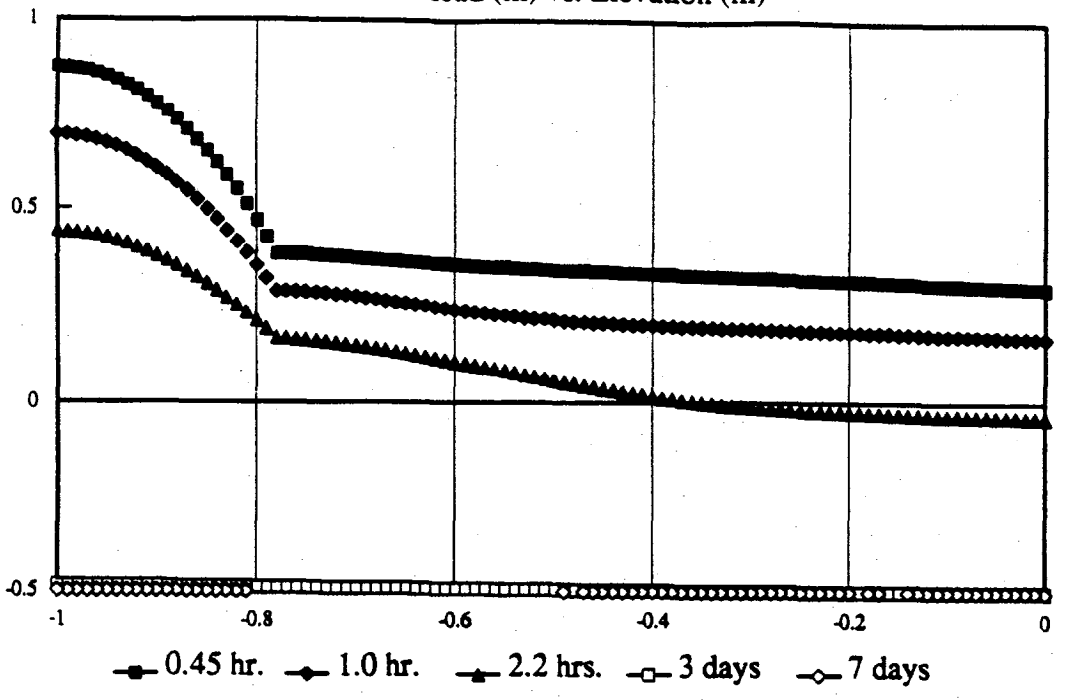

TRIAL 8-10H / NORANDA

(PRESSURE HEAD VS ELEV.)

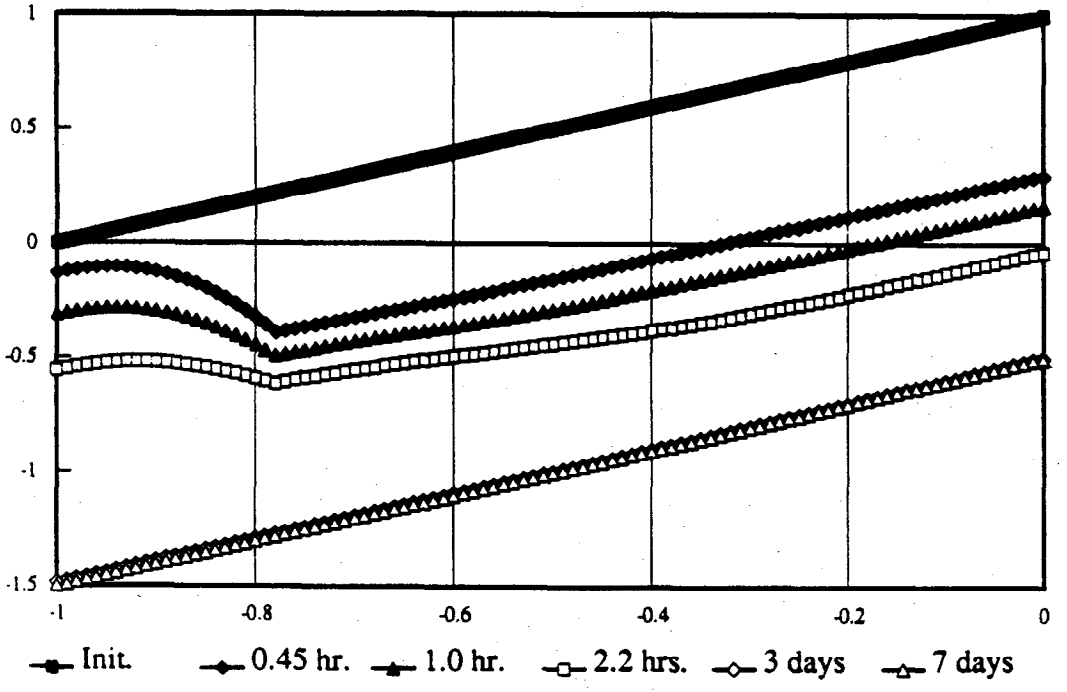

TRIAL 8-10I / NORANDA

Total Head (m) vs. Elevation (m)

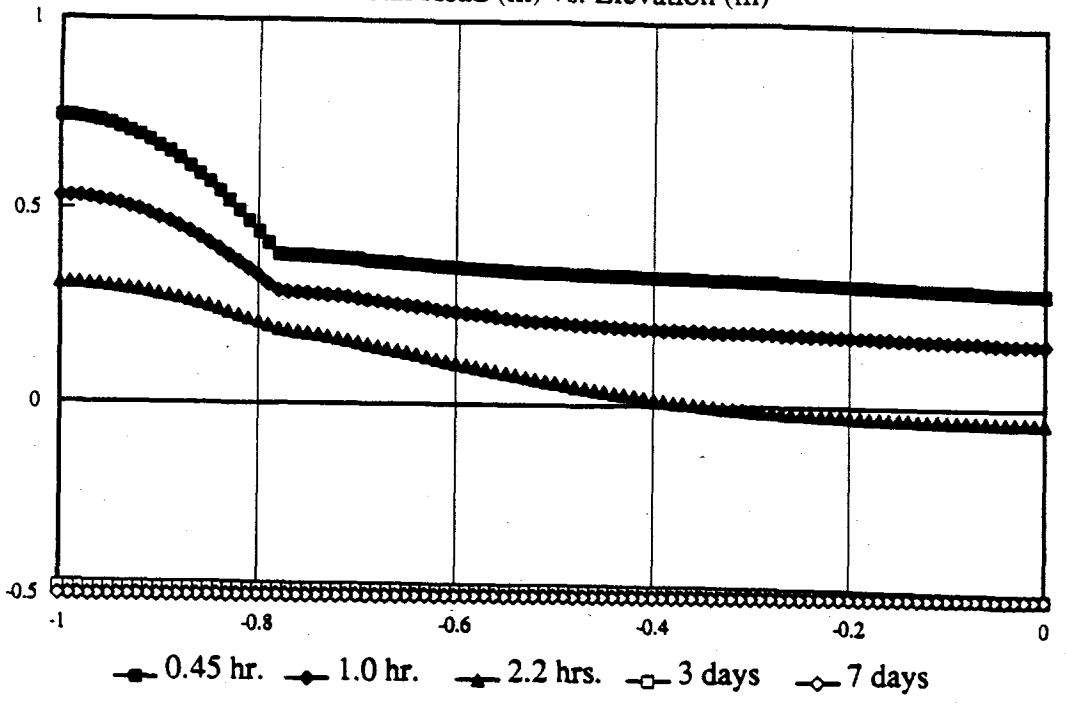

TRIAL 8-10I / NORANDA

Pressure Head (m) vs. Elevation (m)

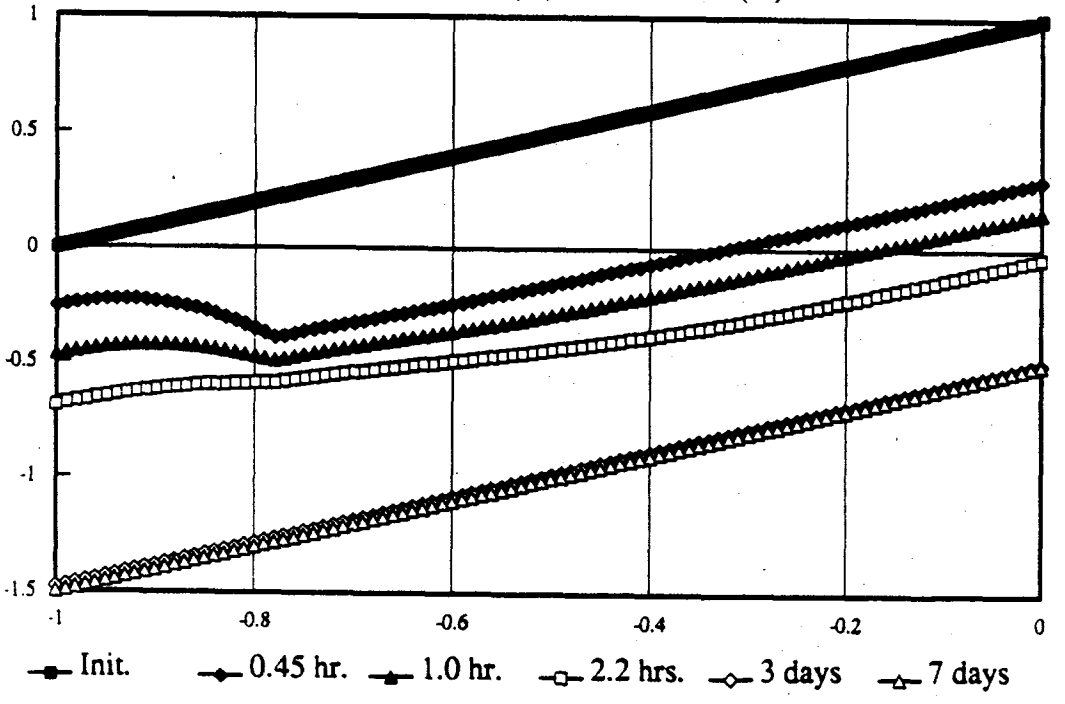

TRIAL 8-10J / NORANDA

Total Head (m) vs. Elevation (m)

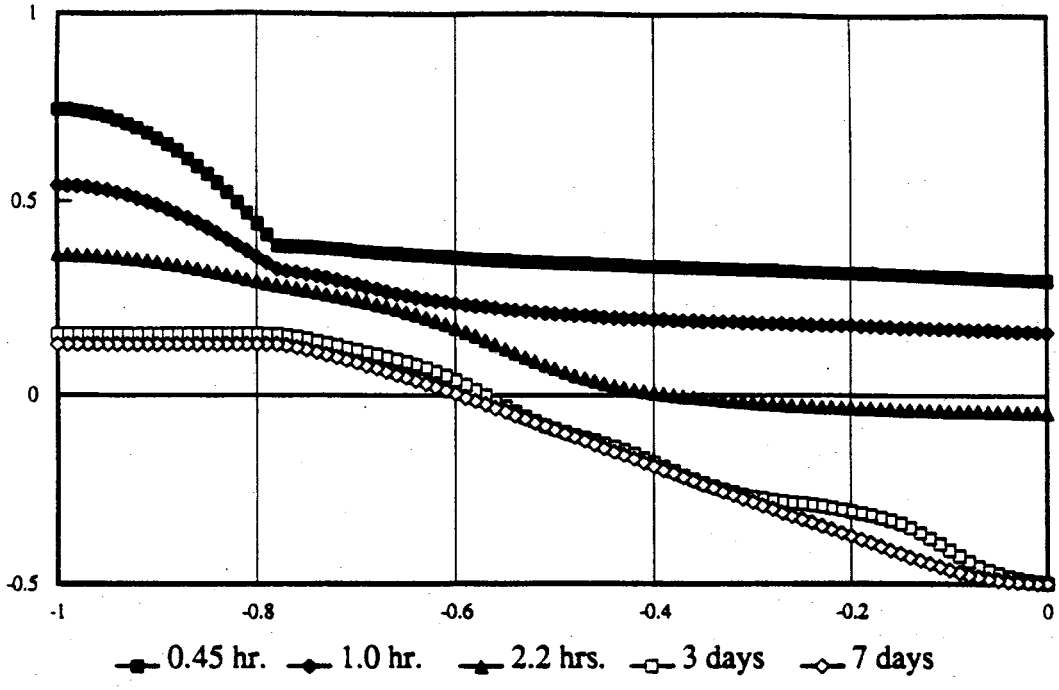

TRIAL 8-10J / NORANDA

Pressure Head (m) vs. Elevation (m)

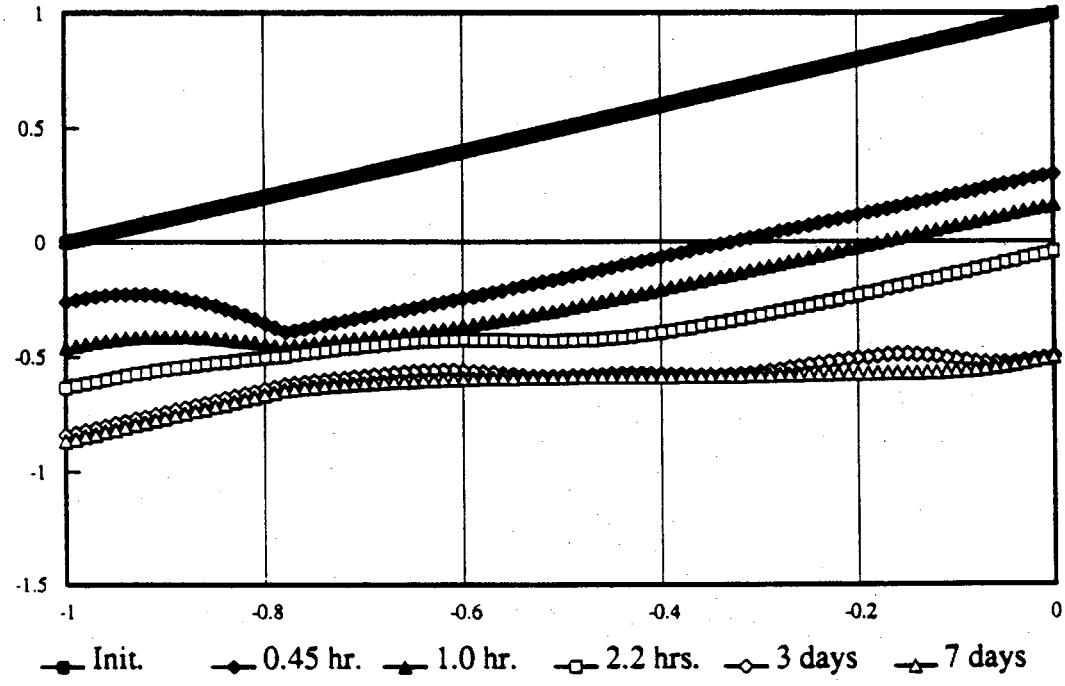

TRIAL 8-10K / NORANDA

Total Head (m) vs. Elevation (m)

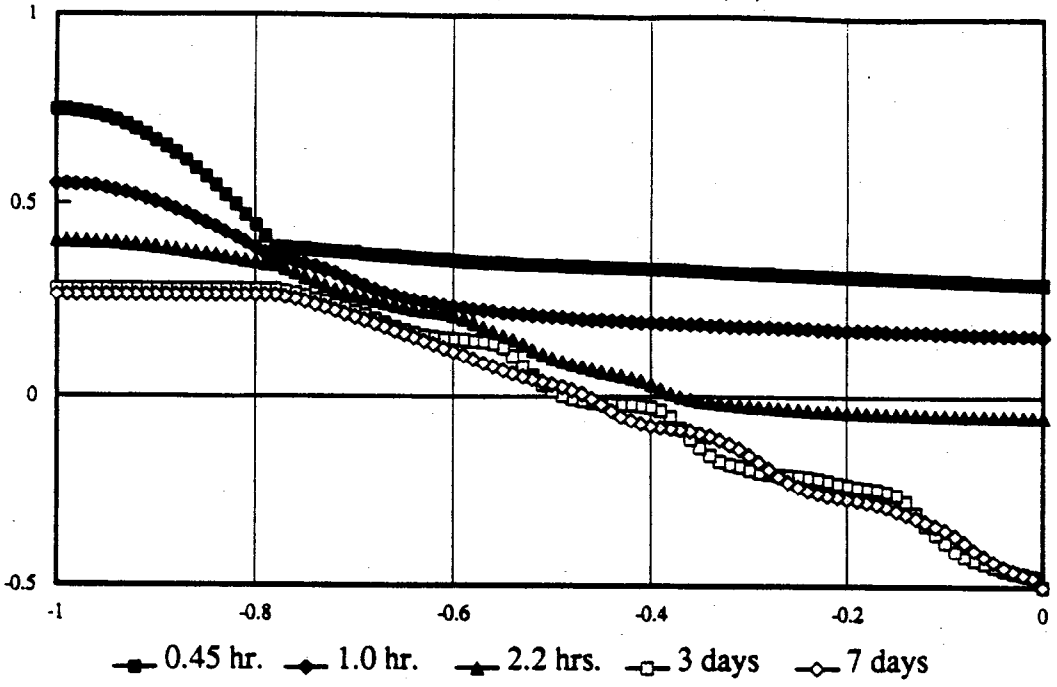

TRIAL 8-10K / NORANDA

Pressure Head (m) vs. Elevation (m)

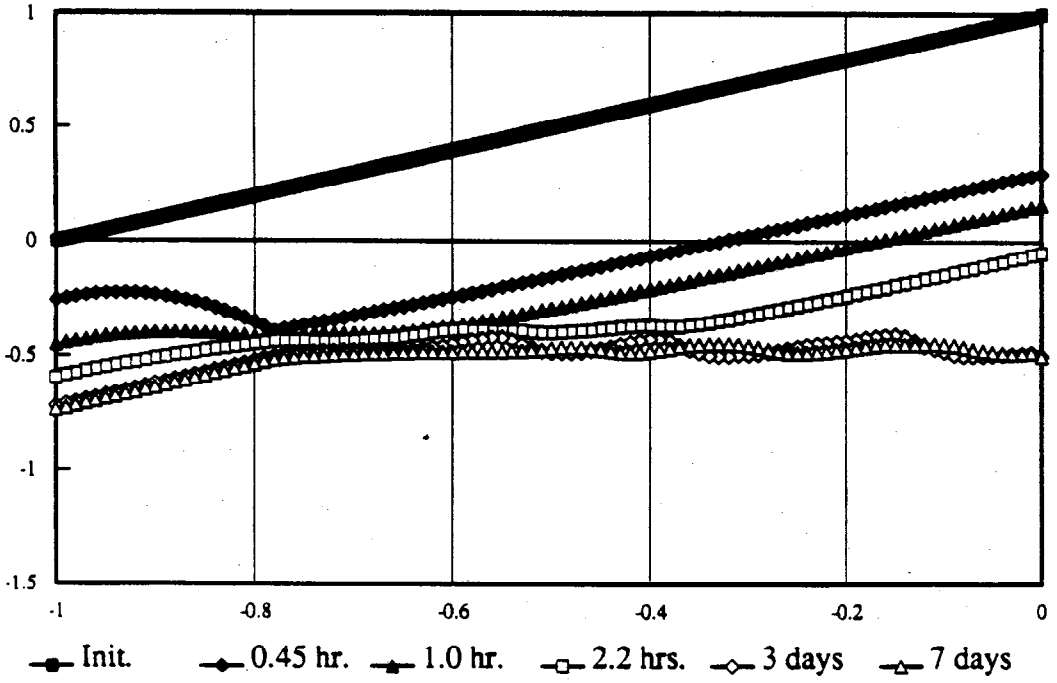

TRIAL 8-10L / NORANDA

Total Head (m) vs. Elevation (m)

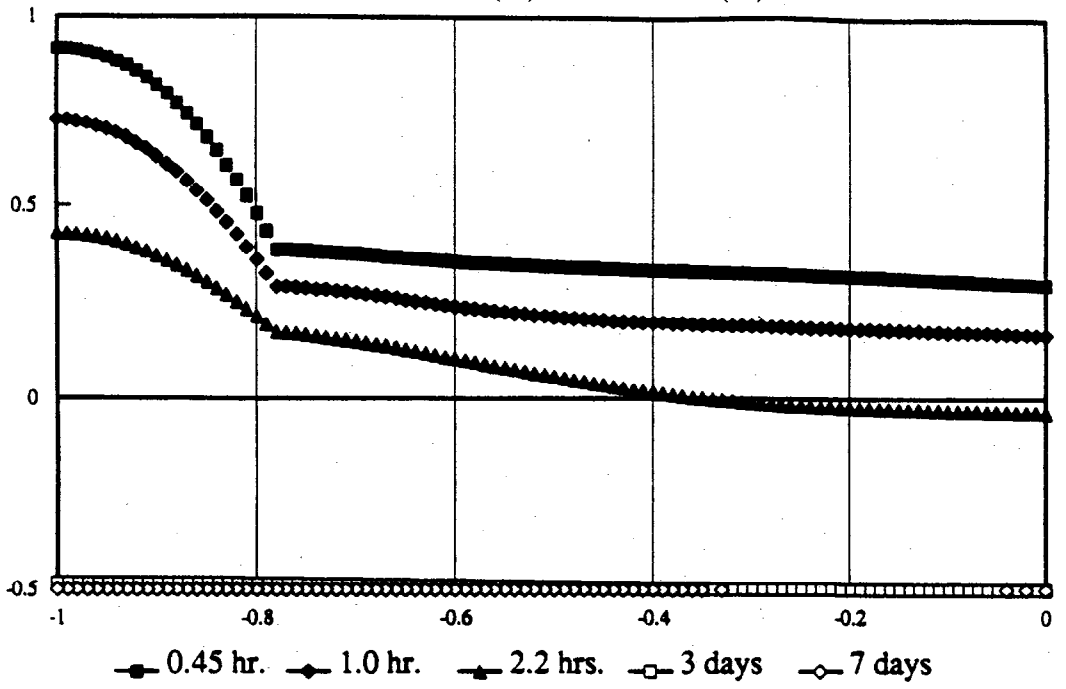

TRIAL 8-10L / NORANDA

Pressure Head (m) vs. Elevation (m)

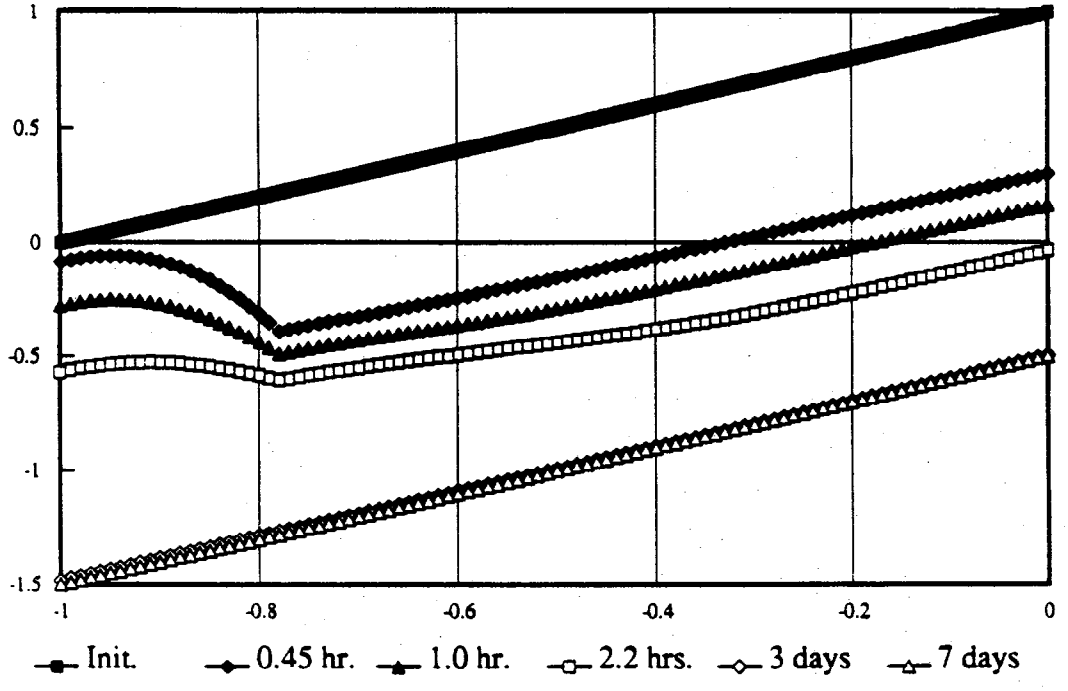

TRIAL 8-10M / NORANDA

Total Head (m) vs. Elevation (m)

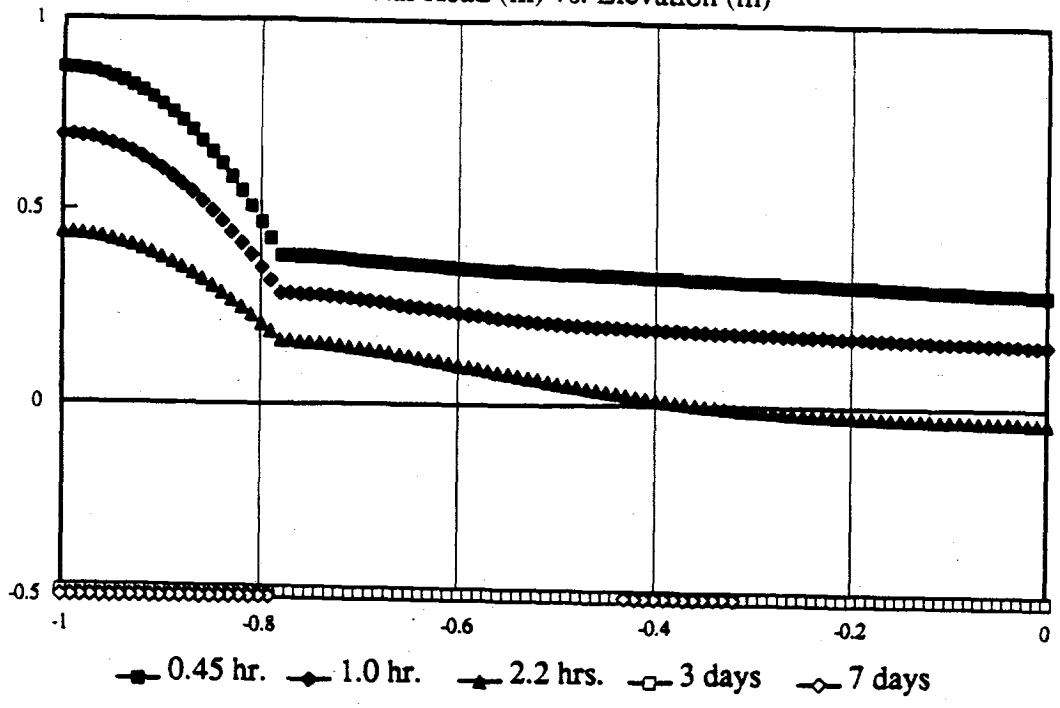

TRIAL 8-10M / NORANDA

Pressure Head (m) vs. Elevation (m)

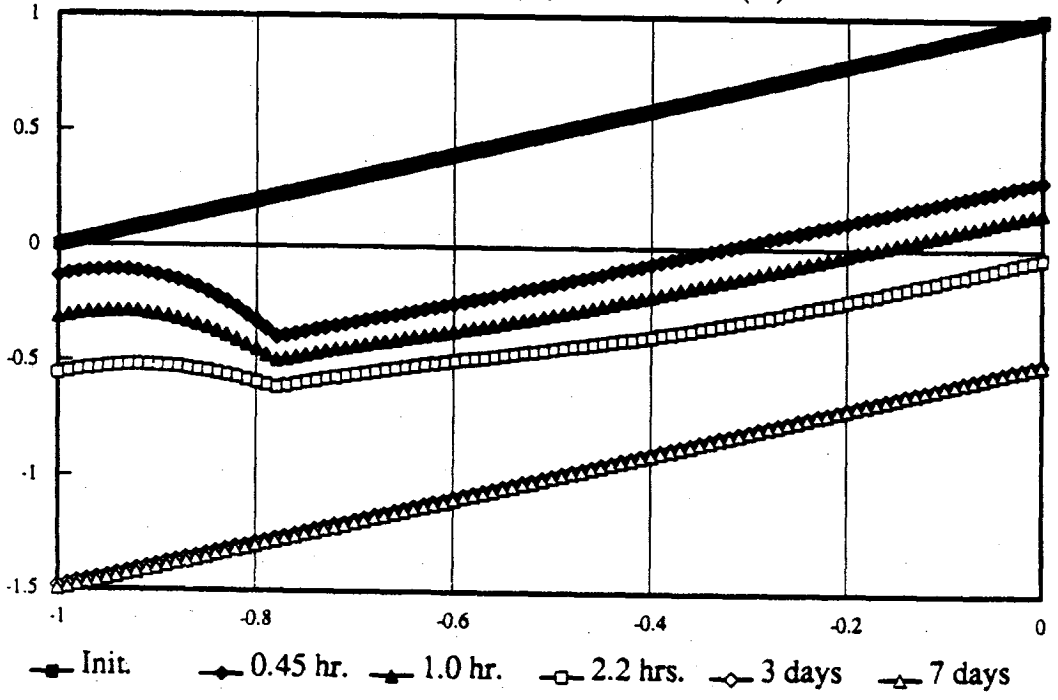

TRIAL 8-10N / NORANDA

Total Head (m) vs. Elevation (m)

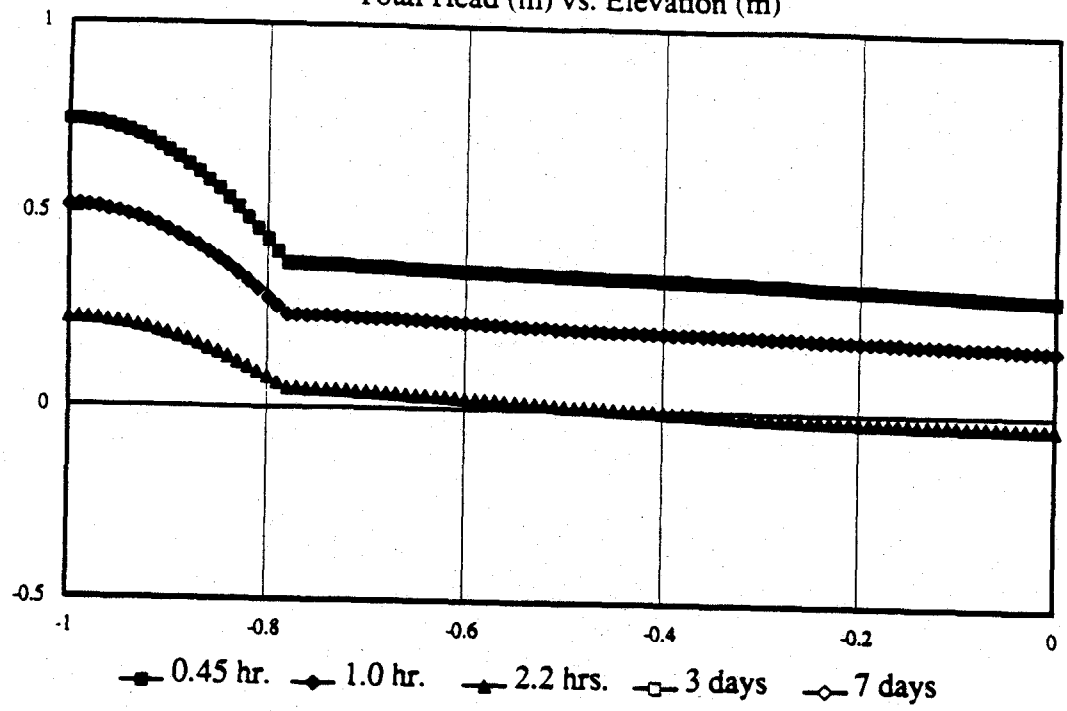

TRIAL 8-10N / NORANDA

Pressure Head (m) vs. Elevation (m)

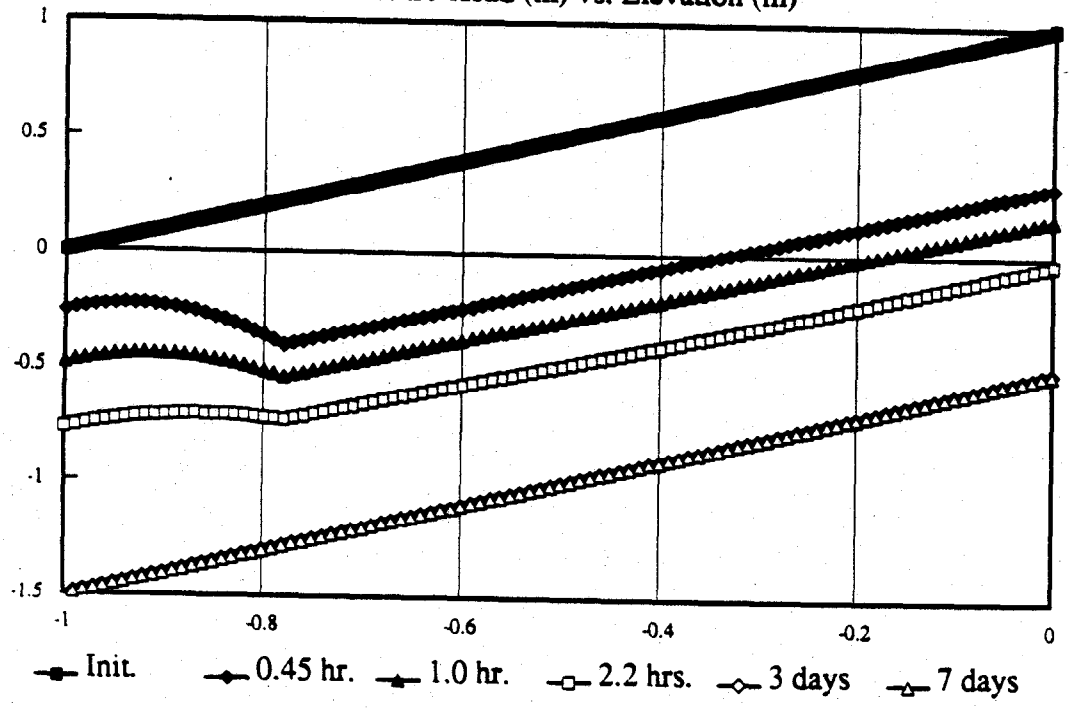

TRIAL 8-10O / NORANDA

Total Head (m) vs. Elevation (m)

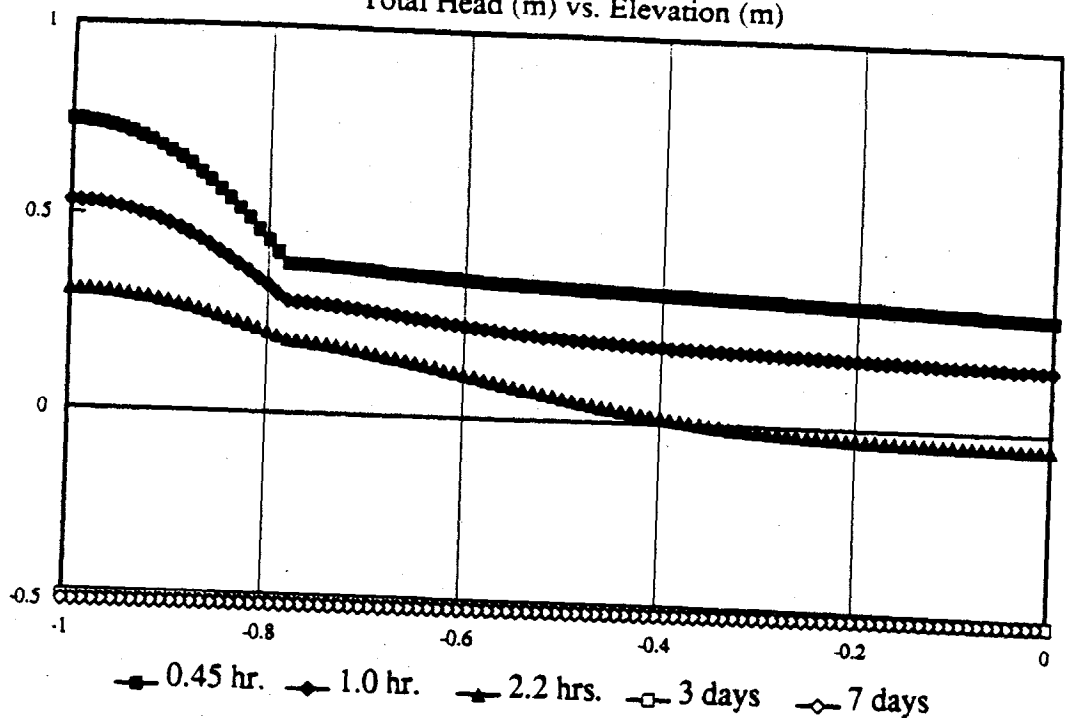

TRIAL 8-10O / NORANDA

Pressure Head (m) vs. Elevation (m)

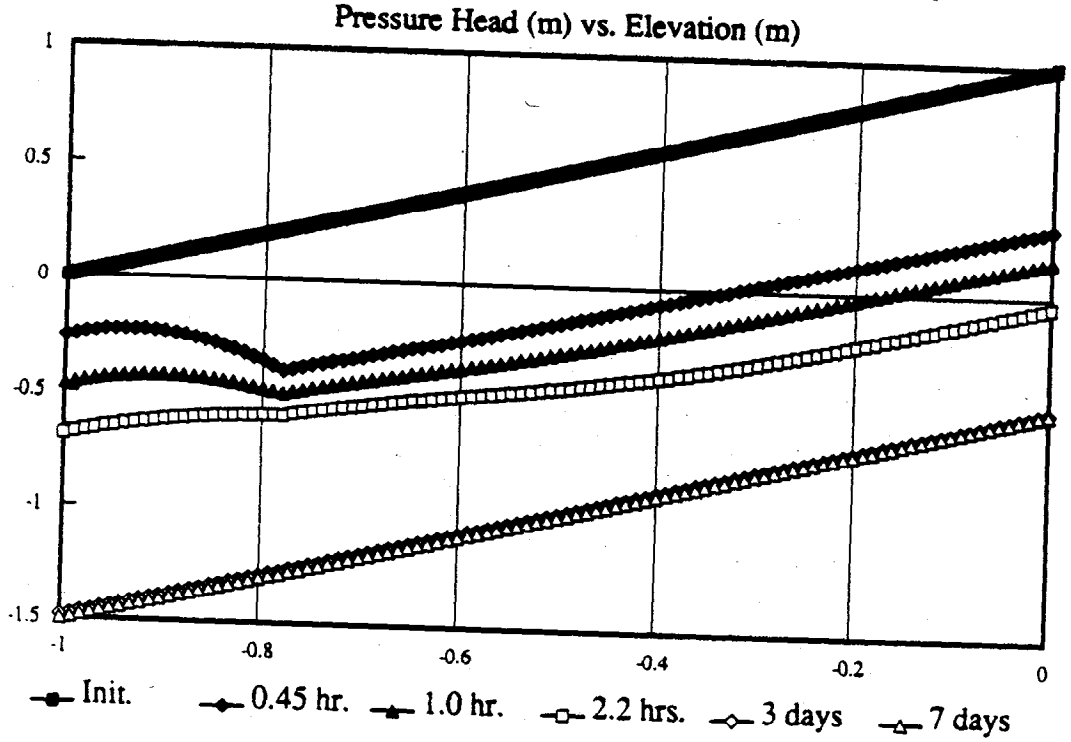

TRIAL 8-10P / NORANDA

Total Head (m) vs. Elevation (m)

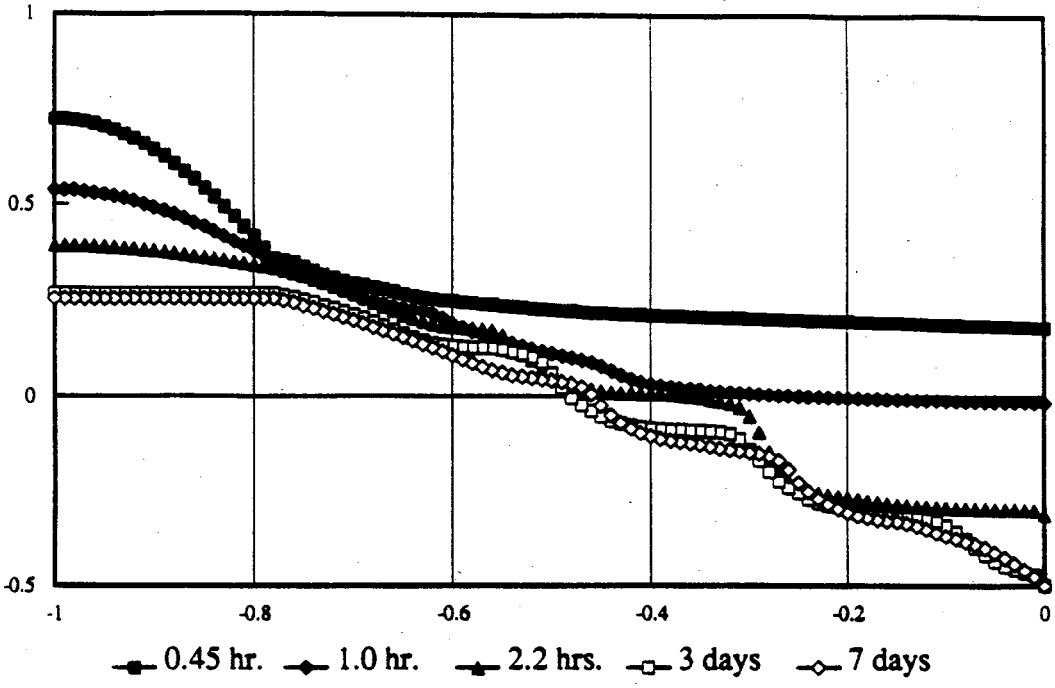

TRIAL 8-10P / NORANDA

Pressure Head (m) vs. Elevation (m)

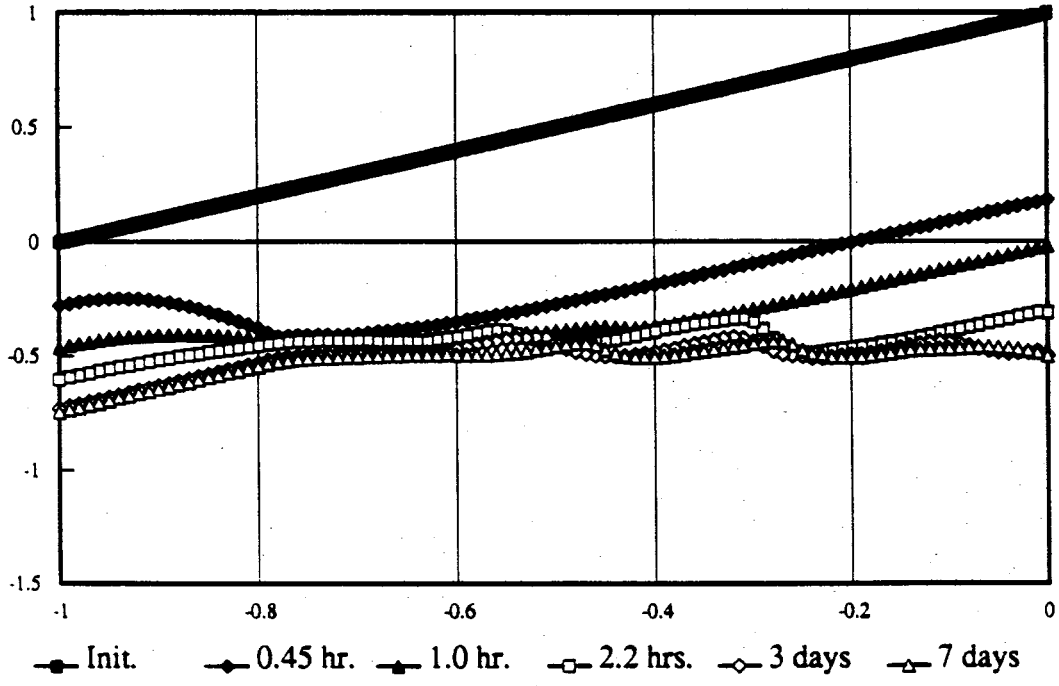

TRIAL 8-10Q / NORANDA

Total Head (m) vs. Elevation (m)

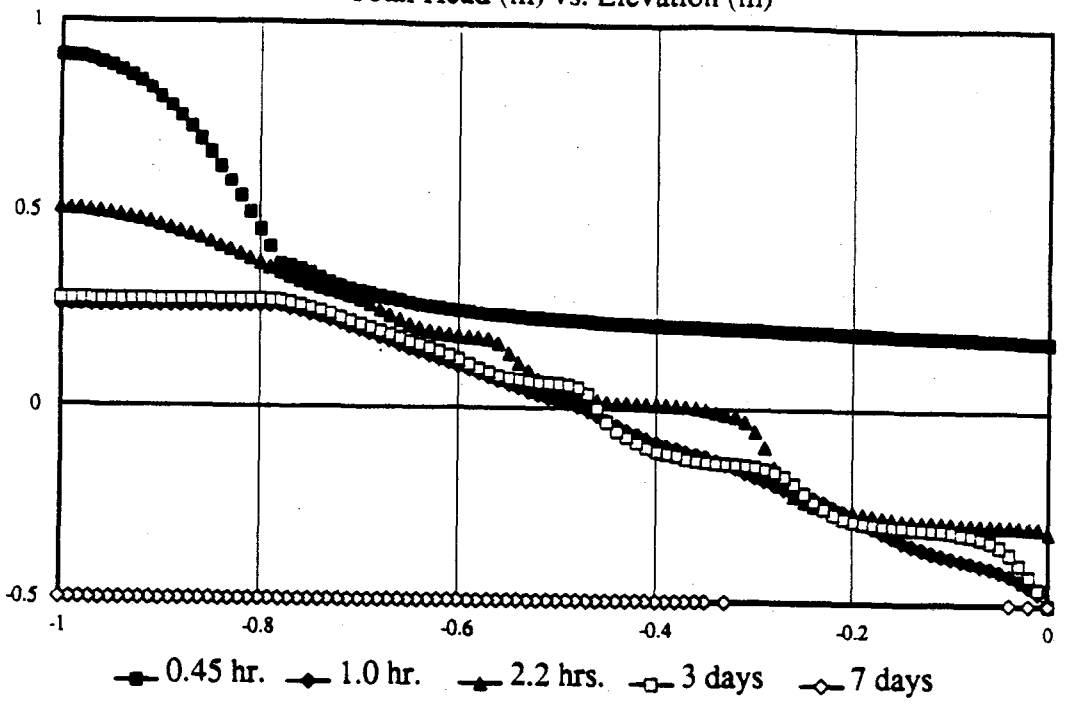

TRIAL 8-10Q / NORANDA

Pressure Head (m) vs. Elevation (m)

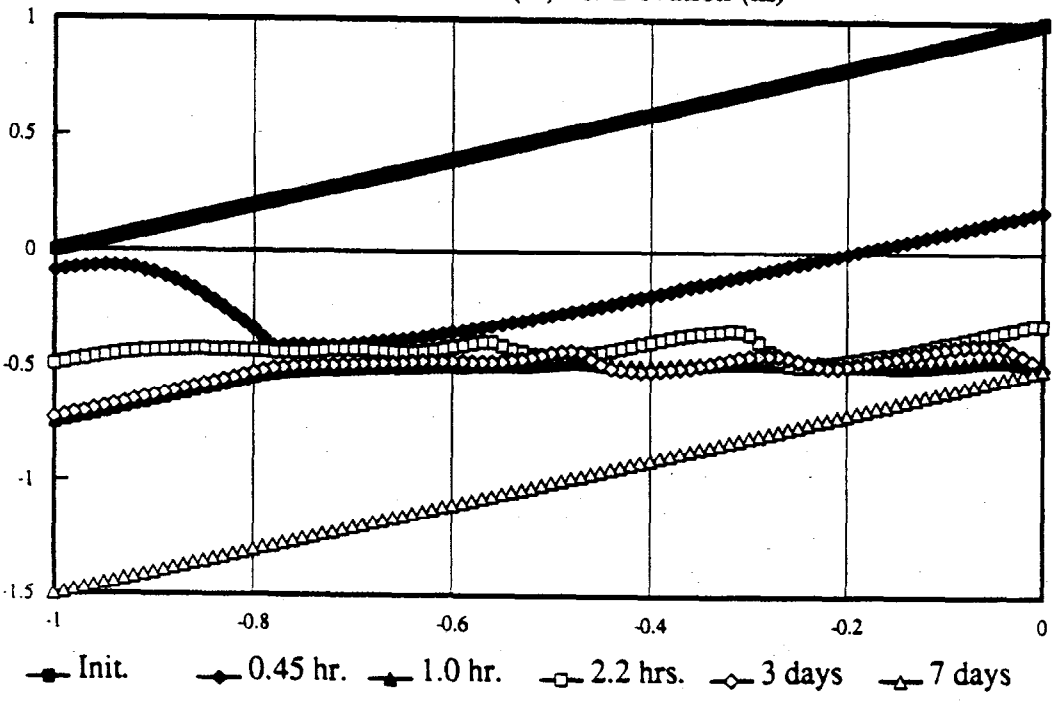

TRIAL 8-10R / NORANDA

Total Head (m) vs. Elevation (m)

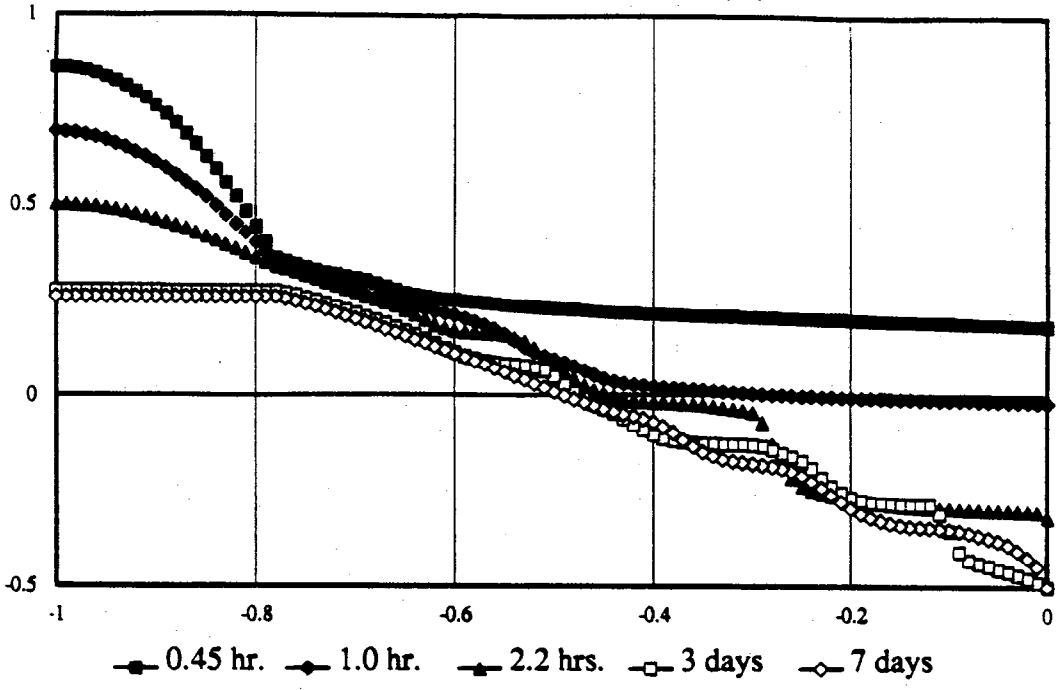

TRIAL 8-10R / NORANDA

Pressure Head (m) vs. Elevation (m)

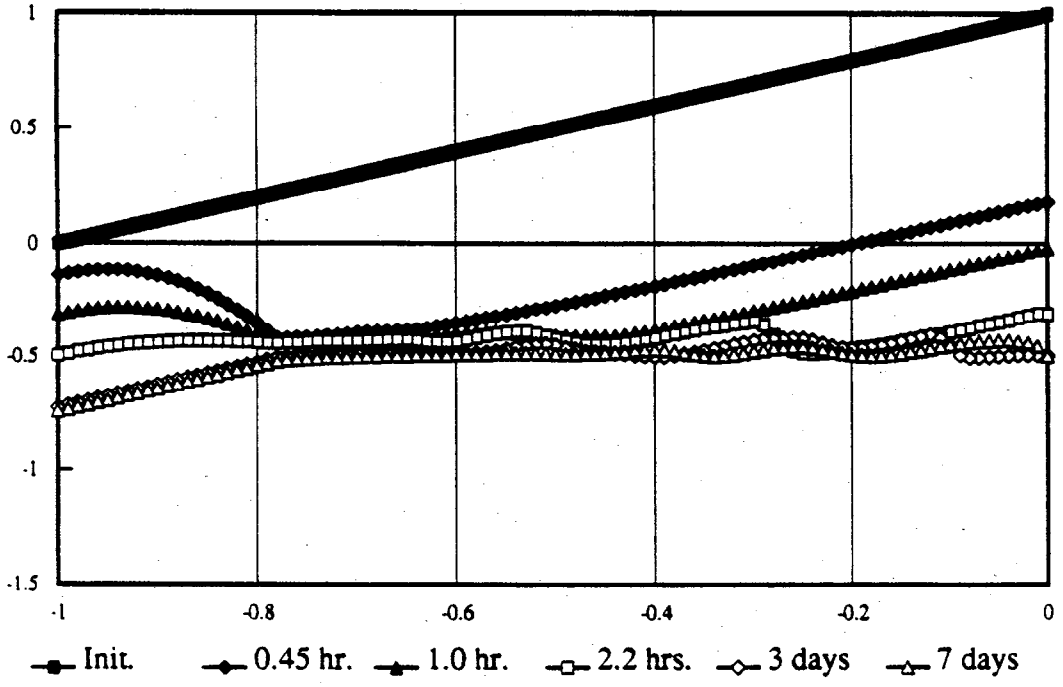

TRIAL 8-10S / NORANDA

Total Head (m) vs. Elevation (m)

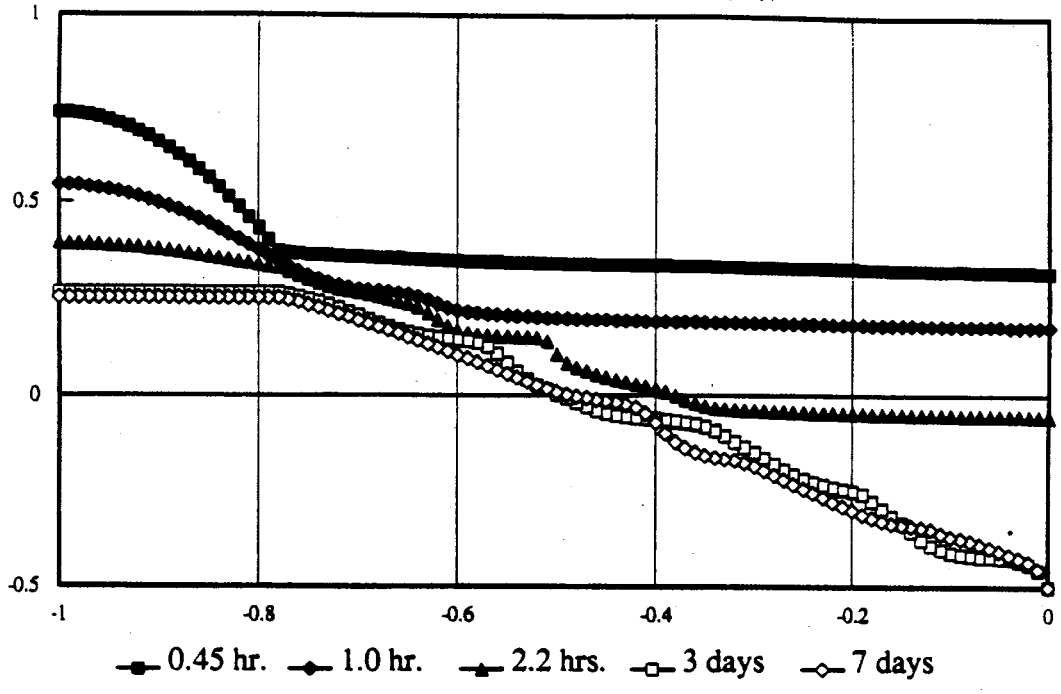

TRIAL 8-10S / NORANDA

Pressure Head (m) vs. Elevation (m)

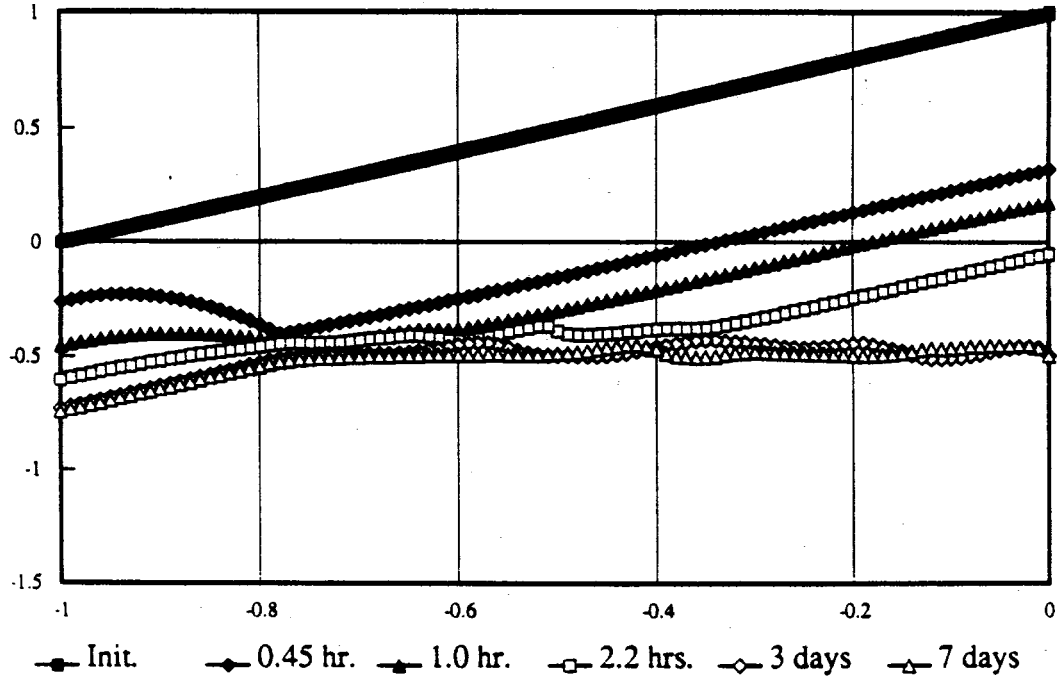

TRIAL 8-10T / NORANDA

Total Head (m) vs. Elevation (m)

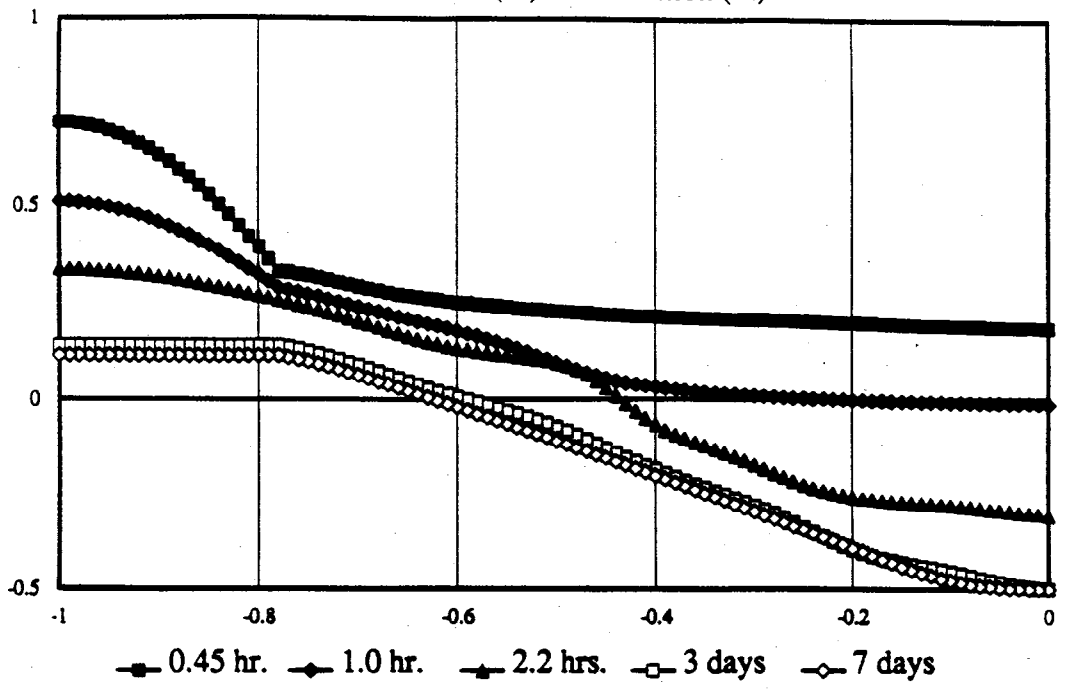

TRIAL 8-10T / NORANDA

Pressure Head (m) vs. Elevation (m)

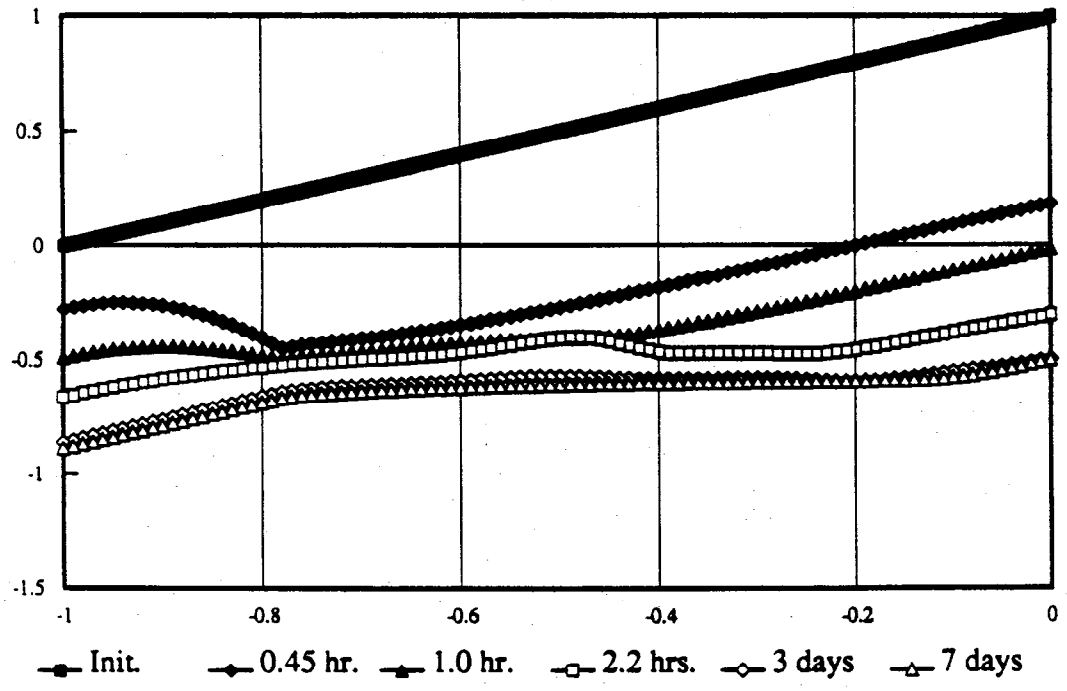

TRIAL 8-10U / NORANDA

Total Head (m) vs. Elevation (m)

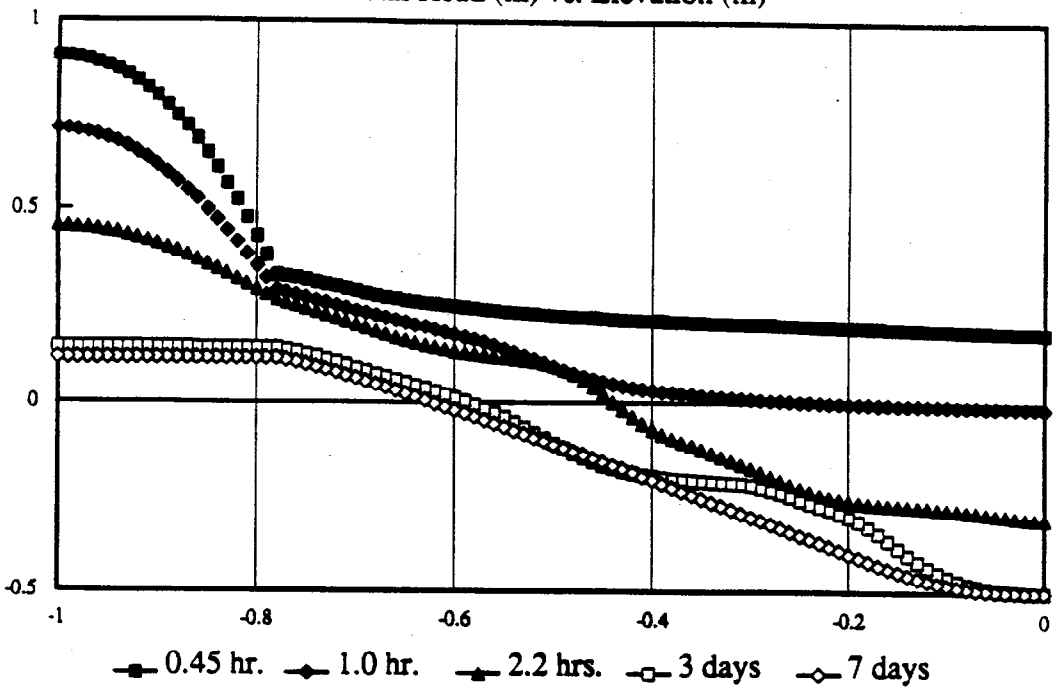

TRIAL 8-10U / NORANDA

Pressure Head (m) vs. Elevation (m)

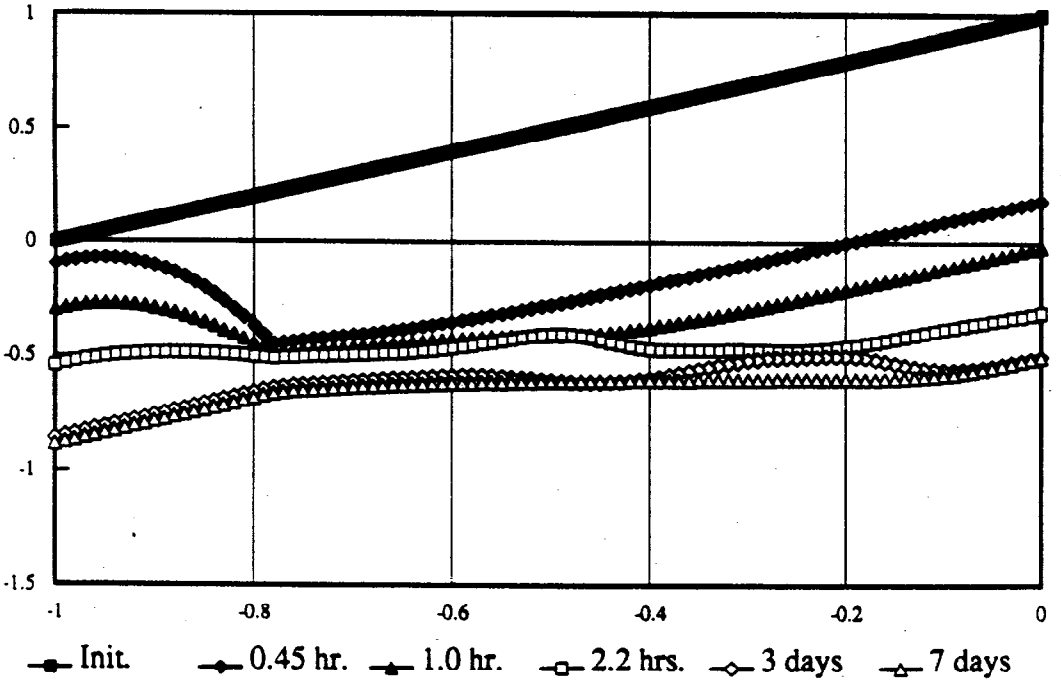

TRIAL 8-10V / NORANDA

Total Head (m) vs. Elevation (m)

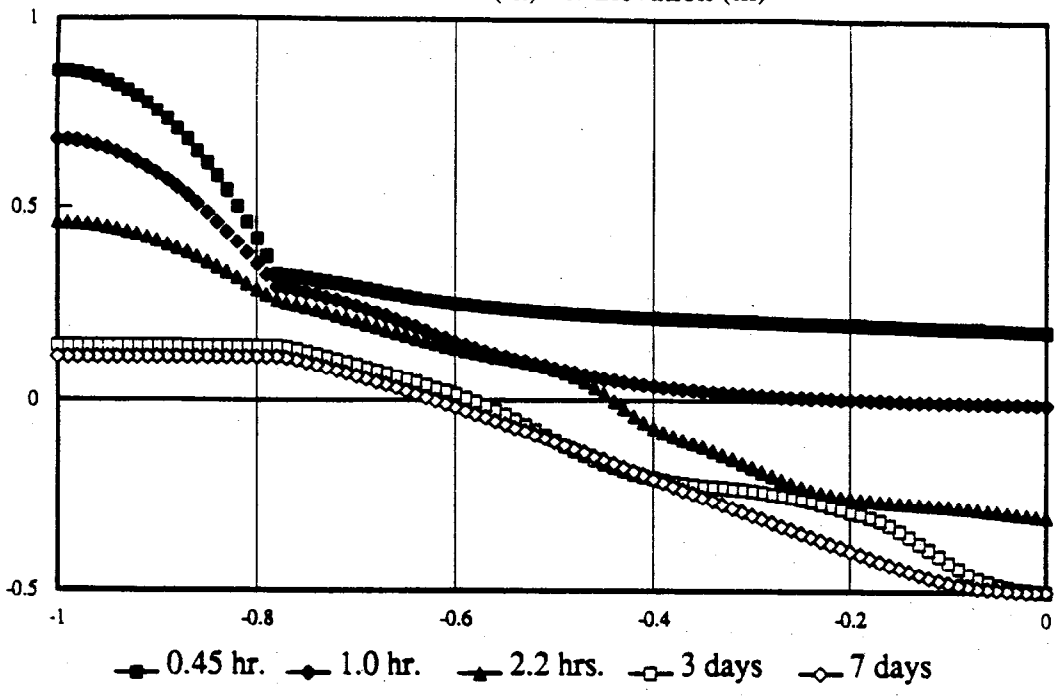

TRIAL 8-10V / NORANDA

Pressure Head (m) vs. Elevation (m)

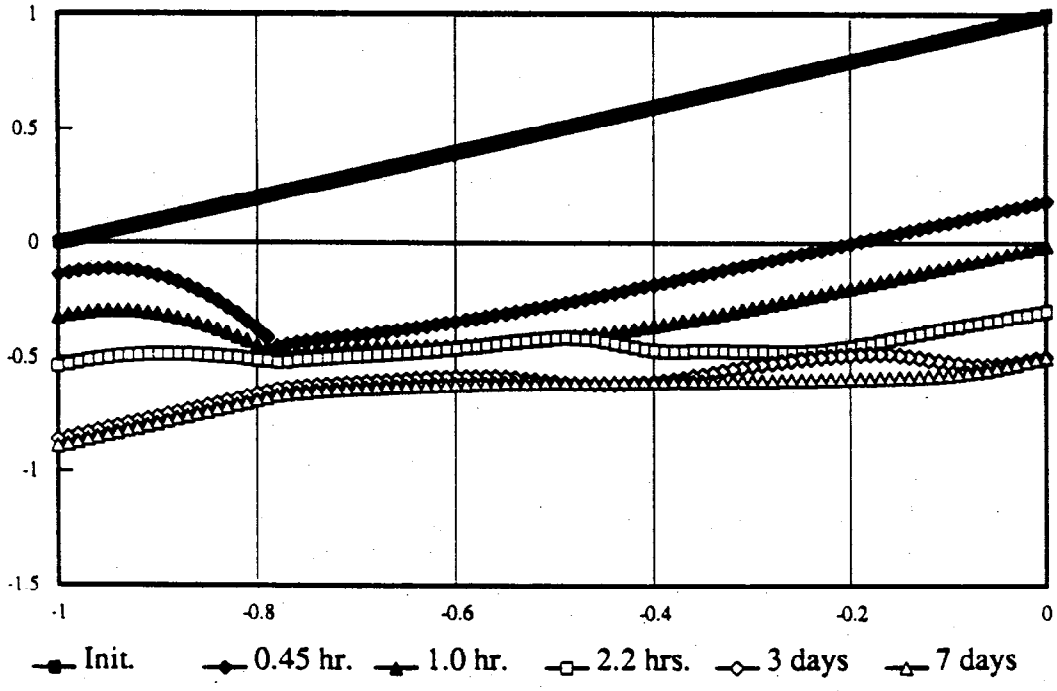

TRIAL 8-10W / NORANDA

Total Head (m) vs. Elevation (m)

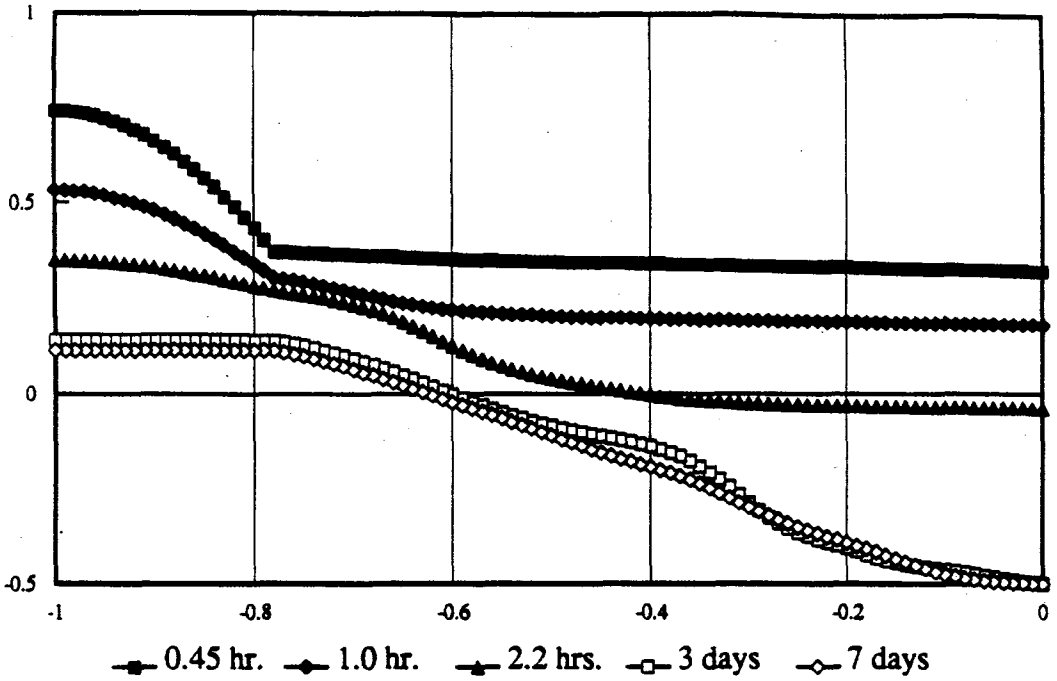

TRIAL 8-10W / NORANDA

Pressure Head (m) vs. Elevation (m)

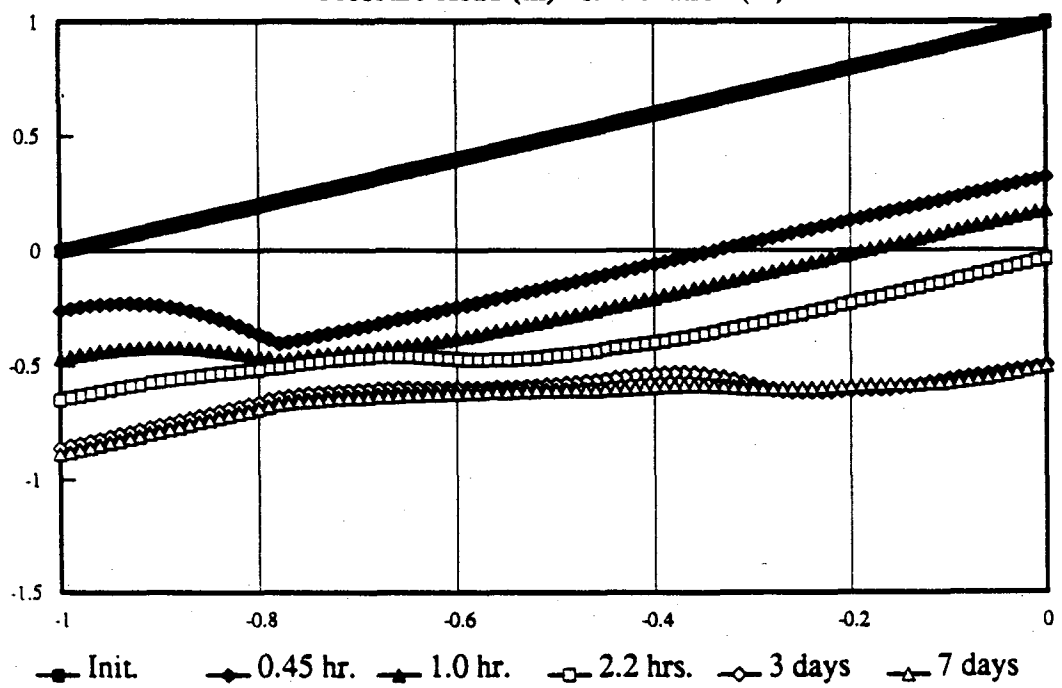

TRIAL 8-10X / NORANDA

Total Head (m) vs. Elevation (m)

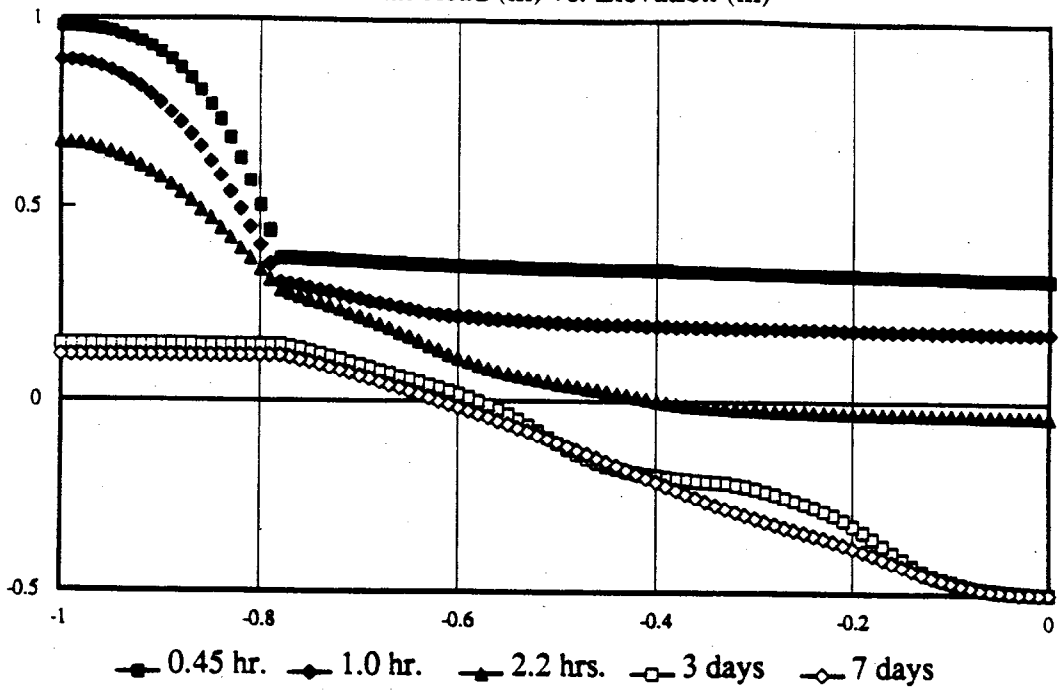

TRIAL 8-10X / NORANDA

Pressure Head (m) vs. Elevation (m)

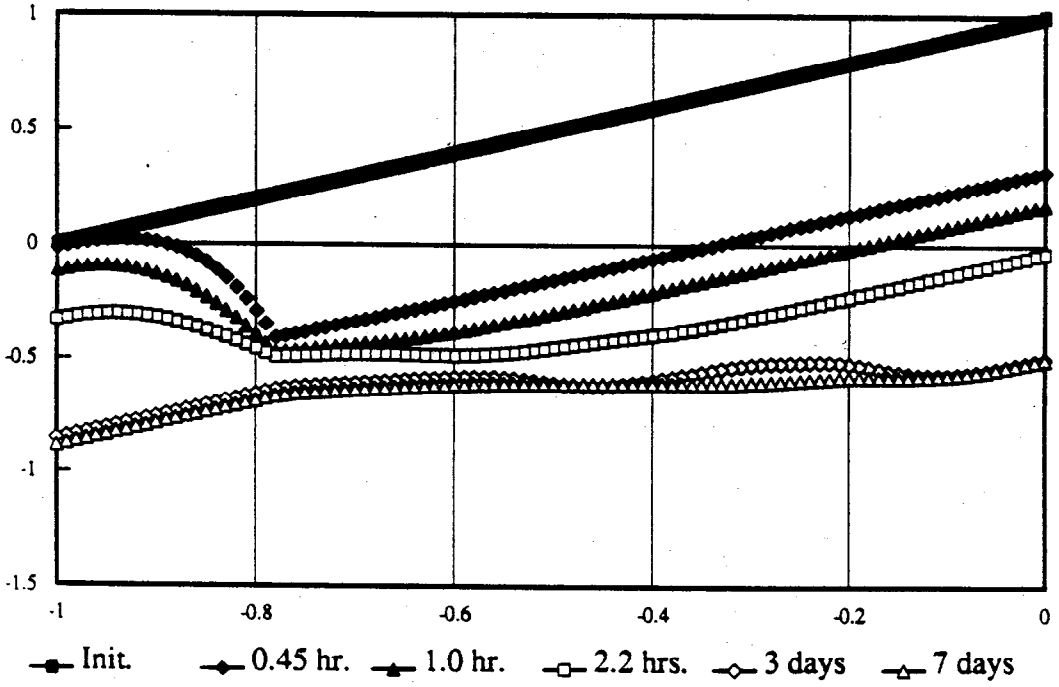

TRIAL 8-10Y / NORANDA

Total Head (m) vs. Elevation (m)

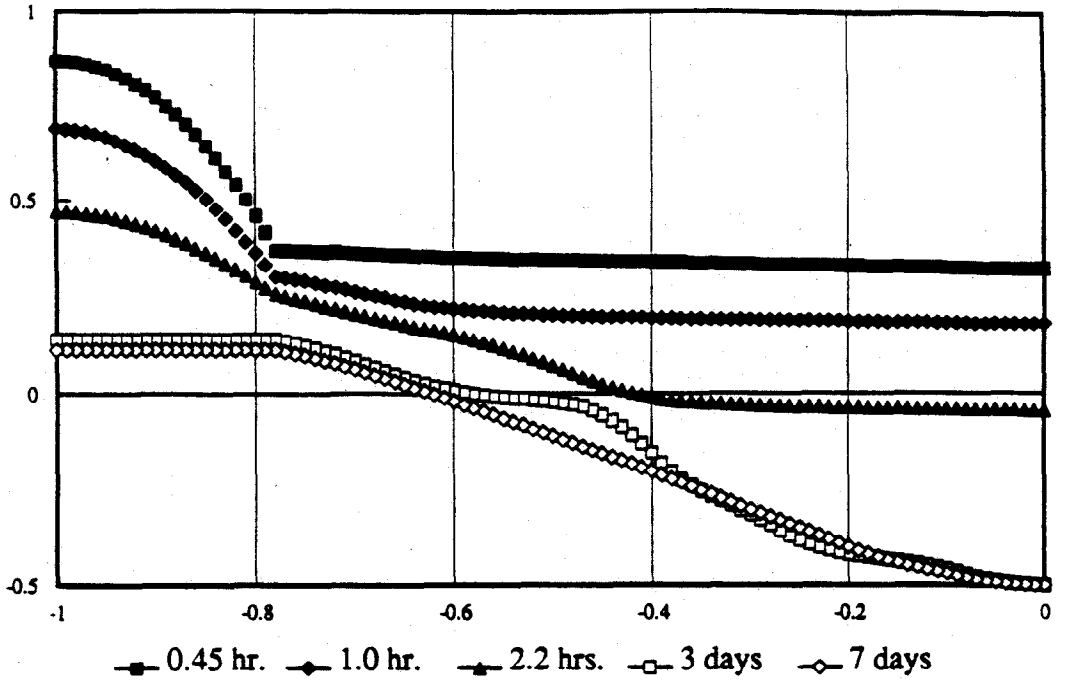

TRIAL 8-10Y / NORANDA

Pressure Head (m) vs. Elevation (m)

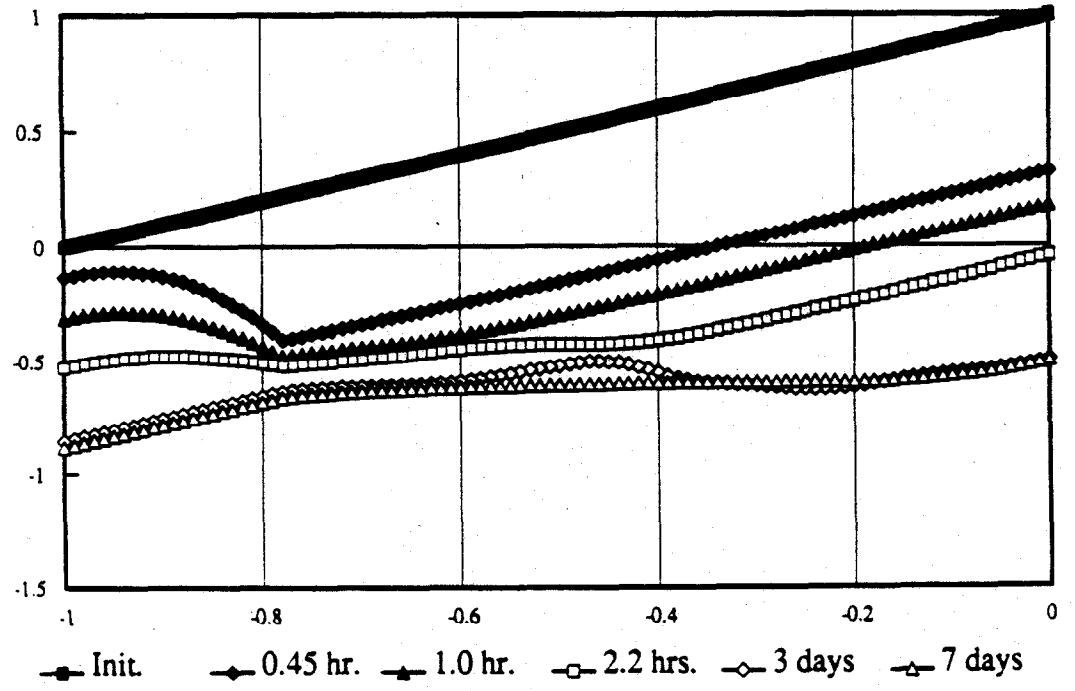

TRIAL 8-10Z / NORANDA

Total Head (m) vs. Elevation (m)

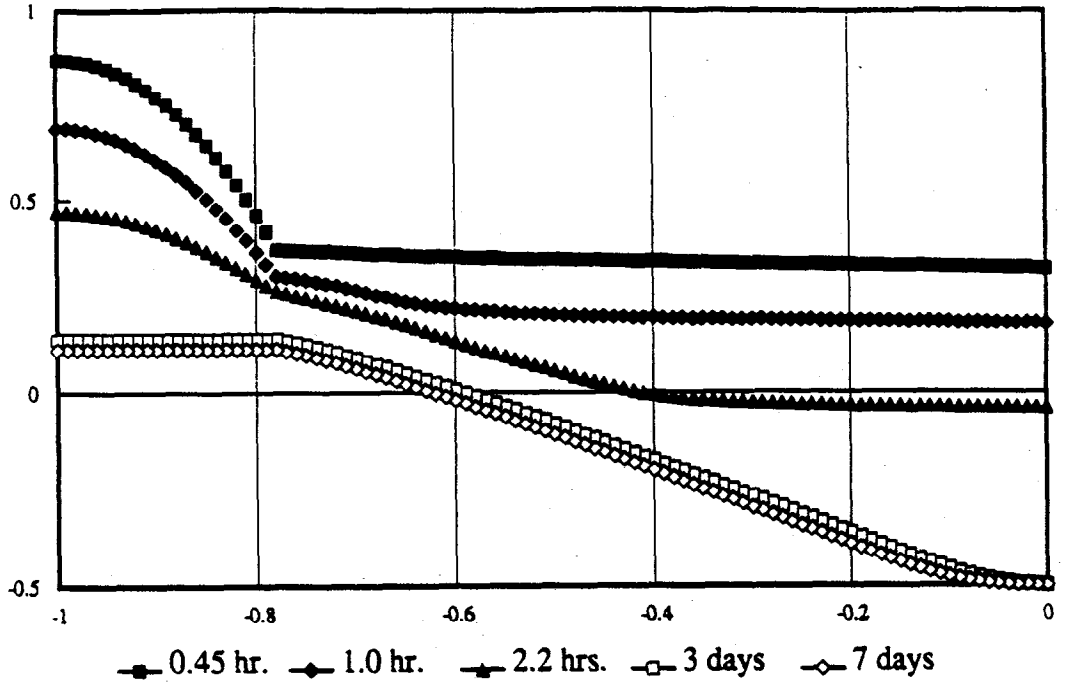

TRIAL 8-10Z / NORANDA

Pressure Head (m) vs. Elevation (m)

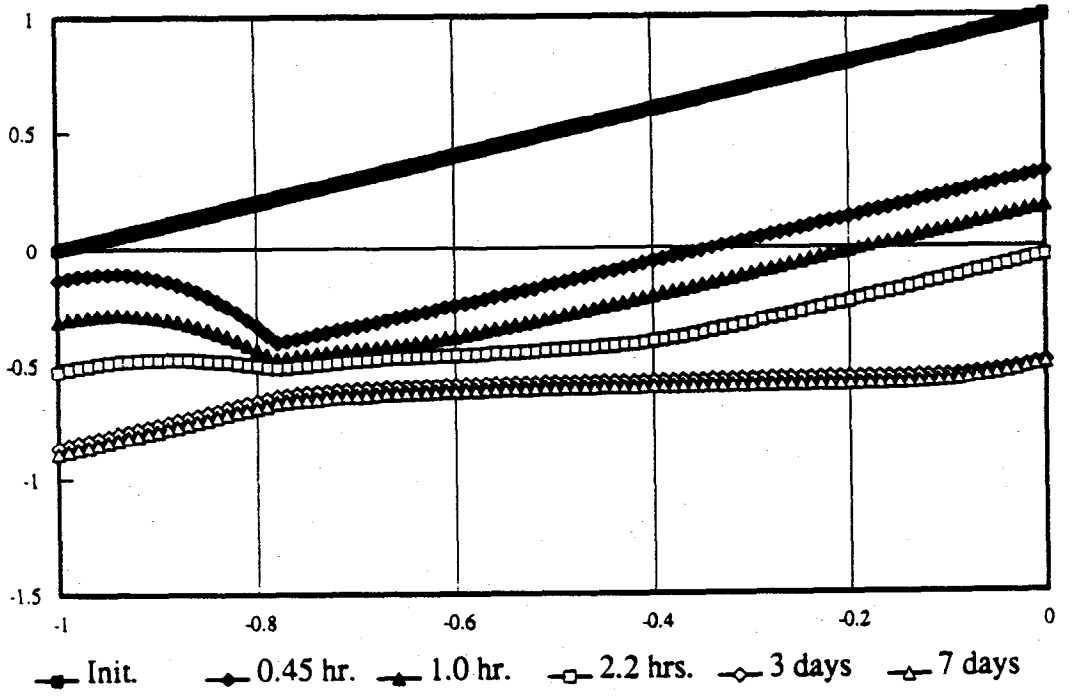

TRIAL 8-10AA / NORANDA

Total Head (m) vs. Elevation (m)

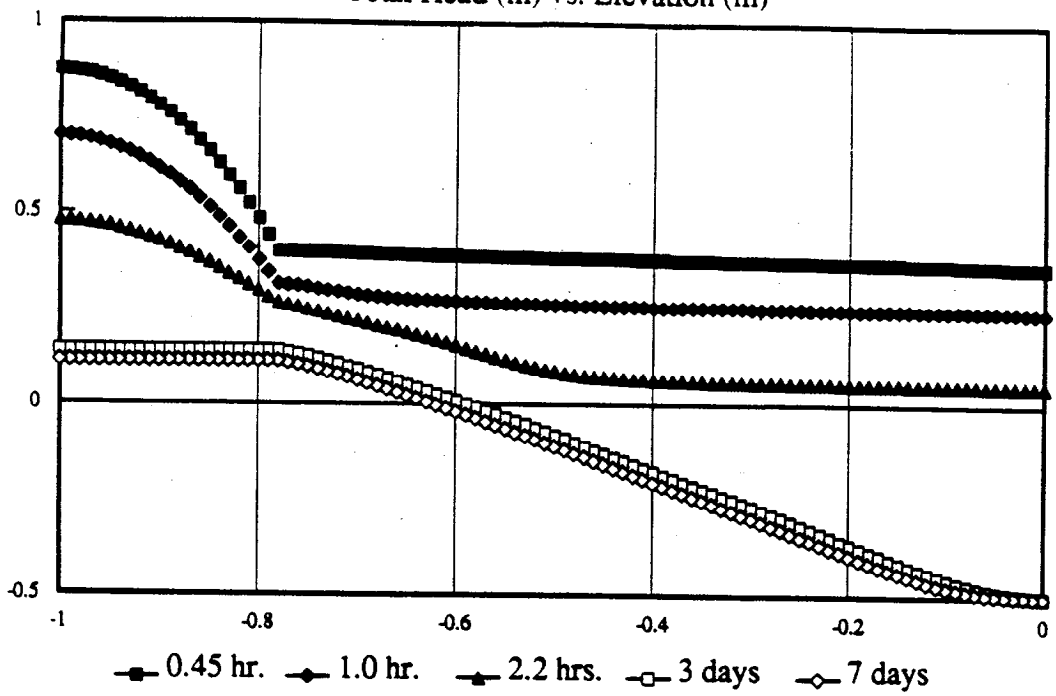

TRIAL 8-10AA / NORANDA

Pressure Head (m) vs. Elevation (m)